

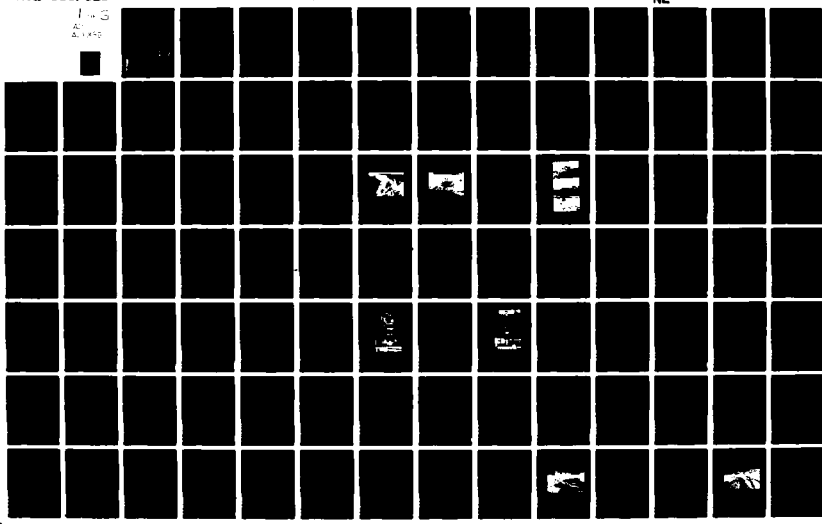
AD-A101 389

SOIL CONSERVATION SERVICE OXFORD MS SEDIMENTATION LAB F/8 8/13
STREAM CHANNEL STABILITY. APPENDIX D, BANK STABILITY AND BANK M--ETC(U)
APR 81 C R THORNE, J B MURPHEY, W C LITTLE

UNCLASSIFIED

1 of 3
2 of 3
3 of 3

NL



~~LEVEL~~

~~#~~

(1)

ADA101389

STREAM CHANNEL STABILITY

APPENDIX D

BANK STABILITY AND BANK MATERIAL PROPERTIES IN THE BLUFFLINE STREAMS OF NORTHWEST MISSISSIPPI

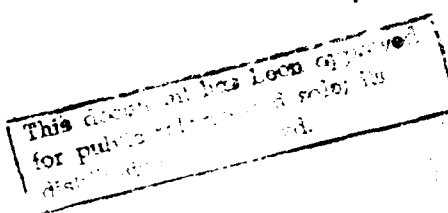
Project Objectives 3 and 5

by

C. R. Thorne, J. B. Murphey
and W. C. Little

USDA Sedimentation Laboratory
Oxford, Mississippi

April 1981



Prepared for
US Army Corps of Engineers, Vicksburg District
Vicksburg, Mississippi

Under
Section 32 Program, Work Unit 7

DTIC
ELECTRONIC
JUL 15 1981
S D
H

81 7 14 103

STREAM CHANNEL STABILITY

APPENDIX D

Bank Stability and Bank Material Properties in the Bluffline Streams
of Northwest Mississippi.

Project Objectives 3 and 5

by

C. R. Thorne¹, J. B. Murphey² and W. C. Little³

USDA Sedimentation Laboratory

Oxford, Mississippi

April 1981



Prepared for

US Army Corps of Engineers, Vicksburg District
Vicksburg, Mississippi

Under

Section 32 Program, Work Unit 7

- 1/ Visiting Scientist, Erosion and Channels Research Unit, USDA Sedimentation Laboratory, Oxford, MS; on leave from School of Environmental Sciences, University of East Anglia, Norwich, England.
- 2/ Geologist, Erosion and Channels Research Unit, USDA Sedimentation Laboratory, Oxford, MS.
- 3/ Research Hydraulic Engineer, Erosion and Channels Research Unit, USDA Sedimentation Laboratory, Oxford, MS.

4/1/81

Preface

This report describes the analyses of processes and mechanisms of streambank erosion in the bluff line streams of Northwest Mississippi.

Bank instabilities occur as a result of general channel degradation by headcutting and as a result of local scouring at the outerbank in bendways. Bank retreat takes place primarily by mass failures of overheightened and oversteepened banks. Failures are usually associated with the development of extensive tension cracks behind the bank and follow periods of heavy precipitation that maximize the bank material weight and minimize its strength.

Slope stability analyses can be used to assess the stability of streambanks and to predict limiting values for the bank height and slope angle. In this report, the limit analysis for a log spiral toe failure is used. This requires data on the distribution and strength properties of the bank materials. These data were obtained from a borehole survey of bank stratigraphy and from in situ and laboratory strength tests.

The accuracy of the stability analysis was tested using field observations of bank geometry. The tests indicated a good degree of success and this suggests that the analysis can be used as an aid in redesigning unstable banks with confidence.

Accession For		
NTIS CRA&I <input checked="" type="checkbox"/>		
DTIC TAB <input type="checkbox"/>		
Unpublished <input type="checkbox"/>		
Classification <i>Per form 50</i>		
Distribution <i>Rev ad file</i>		
Availability Codes		
Avail and/or Dist Special		
A		

Table of Contents

5.3.1	<u>Johnson Creek at Tommy Florence's</u>	75
5.3.2	<u>Johnson Creek at T.A. Woodruff's</u>	92
5.3.3	<u>Goodwin Creek at Katherine Leigh's</u>	95
5.3.4	<u>Hotophia Creek</u>	98
6	ENGINEERING APPLICATIONS	111
6.1	BANK STABILIZATION	111
6.2	CONCLUSIONS	113
7	ACKNOWLEDGEMENTS BY THE SENIOR AUTHOR	114
8	REFERENCES	115

ADDENDUMS

1	FIELD SITES	118
1.1	INTRODUCTION	122
1.2	TEST SITE LOCATIONS & DESCRIPTIONS	132
1.3	BOREHOLE PREPARATION & SAMPLING PROCEDURES	132
1.4	WELL LOGS OF BOREHOLES	160
2	IOWA BOREHOLE SHEAR TESTER	188
2.1	INTRODUCTION	190
2.2	THEORY	190
2.3	APPARATUS	192
2.4	TESTING PROCEDURE	192
2.5	DISCUSSION	199
3	BOREHOLE SHEAR TESTS: TABLES OF RESULTS	202
4	UNCONFINED COMPRESSION AND TENSION TESTER	251
4.1	INTRODUCTION	253
4.2	UNCONFINED COMPRESSION TESTS	253
4.3	UNCONFINED TENSION TESTS	254

List of Tables

Table No.	Title	Page
1	Critical Slope Heights (After Bradford and Piest, 1980)	24
2	Maximum Slope Heights (After Turnbull, 1948)	24
3	Direct Tension Tests on Loess (After Lutton, 1974)	28
4	Laboratory Direct Shear Tests on Reworked Loess (After Bradford and Piest, 1980)	29
5	Vertical and Horizontal Shear Strength of Western Iowa Bluff-Line Loess (After Lohnes and Handy, 1968)	29
6	Stability factor $N_s = H_c(\gamma/c)$ by limit analysis (logspiral passing through the toe, Fig. 9)	38
7	Borehole Shear Tests	49
8	Borehole Shear Tests: Mean Values	51
9	Unconfined Compression and Tension Tests	52
10	Unconfined Compression and Tension Tests: Mean Values	56
11	Mean and Worst Case Soil Strength Parameters	64
12	Bank Geometry Data: October 1980	66
13	Bank Survey Data: Hotophia Creek, Panola County, January 1978 and June 1979	67
14	Weighted Mean Soil Parameters for Surveyed Bank Sections at Tommy Florence's site	72
15	Weighted Mean Soil Parameters for Surveyed Bank Sections at T. A. Woodruff's site	73
16	Weighted Mean Soil Parameters for Surveyed Bank Sections at Katherine Leigh's site	74
17	Soil Parameters for Hotophia Creek	100
1.1	Boring and Testing Record; Tommy Florence property - Lower Johnson Creek, SE $\frac{1}{4}$, NW $\frac{1}{4}$, SE $\frac{1}{4}$, Sec. 3, T.10S., R.7W	154
1.2	Boring and Testing Record; T. A. Woodruff property - Upper Johnson Creek, SW $\frac{1}{4}$, NE $\frac{1}{4}$, Sec. 20, T.9S., R.6W	155
1.3	Boring and Testing Record; Katherine Leigh property - Lower Goodwin Creek, NW $\frac{1}{4}$, SE $\frac{1}{4}$, SW $\frac{1}{4}$, Sec. 2, T.10S., R.7W	156
3	Borehole Shear Tests: Results Tables	202
3.1	Test 1, Davidson Creek, at USDA Sedimentation Lab, BH1	205

3.2 Test 2, Davidson Creek, at USDA Sedimentation Lab, BH2	206
3.3 Test 3, Johnson Creek at Tommy Florence site (J/TF), BH1	207
3.4 Test 4, J/TF, BH1	208
3.5 Test 5, Goodwin Creek at Katherine Leigh site (G/KL), BH1	209
3.6 Test 6, G/KL, BH1	210
3.7 Test 7, G/KL, BH2	211
3.8 Test 8, G/KL, BH2	212
3.9 Test 9, G/KL, BH2	213
3.10 Test 10, Johnson Creek at T. A. Woodruff site (J/TAW), BH2	214
3.11 Test 11, J/TAW, BH2	215
3.12 Test 12, J/TAW, BH2	216
3.13 Test 13, J/TAW, BH2	217
3.14 Test 14, J/TAW, BH3	218
3.15 Test 15, J/TAW, BH3	219
3.16 Test 16, J/TAW, BH2	220
3.17 Test 17, J/TAW, BH4	221
3.18 Test 18, J/TAW, BH4	222
3.19 Test 19, J/TAW, BH4	223
3.20 Test 20, J/TAW, BH5	224
3.21 Test 21, J/TAW, BH6a	225
3.22 Test 22, J/TAW, BH6	226
3.23 Test 23, J/TAW, BH6a	227
3.24 Test 24, J/TAW, BH9	228
3.25 Test 25, J/TAW, BH10	229
3.26 Test 26, J/TAW, BH11	230
3.27 Test 27, J/TF, BH2	231
3.28 Test 28, J/TF, BH2	232
3.29 Test 29, J/TF, BH4	233
3.30 Test 30, J/TF, BH4	234
3.31 Test 31, J/TF, BH3	235
3.32 Test 32, J/TF, BH3	236
3.33 Test 33, J/TF, BH2	237
3.34 Test 34, J/TF, BH2	238
3.35 Test 35, J/TF, BH3	239
3.36 Test 36, J/TF, BH2	240

3.37 Test 37, J/TF, BH4	241
3.38 Test 38, J/TF, BH4	242
3.39 Test 39, J/TF, BH5	243
3.40 Test 40, J/TF, BH5	244
3.41 Test 41, J/TF, BH5	245
3.42 Test 42, G/KL, BH5	246
3.43 Test 43, G/KL, BH5	247
3.44 Test 44, G/KL, BH6	248
3.45 Test 45, G/KL, BH6	249
3.46 Test 46, G/KL, BH6	250

List of Figures

Figure No.	Title	Page
1	Shear failure along a planar slip surface through the toe (After Lohnes and Handy, 1968)	19
2	Slab failure of a vertical bank by tension cracking and plane slip (After Lohnes and Handy, 1968)	20
3	Sequence of bank failure observed by Bradford and Piest (1977). 1. Initial Slope. 2. "Pop out" failure. 3. Final Canti- lever Failure. k is the saturated hydraulic conductivity for the two soils	21
4	Comparison of shear strength for different directions of shear for typical silty loess soil (After Turnbull, 1948)	25
5	Linear yield envelopes for loess at various degrees of saturation S_o (After Lutton, 1974)	27
6	Imminent slab failure observed on Goodwin Creek at Katherine Leigh site, Panola County	32
7	Slab failure on Goodwin Creek, Panola County	33
8	Slab failure with a) more or less intact failure block, b) disintegration of failure block into a soil fall and c) disintegration of failure block into a soil flow	35
9	Stability Number, N_s , as a function of slope angle, i , for a log-spiral failure surface passing through the toe (After Chen, 1975)	37
10	Mohr Diagram for Consolidated, Undrained Triaxial Tests on Old Paleosol from T. A. Woodruff's site, Johnson Creek	57
11	Example of tension failure plane following horizontal bedding planes in the Post Settlement Alluvium	60
12	Example of tension failure in a soil without horizontal bedding planes. Failure surface is horizontal with micro- topography of inclined planes	62
13	Idealized bank failure. a. Just prior to failure the bank height and angle and the tension crack depth are close to their critical values. b. Just after failure the new bank profile may be used to estimate the tension crack depth (y) and the failure block width (b)	70

14a	Bank Stability Graph for Johnson Creek at Tommy Florence's site	76
14b	Bank Stability Graph for Johnson Creek at Tommy Florence's site	77
14c	Bank Stability Graph for Johnson Creek at Tommy Florence's site	78
14d	Bank Stability Graph for Johnson Creek at Tommy Florence's site	79
15a	Bank Stability Graph for Johnson Creek at T. A. Woodruff's site	80
15b	Bank Stability Graph for Johnson Creek at T. A. Woodruff's site	81
15c	Bank Stability Graph for Johnson Creek at T. A. Woodruff's site	82
15d	Bank Stability Graph for Johnson Creek at T. A. Woodruff's site	83
15e	Bank Stability Graph for Johnson Creek at T. A. Woodruff's site	84
16a	Bank Stability Graph for Goodwin Creek at Katherine Leigh's site	85
16b	Bank Stability Graph for Goodwin Creek at Katherine Leigh's site	86
16c	Bank Stability Graph for Goodwin Creek at Katherine Leigh's site	87
16d	Bank Stability Graph for Goodwin Creek at Katherine Leigh's site	88
16e	Bank Stability Graph for Goodwin Creek at Katherine Leigh's site	89
17	View of Tommy Florence's Site showing eroding bank located at the outside of a developing bendway	91
18	View of T. A. Woodruff's Site showing straight channel and vegetated banks above the headcut (now stabilized by a grade control structure)	94
19	View of Katherine Leigh's Site showing eroding bank on the outside of a developing bendway and resistant materials at section 3	96

20	Bank Stability Graph for Hotophia Creek	101
21	Bank Cross Sectional Profile at section T-51-8(L) on Hotophia Creek	102
22	Cross Sectional Profiles on Hotophia Creek. a) Section T-52-1. b) T-51-9	104
23	Bank Cross Sectional Profile at section T-49-1(L) on Hotophia Creek	105
24	Bank Cross Sectional Profiles on Hotophia Creek showing vertical top sections, taken to indicate the depth of tension cracking at the time of failure, and retreat of bank top, taken to indicate failure block width	107
25	Observed and Predicted Tension Crack Depths for Hotophia Creek	108
26	Observed and Predicted Failure Block Widths for Hotophia Creek	110
1.1	Physiographic Setting of Peters Creek Watershed	123
1.2	Geologic Map of Peters and Hotophia Creek Watersheds after Vestal (1956)	124
1.3	Geographic Locations of the Test Sites shown on Soil Map of Area	130
1.4	Valley-normal soil transects at each test site (schematic) . . .	131
1.5	Aerial Photo of Lower Johnson Creek (Florence) site	133
1.6	Locations of Florence site test holes & cross sections	134
1.7	Florence site Cross Section XS-1	135
1.8	Florence site Cross Section XS-2	136
1.9	Florence site Cross Section XS-3	137
1.10	Florence site Cross Section XS-4	138
1.11	Florence site Cross Section XS-5	139
1.12	Aerial Photo of Upper Johnson Creek (Woodruff) site	140
1.13	Locations of Woodruff site test holes & cross sections	141
1.14	Woodruff site Cross Section XS-1	142
1.15	Woodruff site Cross Section XS-2	143
1.16	Woodruff site Cross Section XS-3	144
1.17	Woodruff site Cross Section XS-4	145
1.18	Woodruff site Cross Section XS-5	146

1.19 Aerial Photo of Lower Goodwin Creek (Leigh) site	147
1.20 Locations of Leigh site test holes & cross sections	148
1.21 Leigh site Cross Section XS-1	149
1.22 Leigh site Cross Section XS-2	150
1.23 Leigh site Cross Section XS-3	151
1.24 Leigh site Cross Section XS-4	152
1.25 Leigh site Cross Section XS-5	153
1.26 Drill rig used in Borehole Shear Test program	157
1.27 2" & 3" Quick-Relief Soil Tubes, Bits, and Vacuum-ball Soil Tube Heads	157
1.28 Split-spoon Samplers	159
1.29 Borehole Cover Plug	159
1.30 Well Log Legend	161
1.31 T. Florence site - Borehole #1	162
1.32 T. Florence site - Borehole #2	163
1.33 T. Florence site - Borehole #3	164
1.34 T. Florence site - Borehole #4	165
1.35 T. Florence site - Borehole #5	166
1.36 T. Florence site - Borehole #7	167
1.37 T. Florence site - Borehole #9	168
1.38 T. A. Woodruff site - Borehole #1	169
1.39 T. A. Woodruff site - Borehole #2	170
1.40 T. A. Woodruff site - Borehole #3	171
1.41 T. A. Woodruff site - Borehole #4	172
1.42 T. A. Woodruff site - Borehole #5	173
1.43 T. A. Woodruff site - Borehole #6	174
1.44 T. A. Woodruff site - Borehole #6a	175
1.45 T. A. Woodruff site - Borehole #7	176
1.46 T. A. Woodruff site - Borehole #8	177
1.47 T. A. Woodruff site - Borehole #9	178
1.48 T. A. Woodruff site - Borehole #10	179
1.49 T. A. Woodruff site - Borehole #11	180
1.50 K. Leigh site - Borehole #1	181
1.51 K. Leigh site - Borehole #2	182
1.52 K. Leigh site - Borehole #3	183

1.53 K. Leigh site - Borehole #4	184
1.54 K. Leigh site - Borehole #5	185
1.55 K. Leigh site - Borehole #6	186
1.56 K. Leigh site - Borehole #7	187
2.1 Direct Shear Test for Laboratory Testing	191
2.2 Borehole Shear Test, essentially a direct shear test performed on the soil inside the borehole	193
2.3 Borehole Shear Test Apparatus	194
2.4 Shear Head and Connecting Rods ready for insertion into the borehole	195
2.5 Pulling Assembly, Base Plate and Gas Control Console	197
2.6 Pulling force is applied by cranking the handle at a rate of two turns per second	198
2.7 Old and New (High Pressure) Borehole Shear Test Shear Plates . .	201
4.1 Unconfined compression test on a sample of young paleosol	255
4.2 Unconfined compression apparatus modified for unconfined tension testing	256
4.3 Soil lathe for turning down samples strong in tension	258

**CONVERSION FACTORS, U.S. CUSTOMARY TO METRIC (SI) AND
METRIC (SI) TO U.S. CUSTOMARY UNITS OF MEASUREMENT^{1/}**

Units of measurement used in this report can be converted as follows:

To convert	To	Multiply by
mils (mil)	micron (μm)	25.4
inches (in)	millimeters (mm)	25.4
feet (ft)	meters (m)	0.305
yards (yd)	meters (m)	0.914
miles (miles)	kilometers (km)	1.61
inches per hour (in/hr)	millimeters per hour (mm/hr)	25.4
feet per second (ft/sec)	meters per second (m/sec)	0.305
square inches (sq in)	square millimeters (mm^2)	645.
square feet (sq ft)	square meters (m^2)	0.093
square yards (sq yd)	square meters (m^2)	0.836
square miles (sq miles)	square kilometers (km^2)	2.59
acres (acre)	hectares (ha)	0.405
acres (acre)	square meters (m^2)	4,050.
cubic inches (cu in)	cubic millimeters (mm^3)	16,400.
cubic feet (cu ft)	cubic meters (m^3)	0.0283
cubic yards (cu yd)	cubic meters (m^3)	0.765
cubic feet per second (cfs)	cubic meters per second (cms)	0.0283
pounds (lb) mass	grams (g)	454.
pounds (lb) mass	kilograms (kg)	0.453
tons (ton) mass	kilograms (kg)	907.
pounds force (lbf)	newtons (N)	4.45
kilogram force (kgf)	newtons (N)	9.81
foot pound force (ft lbf)	joules (J)	1.36
pounds force per square foot (psf)	pascals (Pa)	47.9
pounds force per square inch (psi)	kilopascals (kPa)	6.89
pounds mass per square foot (lb/sq ft)	kilograms per square meter (kg/m^2)	4.88
U.S. gallons (gal)	liters (L)	3.79
quart (qt)	liters (L)	0.946
acre-feet (acre-ft)	cubic meters (m^3)	1,230.
degrees (angular)	radians (rad)	0.0175
degrees Fahrenheit (F)	degrees Celsius (C) ^{2/}	0.555

^{2/} To obtain Celsius (C) readings from Fahrenheit (F) readings, use the following formula: $C = 0.555 (F-32)$.

Metric (SI) to U.S. Customary

To convert	To	Multiply by
micron (μm)	mils (mil)	0.0394
millimeters (mm)	inches (in)	0.0394
meters (m)	feet (ft)	3.28
meters (m)	yards (yd)	1.09
kilometers (km)	miles (miles)	0.621
millimeters per hour (mm/hr)	inches per hour (in/hr)	0.0394
meters per second (m/sec)	feet per second (ft/sec)	3.28
square millimeters (mm^2)	square inches (sq in)	0.00155
square meters (m^2)	square feet (sq ft)	10.8
square meters (m^2)	square yards (sq yd)	1.20
square kilometers (km^2)	square miles (sq miles)	0.386
hectares (ha)	acres (acre)	2.47
square meters (m^2)	acres (acre)	0.000247
cubic millimeters (mm^3)	cubic inches (cu in)	0.0000610
cubic meters (m^3)	cubic feet (cu ft)	35.3
cubic meters (m^3)	cubic yards (cu yd)	1.31
cubic meters per second (cms)	cubic feet per second (cfs)	35.3
grams (g)	pounds (lb) mass	0.00220
kilograms (kg)	pounds (lb) mass	2.20
kilograms (kg)	tons (ton) mass	0.00110
newtons (N)	pounds force (lbf)	0.225
newtons (N)	kilogram force (kgf)	0.102
joules (J)	foot pound force (ft lbf)	0.738
pascals (Pa)	pounds force per square foot (psf)	0.0209
kilopascals (kPa)	pounds force per square inch (psi)	0.145
kilograms per square meter (kg/m^2)	pounds mass per square foot lb/sq ft)	0.205
liters (L)	U.S. gallons (gal)	0.264
liters (L)	quart (qt)	1.06
cubic meters (m^3)	acre-feet (acre-ft)	0.000811
radians (rad)	degrees (angular)	57.3
degrees Celsius (C)	degrees Fahrenheit (F) ^{3/}	1.8

1/ All conversion factors to three significant digits.

3/ To obtain Fahrenheit (F) readings from Celsius (C) readings, use the following formula: $F = 1.8C + 32$.

NOTATION

b	Width of Failure Block
c	cohesion
H	bank height
H_c	critical bank height
H_{cr}	critical vertical bank height
H'_c	critical bank height with tension crack
H'_{cr}	critical vertical bank height with tension crack
i	bank angle
N_s	Stability Number
r	ratio of σ_{tc} to σ_{cc} , expressed in %
s	shear strength
s_o	degree of saturation
y	depth of tension crack
Z_o	depth of tensile stress
α	backslope angle
γ	bulk unit weight
ϕ	friction angle
σ	normal stress
σ_{cc}	unconfined compression strength
σ_t	tensile stress
σ_{tc}	unconfined tensile strength

INTRODUCTION

Many of the bluff line streams of Northwest Mississippi have degraded very seriously during the last fifty years. This degradation is the result of changes in land use, channel straightening and lowering of effective base level by trunk stream regulation (Whitten and Patrick, 1980). Degradation takes place primarily by the upstream movement of a knickpoint, often in the form of a headcut or overfall. This headcut forms where the channel bed breaks through resistant substrata of ironstone or clay. The streams lack any bedrock control and are erodible channels. Upstream of a headcut, channels appear to be reasonably stable and they conform to regime equations for alluvial rivers. However, downstream of a headcut the channels lose their stability and their coherent hydraulic geometry.

Although the main fluvial response of the channels is to degrade by bed scouring, the channel banks are also seriously affected. Scour of the bed and bank toe increases the bank's height and slope angle, decreasing its stability with respect to mass failure under gravity. Overheightening and oversteepening of the bank continue until a state of limiting stability is reached, when the forces tending to cause failure balance those tending to oppose failure, and mass failure is imminent. The mechanism of failure depends on the size and stratigraphy of the bank and the physical properties of the bank materials (Thorne, 1978; 1981).

Slope stability analyses can be applied to streambanks to determine their stability and define the most critical mechanism of failure.

In this study, a literature survey was used to identify possible approaches to the problem of describing and analyzing bank stability in the bluff line streams. On the basis of the survey, preliminary field investigation, and previous experience, we decided to use the limit analysis method presented by Chen (1975) to assess bank stability. This requires data on the strength properties of the bank material. Such data usually are obtained from detailed site investigations and laboratory tests on intact samples of soil. However this approach is seldom feasible in the study of bank erosion on a catchment-wide basis, and so another approach must be adopted.

Two relatively new instruments were selected for soil strength measurements. The Iowa Borehole Shear Tester was used to make in situ measurements of the cohesion and friction angle and an Unconfined Compression Tester was modified to conduct both compression and tension tests. The instruments are not widely used and are not well documented, so they are described and discussed in some detail. In this report, the strength measurements are used with bank geometry data from three bluff line streams to test whether reasonable predictions of critical bank heights and slope angles can be made. Finally, the engineering applications are considered and recommendations are made concerning future research.

2.1 BANK STABILITY ANALYSES

Problems of channel degradation and bank instability are not confined to Northwest Mississippi. Lohnes and Handy (1968), Bradford and Piest (1977, 1980) and Lohnes, Klaiber and Dougal (1980) encountered similar problems in western Iowa. Lohnes and Handy (1968) investigated the relationship between the height, slope angle and strength properties of banks formed in loess. Two main mechanisms of failure were identified: shear failure along a planar slip surface through the toe (Fig. 1.) and slab failure of vertical banks by tension cracking and plane slip (Fig. 2.). The Culmann method (Lambe and Whitman, 1979) was used to analyze shear failure and predict maximum bank height for non-vertical slopes. For vertical slopes, stability with respect to slab failure was also analyzed using the Culmann method, but modified to take into account tension cracking behind a vertical cut. As Lohnes and Handy point out, their approach can only be approximate because the basic assumptions on which it is based are not fully satisfied in a real streambank. For example, the Culmann method is a total stress analysis that takes no account of pore pressure. Consequently it should only be applied to highly permeable soils and those with a low degree of saturation. Also it is a limit-equilibrium analysis for a rigid-plastic material. Real soils are elasto-plastic and experience some strain prior to failure, so that failure may occur progressively along a failure plane rather than simultaneously at all points. Finally, the distribution of forces in the bank would be radically altered as soon as a tension crack started to develop, and this is not taken into consideration. Despite these limitations, the analysis and equations developed by Lohnes and Handy did give reasonable results when applied to steep eroding streambanks in loessial material in Iowa, and it might well be applicable to the bluff line streams of Northwest Mississippi.

Bradford and Piest (1977) also considered the stability of steep banks in loessial material, but in their case the soil had been redeposited fluvially. In a field experiment they used a water filled trench to raise the water table in a vertical bank and observed failure as a function of pore water pressure. Failure occurred by a "pop out" near the toe, leaving an overhang which failed subsequently in shear (Fig. 3.). A conventional

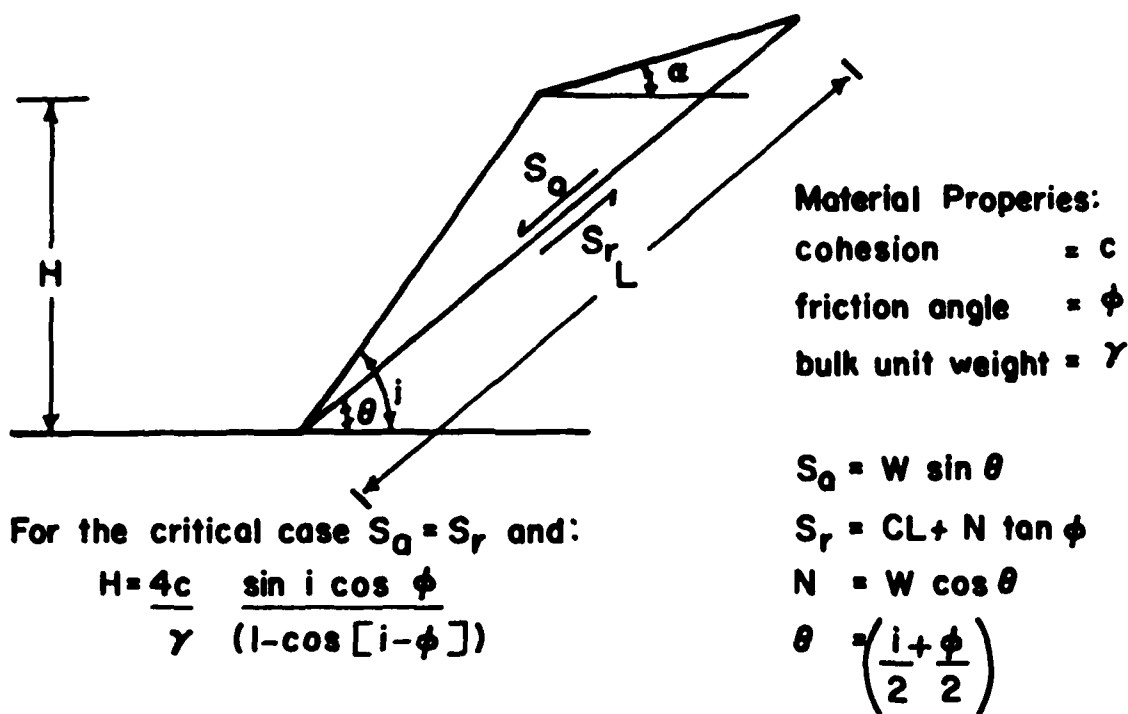
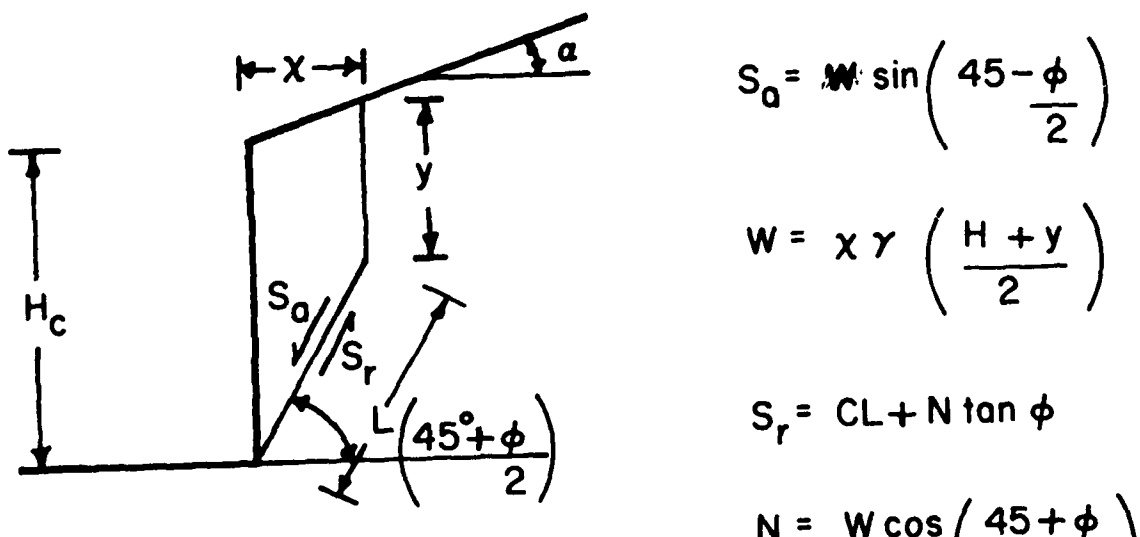


Figure 1. Shear failure along a planar slip surface through the toe (After Lohnes and Handy, 1968).



$$S_a = w \sin\left(\frac{45 - \phi}{2}\right)$$

$$w = x \gamma \left(\frac{H_c + y}{2}\right)$$

$$S_r = CL + N \tan \phi$$

$$N = w \cos\left(\frac{45 + \phi}{2}\right)$$

For the critical case $S_a = S_r$ and:

$$\begin{aligned} H_c &= \frac{4c}{\gamma [\cos \phi - 2 \cos^2(45 + \phi/2) \tan \phi]} - y \\ &= \frac{4c}{\gamma} \tan\left(\frac{45 + \phi}{2}\right) - y \end{aligned}$$

Figure 2. Slab failure of a vertical bank by tension cracking and plane slip (After Lohnes and Handy, 1968).

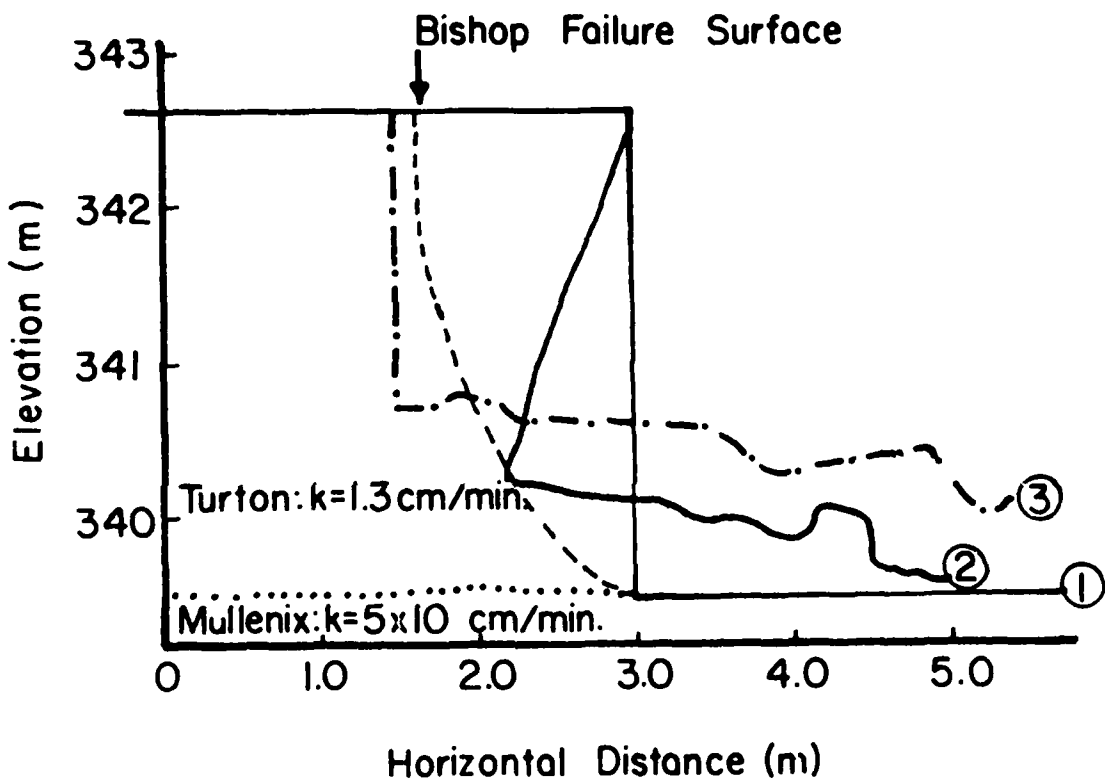


Figure 3. Sequence of bank failure observed by Bradford and Piest (1977).
 1. Initial Slope. 2. "Pop out" failure. 3. Final Cantilever Failure. k is the saturated hydraulic conductivity for the two soils.

slope stability analysis, based on the Bishop version of the Method of Slices (Fellenius, 1939) for a circular arc toe failure, was unsuccessful in predicting the factor of safety, see Fig. 3. This is to be expected, as the failure in no way approximated a circular arc through the toe. The failure of the toe in a "pop out" mechanism could be attributed to drainage in the bank. Probably drainage from the trench was nearly vertical, down to an impermeable layer of Mullenix soil at about toe elevation as shown in Figure 3. This produced strong horizontal seepage at the elevation of the toe along the interface with the impermeable underlying layer. This pattern of drainage might be expected on the basis of piezometer data from loess dams (Turnbull, 1948). Seepage at the toe would promote "pop out" failure, as a result of weakening due to saturation, and possible collapse of the loessial soil on thorough wetting. Bradford and Piest (1977) state emphatically that "seepage force exerted by the flowing groundwater had little effect."

In a later paper, Bradford and Piest (1980) report further on their observations of gully wall stability. Three major mechanisms of failure were identified. These were deep seated circular arc toe failure, slab failure and "pop out" failure with shear failure of the remaining cantilever. Circular arc failures were found on the comparatively low angle banks some distance downstream of a headcut. Slab failures like those noted by Lohnes and Handy (1968) were found on steep banks just downstream of a headcut. "Pop out" failures were associated with steep banks and a high degree of saturation at the toe leading to loss of strength and collapse. It was felt that stress relief at the toe might also be a cause of "pop out" failure. Failed soil units did not usually remain intact but disintegrated to a debris wedge of block rubble and soil flows.

Lutton (1969, 1974) identified similar mechanisms of failure. Vertical cuttings in Vicksburg loess failed in columns, corresponding to slab failure. "Pop out" and alcove failures at the toe were also observed. Lutton attributed these to weakening by saturation or undercutting by flowing water.

These observations are entirely consistent with mechanisms of failure observed on streambanks as summarized by Thorne (1981). Rotational failures are critical in cohesive banks of great height and comparatively low slope. This is the case because in sloping cohesive banks the orientation of the principal stresses changes with depth. For near vertical banks, there is little change of orientation and the failure

surface is almost planar (Carson and Kirkby, 1972). Behind steep banks, tensile stress is generated adjacent to the upper part of the bank. This leads to the development of vertical tension cracks which promote failure by the slab mechanism. The presence of a tension crack has a very important effect in determining the critical mechanism of failure and hence the limiting bank height. For example, Bradford and Piest (1980) applied the simplified Bishop analysis for circular arc toe failure and Lohnes and Handy's slab failure equation (Eq. 8 in Section 3.2.3) to various loess units in Western Iowa (Table 1.). The calculations show that the critical height for slab failure of a vertical bank with a tension crack is smaller than that for a circular arc failure. Hence, slab failure would be more critical than circular arc failure. However, if no tension cracks are present then circular arc failure is more critical than plane shear failure, and the limiting bank height increases by about 70%. Clearly tension cracking plays an extremely important role in controlling the stability, critical mode of failure and limiting height of steep banks.

2.2 MEASUREMENT OF SOIL STRENGTH

In order to apply slope stability analysis, data on the strength of the bank materials are required. These tests fall into two main groups: laboratory tests on core samples of soil, and field tests on the soil in situ. Laboratory tests are usually either compression tests (with or without confining pressure) or direct shear tests. Detailed accounts of testing procedures may be found in standard civil engineering texts and are not covered here (Terzaghi and Peck, 1948; Bishop and Henkel, 1957; Lambe and Whitman, 1979).

Turnbull (1948) carried out direct quick shear tests on saturated and unsaturated samples of loess from South-central Nebraska. Tests were performed on core samples taken vertically, horizontally and at 45°, and no strength anisotropy was detected. The results of Turnbull's shear tests are presented in Figure 4. Consolidation tests showed a rapid decrease in voids ratio as pressures rose above about 22 kiloPascals (kPa) (10 tons per square foot). Also, there was a large amount of consolidation and resulting settlement in the loess as it became saturated. This may be the reason for the "alcove" and "pop out" failures described previously. Steep cuttings in loess remained stable to considerable heights (Table 2.). Loess earth

Table 1: Critical Slope Heights (After Bradford and Piest, 1980).

Soil Deposit	Slope Angle (degrees)	Max. Slope Height (Bishop Slip Circle) (m)	Max. Slope Height (Lohnes and Handy) $y = \text{tension crack depth}$	
			$y = 0$ (m)	$y = z_o$ (m)
Turton	90	3.50	4.04	2.02
Mullinex	90	1.80	2.17	1.08
Hatcher	90	3.00	3.49	1.75
Watkins	90	2.10	2.48	1.24
1 foot = 0.3048m				

Table 2: Maximum Slope Heights (After Turnbull, 1948).

Material	Slope Angle (°)	Maximum Height (m)
Sandy Loess	76	12.2
Silty Loess	76	16.8
Sandy Loess	63	19.8
Silty Loess	63	24.4
Coarse sandy	53	>24.0
Loess or sand	34	Any Height
1 foot = 0.3048m		

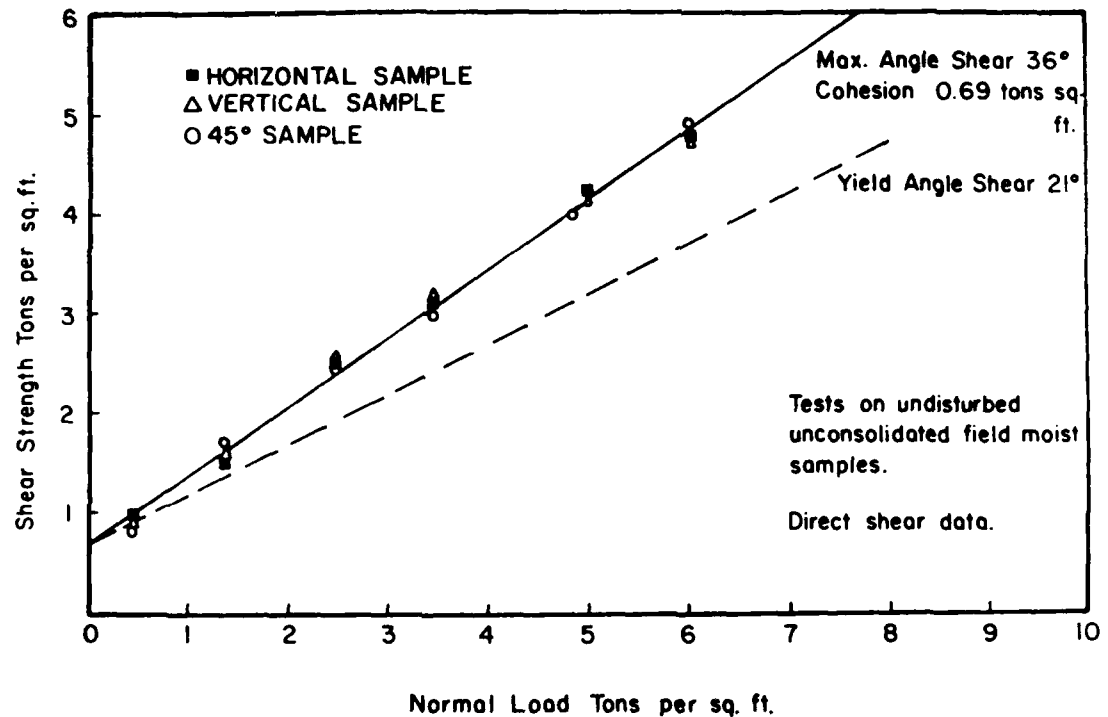


Figure 4. Comparison of shear strength for different directions of shear for typical silty loess soil (After Turnbull, 1948).

fill dams (Turnbull, 1948) were stable too, if allowance was made for unequal settlement upon wetting. Seepage below the dams was monitored using piezometers. The data showed that seepage was nearly vertical below the dams, extending to a deep gravel aquifer.

Lutton (1969, 1974) used unconfined compression tests and both unconsolidated and consolidated undrained triaxial tests to obtain shear strength data for Vicksburg loess. Consolidated tests gave considerably different results from unconsolidated tests. Lutton attributed this to a loss of cohesion through destruction of the soil structure in the consolidated tests. For this reason he places stronger reliance on the unconsolidated test data. Some flattening of the Mohr-Coulomb rupture line was evident in the results for unconsolidated tests run at greater than 320 to 430 kPa (3-4 tons/ft²), probably as a result of structural collapse. Consolidation tests support this theory. Lutton found a strong variation in strength with degree of saturation. There seemed to be a marked but gradual decrease in strength with increasing degrees of saturation (Fig. 5.). Tests performed on vertical and horizontal samples did not reveal any significant strength anisotropy and Lutton did not agree that the stability of vertical slopes could be attributed to strength anisotropy associated with loess soil structure such as root tubes. In his later study Lutton performed some simple direct pull tension tests on intact soil cores. Sample cores were cut to an hour glass shape and attached to end caps using soil sampling wax. The sample was then suspended vertically and weight added in increments to a tray hung from the lower cap until tensile failure occurred. This apparatus is very similar to one developed independently by Thorne (1978) and subsequently further developed into a recording unconfined tension test (Thorne, Tovey and Bryant, 1980). No stress-strain measurements were made but Lutton's apparatus seemed to give reliable results. The tensile strength of the soil was, in some cases, remarkably high and was significantly larger than that measured in a Brazil or splitting test (Table 3.). Bradford and Piest (1977, 1980) carried out consolidated drained triaxial tests, laboratory direct shear tests, and field measurements using a Pilcon vane tester (Table 4.). They stated that "Any stability analysis of slopes is limited by our ability to accurately measure soil properties within each horizon of the failure mass."

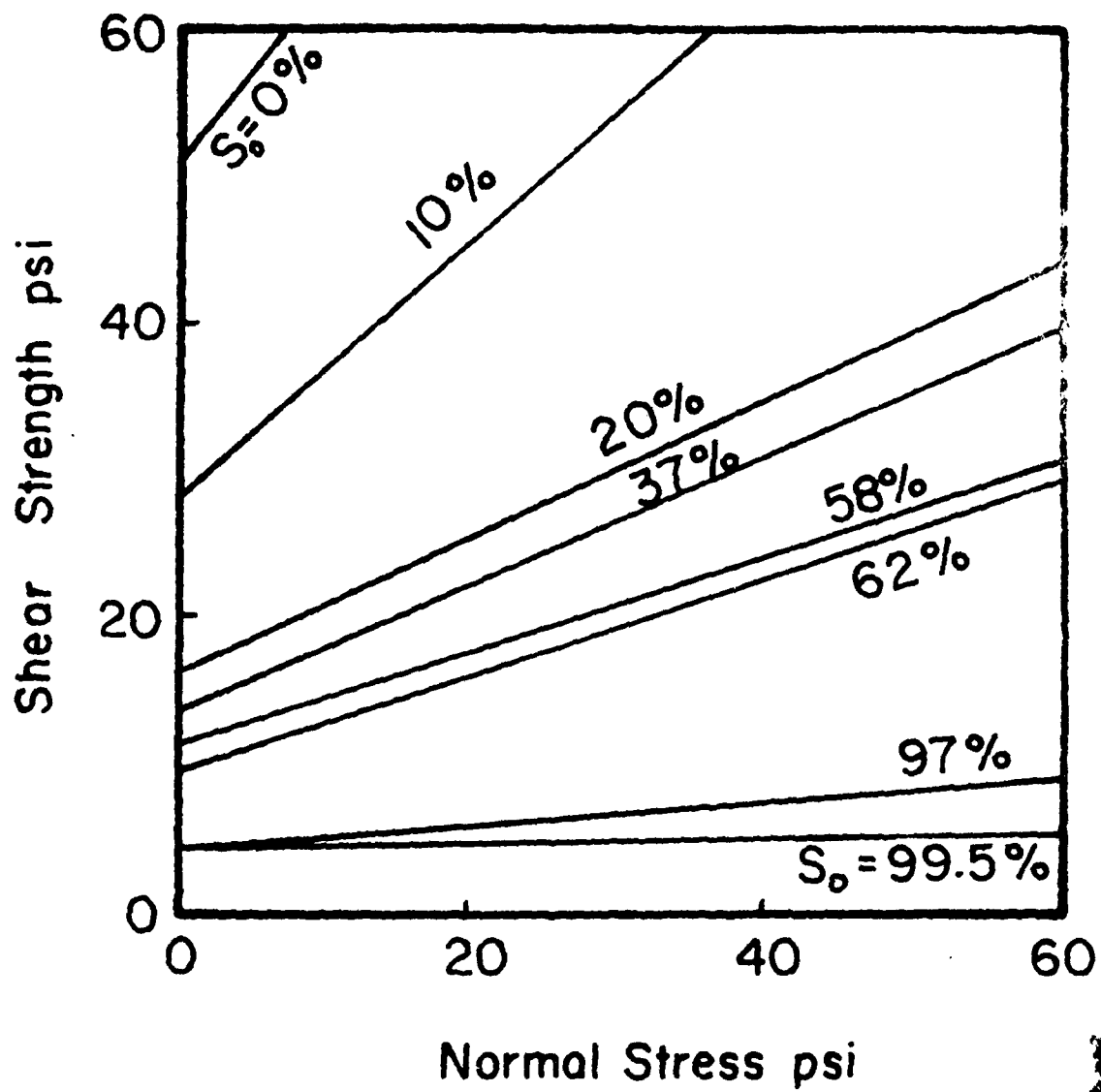


Figure 5. Linear yield envelopes for loess at various degrees of saturation S_o (After Lutton, 1974).

Table 3: Direct Tension Tests on Loess (After Lutton, 1974).

Sample Orientation	Tensile Strength (kPa)	Water Content (percent dry weight)	Degree of Saturation (percent)
v	28.3	10.3	30.9
v	23.4	11.3	33.9
v	55.8	11.1	33.3
v	36.5	7.7	23.1
v	16.5	13.8	41.4
v	14.5	13.4	40.2
v	22.1	9.4	28.2
v	27.6	11.5	34.5
v	24.1	10.6	31.8
H	22.1	8.9	26.7
v	21.4	25.2	76.0
v	40.0	25.8	77.0
v	16.5	24.5	74.0
v	17.2	24.1	72.0
v	80.7	1.0	3.0
v	64.8	1.7	5.0
v	54.5	1.6	5.0
H	19.3	23.7	71.0
v	82.7	4.3	13.0

1 psi = 6.895 kPa

Table 4: Laboratory Direct Shear Tests on Reworked Loess (After Bradford and Piest, 1980).

Soil Deposit	Soil Depth (m)	Sample Depth (m)	Cohesion (kPa)	Friction Angle degrees	Bulk Unit Weight (kNm ⁻²)
Turton	0.00-1.52	0.8-1.0	13.5	15	12.2
Mullenix	1.52-2.74	1.9-2.1	6.9	20	13.1
Hatcher	2.74-5.03	4.0-4.2	12.2	16	14.0
Watkins	5.03-	7.4-7.6	7.6	23	13.6
	1 foot = 0.3048m		1 gm/cm ² = 0.098 kPa		1 gm/cm ³ = 9.81 kNm ⁻³
			1 psi = 6.895 kPa		

Table 5: Vertical and Horizontal Shear Strength of Western Iowa Bluff-Line Loess (After Lohnes and Handy, 1968).

Location and test depth (m)	Cohesion (kPa)		Friction Angle (°)	
	Vertical	Horizontal	Vertical	Horizontal
Sioux City:				
Bluff St.	6.7	3.45	2.76	24.5
Perry St.	4.6	12.41	20.00	27.0
Dodge St.	5.2	11.03	8.27	19.6
Turin Pit	6.1	8.27	8.96	24.4
Loveland Sect.	10.1	20.69	17.93	24.3
Honey Creek	7.3	6.90	6.90	22.0
Average Values		10.34	11.03	23.6
Standard Deviation		4.83	6.21	2.3
(1 psi = 6.895 kPa)				

Lohnes and Handy (1968) used a relatively new instrument, the Iowa Borehole Shear Tester, to conduct in situ quick, drained, direct shear tests on the walls of boreholes drilled into the bank material. This test is unique as a field test in that it allows separate evaluation of the cohesion, c , and friction angle, ϕ , rather than simply measuring the in situ shear strength. Vertical and horizontal tests showed no significant difference in either ϕ or c , though the horizontal tests had more variability (Table 5.). The success of Lohnes and Handy's analysis in predicting limiting bank heights and angles using borehole shear data suggests that the instrument does provide reasonable strength measurements. Its ease of use and rapidity make the test an attractive alternative to laboratory testing.

3.1 GENERAL APPROACH

The general approach adopted in this study was to assemble stability charts to describe the critical bank height and slope angle of eroding streambanks with respect to mass failure, to collect the field data necessary to apply the bank stability charts, and then to test the accuracy of the predictions of critical bank height and angle using observed bank geometry data.

3.2 ANALYSIS OF BANK STABILITY

3.2.1 Introduction

Slope stability analyses can be used to assess the stability of a streambank with respect to mass failure under gravity. Many mechanisms of failure are possible depending on the size, geometry and structure (stratigraphy) of the bank and the strength properties of the bank material (Thorne, 1981). Eroding banks in the bluff line streams are usually between about 3 to 10 m (10 to 33 feet) high and stand at angles between about 50° and 90°. In engineering terms, they are low, steep slopes. It would be expected that the dominant mode of failure for such banks would be slab failure (Terzaghi, 1943; Terzaghi and Peck, 1948; Carson, 1971; Carson and Kirkby, 1972). In this type of failure a tension crack develops vertically downwards from the ground surface behind the bank. Failure occurs by shearing along a slip surface between the toe and the bottom of the tension crack.

3.2.2 Field Observations

Observations of bank erosion and failure in the bluff line streams made by the Channel Stability Research Unit of the Sedimentation Laboratory over several years, and by the authors in a preliminary field survey in the fall of 1979, confirmed that slab failure is the dominant failure mechanism (Fig. 6. and 7.). Unstable banks show deep tension cracking prior to shear failure. Tension cracks develop from the ground surface down, almost parallel to the bank line. Often they seem to begin during a dry period that produces shrinking and cracking in the soil. They further develop mostly during wet periods, owing to the increased weight of the soil, which tends to pull the crack open. The passage of water down the tension crack



Figure 6. Imminent Slab Failure observed on Goodwin Creek at Katherine Leigh site, Panola County.



Figure 7. Slab failure on Goodwin Creek, Panola County.

D.33

widens it. In times of extremely heavy precipitation and surface flow, cracks can fill with water. The resulting hydrostatic pressure produces a horizontal force which is very effective in further wedging the crack open.

Shear failure slip surfaces are slightly curved. The degree of curvature of the slip surface, and the width of the failing block, together control whether blocks topple forwards into the channel, slide outward and downwards, or rotate with back tilting of the upper surface. Depending on the strength, fabric, and internal stress distribution of the failing block, it either remains more or less intact or disintegrates into a soil fall or flow during failure (Fig. 8.).

Fluvial erosion of intact in situ material from the bank surface does not seem to contribute significantly to bank retreat. Support for this statement comes from Bradford and Piest (1980) who noted that under similar circumstances, "Little soil is eroded from the standing banks by tractive forces of the flowing water". This is the case because of the high degree of channel incision which results in an extremely low frequency of bankfull flow, so that the flow rarely if ever attacks anything above the bank toe.

Fluvial erosion does play a very important role in controlling bank stability and retreat rate however, by determining the state of 'basal endpoint control' (Thorne, 1981 and Section 5.3.4). The flow is responsible for eroding failed material from the basal area resulting in steeper banks. Without basal scour and toe erosion, mass failures lead to bank slope reductions and stabilization within a few years (Lohnes and Handy, 1968; Brunsden and Kesel, 1974; Thorne, 1981).

3.2.3 Theory

The analysis of slope stability may be undertaken in a number of ways to produce a dimensionless stability equation of the general form:

$$\frac{\gamma H_c}{c} = N_s = \text{function } (\phi, i) \quad (1)$$

H_c = critical bank height
 γ = bulk unit weight
c = cohesion

ϕ = friction angle
i = slope angle
 N_s = dimensionless stability number

The nature of the functional relationship depends on assumptions made regarding the shape of the failure surface and the method of analysis applied to obtain a solution (Chen, 1975). For example, the Culmann Method, based on a plane shear failure through the toe, produces:



Figure 8. Slab failure with a) more or less intact failure block, b) disintegration of failure block into a soil fall and c) disintegration of failure block into a soil flow.

$$\frac{\gamma H_c}{c} = N_s = \frac{4 \sin i \cos \phi}{(1 - \cos(i - \phi))} \quad (2)$$

This analysis was used by Lohnes and Handy (1968) and Bradford and Piest (1980). For a vertical bank ($i = 90^\circ$), equation (2) reduces to:

$$N_s = \frac{\gamma H_{cr}}{c} = 4 \tan(45 + \frac{\phi}{2}) \quad (3)$$

H_{cr} = critical height of a vertical bank

If a curved (log spiral) failure surface is used instead of a planar one, a slightly lower value of N_s is produced (Fellenius, 1939),

$$N_s = \frac{\gamma H_{cr}}{c} = 3.83 \tan(45 + \frac{\phi}{2}) \quad (4)$$

The lower value of N_s indicates lower stability and shows that a log-spiral failure surface is more critical than a plane surface. Consequently the plane slip analysis tends to overestimate slope stability. The error is not serious for vertical banks, but increases rapidly with decreasing slope angle (Taylor, 1948).

Chen (1975) used a log-spiral toe failure in a limit-analysis approach to slope stability to produce dimensionless stability charts and tables (Fig. 9 and Table 6). This approach produces more reliable solutions than limit-equilibrium analyses because it satisfies equilibrium and does not violate the yield criterion at any point in the bank. By contrast, in limit-equilibrium methods like the Culmann Analysis, the condition of equilibrium is satisfied for the assumed failure surface, but it is not known whether the yield criterion has been violated elsewhere.

In practice, it is found that the results obtained from the limit-analysis are practically identical to those obtained from limit-equilibrium methods like the ϕ -circle method (Taylor, 1948) and the Method of Slices (Fellenius, 1939). Chen's charts may be used to assess bank stability with respect to log-spiral toe failure. The possibility of base failure along a surface passing below the toe is not considered, but this is not a major problem as base failures are associated with instability in banks of lower slope angles than those encountered in this study (Taylor, 1948; Chen, 1975).

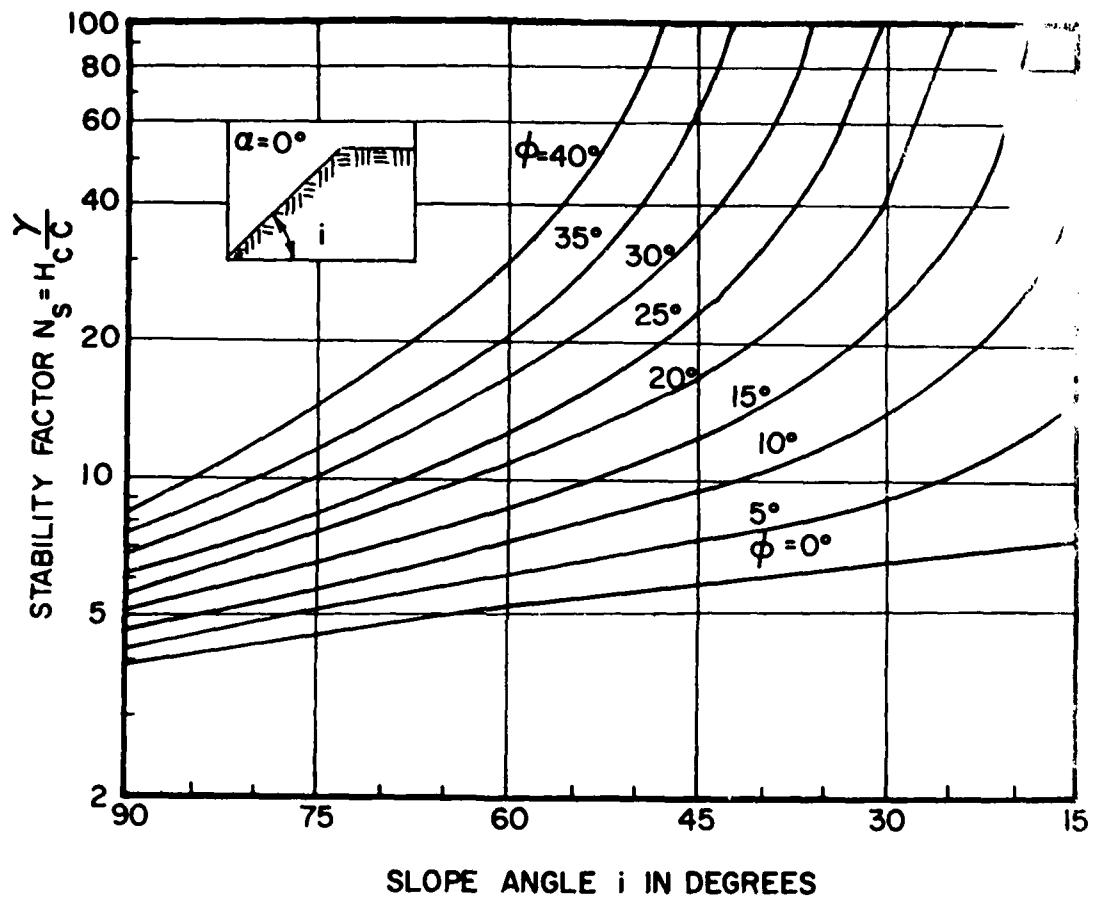


Figure 9. Stability Number, N_s , as a function of slope angle, i , for a log-spiral failure surface passing through the toe (After Chen, 1975).

Table 6: Stability factor $N_s = H_c(\gamma/c)$ by limit analysis (logspiral passing through the toe, Fig. 9.).

Friction angle ϕ (°)	Back slope angle α (°)	Slope angle i (°)					
		90	75	60	45	30	15
0	0	3.83	4.57	5.25	5.86	6.51	7.35
5	0	4.19	5.14	6.17	7.33	9.17	14.80
	5	4.14	5.05	6.03	7.18	8.93	14.62
10	0	4.59	5.80	7.26	9.32	13.53	45.53
	5	4.53	5.72	7.14	9.14	13.26	45.15
	10	4.47	5.61	6.98	8.93	12.97	44.56
15	0	5.02	6.57	8.64	12.05	21.71	
	5	4.97	6.49	8.52	11.91	21.50	
	10	4.90	6.39	8.38	11.73	21.14	
	15	4.83	6.28	8.18	11.42	20.59	
20	0	5.51	7.48	10.39	16.18	41.27	
	5	5.46	7.40	10.30	16.04	41.06	
	10	5.40	7.31	10.15	15.87	40.73	
	15	5.33	7.20	9.98	15.59	40.16	
	20	5.24	7.04	9.78	15.17	39.19	
25	0	6.06	8.59	12.75	22.92	120.0	
	5	6.01	8.52	12.65	22.78	119.8	
	10	5.96	8.41	12.54	22.60	119.5	
	15	5.89	8.30	12.40	22.37	118.7	
	20	5.81	8.16	12.17	21.98	117.4	
	25	5.71	7.97	11.80	21.35	115.5	
30	0	6.69	9.96	16.11	35.63		
	5	6.63	9.87	16.00	35.44		
	10	6.58	9.79	15.87	35.25		
	15	6.53	9.67	15.69	34.99		
	20	6.44	9.54	15.48	34.64		
	25	6.34	9.37	15.21	34.12		
	30	6.22	9.15	14.81	33.08		
35	0	7.43	11.68	20.94	65.53		
	5	7.38	11.60	20.84	65.39		
	10	7.32	11.51	20.71	65.22		
	15	7.26	11.41	20.55	65.03		
	20	7.18	11.28	20.36	64.74		
	25	7.11	11.12	20.07	64.18		
	30	6.99	10.93	19.73	63.00		
	35	6.84	10.66	19.21	60.80		

Table 6, Cont'd.

Friction angle ϕ ($^{\circ}$)	Slope angle α ($^{\circ}$)	Back slope angle i ($^{\circ}$)				
		90	75	60	45	30
40	0	8.30	14.00	28.99	185.6	
	5	8.26	13.94	28.84	185.5	
	10	8.21	13.85	28.69	185.3	
	15	8.15	13.72	28.54	185.0	
	20	8.06	13.57	28.39	184.6	
	25	7.98	13.42	28.16	184.0	
	30	7.87	13.21	27.88	183.2	
	35	7.76	12.95	27.49	182.3	
	40	7.61	12.63	26.91	181.1	

A problem arises in that the analysis does not take into account the possibility for tension cracking behind steep slopes. It was noted in the field survey that deep tension cracks often develop from the ground surface behind the bank prior to shear failure. Tension cracks occur because of tensile stress in this region (Terzaghi, 1943). The depth to which there can be tensile stress in a soil can be predicted from the Mohr diagram (Sowers and Sowers, 1965) and is given by,

$$Z_o = \frac{2c}{\gamma} \tan \left(45 + \frac{\phi}{2} \right) \quad (5)$$

Z_o = depth of tensile stress

The critical height of a bank will be reduced if a tension crack is present. This may be taken into account by modifying the basic stability equation to produce:

$$\frac{\gamma (H'_c + y)}{c} = N_s \approx \text{function } (\phi, i) \quad (6)$$

y = depth of tension cracking

H'_c = critical height of a slope with a tension crack.

Thus, the Culmann Method now produces:

$$\frac{\gamma (H'_c + y)}{c} = N_s = \frac{4 \sin i \cos \phi}{1 - (\cos i - \phi)} \quad (7)$$

which is the equation for slab failure used by Lohnes and Handy (1968). For a vertical bank:

$$H'_{cr} = \frac{4c}{\gamma} \tan \left(45 + \frac{\phi}{2} \right) - y \quad (8)$$

H'_{cr} = critical height of a vertical bank with a tension crack.

If the tensile strength of the soil is zero, the crack will extend to the full depth of tensile stress so that, $Z_o = y$ and equations (5) and (8) may be combined to produce:

$$H'_{cr} = \frac{2c}{\gamma} \tan (45 + \frac{\phi}{2}) \quad (9)$$

and hence, $H'_{cr} = H_{cr}/2$

There is much empirical evidence to support the implication that the maximum depth of tension cracking of a vertical cut is about half the bank height (Terzaghi, 1943).

If the tensile strength of the soil is not zero, the extent of tension cracking may be limited to depths less than Z_o . Lohnes and Handy (1968) presented equations to estimate the depth of tension cracking in a soil of finite tensile strength:

$$y = Z_o \left(1 - \frac{\sigma_{tc}}{\sigma_t}\right) \quad (10)$$

σ_{tc} = tensile strength

σ_t = tensile stress at ground surface, given by:

$$\sigma_t = 2c \tan (45 - \frac{\phi}{2}) \quad (11)$$

and, for vertical banks with a back slope, the width of the failing slab:

$$b = \frac{H-y}{\tan (45+\frac{\phi}{2})-\tan \alpha} \quad (12)$$

α = backslope angle

These equations are only approximate since the stress distribution will be altered as soon as a crack begins to develop. Lohnes and Handy did not apply equations (10) and (11) but instead made the assumption that the tensile strength is zero. This assumption, also made by Bradford and Piest (1980), is a general one and results in an error on the safe side in soils of finite tensile strength. This is quite permissible when designing embankments or cuts but, it results in estimates of critical bank height which tend to be conservative.

Direct measurements of tension strength by the author (Thorne, 1978; Thorne, Tovey and Bryant, 1980) and reported in the literature (Bishop and Garga, 1969; Ajaz and Parry, 1974; Lutton, 1974) show that soils tend to have an unconfined tensile strength of between 5 and 15 percent of their

unconfined compression strength. This would suggest that the accuracy of calculations of critical height and angle using equation (6) could be improved if, given an independent estimate of the tensile strength of the soil, equation (10) was used to predict the crack depth, after equations (5) and (11) had been used to calculate the depth of tensile stress and tensile stress at the ground surface, respectively.

To test this hypothesis, data are required on the cohesion, friction angle, tensile strength and bulk unit weight of the soil, and the heights and bank angles found in the field.

3.3 DATA COLLECTION

3.3.1 Introduction

The data required were collected from three field sites on two bluff line streams in Northwest Mississippi. Two sites are on Johnson Creek and one on Goodwin Creek. The field sites, soil units, and experimental procedure are described in section 3.3.2 and in Addendum 1. The techniques of soil strength and weight measurement are described in section 3.3.3.

3.3.2 Field Sites and Procedure

The first site was on lower Johnson Creek on property owned by Mr. Tommy Florence in Section 3, T.10S., R.7W. Seven test holes were drilled on this property and sixteen horizons of soil were subjected to Borehole Shear Tests. The second site was on upper Johnson Creek on property owned by Mr. T. A. Woodruff in Section 20, T.9S, R.6W. Twelve test holes were drilled on this property and nineteen horizons were subjected to Borehole Shear Tests. The third site was on lower Goodwin Creek on property owned by Ms. Katherine Leigh in Section 2, T.10S., R.7W. Seven test holes were drilled on this property and eleven horizons of soil were subjected to Borehole Shear Tests. More data on these site locations and test depths may be found in Addendum 1.

All three sites are located in valleys of streams tributary to Peters Creek, a tributary to the Yocona River, which exits the bluff line about four miles west of its confluence with Peters Creek. The valleys of both streams are filled with alluvial material washed from the tops and sides of the adjacent loess-covered hills.

The soils exposed on the surface in the valleys are primarily Collins & Falaya silt loams and are described in the SCS's Soil Survey, Panola Co.,

MS, Series 1960, No. 10 (Dent, et al., 1963). Following is a general summation of the properties of the soil association from that report.

"The Collins-Falaya-Grenada-Calloway soil association consists of somewhat poorly drained and moderately well drained, silty soils in alluvium on nearly level flood plains and benches, or in thick loess on nearly level to moderately sloping uplands.

This soil association is in large areas along the Little Tallahatchie and Yocona Rivers and is in small areas along small streams in the northern part of the county. In most places the association is surrounded by the Loring-Grenada-Memphis association. The Collins and Falaya soils are on flood plains and benches in alluvium from soils formed in loess. The Grenada and Calloway soils are in thick, loessial deposits on uplands.

The Collins soils make up more than half of this soil association. These nearly level, moderately well drained soils have a dark-brown silt loam surface layer and upper subsoil. Their lower subsoil is mottled, brown and gray silt loam. The Falaya soils are nearly level and somewhat poorly drained. Their surface layer is dark-brown silt loam or silty clay loam, and their subsoil is mottled, gray and brown silt loam to silty clay loam. The Grenada soils are nearly level to moderately sloping and moderately well drained. The surface layer of Grenada soils is brown or dark-brown silt loam, and the subsoil is brown or dark-brown heavy silt loam. A fragipan occurs at a depth of about 24 inches. The Calloway soils are nearly level to gently sloping and somewhat poorly drained. They have a dark grayish-brown silt loam surface layer, a yellowish-brown heavy silt loam subsoil, and a fragipan at a depth of about 16 inches.

This soil association covers about 23 percent of the land in the county. The Collins soils occupy about 54 percent of the association, the Falaya about 35 percent, the Grenada about 3 percent, and the Calloway about 5 percent. Henry soils, Waverly soils, and Mixed alluvial land occupy the remaining 3 percent.

Most of this soil association has been cleared and is in cotton, corn, or pasture. The association includes some of the best agricultural land in the county."

The soils described above are primarily developed on post settlement alluvium and are only the surface veneer in the valleys. Of considerably more age and importance are the underlying paleosols which control bank failure mechanisms. Determination of bank material strengths and weaknesses is the main target of this study.

Field procedure involved the boring of 3 inch diameter test holes with a small hydraulic drill rig and various types of sampling tools suited to the particular strata, extracting the sampled material in as undisturbed a state as possible, reaming the hole to a smooth uniform diameter and performing the downhole *in situ* shear tests with the Iowa Borehole Shear Tester are described in Addendum 2. Samples taken from the holes, were returned to the laboratory where they were tested for unconfined compression and unconfined tension strength as described in Addendum 4.

The field sites, equipment, procedures and results are described in more detail in Addendum 1.

3.3.3 Soil Strength Parameters

Cohesion and friction angle of the various soil units were determined from data obtained by *in situ* measurements using an Iowa Borehole Shear Tester. Conventionally these data are obtained from laboratory triaxial compression tests on core samples (Bishop and Henkel, 1957). This requires specialized laboratory equipment and technical back-up which were not available at Oxford, and thus precluded extensive triaxial testing. It was noted in the literature survey (section 2.2) that the borehole shear test (BST) seemed to give measurements of c and ϕ which could be used with success in analyzing slope stability (Lohnes and Handy, 1968). Also, BST data seem to be similar to those produced by triaxial and direct shear tests, but are obtained in about a tenth of the time necessary for the laboratory tests (Handy and Fox, 1967). Since a borehole shear tester could be obtained fairly easily, it was used to measure c and ϕ . The instrument was loaned to the Sedimentation Laboratory at Oxford by the SCS National Soil Survey Laboratory in Lincoln, Nebraska.

The instrument, its use, and its limitations are discussed in detail in Addendum 2. The interested reader is referred to that addendum and the references listed there. Therefore, only a brief outline of the testing apparatus and procedure is included here.

The borehole shear test (BST) is essentially a simple direct shear test performed on the walls of a borehole. The apparatus consists of an expanding head and shear plates, a pulling device and a gas control console. The head is slightly less than 76 mm (3 inches) in diameter when contracted, so that it slides into a 76 mm (3 inches) borehole. The borehole is reamed and smoothed using a reamer supplied with the apparatus and the head is lowered to the required depth using connecting rods. It is then coupled to the pulling device. Pressure lines are connected to a gas cylinder through the control console and the head expanded using a known pressure, so that the shear plates are forced against the walls of the borehole. After ten minutes consolidation time the head is pulled axially up the borehole using the pulling device. The axial load is measured hydraulically. The head is pulled up the hole until the soil next to the plates shears. The peak axial load is recorded. When divided by the area of the shear plates, the expanding and axial forces are converted to normal stress (σ) and the shear strength (s). Pairs of σ and s values plot on a σ - s graph as points on the Mohr-Coulomb rupture line.

The test may be run as a stage test or a nonstage test. After a test in which the peak axial load has been exceeded, the axial load is removed, without contracting the shear plates, until the axial load is zero. Then the normal stress (shear plate pressure) is increased by an arbitrary increment and the soil is sheared again. This test is repeated as many times as desired with the shear plates in the same vertical position until sufficient points are generated to define the Mohr-Coulomb line. This constitutes a stage test. In a nonstage test the head is contracted, removed, and cleaned after each shear test. It is then returned to the same soil stratum but in a slightly different location, for the next pressure increment.

In this study, tests were performed on vertical holes which were bored using a Giddings drill rig mounted on a trailer. No horizontal or inclined holes were drilled because results in the literature (Table 5) suggested that there would be no significant strength anisotropy in soils of the type encountered (Turnbull, 1948; Lohnes and Handy, 1968; Lutton, 1969, 1974; Bradford and Piest, 1977, 1980). BSTs were carried out on the soil units identified from the borehole logs. The data are listed and discussed in Section 4.1.

Unconfined compression and unconfined tension tests were performed on intact core samples from the boreholes. Samples were obtained using thin walled sampling tubes of 76 mm (3 inches) and 51 mm (2 inches) diameters that produced cores of about 68 mm (2.7 inches) and about 41 mm (1.6 inches) in diameter, respectively. These tests and the testing apparatus are described in detail in Addendum 4.

In some cases it was possible to run unconfined compression and tension tests on cores from the same depth as BST testing. This provided a check on the validity of the BST since in theory the Mohr-Coulomb rupture line should be a tangent to the Mohr failure circle produced by plotting a circle of radius, $\sigma_{cc}/2$ (σ_{cc} is the unconfined compression strength) centered at coordinates $(\sigma_{cc}/2, 0)$ on the σ - s graph (Terzaghi and Peck, 1948; Bishop and Henkel, 1957).

If the Mohr-Coulomb line is approximately straight, then its extrapolation left of the ordinate into the tension quadrant should produce a line which is tangential to the Mohr failure circle for the unconfined tension test. This is of radius of $\sigma_{tc}/2$, centered at coordinates $(\sigma_{tc}/2, 0)$. Data from tests on alluvial soils in Britain suggest that the Mohr-Coulomb line cannot be extrapolated in this way (Thorne, 1978). The test data collected here can be used to confirm or disprove this suggestion.

The data are listed and discussed in Section 4.2.

Bulk unit weight and moisture content of the soil units were calculated from the weights of soil samples used in the unconfined compression and tension tests. Soil cores were weighed prior to testing to determine the field unit weight. Samples were weighed before and after oven drying at 105° C to determine the moisture content. Additional laboratory tests on Atterburg limits, particle size distribution, specific gravity of solids, voids ratio and chemical composition are planned but have not yet been completed.

4.1 BOREHOLE SHEAR TESTS (BST)

Initially borehole shear tests were performed according to the stage testing procedure recommended in the BST instruction manual and outlined in Addendum 2. The shear plates supplied with the tester were of the original multi-tooth design (Figure 2.7, Addendum 2).

Preliminary tests were run, on the bank of Davidson Creek on the Sedimentation Laboratory grounds, to test the procedure. The data were very encouraging, producing reasonable values for c and ϕ and remarkably high regression coefficients (Results Tables 3.1 and 3.2, Addendum 3).

Stage tests at T.A. Woodruff's and Tommy Florence's fields on Johnson Creek and Katherine Leigh's field on Goodwin Creek produced results of remarkable linearity (Results Tables 3.3 to 3.22, Addendum 3) but by mid-June it was becoming apparent that the data were not consistent with the unconfined compression tests. Values for cohesion were consistently low or even negative, and values for the friction angle were rather high for soils of the type being tested. There were exceptions: for example, some of the data for the soft soils (Results Table 3.22, Addendum 3) did not seem unreasonable. However, curving of the failure line was apparent in many cases (Results Tables 3.9, 3.13, 3.16, 3.19, Addendum 3) and the authors were not happy with the data.

The problem was probably associated with incomplete seating of the shear plates and progressive filling of shear teeth with increasing pressure in the stage tests, producing an artificially high friction angle. After consultations with Prof. R.L. Handy of Iowa State University (inventor of the BST device) and Dr. Mausbach of the NSS Lab, Lincoln, Nebraska, new high pressure shear plates of a different design (Figure 2.7) were used in place of the original plates and stage testing was abandoned (as suggested by Luttenegger, Remmes and Handy (1978)). The new plates and nonstage tests produced much better correlation between the results of BST and unconfined compression tests and values of c and ϕ which seemed much more reasonable. Complete records of the BST tests using the new shear plates are listed in Results Tables 3.23-46, Addendum 3.

The summarized BST data are listed here in the main text in Table 7 with mean values listed in Table 8.

4.2. UNCONFINED COMPRESSION AND TENSION TESTS

Eighty-four unconfined compression and tension tests were carried out on intact soil cores from the three field sites, as outlined in Addendum 4. The test records (stress/strain data, and peak strength) may be obtained from the data files of the U.S.D.A. Sedimentation Laboratory, Oxford, Mississippi, or from the Vicksburg District Office, U.S. Army Corps of Engineers, Vicksburg, Mississippi. The results are summarized and listed here in the main text in Table 9. Mean values, by soil type and site, are listed in Table 10.

In addition, four triaxial tests were run on samples of old paleosol from T.A. Woodruff's field on Johnson Creek. These tests were run to check if the estimates for cohesion and friction angle produced by more conventional tests were comparable to those produced by the bore hole shear test. The results of the triaxial test are presented in Figure 10.

Values calculated for the bulk unit weight are listed in column 7 of Table 9 and column 6 of Table 10. Column 8 in Table 9 contains values for the ratio (r) of the unconfined tension to the unconfined compression strength.

4.3 DISCUSSION OF FIELD DATA

4.3.1 Cohesion and Friction Angle

The values of cohesion and friction angle produced from the BST tests with the high pressure plates are very reasonable compared with data presented in the literature survey (Tables 4 and 5) for somewhat similar soils in Iowa. Mean friction angles are very similar, but generally the Mississippi soils are more cohesive. This may well be a real difference in the soils, or it may be due to the fact that the tests in Mississippi were performed in summer when the soils were rather dry. Possibly the degree of cohesion would be similar to that in Iowa if further data for wet conditions were included.

The single set of triaxial test data (Fig. 10) are quite consistent with BST data for the Old Paleosol in general but the equivalent BST test

Table 7: Borehole Shear Tests.

Test Number	Location Creek/Site	Borehole No. and Depth (m)	Angle of Friction (°)	Cohesion (kPa)	Moisture Content (%dw)
<u>Post Settlement Alluvium</u>					
28 (43a)	J/TF	2/0.8	12	24.0	11.6
29 (55)	J/TF	4/0.6	23	64.2	14.3
38 (57)	J/TF	4/1.1	22	32.3	18.5
26 (39)	J/TAW	11/0.7	29	31.0	-
42 (71)	G/KL	5/0.8	21	20.8	23.0
44 (79)	G/KL	6/0.9	21	41.4	-
<u>Young Paleosol</u>					
39 (4, 22)	J/TF	5/1.9	24	55.2	18.5
40 (4, 22)	J/TF	5/1.4	26	68.6	19.0
24 (8)	J/TAW	9/1.5	20	71.2	-
23 (33b)	J/TAW	6a/2.1	16	21.3	-
45 (73)	G/KL	6/1.5	15	63.5	-
46 (75)	G/KL	6/2.4	25	16.5	-

Test number in parentheses indicates equivalent unconfined compression test.

Creeks: J = Johnson Creek, G = Goodwin Creek

Sites: TF = Tommy Florence's; TAW = T.A. Woodruff's; KL = Katherine Leigh's

1 kiloPascal \approx 0.145 psi \approx 47.88 psf, 1 meter \approx 3.28 feet

Table 7: Borehole Shear Tests (Continued).

<u>Old Paleosol</u>						
27 (41)	J/TF	2/3.1	27	44.0	-	
30 (59, 61)	J/TF	4/2.7	26	54.5	21.2	
31 (51)	J/TF	3/2.4	21	98.5	23.4	
32 (47, 49, 51)	J/TF	3/2.0	25	52.0	23.9	
33 (41)	J/TF	2/3.0	28	34.5	22.6	
34* (45)	J/TF	2/1.6	40	3.9	20.2	
35 (46, 49)	J/TF	3/1.8	27	15.2	21.4	
36 (436, 67)	J/TF	2/4.4	27	73.0	17.7	
37 (61)	J/TF	4/3.3	19	106.0	23.1	
41 (59, 63)	J/TF	5/3.7	14	118.3	-	
25 (36)	J/TAW	10/3.3	11	20.1	-	
43 (67)	G/KL	5/3.7	8	104.5	19.7	
<u>Fine Sand/Silt</u>						
34 (45)	J/TF	2/1.6	40	3.9	20.2	

* Listed as old paleosol (according to borehole log) but believed to be a small sand lens.

Table 8: Borehole Shear Tests: Mean Values.

Soil and Site	Number of Tests	Angle of Friction ($^{\circ}$)	Cohesion (kPa)	Moisture Content (%dw)
PSA				
TF	3	19	40.2	14.8
TAW	1	29	31.0	-
KL	2	21	31.1	23.0
OVERALL MEANS				
MEANS	6	21	35.6	16.9
YOUNG PALEOSOL				
TF	2	25	61.9	18.8
TAW	2	18	46.3	-
KL	2	20	40.0	-
OVERALL MEANS				
MEANS	6	21	49.4	18.8
OLD PALEOSOL				
TF	9	24*	60.2*	21.9
TAW	1	11	20.1	-
KL	1	8	104.5	19.7
OVERALL MEANS				
MEANS	11	21	65.5	21.5
FINE SAND/SILT				
TF	1	40	3.9	20.2

* Omitting ϕ for test 34.

Table 9: Unconfined Compression and Tension Tests.

Test Number	Location Creek/Site	Borehole No. /Depth (m)	Compressive Strength (kPa)	Tensile Strength (kPa)	Moisture Content (%dw)	Bulk Unit Weight (kNm^{-3})	� (%)
POST SETTLEMENT ALLUVIUM							
1	J/TF	1/0.6	96.8	-	18.9	-	
2	J/TF	1/1.1	71.4	-	27.6	-	
3	J/TF	1/1.3	65.1	-	-	-	
43a	J/TF	2/0.8	52.6	-	20.4	-	
53	J/TF	4/0.4	28.8	-	20.3	18.0	11.0
54	J/TF	4/0.3	-	3.2	18.0	-	
55	J/TF	4/0.6	66.6	-	21.2	17.8	3.0
56	J/TF	4/0.6	-	2.0	21.2	17.8	
57	J/TF	4/1.0	109.0	-	18.7	25.5	10.7
58	J/TF	4/1.0	-	11.7	24.8	-	
6	J/TAW	2/0.3	61.1	-	16.9	-	
32	J/TAW	6a/1.2	58.5	-	23.7	-	14.6
33a	J/TAW	6a/0.9	-	8.5	22.9	-	
39a	J/TAW	11/0.7	80.5	-	20.2	-	
65	G/KL	5/0.6	238.7	-	5.0	15.8	3.0
66	G/KL	5/0.6	-	7.2	4.1	-	
69	G/KL	6/0.6	237.9	-	3.8	15.2	1.4
70	G/KL	6/0.6	-	3.4	4.8	-	
71	G/KL	6/0.9	37.4	-	7.2	15.4	21.7
72	G/KL	6/0.9	-	2.4	8.1	-	
79	G/KL	7/0.5	71.0	-	-	-	4.6
80	G/KL	7/0.5	-	3.3	-	-	

Table 9: Unconfined Compression and Tension Tests (Continued).

YOUNG PALEOSOL						
7	J/TAW	2/0.8	39.8	-	24.3	-
8	J/TAW	2/1.7	61.4	-	19.5	16.5
22	J/TAW	7a/0.3	167.5	-	18.4	20.3
23	J/TAW	7a/0.6	76.9	-	23.5	18.7
33b	J/TAW	6a/1.8	37.0	-	28.8	- } 8.5
34	J/TAW	6a/1.8	-	3.1	28.4	-
35	J/TAW	6a/3.5	97.6	-	17.5	-
39b	J/TAW	11/2.5	43.0	-	24.6	18.2 } 16.3
40	J/TAW	11/2.6	-	7.0	24.6	18.2
<hr/>						
4	G/KL	1/1.2	92.6	-	18.3	-
5	G/KL	1/2.3	86.5	-	19.2	-
73	G/KL	6/1.5	87.2	-	5.0	- } 12.7
74	G/KL	6/1.5	-	11.1	4.0	-
75	G/KL	6/2.4	73.8	-	14.1	16.9 } 12.2
76	G/KL	6/2.4	-	9.0	-	-
<hr/>						
OLD PALEOSOL						
41	J/TF	2/3.1	140.4	-	23.2	19.2 } 6.5
42	J/TF	2/3.4	-	9.1	17.0	-
45*	J/TF	2/2.0	119.5	-	43.2	19.6
46	J/TF	3/1.6	75.0	-	22.0	17.6 (with test 48) 10.0
47	J/TF	3/1.9	84.1	-	-	15.5 } 8.9
48	J/TF	3/1.9	-	7.5	23.7	-
49	J/TF	3/2.2	71.3	-	-	19.2 } 18.1
50	J/TF	3/2.2	-	12.9	22.4	-
51	J/TF	3/2.5	116.8	-	-	19.2 } 6.9
52	J/TF	3/2.5	-	8.1	22.7	-
59	J/TF	4/3.7	229.4	-	20.9	20.6 } 11.7
60	J/TF	4/3.7	-	26.9	11.9	- } 14.3
61	J/TF	4/3.7	188.7	-	18.2	21.0 } 22.8
62	J/TF	4/3.7	-	43.0	19.3	- (with test 59) 18.7

* Listed as old paleosol (according to borehole log) but believed to be a small sand lens.

Table 9: Unconfined Compression and Tension Tests (Continued).

<u>OLD PALEOSOL, (Continued)</u>							
63	J/TF	5/3.8	203.6	-	20.9	20.2	11.4
64	J/TF	5/3.8	-	23.2	-	-	(with test 59) 10.1
9	J/TAW	2/1.8	134.3	-	20.7	19.6	
10	J/TAW	2/2.9	165.2	-	17.0	19.9	
11	J/TAW	2/3.0	232.7	-	20.3	-	12.9
12	J/TAW	2/3.1	-	30.1	20.3	20.9	14.1
13	J/TAW	2/3.1	213.3	-	20.0	21.0	
14	J/TAW	2/3.2	217.9	-	20.2	20.9	(with test 12) 13.8
15	J/TAW	4/2.4	268.9	-	17.0	20.4	9.6
16	J/TAW	4/2.6	-	25.9	17.0	-	12.0
17	J/TAW	5/2.7	215.1	-	17.6	19.8	12.5
18a	J/TAW	5/2.9	-	26.8	15.3	-	(with test 15) 10.0
18b	J/TAW	5/3.1	-	65.1	13.8	20.0	
19	J/TAW	5/4.0	82.7	-	23.2	20.3	21.5
20	J/TAW	5/3.7	-	17.8	20.6	-	
21	J/TAW	5/4.3	59.9	-	20.8	20.5	
24	J/TAW	7a/1.1	167.0	-	21.4	19.6	20.9
25	J/TAW	7a/1.1	-	34.9	21.0	-	
26	J/TAW	7a/3.1	132.0	-	16.9	20.4	12.7
27	J/TAW	7a/3.1	-	16.7	17.6	-	
28	J/TAW	7a/1.5	180.9	-	19.2	20.0	(with test 25) 19.3
29	J/TAW	7/3.5	112.3	-	21.3	20.3	(with test 27) 14.9
30	J/TAW	7/3.5	-	58.4	19.4	-	52.0
31	J/TAW	7a/3.5	124.9	-	22.2	21.2	(with test 20) 14.3
36	J/TAW	6a/3.7	107.1	-	20.0	-	(with test 20) 16.6
37	J/TAW	6a/4.0	132.6	-	20.0	-	13.4
38	J/TAW	6a/4.0	-	17.8	18.3	-	

Table 9: Unconfined Compression and Tension Tests (Continued).

<u>FINE SAND/SILT</u>							
43b	J/TF	2/4.7	127.8	-	-	22.7	2.1
44	J/TF	2/4.7	-	2.7	-	-	
45*	J/TF	2/2.0	119.5	-	43.2	19.6	
67	G/KL	5/4.0	124.4	-	29.6	-	3.0
68	G/KL	5/4.0	-	3.7	-	-	
77	G/KL	6/5.5	129.0	-	18.6	21.6	
78	G/KL	6/5.5	256.6	-	16.5	20.5	

Table 10: Unconfined Compression and Tension Tests: Mean Values.

Soil and Site	Total Number of Tests	Compressive Strength (kPa)	Tensile Strength (kPa)	Moisture Content (% dw)	Bulk Unit Weight (kNm ⁻³)	r (%)
PSA						
TF	10	70.0	5.6	21.2	20.4	8.2
TAW	5	69.5	8.5	20.7	-	14.6
KL	8	146.3	4.1	5.5	15.5	7.7
OVERALL						
MEANS	23	90.2	5.2	16.4	18.0	8.8
YP						
TAW	9	74.7	5.1	23.3	18.4	12.4
KL	6	85.0	10.1	12.1	16.9	12.5
OVERALL						
MEANS	15	78.5	7.6	19.3	18.1	12.4
OP						
TF	16	138.7	15.7	20.2	19.1	12.6
TAW	25	159.2	32.6	19.2	20.3	16.9
OVERALL						
MEANS	41	146.3	25.2	19.5	19.9	15.2
FINE SAND/SILT						
TF	2	123.7	2.7	-	21.1	2.1
KL	4	170.0	3.7	21.6	21.1	3.0
OVERALL						
MEANS		151.5	3.2	21.6	21.1	2.6
CHANNEL FILL						
TAW		86.6	9.8	22.5	-	12.1

Johnson Creek at T. A. Woodruff's
Old Paleosol

Borehole 10

3.12m to 4.04m

Triaxial Tests [Consolidated Undrained, Partly Saturated]

Test No.	σ_1 kPa	σ_3 kPa
1	223.7	41.4
2	298.5	82.7
3	115.4	0
4	355.9	124.1

cohesion intercept = 44 kPa (6.38 psi, 919 psf)
friction angle = 19°

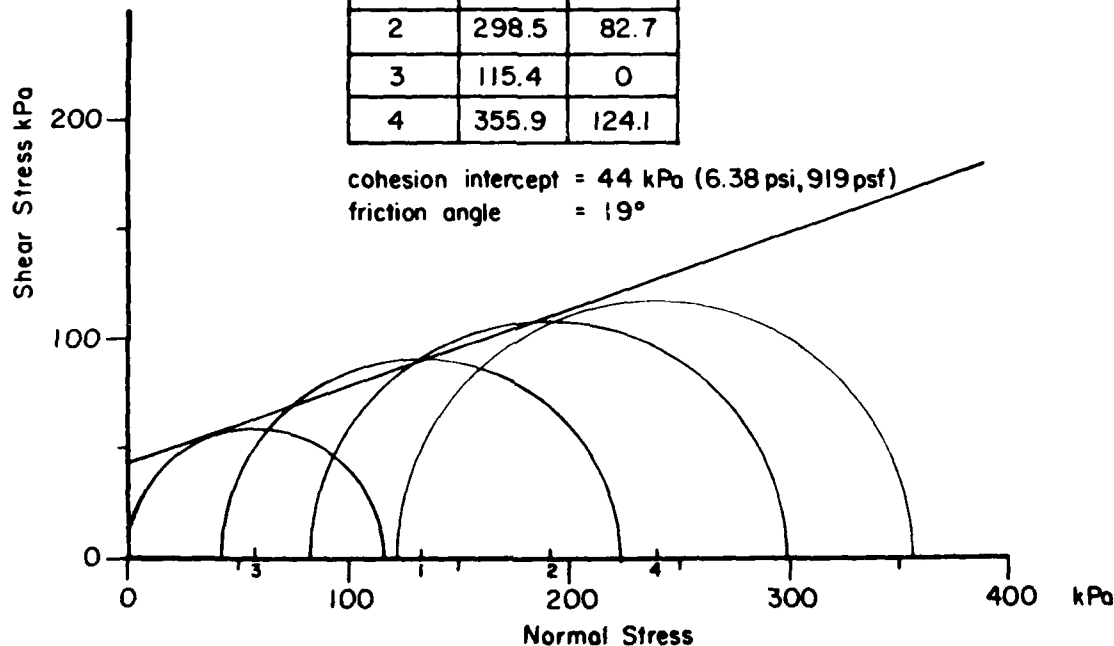


Figure 10. Mohr Diagram for Consolidated, Undrained Triaxial Tests on Old Paleosol from T. A. Woodruff's site, Johnson Creek.

(number 25 in Table 7) yielded lower strength values. However, that particular test was not very satisfactory and the strength values (based on only two points) are speculative.

There is good general agreement between the BST data and the unconfined compression tests. Theoretically, the rupture lines defined by the BST points should be tangents to the failure circles for the equivalent unconfined compression tests (Results Tables, Addendum 3). In 11 tests this is the case, but in 8 tests the circle plots below the line. There are 3 reasons which may explain this. First, it may be due to disturbance of the soil core, in its handling and preparation, resulting in a lower strength than in the soil *in situ*. Second, it may be due to the presence of a critically oriented fissure in the core sample, which results in a low value for the unconfined compression strength. The shear plates in the BST were relocated after each test point, so that when a fissure was encountered in the soil, it would produce only one low point. Such a low point would be either discounted in the regression analysis, or else would have a marginal effect on the overall cohesion and friction angle. Third, the failure circles may in fact be consistent with the BST data, indicating, at low levels of stress, that the rupture line is not straight, but curves downwards towards the abscissa. Further tests and experiments are required to investigate these hypotheses. In just 4 cases the rupture line intersects the failure circle significantly. This might have been due to strengthening of the core sample by the development of negative pore pressures during compression (which was undrained). Alternatively the cores might have been strengthened by some drying out between sampling and testing.

There are not enough tests to allow a statistical analysis to compare the various soil units and sites. Even so, the results may be compared less rigorously. The friction angles of the PSA, YP and OP are very similar. Indeed, the overall mean values (Table 8) are the same. The fine sand/silt has a much higher friction angle of 40°. Since the material is very closely packed, this can be expected. There is a 40% increase in cohesion from the PSA to the YP and a further increase of 33% between the YP and the OP. Considering the composition and morphology of the three soils, this is quite reasonable (see Appendix E of this report).

The data show considerable scatter both within and between sites. Much of this is probably due to variation in moisture content but there are insufficient data to construct a diagram like that of Lutton (1974), Figure 5. Scatter is also to be expected as a result of local variations in soil strength.

4.3.2 Bulk Unit Weight

Values for the bulk unit weight also show considerable variation, but again there is insufficient data to define a relationship with moisture content. Mean values are very similar for the PSA and YP, but the OP is heavier by about 10%. The sandy silt is the most dense material, its bulk unit weight is about 6% greater than that of the OP. These figures are, in absolute and relative terms, very reasonable.

4.3.3 Tensile Strength

The tension tests worked very well and have provided reliable data on the unconfined tension strength of the various soils. These data may be used in the equations presented in section 3.2.3, to predict the depth of tension cracking and may be used in the future to investigate the tensile behavior of soils and the relationship between the tensile and compressive strength.

The mean values of tensile strength increase by about 50% between the Post Settlement Alluvium and the Young Paleosol and by a further 300% between the Young Paleosol and the Old Paleosol. It was quite evident in the field that the Old Paleosol was far stronger in tension than either of the other materials and that the PSA was a little weaker and more friable than the Young Paleosol. The weakest material of all, in tension, was the fine sandy silt, which was almost cohesionless. Consequently both the absolute and relative strengths indicated by the mean values are acceptable.

The results show the PSA and Young Paleosol to be weaker than the loessial soils tested by Lutton (1974), (Table 3). The Old Paleosol yields very similar strength data.

The strength data show considerable scatter, probably due to the presence or absence of fissures in the samples. All the tests were performed on vertical core samples and in the PSA it was observed that the tensile failure surface followed the bedding planes, when present (Fig. 11). Such planes would not be present in horizontal samples, but vertical

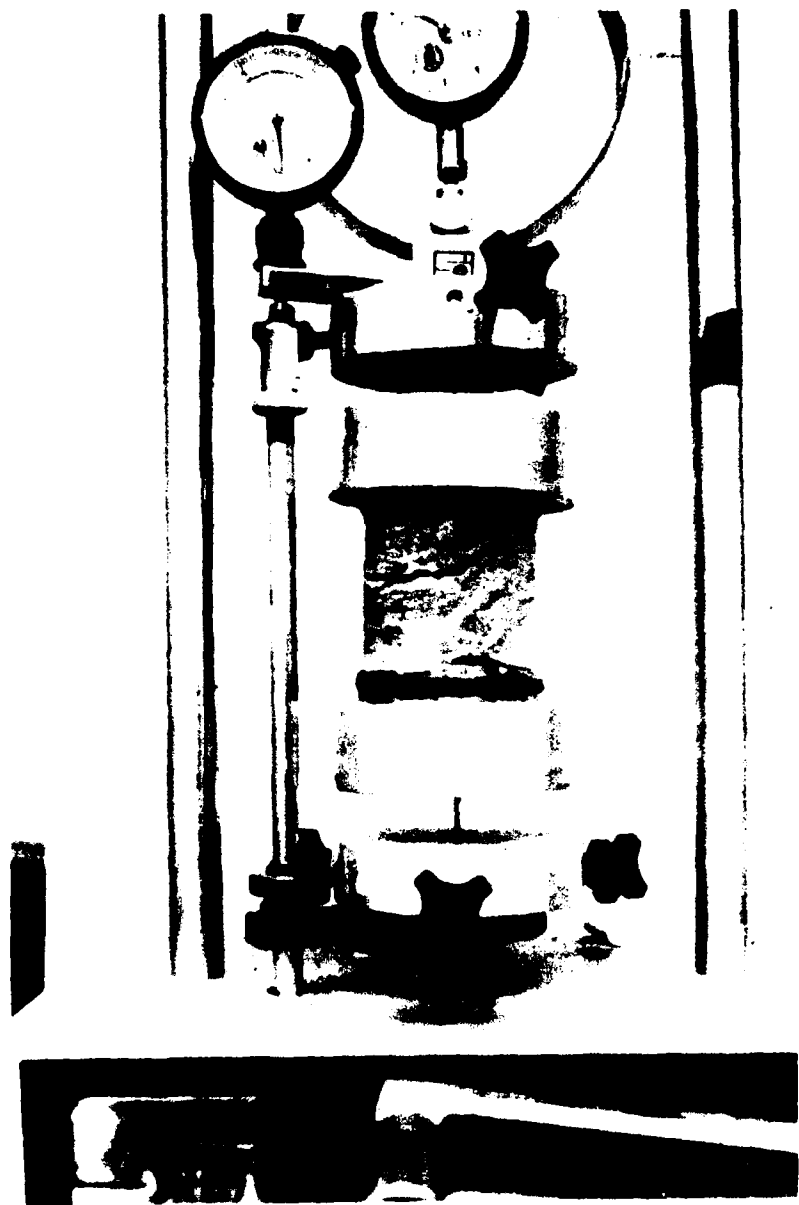


Figure 11. Example of tension failure plane following horizontal bedding planes in the Post Settlement Alluvium.

fissures due to desiccation cracking might present similar planes of weakness. Where bedding planes were absent the failure plane was usually horizontal, often with a microtopography of small inclined failure surfaces (Fig. 12). There was no evidence of bending and it seems fair to conclude that the tests were true uniaxial direct tension tests.

Division of the unconfined tension strength by the compression strength of an adjacent soil sample produces the ratio, r , expressed in percent in Table 9. The mean r value for the PSA is 7.3% with a standard deviation of 5.5%. The wide spread of values is associated with the effects which drying seems to have on the compressive and tensile strengths. The compressive strength increases dramatically at low moisture content (for example, tests 65 and 69) but the tensile strength is not increased much above the average. This leads to a very low r value on dry samples. The explanation of this is probably that drying induces tiny desiccation cracks in the soil. The presence of such cracks has little effect on the compressive strength unless a crack happens to be critically oriented relative to the potential failure plane (Test 71). However, desiccation cracking weakens the tensile strength regardless of crack orientation, offsetting the increase in tensile strength of the intact sections of the sample.

The Young Paleosol has a somewhat higher mean value for r , 12.4%, with a lower standard deviation, 3.2%. The Old Paleosol value of r is 13.8% and $s = 4.3\%$. The values for r are in the same range as those for alluvial soils in British river valleys (Thorne, Tovey and Bryant, 1980).

4.3.4 Worst Case or Operational Parameters

The soil strength data were collected during the summer of 1980. This was unavoidable in a one year study of this type. The soils at the time of testing tended to be rather dry and were on average stronger and lighter than they would have been had the tests been carried out in winter or spring. In calculating bank stability, it is necessary not only to deal with conditions on the day of measurement, but also to predict the bank's stability under the worst likely combination of conditions, which would in this case be a combination of minimum strength and maximum bulk unit weight. Lo (1970) suggested that these parameters should always be used when predicting the stability of a large mass of soil on the basis of test data from small samples.

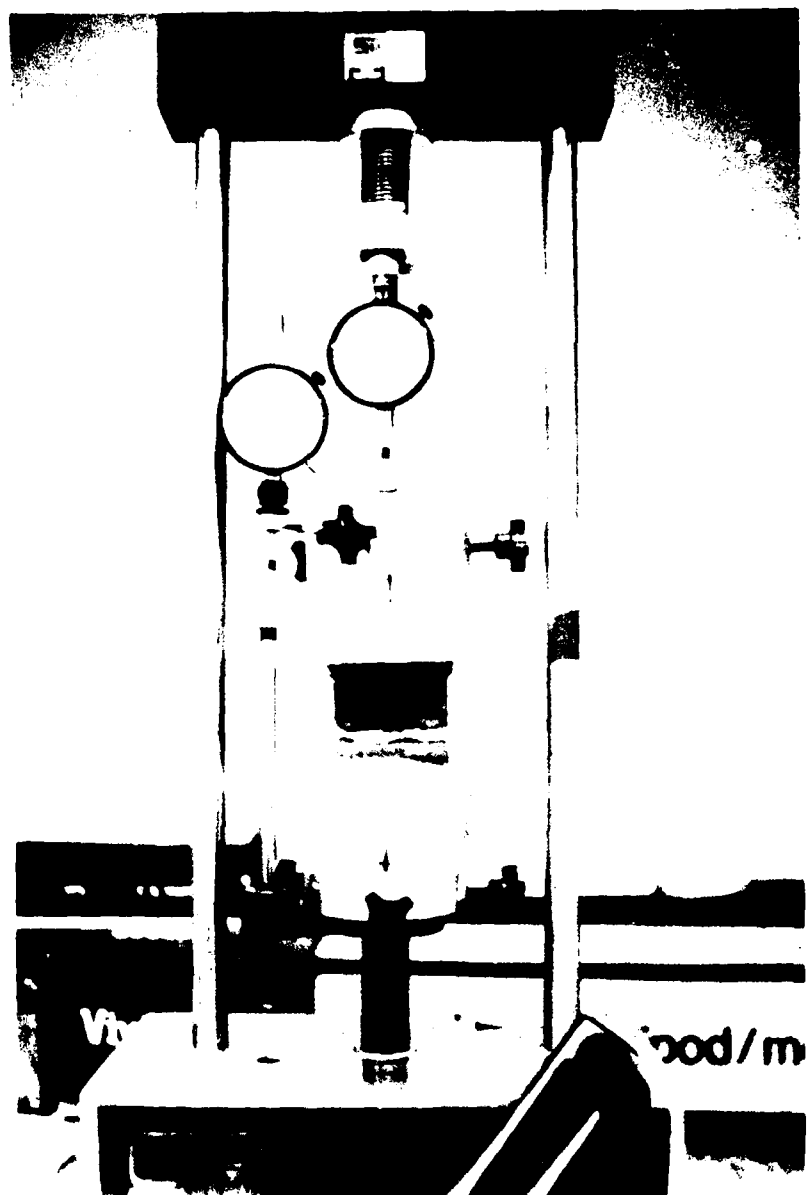


Figure 12. Example of tension failure in a soil without horizontal bedding planes. Failure surface is horizontal with microtopography inclined planes.

This approach has been adopted here. The worst case data are derived simply by noting the lowest values of cohesion, friction angle and tensile strength and the highest value of bulk unit weight for each soil at each site. These values should then represent the long term bulk parameters for each soil and site. The worst case or operational soil parameters and the mean soil parameters are listed in Table 11.

The experimental data are not extensive and in some cases do not adequately cover the full range of possible values. In such cases the data for similar soil types from other sites have been taken into consideration in arriving at the values in Table 11.

Table 11: Mean and Worst Case Soil Strength Parameters.

Soil	Cohesion kPa	Friction Angle degrees	Unit Weight kNm^{-3}	MEAN VALUES			WORST CASE VALUES		
				Bulk Strength kPa	Tensile Strength kPa	Cohesion Angle degrees	Friction Angle degrees	Bulk Unit Weight kNm^{-3}	Tensile Strength kPa
<u>Tommy Florence's</u>									
PSA	40.2	19	17.9	5.6	24	12	21	2.0	2.0
YP	62	25	18.4	5.1	21	15	20.3	3.1	3.1
OP	66.2	24	19.1	15.7	34.5	14	21	7.5	7.5
Silty/sand	3.9	40	21.2	0	0	20	22.7	0	0
<u>T.A. Woodruff's</u>									
PSA	31	29	17	8.5	22	12	21	2.2	2.2
YP	46.3	18	18.4	5.1	21.3	16	20.3	3.1	3.1
OP	80	18	20.3	32.6	20.1	11	22.2	16.7	16.7
Silty/sand	4	40	21	0	0	20	22	0	0
<u>Katherine Leigh's</u>									
PSA	31	21	15.5	4.1	20.8	12	21	2.4	2.4
YP	40	20	16.9	10.1	21	15	20	9	9
OP	104.5	12	19	25.2	35	9	21	7.5	7.5
Silty/sand	5	40	21.1	3.7	0	20	21.6	0	0

APPLICATION OF BANK STABILITY ANALYSIS

5.1 FIELD OBSERVATIONS OF BANK GEOMETRY

The stability charts presented in section 3.2 and the soil property data listed in section 4 may be used to calculate the stability of streambanks of given geometries. Bank geometry data for the experimental sites were collected in a short survey performed at the end of the study by Mr. Paul Hawks of the Sedimentation Lab. Five bank cross sectional profiles were surveyed at each site and the bank heights and angles which were observed at each site are listed in Table 12.

A large number of cross sections for Hotophia Creek were made available by Mr. B. R. Winkley, Mr. Bob Rentschler and Mr. John Brooks of the Potamology Section, Vicksburg District Office, U.S. Army Corps of Engineers (Table 13). This watershed is adjacent to Johnson and Goodwin Creeks. Like the others, this creek is experiencing extreme bed degradation and its banks are known to be highly unstable (Whitten and Patrick, 1980). Hotophia Creek cross sectional profiles are available for January 1978 and June 1979. In many cases bank failures occurred between these dates and are well documented in the resurvey. The shape of the failure surface can be inferred from the bank cross sectional profile. The depth of tension cracking, y , can be approximated to the depth of the near vertical face at the bank top (Lohnes and Handy, 1968; Bob Lohnes, personal communication, 1980) (Fig. 13) and if it can be assumed that all of the observed retreat at a point along the channel took place in a single failure, then the change in bank top location defines the width of the failure block, b . Bank height, slope angle, crack depth, and block width data from the Corps surveys of Hotophia Creek are listed in Table 13.

5.2 STABILITY CALCULATIONS AND GRAPHS

The banks at all the sites are made up of layers of the various soil types. The order of the layers, from top to bottom, is PSA, YP, OP and sand. The order is always the same, but the thickness of individual layers varies from place to place. In some cases one or more soil layers are entirely absent from the sequence.

The layering was taken into account in the stability analysis by calculating overall values for the soil parameters which were weighted

Table 12: Bank Geometry Data: October 1980.

Johnson Creek at Tommy Florence's		
Section	Height	Angle
Number	(m)	(°)
2(L)	6.1	62
3(L)	6.2	58
4(L)	6.2	65
5(L)	6.2	68
(R)	5.3	54
Johnson Creek at T.A. Woodruff's		
Section	Height	Angle
Number	(m)	(°)
1(L)	4.3	32
(R)	4.6	50
2(L)	4.3	25
(R)	4.5	59
3(L)	3.8	18
(R)	4.0	57
4(L)	3.9	64
(R)	4.0	44
5(L)	4.5	60
(R)	4.6	33
Goodwin Creek at Katherine Leigh's		
Section	Height	Angle
Number	(m)	(°)
1(R)	4.5	50
2(R)	4.5	47
3(R)	5.0	66
4(R)	1.3	22
4(L)	5.3	50
5(R)	5.3	61
5(L)	5.5	50

Table 13: Bank Survey Data: Hotophia Creek, Panola County, January 1978
and June 1979.

Section Number		Bank Height (m)	Bank Angle (°)	Stable/Unstable	Crack Depth (m)	Failure Block Width (m)
T-48-2	L	7.2	51	S	2.6	-
	R	8.0	61	U	-	-
T-48-3	L	7.4	53	S	-	-
	R	7.2	51	S	-	-
T-49-1	L	7.7	56	S	-	-
	R	8.1	53	S	-	-
T-49-2	L	7.5	69	U	-	-
	R	8.4	55	S	-	-
T-49-3	L	7.6	47	S	-	-
	R	7.6	57	S	-	-
T-49-4	L	7.9	46	S	2.4	-
	R	7.6	58	S	-	-
T-49-5	L	6.7	51	S	2.3	-
	R	6.9	62	S	-	-
T-49-6	L	6.4	76	U	0	1.4
	R	7.3	66	S	2.7	-
T-49-7	L	6.1	71	S	-	-
	R	7.9	58	S	-	-
T-50-1	L	7.0	78	U	-	-
	R	6.1	62	U	2.6	-
T-50	R	8.2	46	S	-	-
T-50-2	L	7.0	80	U	-	-
	R	6.7	55	S	-	-
T-51-4	L	6.1	59	U	4.3	0.3
	R	5.9	50	S	4.3	-
T-51-5	L	6.7	63	U	-	-
	R	6.2	48	S	2.4	-
T-51-6	L	5.3	86	U	-	-
	R	7.6	67	S	-	-
T-51-7	L	6.4	55	S	-	-
	R	6.9	63	U	-	-
T-51-8	L	6.7	61	S	-	-
	R	5.5	73	U	3.4	1.2
T-51-9	L	6.1	80	U	1.8	1.2
	R	5.6	85	U	-	2.1
T-51-12	L	3.7	80	S	-	-
	R	6.1	64	S	-	-
T-52	L	5.6	65	U	2.1	1.1
	R	6.4	67	U	-	-
T-52-1	L	5.5	58	S	-	-
	R	5.0	60	S	-	-
T-52-2	L	3.4	82	U	3.0	2.1
	R	6.2	63	U	3.2	1.2

Table 13, Cont'd.

T-52-3	L	7.3	52	S	-	-
	R	5.2	68	U	0	1.6
T-52-4	L	5.5	67	U	-	-
	R	5.6	71	U	-	-
T-52-5	L	6.7	50	S	-	-
	R	6.1	62	U	-	-
T-52-6	L	6.9	52	S	-	-
	R	6.9	58	S	-	-
T-52-7	L	6.4	54	S	-	-
	R	6.1	60	S	-	-
T-52-8	L	6.7	60	U	-	-
	R	5.9	60	S	-	-
T-52-9	L	4.2	73	S	-	-
	R	6.4	53	S	-	-
T-53	L	3.7	76	S	-	-
T-53-1	L	4.9	68	S	-	-
	R	6.2	53	S	-	-
T-53-2	L	5.5	68	U	2.9	0.9
	R	5.3	64	S	-	-
T-53-3	L	4.9	74	U	3.7	0.6
	R	5.3	47	S	-	-
T-53-4	L	4.9	71	U	3.5	0.6
	R	5.3	57	S	-	-
T-53-5	L	5.5	59	S	-	-
	R	5.2	61	S	1.8	-
T-53-6	L	4.9	67	S	2.4	-
	R	5.2	61	S	2.3	-
T-53-7	L	4.8	72	U	2.4	0.5
	R	4.5	80	U	0	0.6
T-53-8	L	5.1	62	S	-	-
	R	5.1	79	U	0	0.9
T-53-9	L	5.0	61	S	-	-
	R	4.6	65	S	2.0	-
T-53-10	L	5.2	58	S	1.4	-
	R	4.7	57	S	-	-
JG-11-6	L	7.8	62	U	-	-
	R	7.5	48	S	-	-
JG-11-7	L	5.6	46	S	2.4	1.5
	R	7.6	54	S	-	-
JG-11-8	L	6.4	32	S	-	-
	R	8.5	50	S	-	-
JG-11-9	L	7.6	60	S	-	-
	R	7.6	56	S	-	-
JG-11-10	L	6.1	68	U	-	-
	R	7.0	56	S	-	-
JG-12-1	L	7.0	35	S	-	-
	R	5.5	60	S	2.6	-
JG-12-2	L	6.7	57	S	-	-
	R	7.0	57	S	-	-
JG-12-3	L	7.9	57	U	-	-
	R	7.0	55	S	-	-

Table 13, Cont'd.

JC-12-4	L	7.2	63	U	-	-
	R	7.0	59	S	-	-
JC-12-5	L	8.0	29	S	-	-
	R	7.2	26	S	-	-
JC-12-6	L	7.3	62	S	-	-
	R	7.0	58	S	-	-
JC-12-7	L	6.4	61	S	-	-
	R	7.2	58	S	-	-
JC-14-10	L	7.3	55	S	2.4	1.5
	R	7.3	53	S	2.1	-
JC-15-1	L	7.2	59	U	2.2	0.6
	R	7.8	50	S	-	-
JC-15-2	L	6.7	60	U	-	-
	R	7.3	53	S	-	-
JC-15-3	L	5.9	63	U	-	-
	R	6.7	56	S	-	-
JC-15-4	L	7.0	64	U	2.4	1.2
	R	6.9	54	S	-	-
JC-15-5	L	6.9	60	U	-	-
	R	6.7	62	U	3.6	-
JC-15-6	L	6.0	81	U	2.6	1.6
	R	7.5	51	S	-	-
JC-15-7	L	6.6	60	U	1.8	1.7
	R	7.2	45	S	-	-

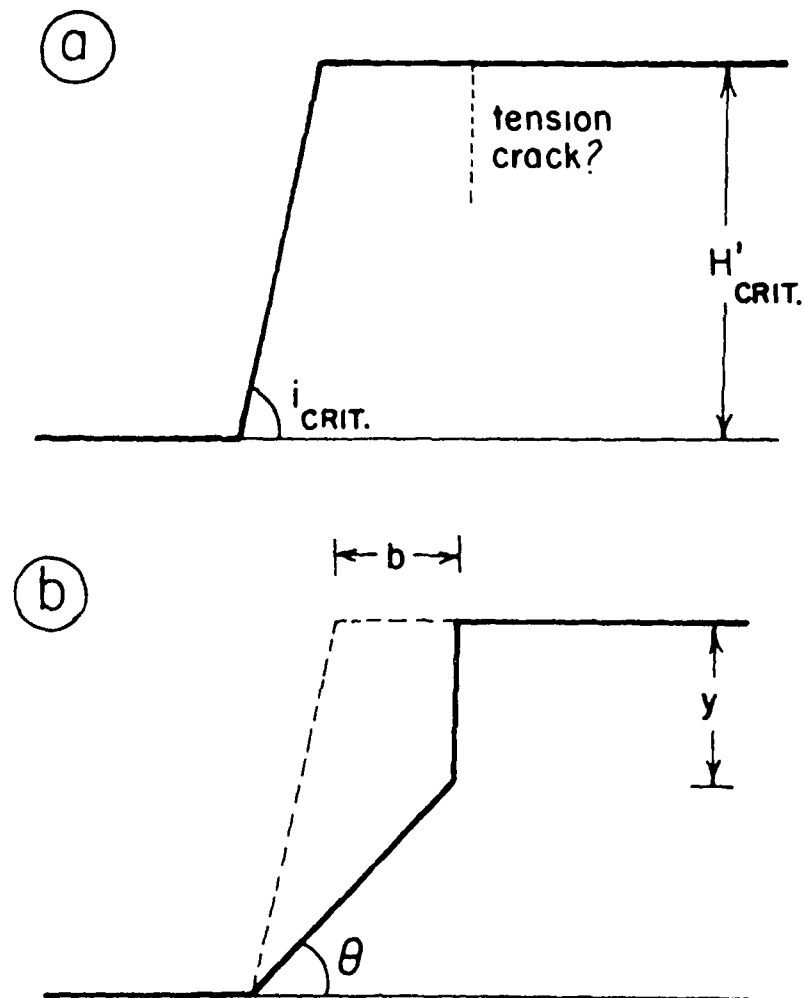


Figure 13. Idealized bank failure. a. Just prior to failure the bank height and angle and the tension crack depth are close to their critical values. b. Just after failure the new bank profile may be used to estimate the tension crack depth (y) and the failure block width (b).

according to the proportion of each soil type present. Stratigraphic information from the borehole closest to the bank profile was used to define the thickness of each layer (See Addendum 1). The proportion of the bank formed in each soil was then found by dividing the layer thickness by the bank height. These proportions were then multiplied by the mean and worst case soil parameter values from Table 11 and the products summed to yield the weighted overall values of cohesion, friction angle and bulk unit weight for each bank section. These data are listed in Tables 14, 15 and 16.

In calculating the depth of the tension crack, y , only the proportion of the upper layers were considered, since it is in these layers that cracks form. It has been shown empirically that the depth of tension cracking in soils seldom exceeds half the bank height (Terzaghi, 1943). Therefore, in the calculation of crack depth the weighted average soil parameters were based on the soil layers in the upper half of the bank.

Values of c , ϕ , γ and y calculated for a given bank section, may be used to replot the stability chart (Fig. 9) in terms H versus i . This is done by obtaining values of N_s corresponding to the fixed value of ϕ and various values of i , using Table 6, and then calculating H from:

$$H = \frac{c}{\gamma} N_s - y \quad (13)$$

These values of H and i define the line of critical stability. Two lines are plotted, one for mean and one for worst case conditions. In some cases the calculated crack depth, y , was greater than half the bank height. This was thought to be unrealistic in view of the empirical evidence that tension cracks seldom exceed half the bank height and so in those cases the crack depth was taken to be half the bank height. This affected the curves only at very low bank heights and high angles, above seventy five degrees.

After constructing the critical curves for mean and worst case conditions, the points for the actual bank height and angle observed in the field were then plotted onto the graph (squares on Figs. 14a through 16e). Banks which plot below the critical line for worst case conditions are stable under all conditions and can only be brought to failure by an increase in height (by bed degradation) or bank angle (by oversteepening through toe erosion). Banks which plot between the mean and worst case

Table 14: Weighted Mean Soil Parameters for Surveyed Bank Sections at
Tommy Florence's site.

Section and Soils	Borehole	Cohesion (kPa)	Friction Angle (°)	Bulk Unit Weight (kNm ⁻³)	Crack Depth (m)	Stability Equations
2 PSA 0.33 OP 0.57	2 Mean W.C.	51.4 27.6	24 14	19 21.2	6.71 3.00	$H_M = 2.71N_s - 6.71$ $H_{WC} = 1.30N_s - 3.00$
Sand 0.10						
3 PSA 0.27 OP 0.41	3 Mean W.C.	39.2 20.6	27.8 15.4	19.5 21.5	7.08 3.10	$H_M = 2.01N_s - 7.08$ $H_{WC} = 0.96N_s - 3.10$
Sand 0.32						
4 PSA 0.18 YP 0.11 OP 0.71	4 Mean W.C.	61.1 31.1	23 13.8	18.8 20.9	7.93 3.03	$H_M = 3.25N_s - 7.93$ $H_{WC} = 1.49N_s - 3.03$
5 PSA 0.22 YP 0.30 OP 0.09	5 Mean W.C.	34.9 14.7	29.4 16.2	19.5 21.5	7.96 2.55	$H_M = 1.79N_s - 7.96$ $H_{WC} = 0.68N_s - 2.55$
Sand 0.39						

Table 15: Weighted Mean Soil Parameters for Surveyed Bank Sections at T.A. Woodruff's site.

Section and Soils	Borehole	Cohesion (kPa)	Friction Angle (°)	Bulk Weight (kNm^{-3})	Crack Depth (m)	Stability Equation
1(Left) 3,4,9,10						
PSA 0.14	Mean	52.3	21.1	19	6.09	$H_M = 2.75N_s - 6.09$
YP 0.46	W.C.	19.5	14.1	21.1	2.49	$H_{WC} = 0.92N_s - 2.49$
OP 0.33						
Sand 0.07						
1(Right) 3,4,9,10						
PSA 0.13	Mean	49.3	22.3	19.1	6.11	$H_M = 2.58N_s - 6.11$
YP 0.43	W.C.	18.3	16.7	21.2	2.49	$H_{WC} = 0.86N_s - 2.49$
OP 0.31						
Sand 0.13						
2(Right) 2						
PSA 0.10	Mean	58.7	19.9	19.6	6.68	$H_M = 2.99N_s - 6.68$
YP 0.24	W.C.	18.4	13.3	21.6	1.99	$H_{WC} = 0.85N_s - 1.99$
OP 0.55						
Sand 0.11						
3(Right) 2						
PSA 0.11	Mean	65.5	19.2	19.4	6.54	$H_M = 3.38N_s - 6.54$
YP 0.27	W.C.	20.6	12.5	21.6	2.11	$H_{WC} = 0.95N_s - 2.11$
OP 0.62						
4(Left) 7						
YP 0.17	Mean	59.1	22.4	20.1	7.35	$H_M = 2.94N_s - 7.35$
OP 0.63	W.C.	16.3	13.7	21.8	1.50	$H_{WC} = 0.75N_s - 1.50$
Sand 0.20						
5(Left) 7						
YP 0.15	Mean	52.1	24.6	20.2	7.42	$H_M = 2.58N_s - 7.42$
OP 0.55	W.C.	14.3	14.5	21.9	1.45	$H_{WC} = 0.65N_s - 1.45$
Sand 0.30						

Table 16: Weighted Mean Soil Parameters for Surveyed Bank Sections at Katherine Leigh's site.

Section and Soils	Borehole Number	Cohesion (kPa)	Friction Angle (°)	Bulk Unit Weight (kNm ⁻³)	Crack Depth (m)	Stability Equation
1	1					
PSA 0.20	Mean	19.7	30.8	19	5.13	$H_M = 1.04N_s - 5.13$
YP 0.27	W.C.	9.83	17.3	21.0	1.99	$H_{AV} = 0.47N_s - 1.99$
Sand 0.53						
2	1					
PSA 0.21	Mean	20.3	30.8	19	5.33	$H_M = 1.07N_s - 5.33$
YP 0.28	W.C.	10.25	17.1	21.2	2.08	$H_{AV} = 0.48N_s - 2.08$
Sand 0.52						
3	1 and 6					
PSA 0.22	Mean	50.3	19	17.2	5.43	$H_M = 2.92N_s - 5.43$
YP 0.53	W.C.	23.1	13.1	21.0	2.12	$H_{AV} = 1.10N_s - 2.12$
OP 0.21						
Sand 0.04						
4	5 and 7					
PSA 0.18	Mean	36.4	26.2	18.6	6.08	$H_M = 1.96N_s - 6.08$
YP 0.28	W.C.	13.3	15.1	20.9	2.22	$H_{AV} = 0.64N_s - 2.22$
OP 0.17						
Sand 0.37						
5	2 and 3					
PSA 0.16	Mean	38.6	20.2	16.7	5.46	$H_M = 2.31N_s - 5.46$
YP 0.84	W.C.	21	14.5	20.2	2.08	$H_{WC} = 1.04N_s - 2.08$

lines are at risk and can fail as a result of weakening through wetting and cracking without any erosion. Any banks which plot above the mean line are highly unstable and could fail at any time. The stability graphs for the bank sections at Tommy Florence's, T. A. Woodruff's and Katherine Leigh's fields are presented in Figures 14, 15 and 16.

5.3 DISCUSSION OF RESULTS

5.3.1 Johnson Creek at Tommy Florence's

Only 4 sections are considered at Tommy Florence's (T.F.) site. Section 1 was located at a point where overbank field drainage intersected the bank. Headward erosion of the resulting gully had produced a complex cross sectional profile which was not suitable for analysis and so section 1 is excluded.

The points for sections 2 and 4 plot (squares indicate bank height and angle for that section) just below the line of critical stability (bottom line) for worst case conditions (Figs. 14a and 14c). Sections 3 and 5 (right bank) plot just above that line (Figs. 14b and 14d). Section 5 (left bank) plots well above the worst case line, midway up to the mean line (Fig. 14d).

The interpretation of the analysis and graphs is that all the bank sections should be stable under conditions like those that existed when the data were collected and as represented by the mean line, but that sections 3, 5 (right bank) and 5 (left bank) would be unstable under worst case conditions. They would be expected to fail sometime during winter or spring when the banks are wet and worst case conditions prevail. Sections 2 and 4 should withstand even these conditions. However the factors of safety, as defined by the critical height divided by the actual height, under worst case conditions would be only 1.1 and 1.2 at sections 2 and 4 respectively. Thus stability would be rather marginal and so the banks could not really be considered safe. Some scour of the bank toe and the bed always occurs during high flows, even if deposition on the recession results in there being no net degradation. This scour increases bank height by basal lowering and increases bank angle by oversteepening, both tending to decrease stability. For section 2 about 1.2 m of basal lowering, or 6° of oversteepening, would put the bank at risk of failure. For section 4 the figures are 2 m and 10°. Basal lowering by over a meter is possible but not particularly likely, but oversteepening by only 10° is

TOMMY FLORENCE'S SECTION 2 ; BOREHOLE 2

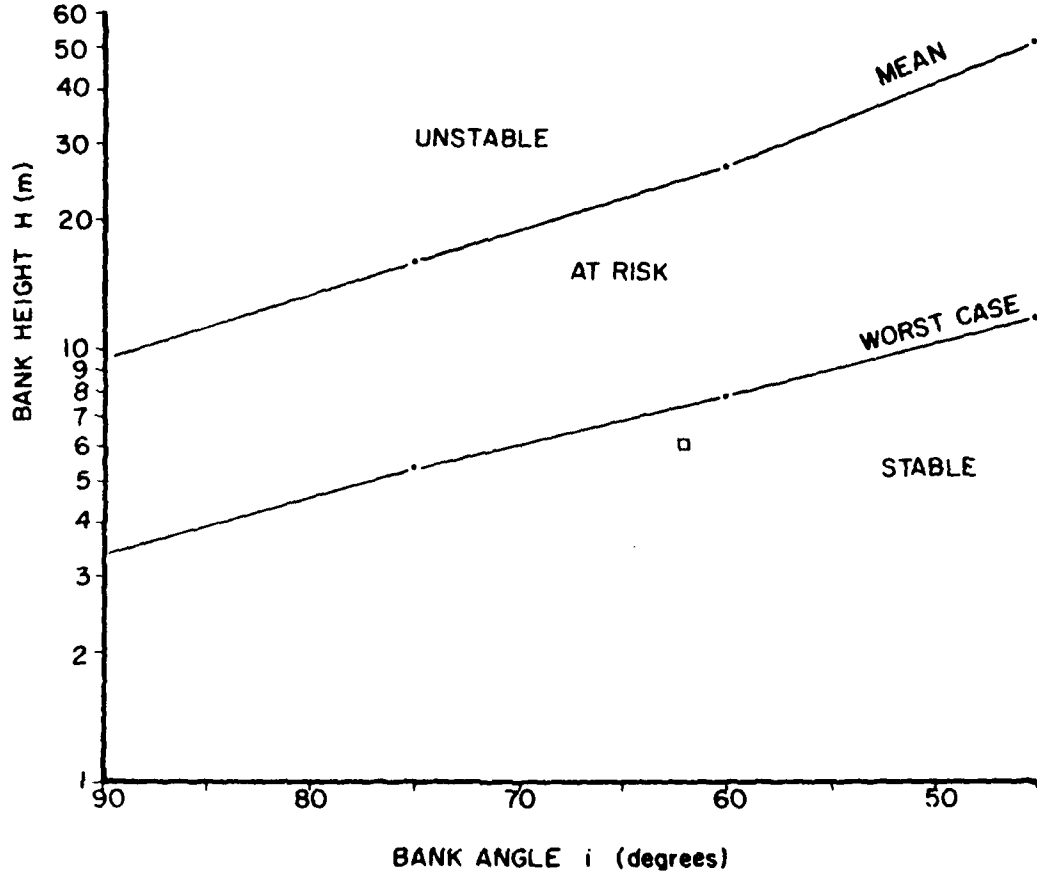


Figure 14a. Bank Stability Graph for Johnson Creek at Tommy Florence's site.

TOMMY FLORENCE'S SECTION 3 ;BOREHOLE 3

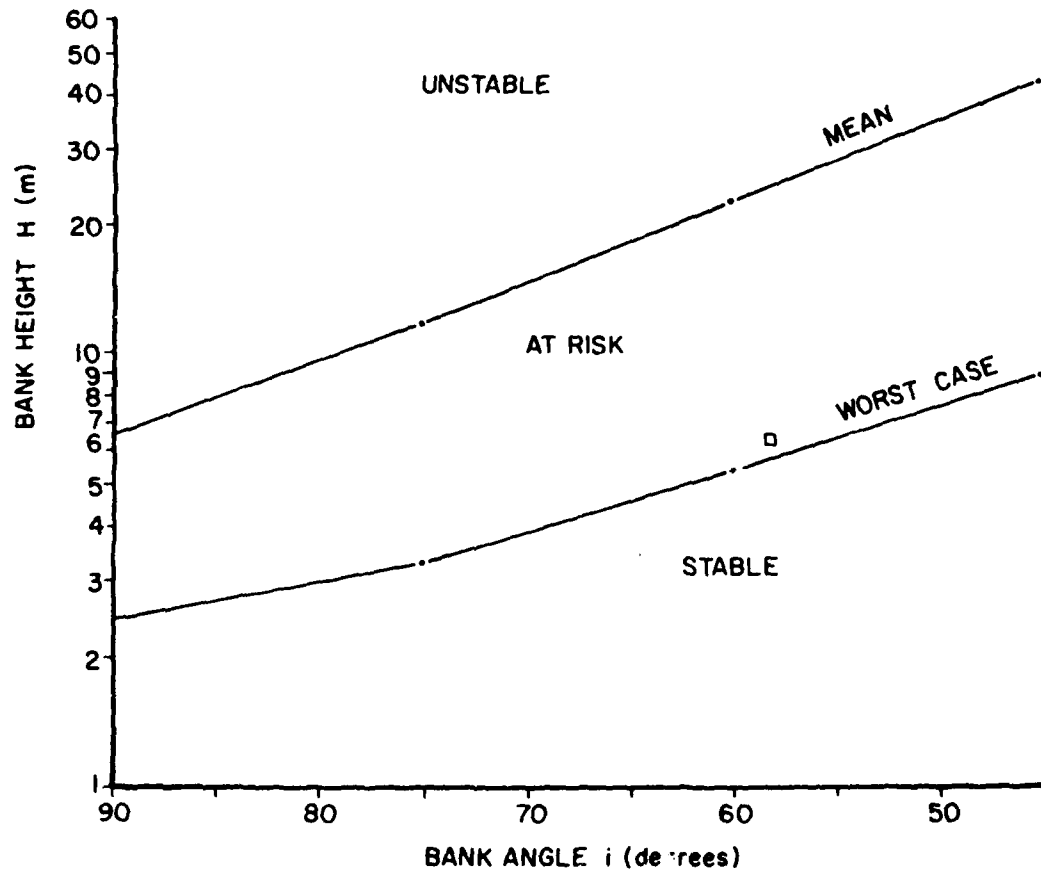


Figure 14b. Bank Stability Graph for Johnson Creek at Tommy Florence's site.

TOMMY FLORENCE'S SECTION 4; BOREHOLE 4

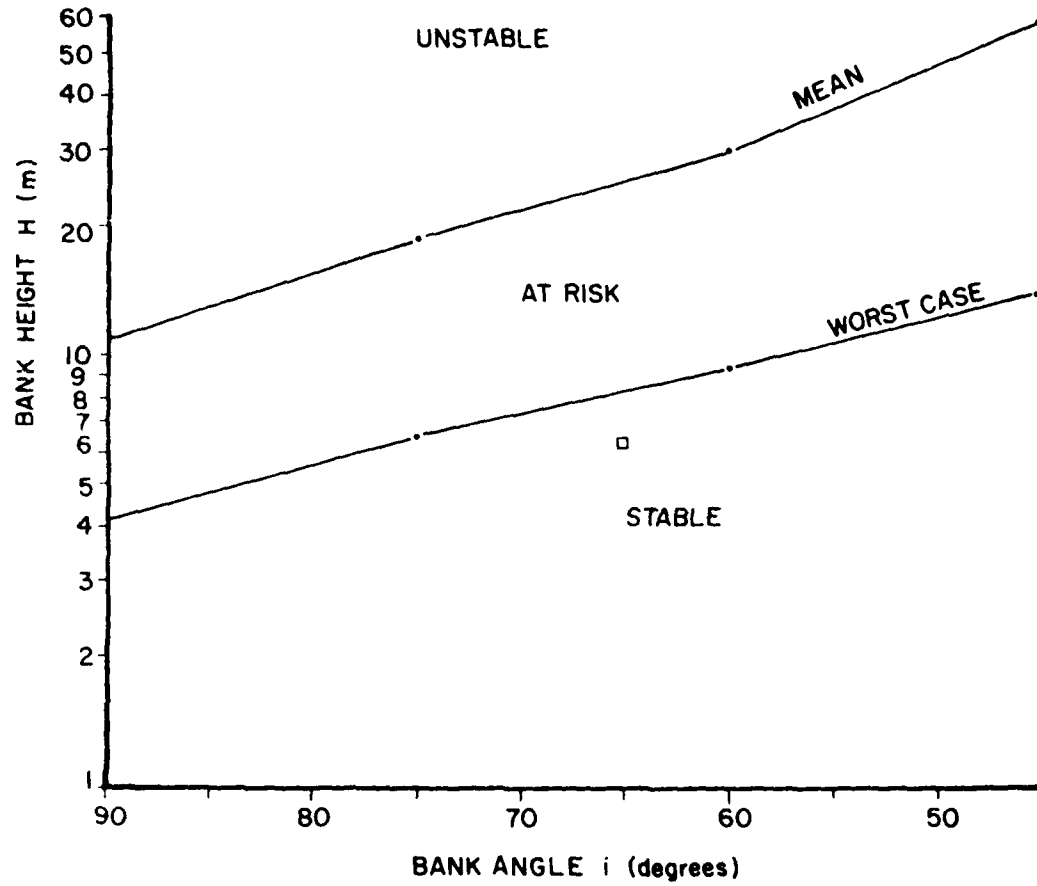


Figure 14c. Bank Stability Graph for Johnson Creek at Tommy Florence's site.

TOMMY FLORENCE'S SECTION 5, BOREHOLE 5

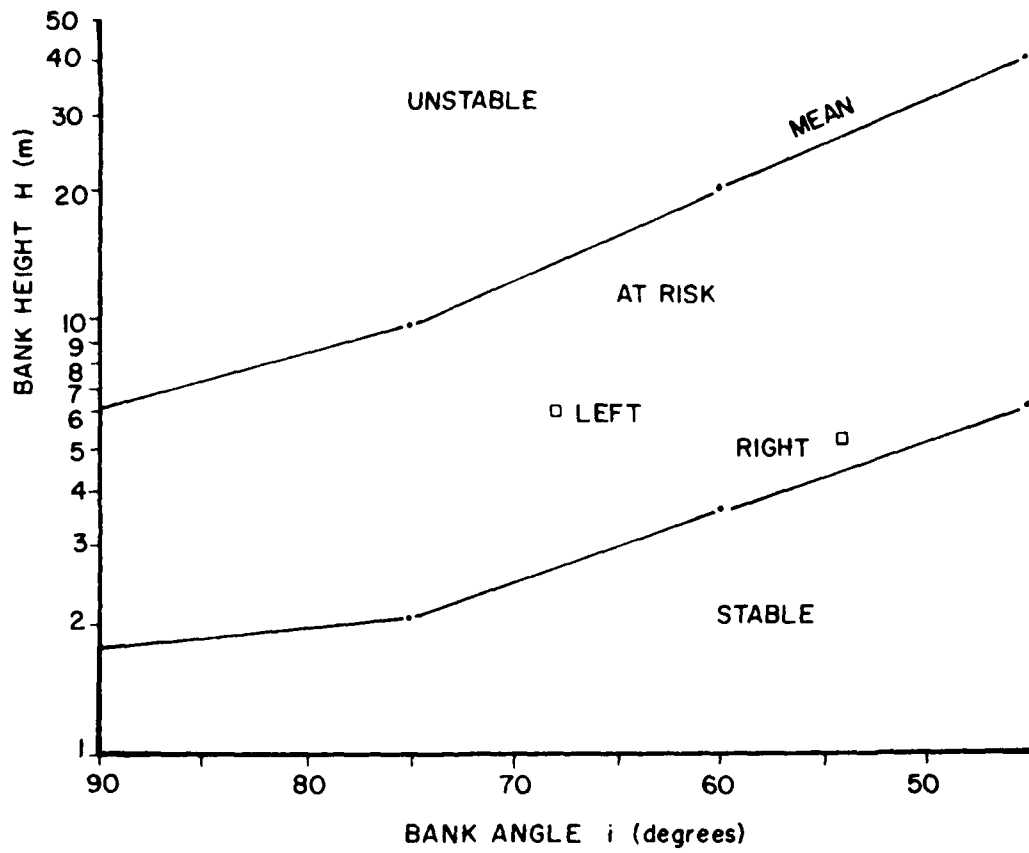


Figure 14d. Bank Stability Graph for Johnson Creek at Tommy Florence's site.

T.A. WOODRUFF'S SECTION I, BOREHOLES 3,4,9,10
(RIGHT BANK)

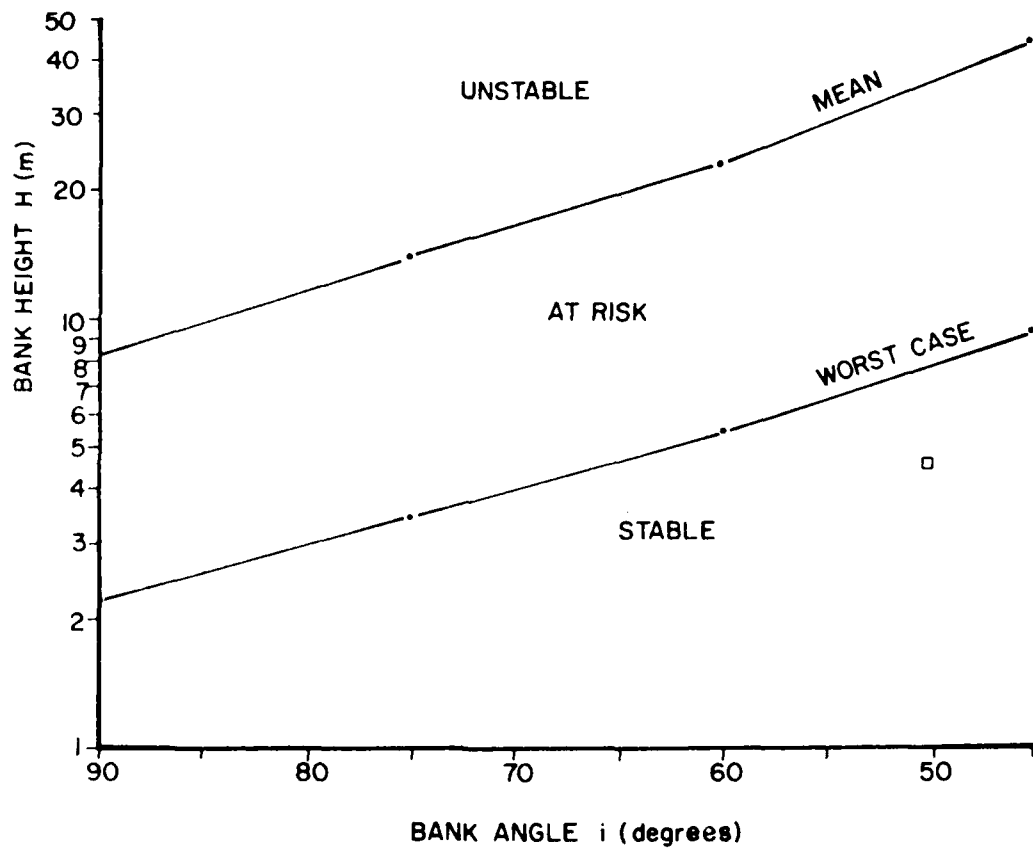


Figure 15a. Bank Stability Graph for Johnson Creek at T. A. Woodruff's site.

T.A. WOODRUFF'S SECTION 2, BOREHOLE 2

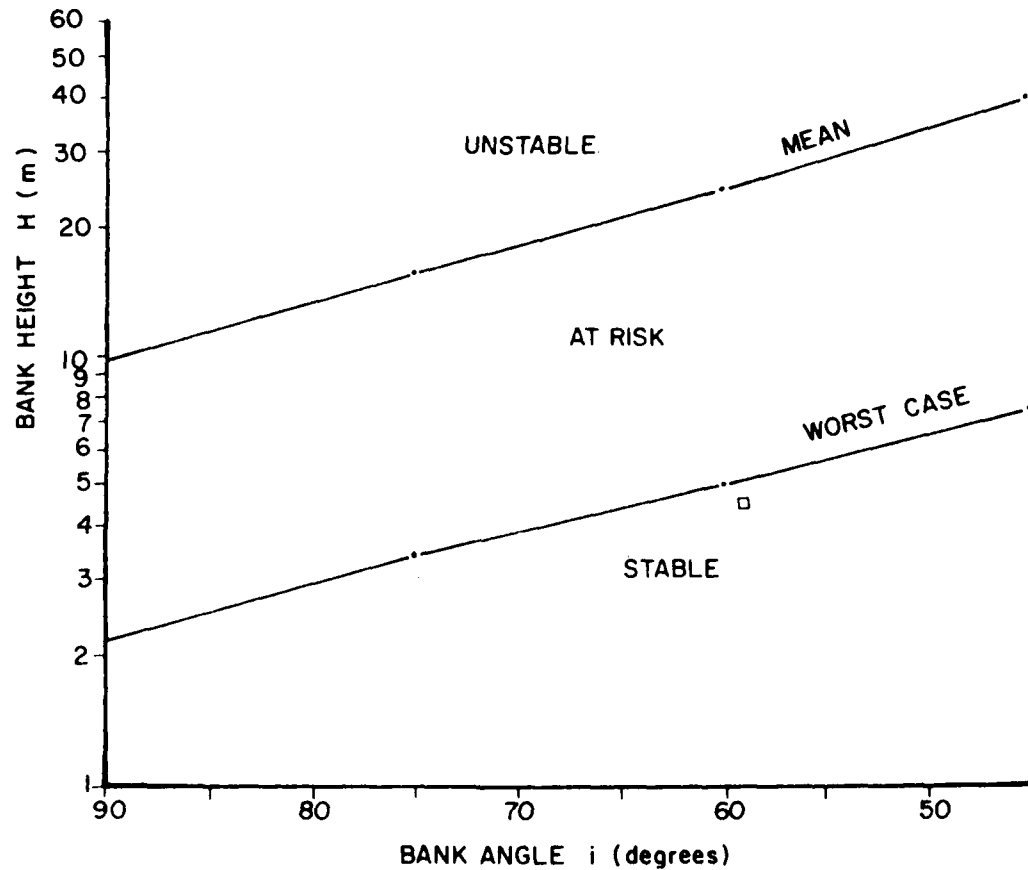


Figure 15b. Bank Stability Graph for Johnson Creek at T. A. Woodruff's site.

T.A.WOODRUFF'S SECTION 3, BOREHOLE 2

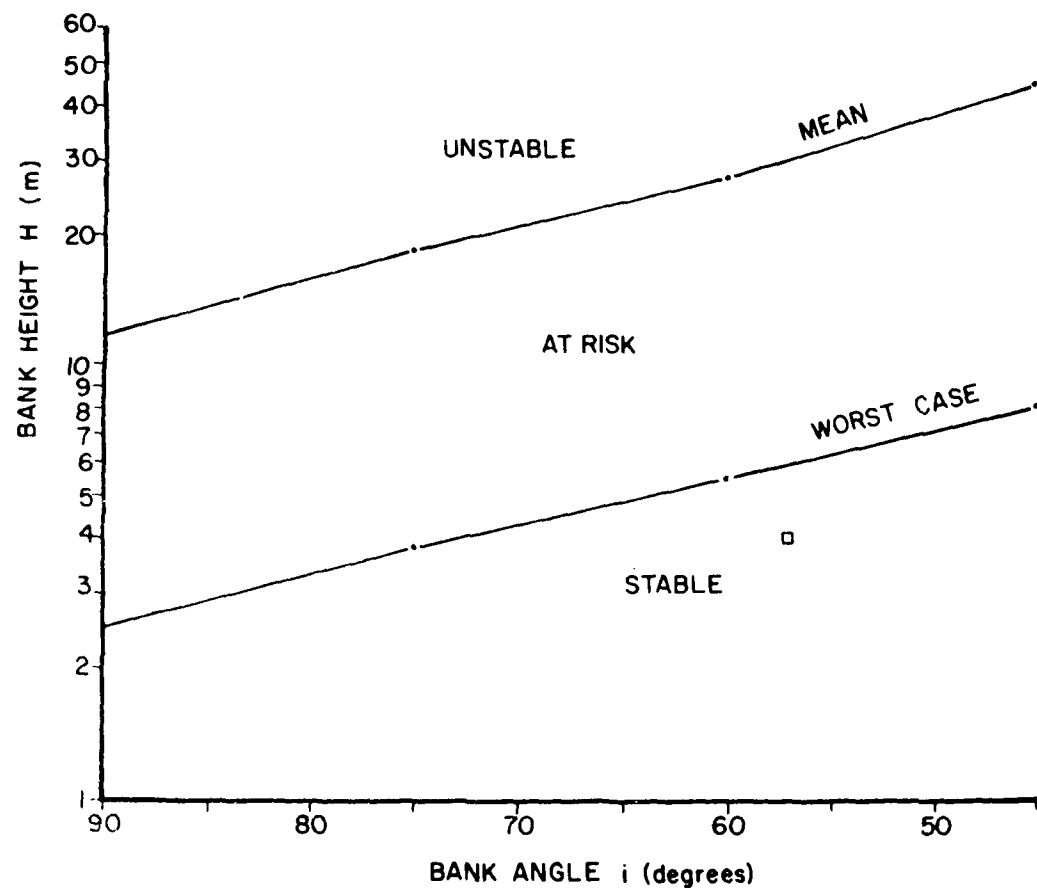


Figure 15c. Bank Stability Graph for Johnson Creek at T. A. Woodruff's site.

T.A. WOODRUFF'S SECTION 4, BOREHOLE 7

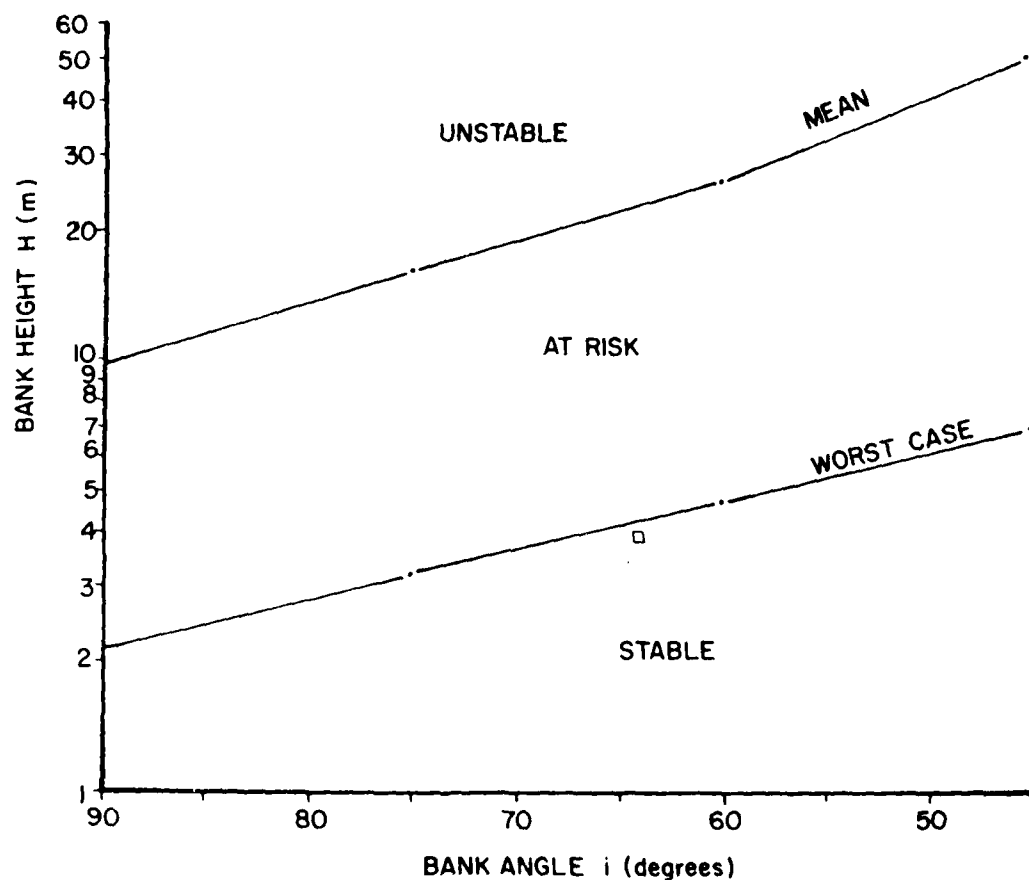


Figure 15d. Bank Stability Graph for Johnson Creek at T. A. Woodruff's site.

T.A. WOODRUFF'S SECTION 5, BOREHOLE 7

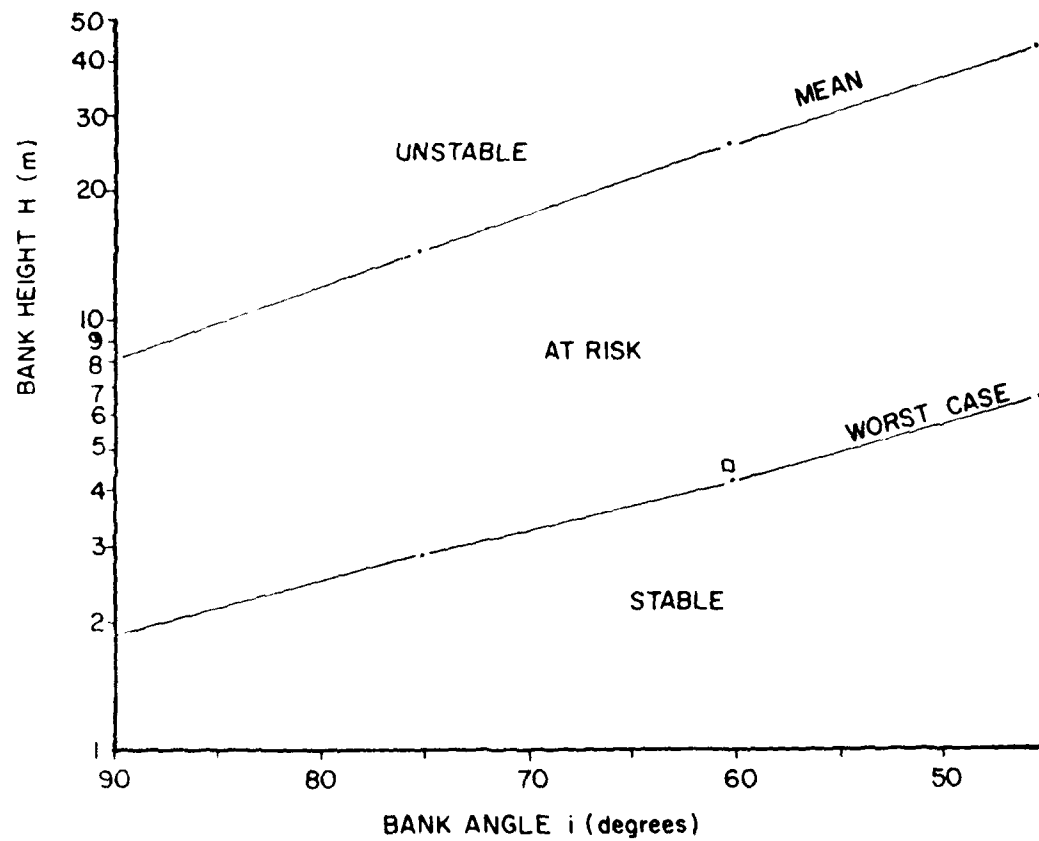


Figure 15e. Bank Stability Graph for Johnson Creek at T. A. Woodruff's site.

KATHERINE LEIGH'S SECTION I, BOREHOLE I

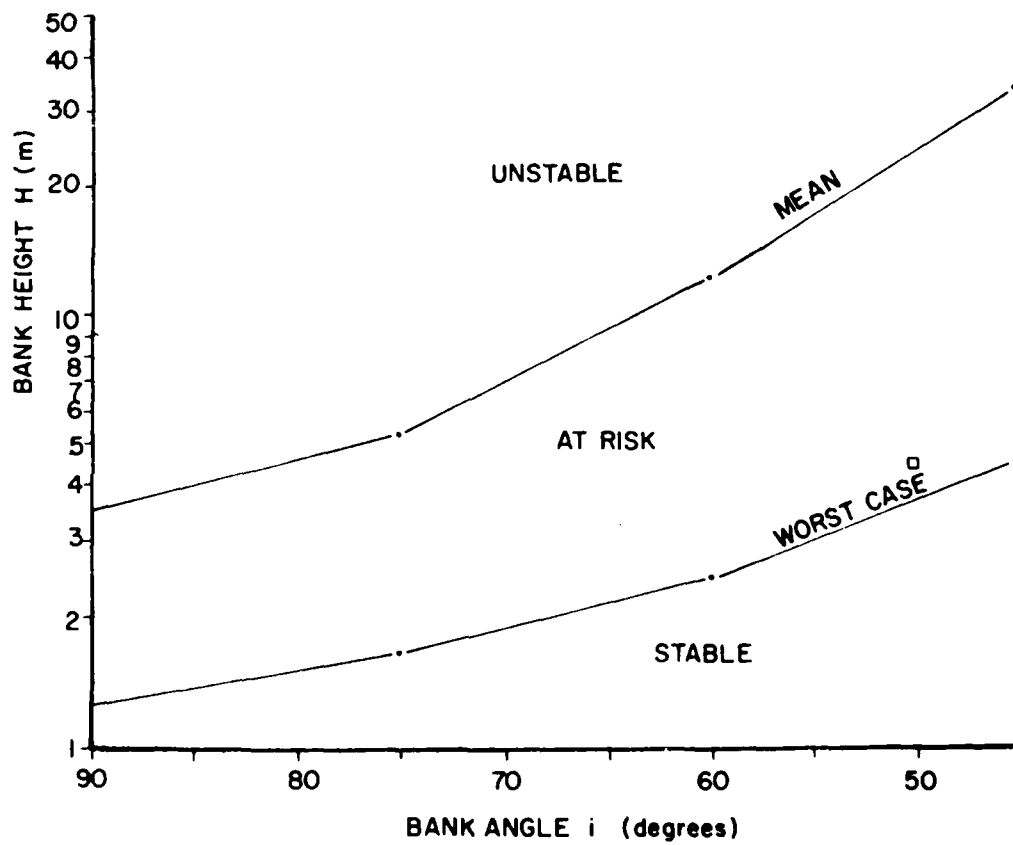


Figure 16a. Bank Stability Graph for Goodwin Creek at Katherine Leigh's site.

KATHERINE LEIGH'S SECTION 2, BOREHOLE I

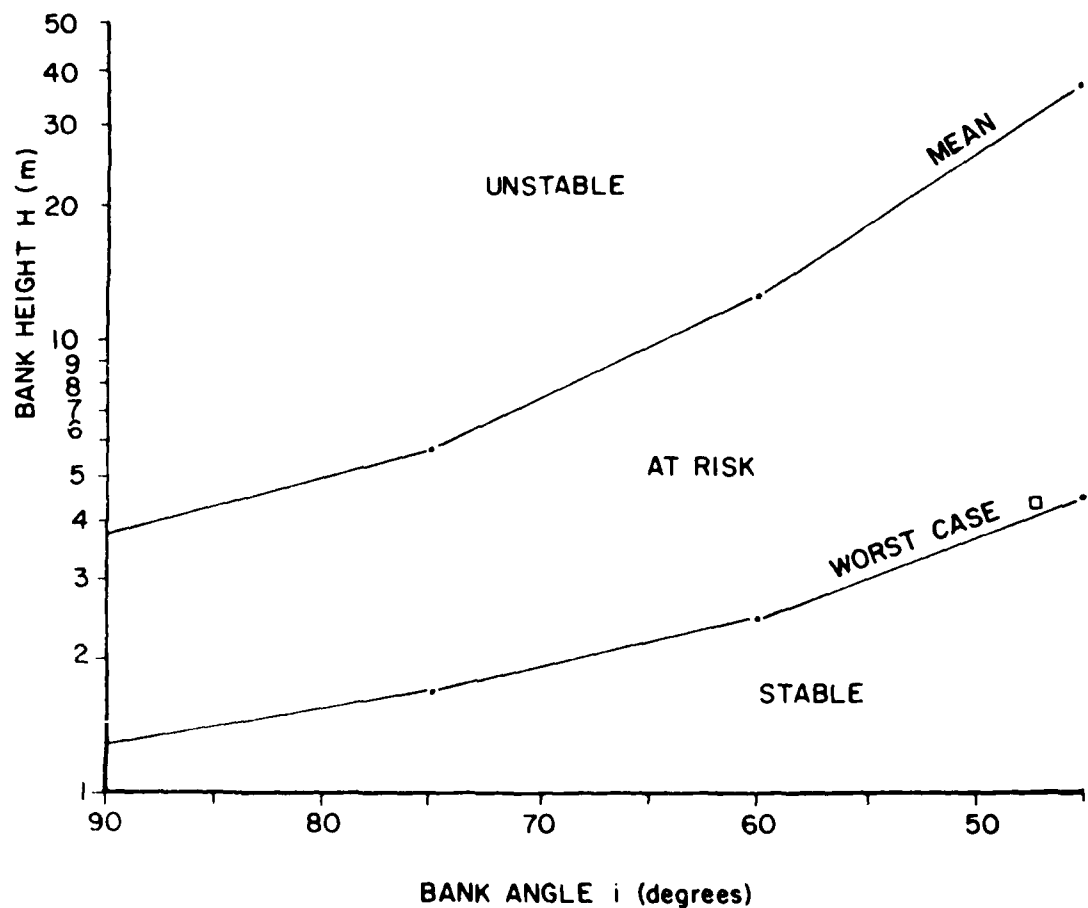


Figure 10b. Bank Stability Graph for Goodwin Creek at Katherine Leigh's site.

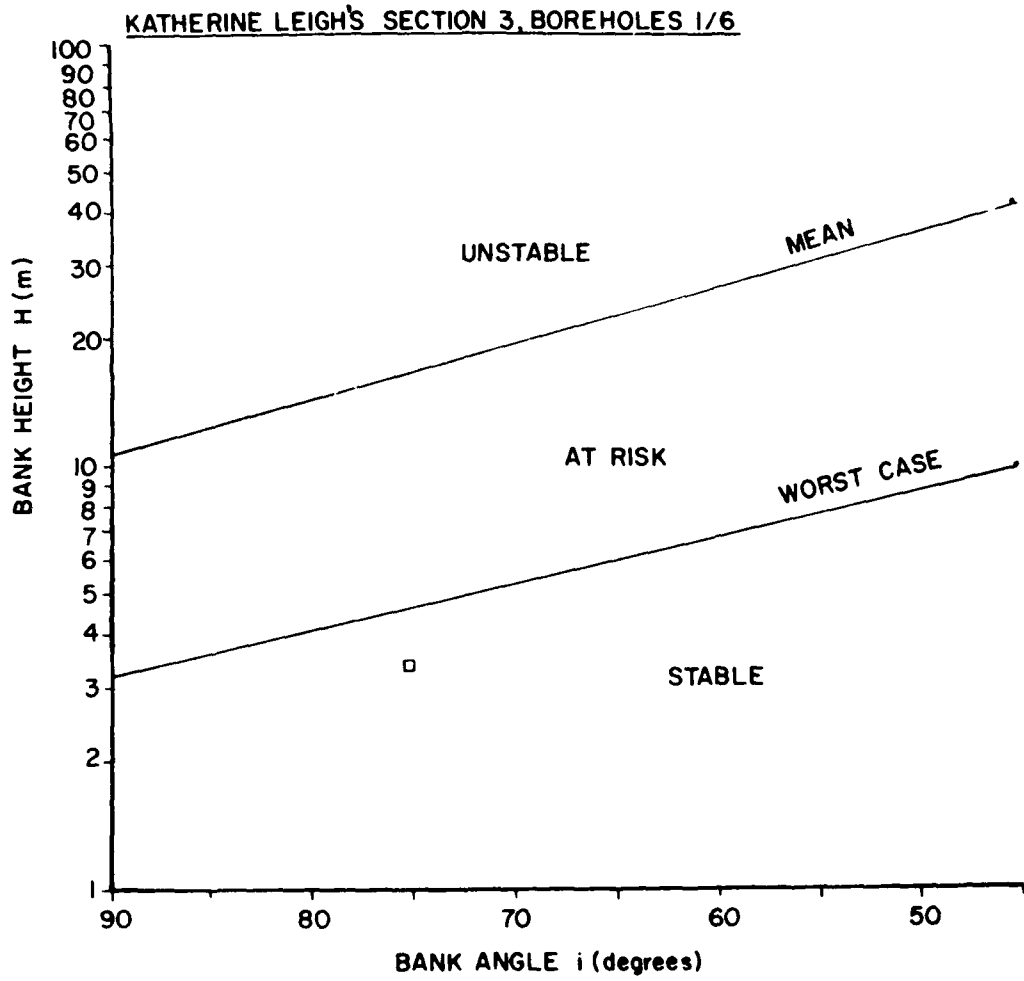


Figure 16c. Bank Stability Graph for Goodwin Creek at Katherine Leigh's site.

KATHERINE LEIGH'S SECTION 4, BOREHOLES 5/7

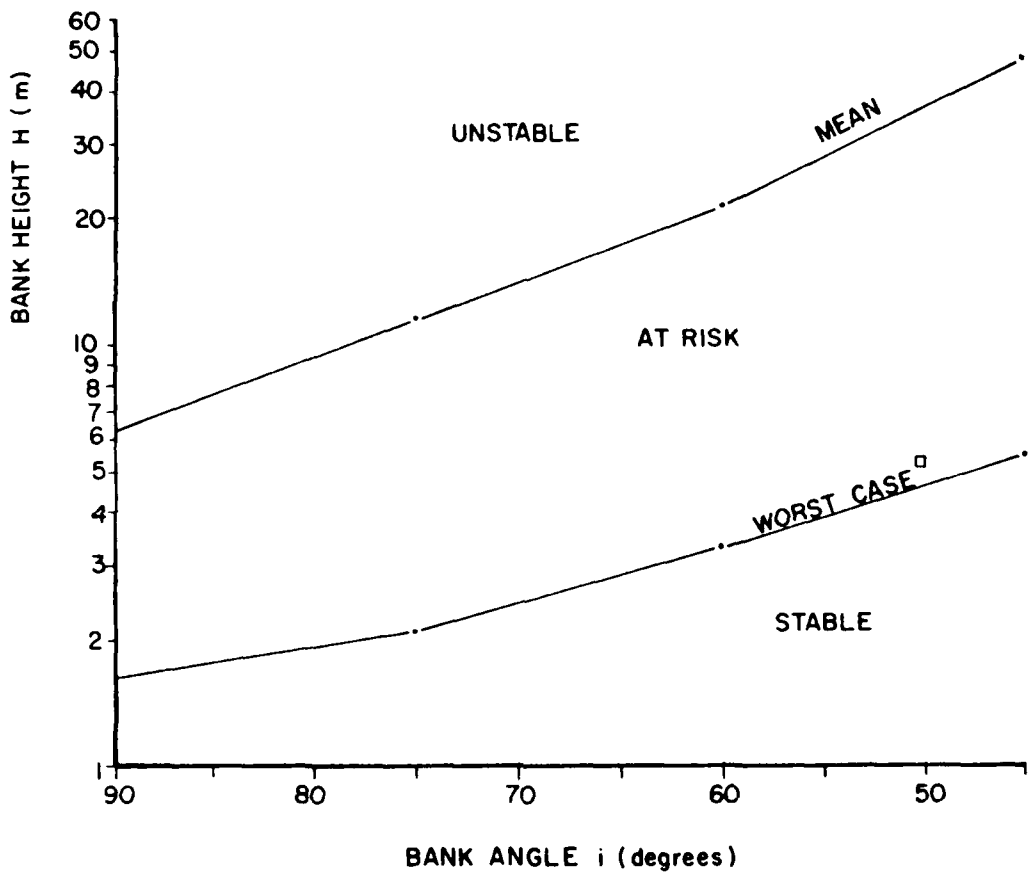


Figure 16d. Bank Stability Graph for Goodwin Creek at Katherine Leigh's site.

KATHERINE LEIGH'S SECTION 5, BOREHOLE 2

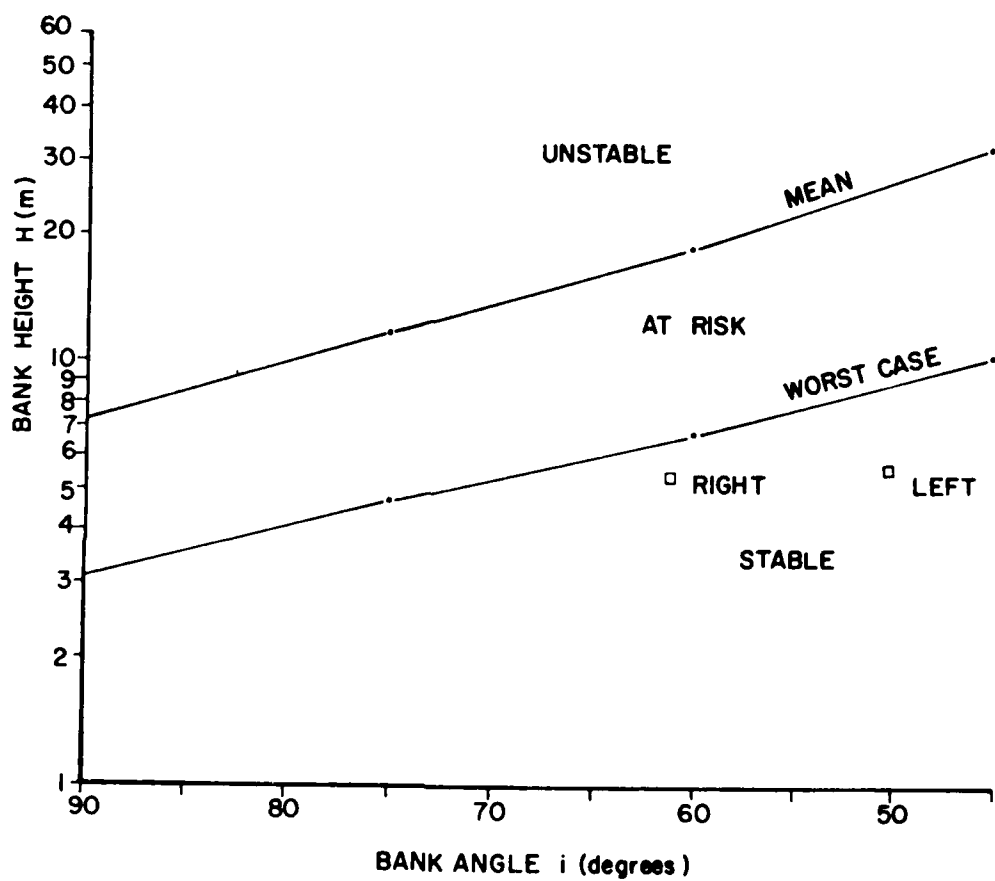


Figure 16e. Bank Stability Graph for Goodwin Creek at Katherine Leigh's site.

very likely to occur because both sections are located on the outside of a bend where high velocities and boundary shear stresses attack the bank toe during high flows (Fig. 17).

The reason that section 5 (left bank) is so much less stable than the other sections is the lack of old paleosol in the profile. At section 5 the present bank line intersects an old channel which is filled with sandy silt, the upper part of which weathered to form the young paleosol. These materials are weaker than old paleosol and also appear to be wetter because the old channel acts as an aquifer. This illustrates very clearly the localized effect that stratigraphy can have on bank stability.

On the basis of the stability analysis and interpretation, the authors draw the following conclusions and make the following predictions. Bank failures by slab failure will occur all along the left bank at the T.F. site and at the right bank in the bend downstream. Failures will be associated with wet periods when worst case conditions occur, especially after high flows have attacked the bank toe, removed basal accumulations of bank debris and oversteepened the bank. Section 5 (left bank) will experience serious retreat and erosion. Bank retreat and flood plain destruction will continue, with the sand bar growing, thus enhancing erosion of the toe of the left bank by deflecting the flow. The bendway will continue to develop, increasing channel sinuosity. The authors predict that serious bank erosion will continue at the T.F. site in years to come unless remedial measures are taken. The nature of remedial action which might be taken is discussed in section 6, 'Engineering Applications'.

In fact the banks at T.F.'s were stable throughout the summer of 1980 when the soil data were collected and this bears out the fact of plots of critical bank angles falling well below the critical line for mean elevations. Historically the left bank is known to be retreating rapidly, so the instability indicated by the analysis is real. Also, field observations show as predicted here, that most retreat takes place by mass failures during or after storm events in winter or spring. Then, to some extent the analysis and interpretation are confirmed. However, further resurveys and site monitoring are necessary to fully verify the conclusions and predictions.



Figure 17. View of Tommy Florence's Site showing eroding bank located at the outside of a developing bendway.

5.3.2 Johnson Creek at T.A. Woodruff's

Five cross-sections were surveyed at T.A. Woodruff's (T.A.W.) site. The sections are all upstream of a headcut, now stabilized by a grade control structure. Sections 2(R) and 4(L) plot just below the line of critical stability for worst case conditions, while section 5(L) plots just above it. All the other sections plot either well below the critical line, or are too gentle to plot on the graph at all (Fig. 15).

The interpretation of the graphs is that all the banks should be stable under mean conditions and that all except section 5(L) should also survive worst case conditions. However, the worst case factors of safety at sections 2(R) and 4(L) are only 1.2 and 1.1 respectively. Section 2(R) could be put at risk of failure by 0.6 m of basal scour, or 5° of oversteepening. For section 4(L) the figures are 0.3 m and 3°. Erosion on this scale could easily occur during high flow and so the authors do not expect these sections to remain stable in the long term. By contrast the other sections 1(L and R), 2(L), 3(L and R), 4(R) and 5(R) require considerable erosion to be put at risk. For example at section 1(R) the worst case factor of safety is 1.7. Nearly 3 m of basal scour or 15° of oversteepening would be needed to bring the bank to potential instability. Erosion on this scale would probably not occur as a result of high flows. It could, however, come about through progressive bed degradation associated with the passage of a headcut through the reach, or through basal attack of either bank due to the development of a meandering thalweg in the presently straight channel. The headcuts working upstream toward this reach have been held up by bands of stiff clay in the bed and have now been stabilized by three grade control structures downstream of the site. There is as yet little tendency for meandering although there are some point bars in the channel.

Section 5(L) is the only one which plots above the critical line for worst case conditions and which would be expected to fail in the near future without any change in geometry. Section 5 has been affected by the construction of the upstream grade control structure. Oversteepening and overheightening resulting from construction are probably the causes of potential instability.

On the basis of this stability analysis and interpretation, the authors draw the following conclusions and make the following predictions.

The banks at T.A. Woodruff's site are much more stable than those at Tommy Florence's. The main reason for this is that they are considerably lower, even though the bank angles, stratigraphy and soil properties are quite similar to those at Tommy Florence's. The banks are lower because the site is further upstream on Johnson Creek and has been much less affected by headcutting. This is an important point, illustrating that if headcuts can be controlled and stabilized, then the channel banks upstream can retain or recover their stability. At T.A.W.'s site the headcuts downstream have been stabilized by grade control structures and there should not be significant bed degradation. There is still the potential for bank instability due to meandering of the thalweg and, in due course, the channel. At T.A. Woodruff's site what potential there is for instability is associated with scouring in the pools opposite point bars in the channel at sections 2 and 4. Clearly instability can result from meander development even if grade control structures are successful in preventing degradation. It appears that most bank instability results from meandering of the thalweg and oversteepening of alternate banks along the channel. Without remedial action eventually this meandering phase can result in the destruction of the present flood plain by a process of lateral channel migration, and its replacement by a new flood plain at a level perhaps 3 to 5 meters lower. The degree to which meanders develop depends on the bed and bank materials, the water and sediment discharge, and perhaps most importantly the channel and valley slopes. In the case of Johnson Creek at T.A. Woodruff's the meandering tendency does not appear to be strong at the moment and the authors do not expect serious bank erosion to result from this process at this site (Fig. 18).

In the field it is clear that both banks at sections 1 and 3 are clearly more stable than those at Tommy Florence's. They are fairly well vegetated and show no signs of recent failures. Sections 2 and 4 have one very stable bank (2(L) and 4(R)) and one marginally stable bank (2(R) and 4(L)). In both cases the very stable bank is located behind the point bar while the less stable bank is next to the scour pool. At section 5 the right bank is stable but the left bank is unvegetated and appears to be potentially unstable. These observations support the stability analysis, interpretation and the conclusions drawn by the authors. Like Tommy Florence's site, T.A. Woodruff's site will be monitored and resurveyed to verify the conclusions and predictions.



Figure 18. View of T. A. Woodruff's Site showing straight channel and vegetated banks above the headcut (now stabilized by a grade control structure).

5.3.3 Goodwin Creek at Katherine Leigh's

Five cross sections were surveyed at Katherine Leigh's (K.L.) site. Sections 1, 2 and 4 plot above the line of critical stability for worst case conditions while sections 3 and 5 plot below that line (Fig. 16). This indicates that sections 1, 2 and 4 are at risk and could fail as a result of weakening by wetting or cracking, without any erosion. The minimum factors of safety at sections 3, 5(R) and 5(L) are 1.2, 1.2 and 1.6 respectively. At section 3, 0.9 m of basal scour or 8° of oversteepening would put the bank at risk of mass failure under worst case conditions. For section 5(R) the figures are 1.2 m and 9°, and for section 5(L), 3.4 m or 28°. The interpretation is that section 5(L) is a safe slope which will not fail due to overheightening unless there is major bed degradation. Considerable oversteepening would be necessary to cause instability and since the section is presently located behind a point bar this is unlikely to occur. The stability of sections 3 and 5(R) is fairly marginal. The amount of bed scour required to cause instability could occur during a flood but the banks are most susceptible to mass failure due to oversteepening - only single-figure increases in bank angle being necessary to put the banks at risk.

Sections 1, 2 and 4 are at risk because their soil profiles include large percentages of sandy silt, which is the weakest of the four materials found in the banks. By contrast the higher stability of section 3 is due to the band of old paleosol present there. Old paleosol is the strongest of the soils. Section 5 is formed in PSA and Young Paleosol and its overall strength lies somewhere between that of 1, 2, 4 and 3. As a result section 5 can support the highest banks at angles greater than 1, 2 and 4 but less than 3, with reasonable stability.

All the unstable or potentially unstable sections are located on the outside of bendways (Fig. 19) where the scour pool is close to the bank toe.

On the basis of this analysis and interpretation the authors draw the following conclusions and make the following predictions. Bank failures and serious bank retreat will occur at all the sections except 5(L) at Katherine Leigh's site. The most rapid retreat will take place at the right bank in the upstream bend, around sections 1 and 2 where the bank materials are weak and the scour pool is next to the toe. The bank at

AD-A101 389

SOIL CONSERVATION SERVICE OXFORD MS SEDIMENTATION LAB F/6 8/13
STREAM CHANNEL STABILITY, APPENDIX D, BANK STABILITY AND BANK M--ETC(U)
APR 81 C R THORNE, J B MURPHAY, W C LITTLE

UNCLASSIFIED

NL

2 x 3
40
201259

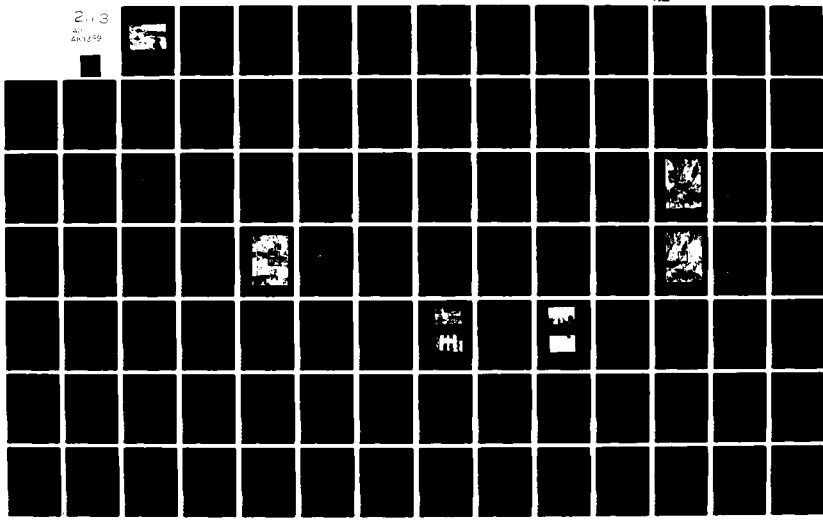




Figure 19. View of Katherine Leigh's Site showing eroding bank on the outside of a developing bendway and resistant materials at section 3.

section 3 should act as a hard point because of the old paleosol. Retreat should be less rapid and this might help to slow down the retreat of the right bank. Conversely, by directing the flow against the left bank it could worsen basal scour there and promote retreat. Conditions at the right bank might change if its retreat reveals old paleosol. This would result in a slowing of retreat, at least until basal scouring and oversteepening brought bank heights and angles back up to critical values. The banks at sections 4 and 5(R) will also continue to retreat, and the sinuosity of the reach will increase. Banks behind the point bars will be stable until downstream progression of the meander bends causes them to be attacked. At Katherine Leigh's site the major phase of downcutting and bed degradation seems to have finished and the site is now undergoing the second phase, that of increasing thalweg sinuosity and meandering. In the meandering channel the bank toe of the outer bank in bendways is attacked during flood flows by high velocities and boundary shear stresses (Bathurst, Thorne and Hey, 1979). The flow is therefore able to remove debris and erode intact bank toe material, oversteepening the bank and putting it at risk of mass failure. Failures are then triggered by worst case conditions associated with wetting. The slump material is removed by the flow to complete the cycle of mass failure. Bank retreat continues over the year, as long as the flow is competent to remove all of the slump debris and erode the toe. The rate of retreat is governed by the rate of toe erosion which in turn depends on the magnitude and frequency of flow events. This process-response system is called basal endpoint control (Thorne, 1981) and explains why toe protection is so vital to bank stability.

In the foreseeable future the authors predict that the flow at Katherine Leigh's site will be competent to remove all the bank debris and continue attacking the toe of the outer bank in the bendways. Very serious destruction of the present floodplain by lateral channel migration and increasing sinuosity will continue unless remedial steps are taken.

Field observation shows the right bank in the upper bendway around sections 1 and 2 to be retreating rapidly. Although it is stable under mean conditions, it appears to be highly unstable when wet. There are extensive tension cracks behind the bank and evidence of recent failures. Sections 3 and 4 are in a similar condition but seen to be retreating less rapidly because of the stiff layer of old paleosol which is present. At

section 5 the left bank is very stable and has a thick growth of vegetation suggesting that it has not failed recently. The right bank shows evidence of instability in the form of tension cracks, unvegetated surfaces and failure scars, and it is retreating. The extensive sand bars in the channel are growing and are responsible for fluvial attack of the toe of the outer banks in the bendways. The sinuosity of the thalweg and the channel at Katherine Leigh's has been increasing in recent years.

These observations support the interpretation and conclusions of the authors. As with the others, Katherine Leigh's site will be monitored and resurveyed to verify the predictions made by the authors.

5.3.4 Hotophia Creek

There were three main reasons why the authors wished to apply the stability analysis to Hotophia Creek. First, the bank sections at Hotophia Creek were resurveyed, so that it was possible to discriminate between banks which were stable and those which were unstable over the period of time between surveys. This made it possible to test the analysis in a way not possible in Johnson and Goodwin Creeks, where resurvey data were not available. Second, the large number of sections available for Hotophia Creek included some freshly failed banks where it was possible to estimate the depth of tension cracking at the time of failure and the width of the failure block. This made it possible to test the ability of the analysis to predict these parameters. Third, Hotophia Creek is perhaps typical of many creeks with bank stability problems but for which detailed bank material data, like those collected in this study, are not available. It is of interest to see whether the analysis could be extended to a creek where only estimates of the soil parameters were available.

It was known that the stratigraphy and the soil units at Hotophia Creek were generally similar to those in the adjacent Johnson and Goodwin Creek watersheds. Therefore the overall soil parameters were estimated from those for the Tommy Florence, T. A. Woodruff and Katherine Leigh sites. The parameters were calculated as follows: First the proportions of the bank made up by each soil unit (PSA, YP, OP and sandy/silt) at the three sites (TF, TAW, and KL) were averaged. Then the average proportion of each soil unit was multiplied by the average soil property (mean and worst case conditions) and the products summed to produce weighted average values for the three sites. These were taken to be representative of

Hotophia Creek. A similar approach was used in producing weighted average values for the calculation of the tension crack depth, but only the soils in the upper half the bank were considered as the crack forms in this part of the bank. The soil data and stability equations are listed in Table 17.

Bank Stability - The overall soil parameters are used together with the bank stability table (Table 6) to plot the lines of critical stability for mean and worst case conditions in Figure 20. The bank heights and angles observed in the field survey of January 1978 (Table 13) are plotted on the graph as dots or crosses depending on whether or not the bank had failed by the time it was resurveyed, in June 1979.

In theory the banks which failed (crosses in Fig. 20), should plot in the "at risk" zone on the stability chart. It would not be expected that points would plot in the "unstable" zone as banks in such an unstable state could not have been surveyed in the first place. Banks which did not fail should plot in the "stable" zone on the chart. Generally this is, in fact, the case in Figure 20 and is strong support for the validity of the stability analysis. Very few banks failed at angles of less than sixty degrees. The distribution of dots in this part of the graph suggests that the stability line is too low and should curve upward at bank angles less than sixty degrees. At higher bank angles, where most failures took place, there is excellent agreement and the line of critical stability for worst case conditions divides the unstable and stable banks most satisfactorily.

There are about six stable sections (dots) which plot significantly above the stability line, in the "at risk" zone and which according to the analysis would have been expected to have failed by the resurvey in June 1979. These could easily be explained by local variations in soil stratigraphy resulting in locally high bank material strength, (as observed at Katherine Leigh's site, section 3 on Goodwin Creek). However, further examination of the cross sectional data reveals another reason. All of the stable banks which plot in the "at risk" zone experienced net basal deposition between the surveys. As a result bank height was decreased (and in some cases bank angle was reduced) and stability was increased. For example, Figure 21 shows section T-51-8(L). The profile for January 1978 yields $H = 7 \text{ m}$, $i = 61^\circ$. This geometry puts the bank in the "at risk" zone in Figure 20, indicating that failure should be expected. The profile for

Table 17: Weighted Mean Soil Parameters for Hotophia Creek.

Soils	Proportion of Total Bank Height	Cohesion kPa	Friction Angle (°)	Bulk Unit Weight (kNm ⁻³)	Crack Depth (m)	Stability Equations
Entire Bank Height						
PSA	0.15					
YP	0.21	Mean	63.2	22.9	19.0	$H_{AV} = 3.32N_s - 6.92$
OP	0.48	W.C.	22.0	13.5	21.2	$H_{WC} = 1.04N_s - 2.45$
SAND 0.16						
Upper Half of Bank Only (for tension crack depth calculation)						
PSA	0.30					
YP	0.42	Mean	54.4	20.8	18.0	6.9
OP	0.28	W.C.	23.9	13.1	20.8	2.5

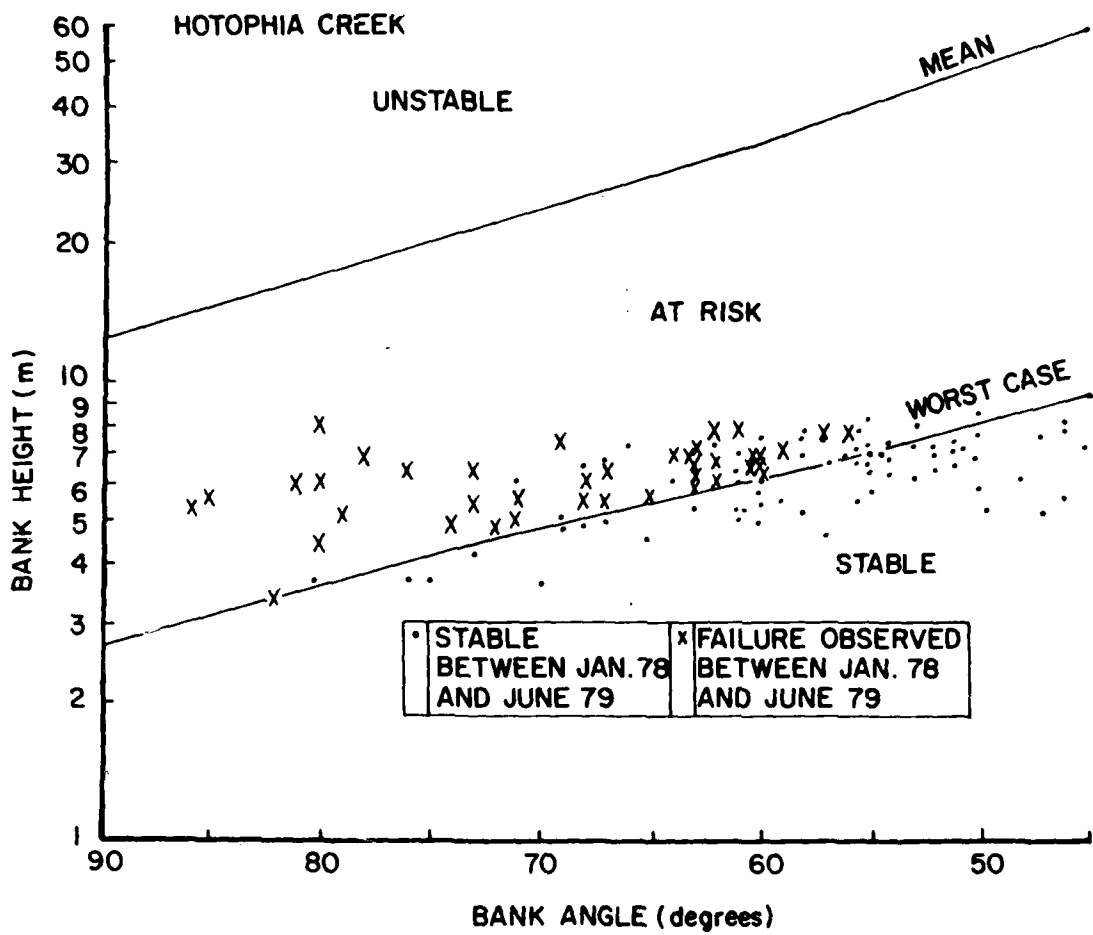
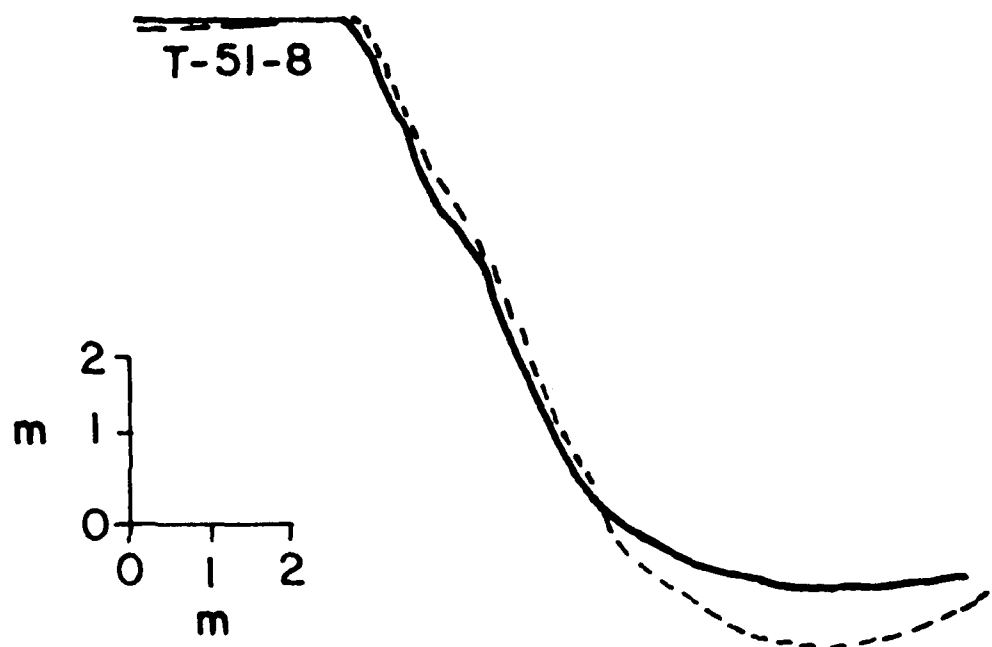


Figure 20. Bank Stability Graph for Hotophia Creek.



	DATE	HEIGHT	ANGLE
-----	JAN. 1978	7.0	61°
———	JUNE 1979	6.1	60°

Figure 21. Bank Cross Sectional Profiles at section T-51-8(L) on Hotophia Creek.

June 1979 shows that no failure did occur but that basal aggradation resulted in reduction of H to 6.1 m and i to 60° . This geometry would put the bank in the "stable" zone in Figure 20. The authors' interpretation of this phenomenon is that the conditions required for failure did not occur while the bank was at risk and that the bank was able to regain stability because of basal aggradation.

In many cases the bank experienced basal scour between the surveys, resulting in increased bank height and slope angle and decreased stability. For example Figure 22a shows section T-52-1 where bed degradation between January 1978 and June 1979 resulted in increases of bank height from 5.5 m and 5.0 m to 7.9 m and 7.5 m for the left and right banks respectively. Using the January 1978 data the banks plot as stable and they were stable up to June 1979. However, replottedting the banks in terms of the June 1979 data would show both banks to be "at risk" and would be expected to fail quite soon. The authors' interpretation of this phenomenon is that bed degradation can rapidly reduce bank stability and put a bank at risk of failure.

In some cases the large input of material associated with bank failure resulted in basal aggradation between January 1978 and June 1979 (Figs. 22b and 23). For example, Figure 23 shows section T-49-1(L). The bank plots as unstable (on January 1978 data) and failure did occur as expected. In its new configuration ($H = 7.3$ m, $i = 57^\circ$) the bank plots on the line of critical stability and could be stable (allowing for measurement error). Its future stability depends on whether it experiences basal aggradation, like section T-51-9 (Fig. 22b) or basal scour, like section T-52-1 (Fig. 22a).

These observations demonstrate the immediate impact of basal aggradation/degradation on bank stability. Thorne (1978, 1981) has shown how an eroding bank's stability and rate of retreat can be explained by the balance of input and removal of material from the bank toe. If the rate of input, from bank failures and upstream transport, exceeds the competence of the flow to remove material, then basal aggradation occurs, decreasing the bank height and slope angle, increasing its stability and reducing its rate of retreat. If the rate of input is smaller than the rate of removal then basal scour occurs, increasing bank height and slope angle, decreasing stability and accelerating the rate of retreat. If the two rates are

CHANNEL CROSS SECTIONS
HOTOPHIA CREEK

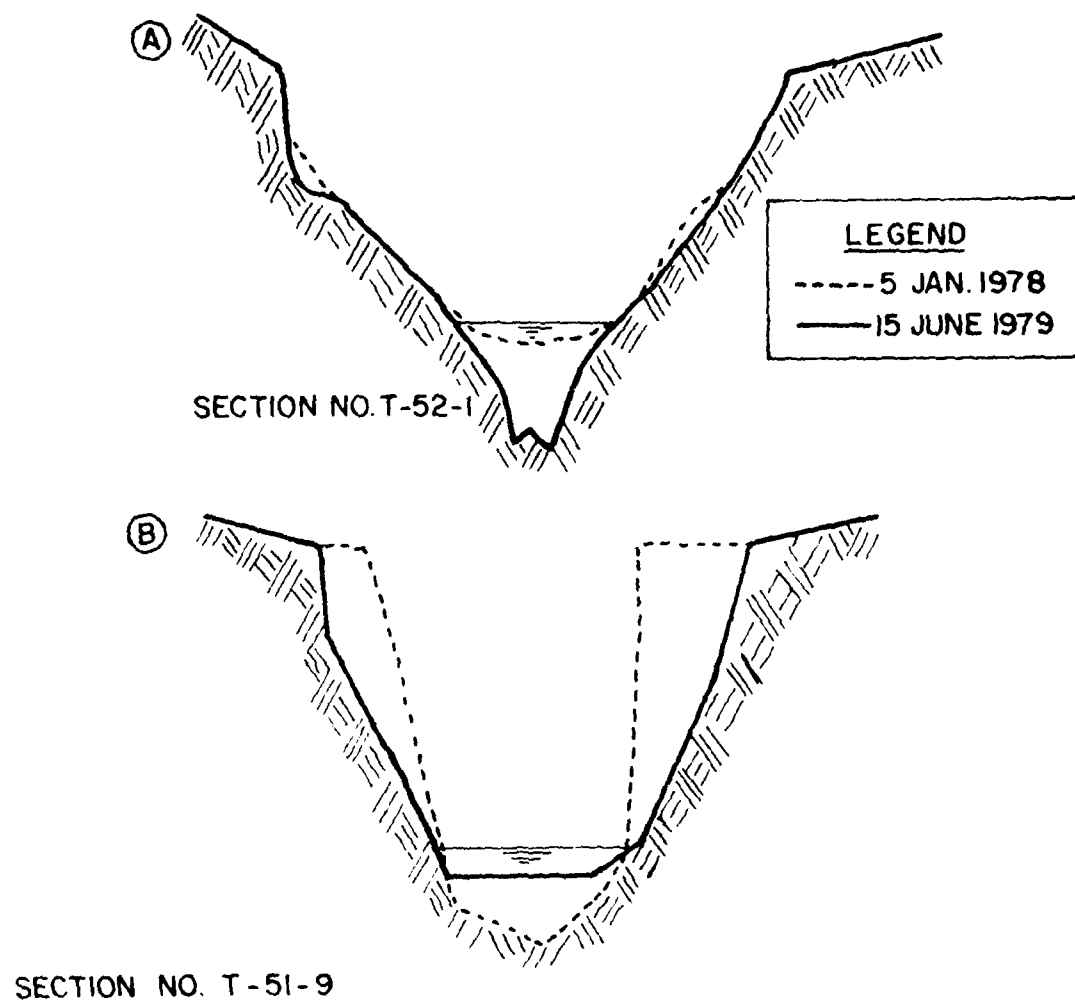
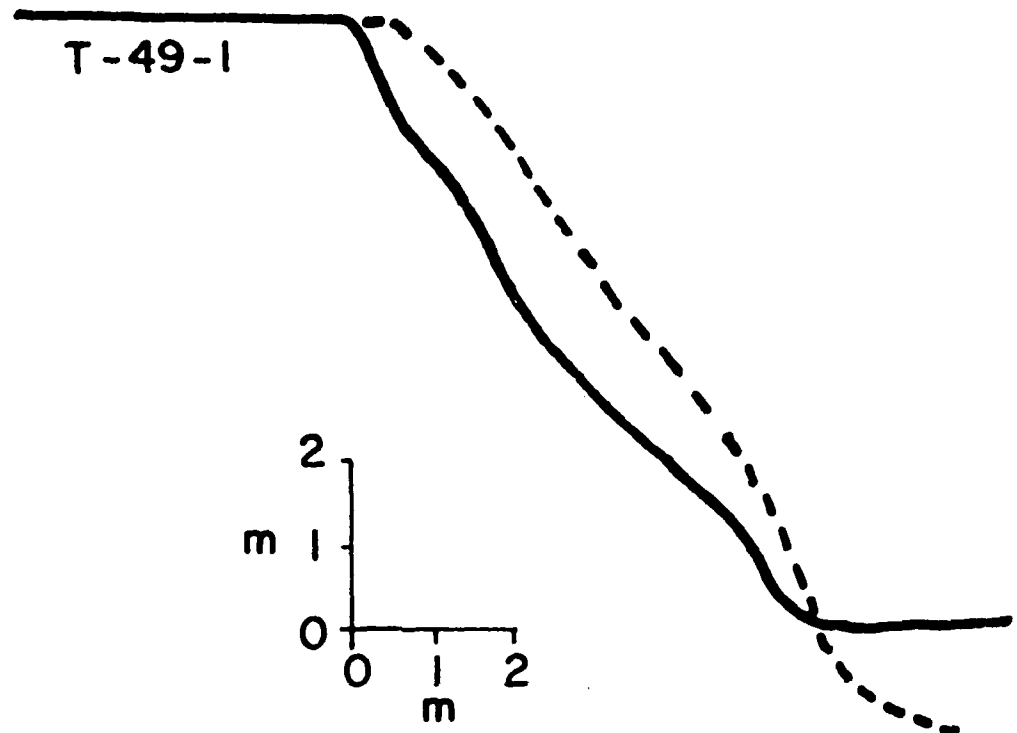


Figure 22. Cross Sectional Profiles on Hotophia Creek. a) Section T-52-1.
b) T-51-9.



	DATE	HEIGHT	ANGLE
-----	JAN. 1978	7.7m	56°
---	JUNE 1979	6.9m	53°

Figure 23. Bank Cross Sectional Profile at section T-49-1(L) on Hotophia Creek.

balanced, the bank retreats at a constant rate determined by the rate of basal removal of bank material by the flow. This concept, first developed for hillslopes by Carson and Kirkby (1972), is called basal endpoint control. The concept of basal endpoint control has been successfully applied to banks of many different structures and scales (Carson and Kirkby, 1972; Brunsden and Kesel, 1973; Thorne and Tovey, 1981).

In the case of the degrading bluff line streams like Hotophia, Johnson and Goodwin Creeks the concept of basal endpoint control explains very clearly why serious bank instability and rapid bank retreat is associated with gross bed degradation and why it is essential to halt bed degradation before attempting to stabilize the channel banks.

Tension Crack Depth - For mean and worst case soil conditions equations (5), (10) and (11) were used to calculate the depth of tension cracking. The depths were 6.9 m (mean) and 2.5 m (worst case). Some of the bank sections at Hotophia Creek showed very clear vertical faces at their tops which could be taken as being old tension cracks. Examples of this type of profile are shown in Figure 24. Plotting the distribution of crack depths as a histogram (Fig. 25) shows an almost normal distribution with a mean depth of 2.6 m and standard deviation of 0.7 m. There is then very good agreement between observed crack depths ($\bar{y} = 2.6$ m) and the prediction based on average, worst case soil properties ($y = 2.5$ m). Agreement for individual sections could probably also be obtained if soil data for those individual sections were available, so that the crack depth for particular cases could be calculated.

It appears from this comparison that calculations based on mean soil parameters overestimate the crack depth and that worst case values are in fact much more representative of field conditions.

Failure Block Widths - Lohnes and Handy (1968) presented an equation to calculate the width of the failure block for a vertical bank. This equation (12) can be modified to be applied to non-vertical banks without backslopes, and this produces:

$$b = \frac{(H_c - y)}{\tan(\frac{i}{2} + \frac{\phi}{2})} - \frac{H_c}{\tan i} \quad (14)$$

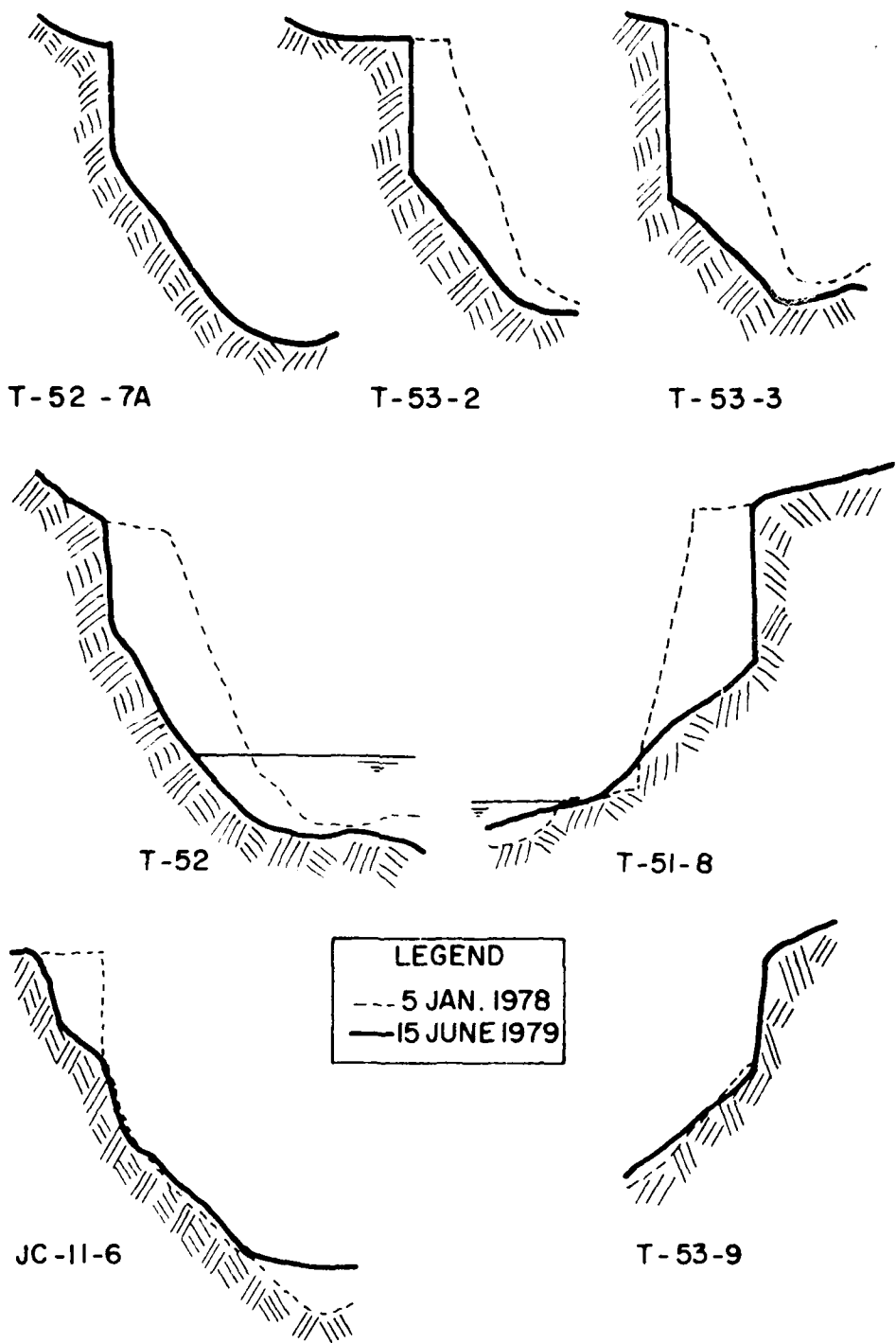


Figure 24. Bank Cross Sectional Profiles on Hotophia Creek showing vertical top sections, taken to indicate the depth of tension cracking at the time of failure, and retreat of bank top, taken to indicate failure block width.

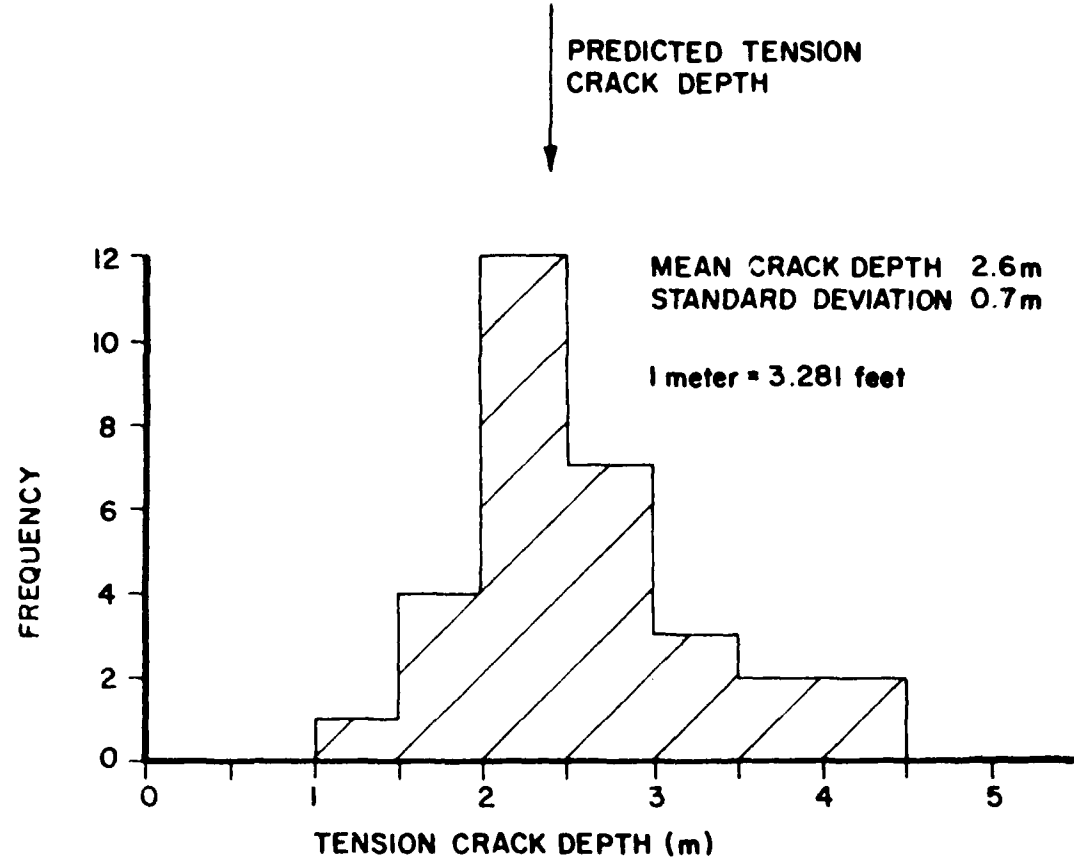


Figure 25. Observed and Predicted Tension Crack Depths for Hotophia Creek.

The equation has been applied to the Hotophia Creek sections where failures occurred between the two surveys and the width of the failure block in the field could be estimated. The observed and predicted failure block widths are compared in Figure 26.

The predictions are not really satisfactory. Agreement would probably be improved if soils data specific to each section were available. Usually the predicted width is an overestimate. The reason for this might well be that, in the field, the width of the failure block is controlled by ped fabric in the soil. This macrofabric consists of a polygonal pattern of evenly spaced, near vertical cracks, caused by lateral shrinkage during drying and desiccation.

This is one aspect of the analysis which requires further study. Also the field data (only 15 points) are not extensive and further observations should be made.

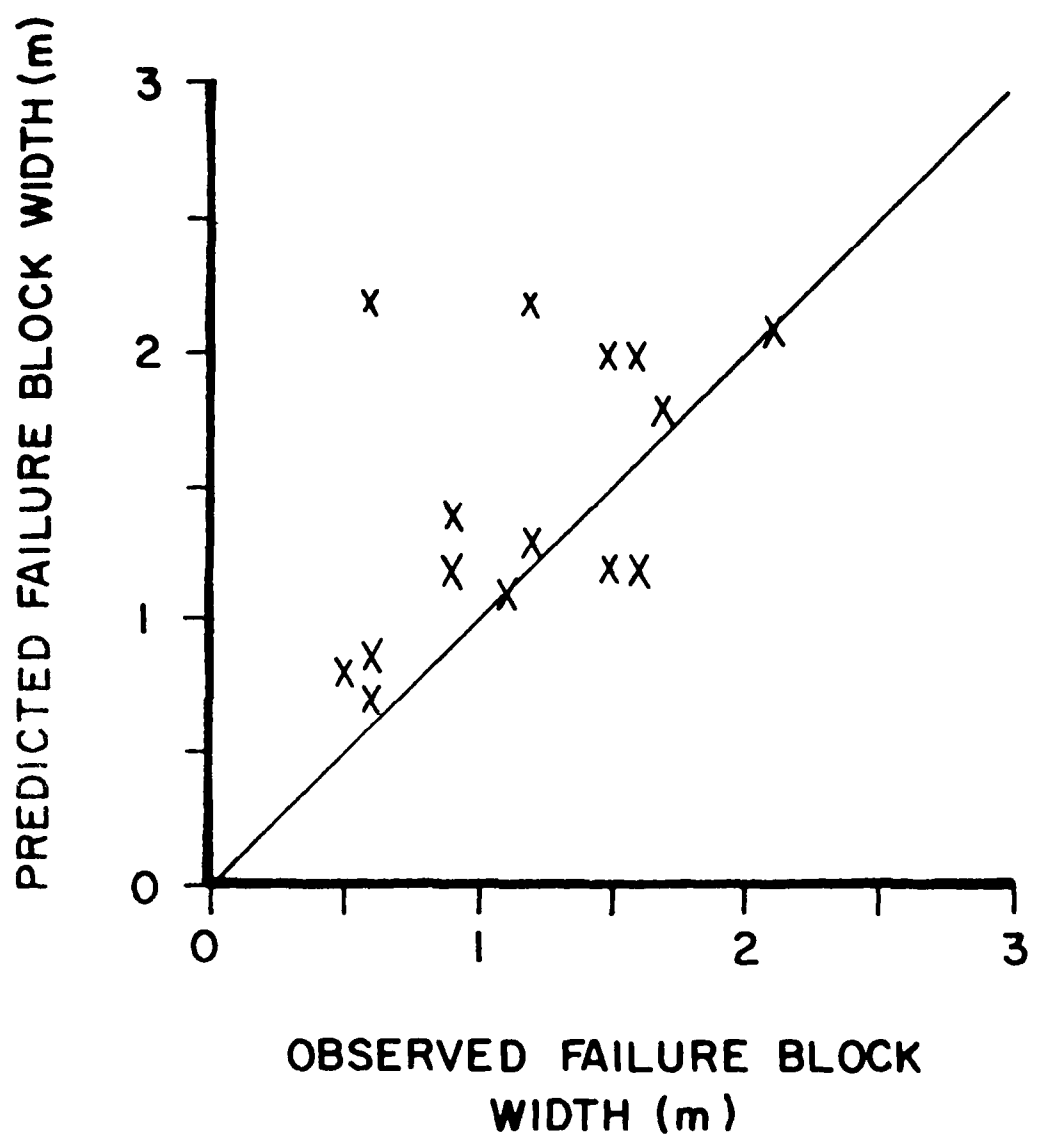


Figure 26. Observed and Predicted Failure Block Widths for Hotophia Creek.

6.1 BANK STABILIZATION

The most damaging impact of channel instability on a region is in the destruction of flood plain land by bank erosion. There are two primary causes of bank erosion in the bluff line streams of Mississippi. First, progressive bed degradation leading to bank instability (primarily through overheightening) and to widening of the channel. Second, toe erosion and basal scour at the outer bank in bendways leading to bank instability (primarily through oversteepening) and to lateral movement of meandering channels. In the field, evidence suggests that a major phase of bed degradation follows lowering of base level and or straightening. When the channel longitudinal profile has stabilized, a second phase of meandering and flood plain destruction occurs. Stability is finally re-established when a new flood plain is formed. This is at a lower level than that which was destroyed, and is an economically inferior soil. The stability analysis and field techniques developed and presented here could be useful when dealing with bank erosion associated with either phase.

In controlling bank erosion associated with bed degradation it is essential that a stable bed be established if bank stabilization measures are to be successful, because continued lowering of the bed will eventually result in the undermining and failure of any bank protection structures. With a lack of natural bed-rock controls on the bluff line streams, grade control structures are required to establish bed stability. However, a question arises immediately of how many structures are needed and how closely they should be spaced along the channel. To some extent this depends on the critical bank height. The stability analysis can be used here as an aid in estimating the maximum bank height which the bank materials can support. For example, at Hotophia Creek, if the bank height could be limited to about 5 m there probably would not be widespread bank failure due to overheightening (Figure 20). Consequently, grade controls should be positioned along the channel so that the degree of incision below the flood plain does not exceed about 5 m. Of course the bank angle is also a factor, and if some regrading of the steeper banks could be incorporated into the channel stability program, higher banks would be permissible.

In dealing with bank erosion in bendways the attack on the bank toe is a major problem. The reason for this is easily explained by the concept of basal endpoint control, outlined in the last section, and by the account of bend flow presented by Bathurst, Thorne and Hey (1979). Therefore it is vital that effective toe protection be established at the outer bank in eroding bendways. Once the toe has been stabilized, the stability analysis can be used as an aid in designing the regraded bank.

The safest approach in redesigning the bank is to grade it so that the bank angle is lower than the worst case friction angle of the bank material. This eliminates tensile stress from the bank and theoretically the bank should be stable to any height (Taylor, 1948). For example, in Johnson Creek the average worst case friction angle is 14.5° . In bank stabilization projects carried out on this creek a gradient of 1 on 3, or 18° has been used successfully and this is rather close to the worst case friction angle, suggesting that theory and practice may agree.

Often it may not be possible to grade the banks at such a comparatively low angle and in such cases higher angles may be used with a good chance of stability, provided they plot well below the line of critical stability for worst case conditions, in the "stable" zone of a stability chart based on the bank material properties. For example, the results for Hotophia Creek (Fig. 20) show that banks at angles with the horizontal of less than about 55° were stable with respect to mass failure. This figure could be used as a rule of thumb in regrading unstable banks on Hotophia Creek with a good chance of success.

The surface of any steep, but not vertical, bank in Mississippi must be protected from surface erosion by water running down the slope. Protection is best provided by carefully controlled overbank drainage and suitable vegetation. The role of vegetation in providing surface protection from both downslope and channel flow is well established, but vegetation can also play an important role in improving bank stability through the effect of plant roots in increasing the strength of the soil. Waldron (1977) has demonstrated that the shear strength of soils and the interfaces between layers of contrasting soils can be increased by 200% by strongly rooted species such as alfalfa. It is expected that even greater increases in the tensile strength would be recorded, and that the extent of

tension cracks behind steep banks could be reduced dramatically by establishing a hedge of strongly rooting species along the bank top. There is great potential for bank stabilization through the use of vegetation in the bluff line creeks if suitable plant species can be discovered. It was intended that part of this study should be devoted to evaluation of some of the plants currently under investigation at the Sedimentation Laboratory, but shortage of time precluded work on this objective. It is recommended that the study be extended to include the effects of vegetation in future.

6.2 CONCLUSIONS

The analysis presented here is not sophisticated. It deals only with log-spiral toe failure of a bank with a tension crack. It cannot account for other types of failure such as transitional failure associated with a very weak layer in the bank. When a very weak layer is present most of the failure plane forms in it and the geometry of the failure plane is no longer log-spiral. Such situations must be dealt with individually, depending on the stratigraphy of the bank and the soil properties.

The reasonable results for the soil strength tests, the success of the analysis as applied to the sites on Johnson and Goodwin Creeks, and the good agreement between observed and predicted stability on Hotophia Creek all suggest that the approach developed here could be used to predict bank stability with some confidence in engineering projects in the bluff line streams. Certainly there is still much research and development work to be done to refine and improve the analysis.

ACKNOWLEDGEMENTS BY THE SENIOR AUTHOR

The work reported in this appendix was undertaken while I was a visiting scientist with the Channel Stability Group at the USDA-SEA Sedimentation Laboratory at Oxford, Mississippi and a visiting professor at Mississippi State University. This visit was made possible only through the efforts and cooperation of Dr. D. G. DeCoursey (Director) and Dr. W. Campbell Little (Group Leader) of the Sedimentation Lab., Mr. B. R. Winkley (Chief) of the Potamology Section, Vicksburg District, Corps of Engineers, and Professor F. D. Whisler, of the Agronomy Department, Mississippi State University. I thank most sincerely each of those individuals and their organizations for all their efforts. Also, I thank the supervisor of my research post in England, Dr. R. D. Hey, and the funding organization, the Natural Environment Research Council, for leave of absence to make the visit.

The project would have been impossible without the help and support I received from the professional, technical and administrative staff of the Sedimentation Laboratory. In this respect Mrs. Tommie Simpson, Administrative Officer, deserves special thanks for solving numerous administrative problems concerned with my visit and arranging for me to be paid at regular intervals. The staff of the Computing Section were especially helpful and I mourn with all of the staff the recent deaths of Mr. Gerald Bolton and Mr. Bob Wilson, two fine men.

I had the pleasure of working with and getting to know Dr. Earl Cressinger, Dr. Carlos Alonso and Mr. Paul Hawks and the joys of field work during the hottest summer on record were shared with me by Mr. Joe Murphey and Mr. Gwyn Smith. One of my co-authors, Mr. Joe Murphey taught me a lot about Mississippi, its flora, fauna and history and for all of that I am very grateful.

Finally, I must mention and thank my good friend and mentor at Oxford, Dr. Neil L. Coleman, who was always available to discuss my problems and counsel me wisely.

To all at Oxford, Thank You.

Colin R. Thorne

REFERENCES

Ajaz, A. and Parry, R. H. G. (1974) "An Unconfined Direct Tension Test for Compacted Clays," *Journal of Testing and Evaluation, ASTM*, 2, No. 3, pp. 163-172.

Bathurst, J. C., Thorne, C. R. and Hey, R. D. (1979) "Secondary Flow and Shear Stress at River Bends," *Journal of the Hydraulics Division, ASCE*, 105, HY10, Proc. Paper 14906, pp. 1277-1295.

Bishop, A. W. and Garga, V. K. (1969) "Drained Tension Tests on London Clay," *Geotechnique*, London, England, Vol. 19, No. 3, pp. 310-313.

Bishop, A. W. and Henkel, D. J. (1957) "The Measurement of Soil Properties in the Triaxial Test," *Edward Arnold*, London (2nd Edition 1962), 227 p.

Bradford, J. M. and Piest, R. F. (1977) "Gully Wall Stability in Loess-Derived Alluvium," *Soil Science Society of America Journal*, 41, No. 1, pp. 115-122.

Bradford, J. M. and Piest, R. F. (1980) "Erosional Development of Valley-Bottom Gullies in the Upper Midwestern United States," In, *Thresholds in Geomorphology*, D. R. Coates and J. D. Vitak (Eds.), pp. 75-101.

Brunsden, D. and Kesel, R. H. (1973) "Slope Development on a Mississippi River Bluff in Historic Time," *Journal of Geology*, 81, pp. 570-598.

Carson, M. A. (1971) "The Mechanics of Erosion," *Pion Press*, 167 p.

Carson, M. A. and Kirkby, M. J. (1972) "Hillslope Form and Process," *Cambridge Univ. Press*, Cambridge, England, 475 p.

Chen, W. F. (1975) "Limit Analysis and Soil Plasticity," *Elsevier Scientific Publishing Co.*, New York, 638 p.

Dent, J. H., Jr., Galberry, H. S., Huddleston, J. S., and Thomas, A. E. (1963) "Soil Survey of Panola County, Mississippi," *Soil Conservation Service, USDA*, 63 p., 122 maps.

Fellenius, W. (1939) "Erdstatische Berechnungen mit Reibung und Kohäsion, Adhäsion, und unter Annahme kreiszylindrischer Gleitflächen," Rev. ed., W. Ernst and Sohn, Berlin.

Handy, R. L. and Fox, N. W. (1967) "A Soil Borehole Direct-Shear Device," *Highway Research Board News*, 27, pp. 42-51.

Handy, R. L. (1975) Discussion of 'Measurement of In situ Shear Strength' by J. H. Schmertmann, in 'In situ Measurement of Soil Properties' *Proceedings of the Specialty Conference of the Geotech. Engrg. Div., ASCE*, V.II, pp. 143-149.

Handy, R. L., Pitt, J. M., Engle, L. E. and Klockow, D. E. (1976) "Rock Borehole Shear Test," Proc. 17th Symposium on Rock Mechanics, pp. 4B6-1 to 4B6-11.

Lambe, T. W., and Whitman, R. V. (1979) "Soil Mechanics, SI Version," John Wiley and Sons, New York, 553 p.

Lo, K. Y. (1970) "The Operational Strength of Fissured Clays," Geotechnique, 20, pp. 57-74.

Lohnes, R. A. and Handy, R. L. (1968) "Slope Angles in Friable Loess," Journal of Geology, 76, pp. 247-258.

Lohnes, R. A., Klaiber, F. W. and Dougal, M. D. (1980) "Alternate Methods of Stabilizing Stream Channels in Western Iowa," Final Report, ISU-ERI-AMES-81047, Project 1421, Iowa State University, Ames, Iowa 50010, 132 p.

Luttenegger, A. J., Remmes, B. D. and Handy, R. L. (1978) "Borehole Shear Test for Stiff Soil," Journal of the Geotechnical Engineering Division, ASCE, Technical Note, 104, GT11, pp. 1403-1407.

Lutton, R. J. (1969) "Fractures and Failure Mechanics in Loess and Applications to Rock Mechanics," Research Report S-69-1, U.S. Army Engineers, WES, Vicksburg, Mississippi, 53 p.

Lutton, R. J. (1974) "Use of Loess Soil for Modeling Rock Mechanics," Misc. Report S-74-28, U.S. Army Engineers, WES, Vicksburg, Mississippi, 163 p.

Schmertman, J. H. (1975) "In Situ Measurement of Soil Strength," In, ASCE Specialty Conference on In Situ Measurement of Soil Properties, Vol. I, pp. 57-179.

Sowers, G. B., and Sowers, G. F. (1965) "Introductory Soil Mechanics and Foundations," 2nd Ed., MacMillan Co., New York, 386 p.

Taylor, D. W. (1948) "Fundamentals of Soil Mechanics," John Wiley and Sons, New York, 700 p.

Terzaghi, K. (1943) "Theoretical Soil Mechanics," John Wiley and Sons, New York, 510 p.

Terzaghi, K. and Peck, R. B. (1948) "Soil Mechanics and Engineering Practice," John Wiley and Sons, New York, 566 p.

Thorne, C. R. (1978) "Processes of Bank Erosion in River Channels," Unpublished thesis submitted to the University of East Anglia, Norwich, England, in complete fulfillment of the requirements of the degree of Doctor of Philosophy, 447 p.

Thorne, C. R., Tovey, N. K. and Bryant, R. (1980) "Recording Unconfined Tension Testing Apparatus," Journal of the Geotechnical Engineering Division, ASCE, 106, G.T.11, pp. 1269-1273.

Thorne, C. R. and Tovey, N. K. (1981) "Stability of Composite River Banks," Earth Surface Processes and Landforms, John Wiley and Sons, London, England, (In Press).

Thorne, C. R. (1981) "Processes and Mechanisms of River Bank Erosion," In Proceedings of the International Workshop on Engineering Problems in the Management of Gravel-Bed Rivers, Gregynog, Wales, June 23-28, 1980. John Wiley and Sons, London, England, In Press.

Turnbull, W. J. (1948) "Utility of Loess as a Construction Material," Proceedings of the International Conference on Soil Mechanics, Rotterdam, 5, pp. 97-103.

Waldron, L. J. (1977) "The Shear Resistance of Root Permeated Homogeneous and Stratified Soil," Soil Sci. Soc. Am. Jour., 41, No. 5, pp. 843-849.

Whitten, C. B. and Patrick, D. M. (1981) "Engineering Geology and Geomorphology of Streambank Erosion, Report 2, The Yazoo River Basin Uplands," U.S. Army Engineers, WES, Vicksburg, Mississippi, Technical Report, In Press.

Wineland, J. D. (1975) "Borehole Shear Device," Proceedings of the Conference on In Situ Measurement of Soil Properties," ASCE, Vol. 1, pp. 511-535.

Yang, K. H. (1975) "Shear Strength of Chemically Modified Soils," Appendix B "Modification of Borehole Shear Contact Plates." Thesis Presented to Iowa State University, Ames, Iowa, in partial fulfillment of the requirements for the Degree of Master of Science.

ADDENDUM 1

FIELD SITES

Addendum 1
List of Tables

Table No.	Title	Page
1.1	Boring and Testing Record; Tommy Florence property - Lower Johnson Creek, SE $\frac{1}{4}$, NW $\frac{1}{4}$, SE $\frac{1}{4}$, Sec. 3, T.10S., R.7W	154
1.2	Boring and Testing Record; T. A. Woodruff property - Upper Johnson Creek, SW $\frac{1}{4}$, NE $\frac{1}{4}$, Sec. 20, T.9S., R.6W	155
1.3	Boring and Testing Record; Katherine Leigh property - Lower Goodwin Creek, NW $\frac{1}{4}$, SE $\frac{1}{4}$, SW $\frac{1}{4}$, Sec. 2, T.10S., R.7W	156

Addendum 1
List of Figures

Figure No.	Title	Page
1.1	Physiographic Setting of Peters Creek Watershed	123
1.2	Geologic Map of Peters and Hotophia Creek Watersheds after Vestal (1956)	124
1.3	Geographic Locations of the Test Sites shown on Soil Map of Area	130
1.4	Valley-normal soil transects at each test site (schematic) . .	131
1.5	Aerial Photo of Lower Johnson Creek (Florence) site	133
1.6	Locations of Florence site test holes & cross sections	134
1.7	Florence site Cross Section XS-1	135
1.8	Florence site Cross Section XS-2	136
1.9	Florence site Cross Section XS-3	137
1.10	Florence site Cross Section XS-4	138
1.11	Florence site Cross Section XS-5	139
1.12	Aerial Photo of Upper Johnson Creek (Woodruff) site	140
1.13	Locations of Woodruff site test holes & cross sections	141
1.14	Woodruff site Cross Section XS-1	142
1.15	Woodruff site Cross Section XS-2	143
1.16	Woodruff site Cross Section XS-3	144
1.17	Woodruff site Cross Section XS-4	145
1.18	Woodruff site Cross Section XS-5	146
1.19	Aerial Photo of Lower Goodwin Creek (Leigh) site	147
1.20	Locations of Leigh site test holes & cross sections	148
1.21	Leigh site Cross Section XS-1	149
1.22	Leigh site Cross Section XS-2	150
1.23	Leigh site Cross Section XS-3	151
1.24	Leigh site Cross Section XS-4	152
1.25	Leigh site Cross Section XS-5	153
1.26	Drill rig used in Borehole Shear Test program	157
1.27	2" and 3" Quick-Relief Soil Tubes, Bits, and Vacuum-ball Soil Tube Heads	157

1.28 Split-spoon Samplers	159
1.29 Borehole Cover Plug	159
1.30 Well Log Legend	161
1.31 T. Florence site - Borehole #1	162
1.32 T. Florence site - Borehole #2	163
1.33 T. Florence site - Borehole #3	164
1.34 T. Florence site - Borehole #4	165
1.35 T. Florence site - Borehole #5	166
1.36 T. Florence site - Borehole #7	167
1.37 T. Florence site - Borehole #9	168
1.38 T.A. Woodruff site - Borehole #1	169
1.39 T.A. Woodruff site - Borehole #2	170
1.40 T.A. Woodruff site - Borehole #3	171
1.41 T.A. Woodruff site - Borehole #4	172
1.42 T.A. Woodruff site - Borehole #5	173
1.43 T.A. Woodruff site - Borehole #6	174
1.44 T.A. Woodruff site - Borehole #6a	175
1.45 T.A. Woodruff site - Borehole #7	176
1.46 T.A. Woodruff site - Borehole #8	177
1.47 T.A. Woodruff site - Borehole #9	178
1.48 T.A. Woodruff site - Borehole #10	179
1.49 T.A. Woodruff site - Borehole #11	180
1.50 K. Leigh site - Borehole #1	181
1.51 K. Leigh site - Borehole #2	182
1.52 K. Leigh site - Borehole #3	183
1.53 K. Leigh site - Borehole #4	184
1.54 K. Leigh site - Borehole #5	185
1.55 K. Leigh site - Borehole #6	186
1.56 K. Leigh site - Borehole #7	187

1.1 INTRODUCTION

The Peters Creek Watershed lies partially within the North Central Hills physiographic subprovince on the east and partially within the Bluff Hills subprovince on the west (Fig. 1.1.). It is tributary to the Yocona River which parallels the southern Panola County boundary. The Yocona River exits the Bluff Hills into the Mississippi Alluvial Valley about 4 miles west of its confluence with Peters Creek.

The western portion of the 87 square mile watershed area is blanketed with layers of loess which thicken to the west. The eastern portion of the watershed has a thin veneer of loess but it is broken more often than not by gulleys and valley incisions into the underlying materials. The valleys are filled with alluvium of fairly recent origin, most derived from erosion of the adjacent low loess covered hills.

The cores of most of the low hills consist of alluvial gravels and sands with some clay lenses. Figure 1.2 is a map of the geology of the area as described by Vestal (1956). Also included is the geology of the Hotophia Creek Watershed area to the north. Investigations of the Channel Stability Unit at the USDA Sedimentation Laboratory over the past four years have determined that the surface material shown as Eocene in the eastern portion of the map (Kosciusko, Zilpha-Winona and Tallahatta formations) is actually much younger alluvium. This entire geologic assemblage lies above a regional erosion surface developed on Tertiary marine shales & mudstones. The alluvial material in the valleys occurs in the same predictable stratigraphic sequence of lithologies throughout the entire area, and therefore is probably the result of regional paleoclimatic conditions (for more discussion, see Appendix E).

The valley stratigraphy consists of only six primary deposits which govern processes affecting bank stability. They are from youngest to oldest: (1) post-settlement alluvium (PSA), a widely variable thickness of layered fines washed into the valleys since cultivation of the uplands by European settlers began in the 1830's; (2) a young buried paleosol (YP), a fine silty to medium sandy channel infilling about 3000 ^{14}C years old; (3) an older buried paleosol (OP), a predominantly fine, highly-weathered, polygonally-cracked, low energy deposition deposit about 8000 to 5000 ^{14}C

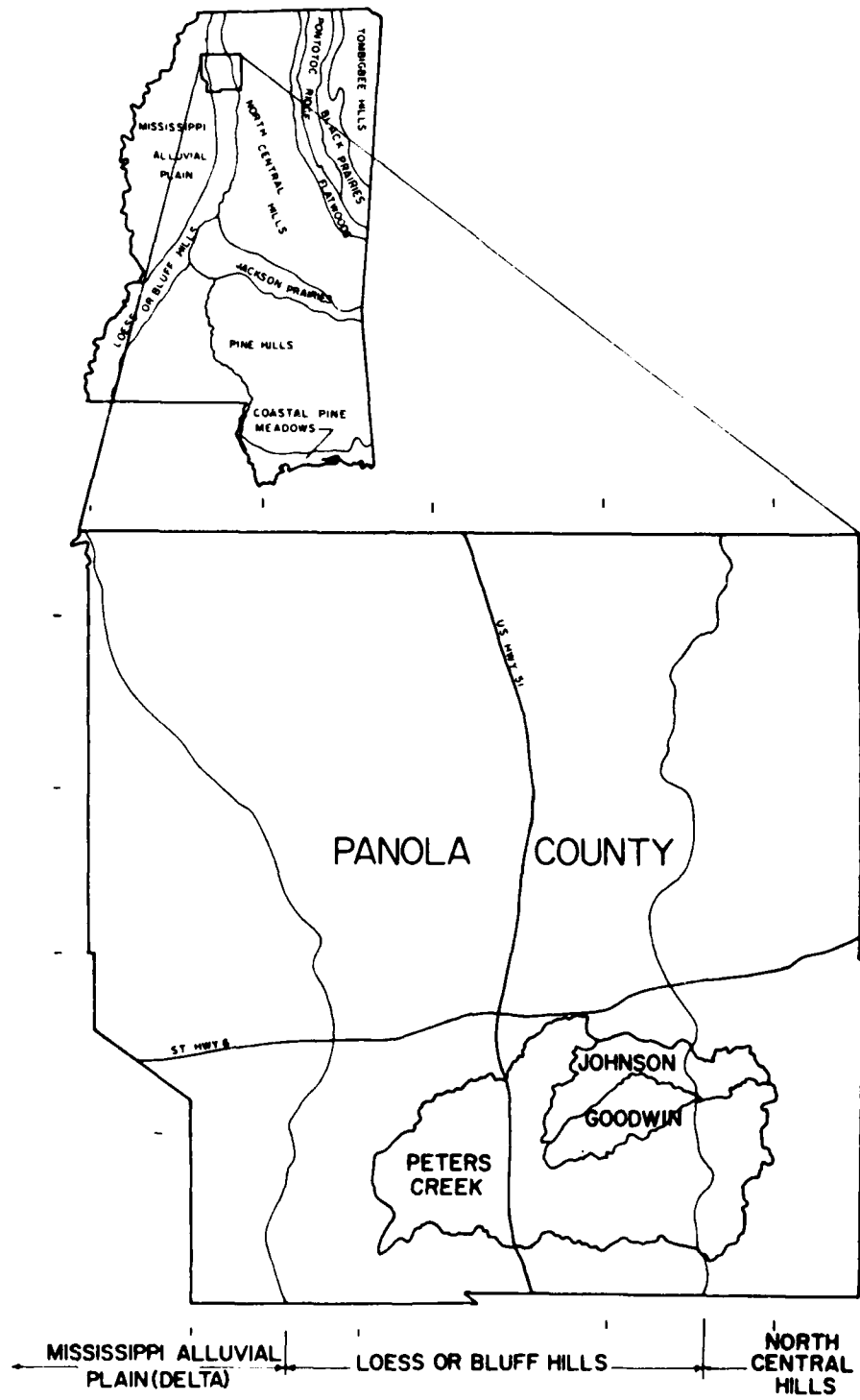


Figure 1.1. Physiographic Setting of Peters Creek Watershed.

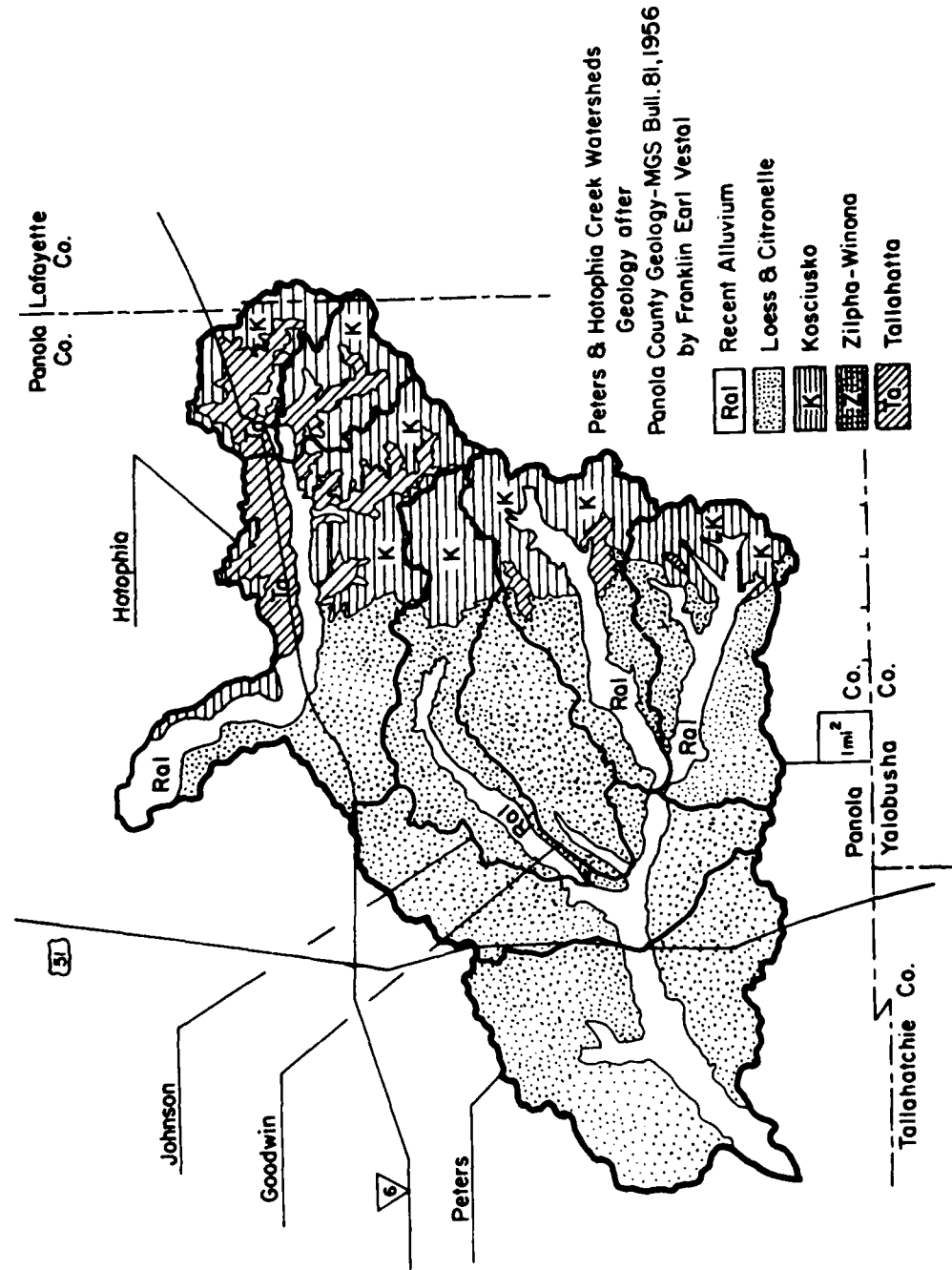


Figure 1.2. Geologic Map of Peters and Hotophia Creek Watersheds after Vestal (1956).

years old; (4) an organic bog deposit liberally interspersed with (5) coarse sand and gravel lag deposits, both of which are about 10,000 ^{14}C years old, and (6) remnants of a layer (or layers) of ferruginous to siliceous sandstones at the base of the above deposits. The precipitates in the sandstones are post-depositional. The sandstones cross many bedding planes, contain some carbon older than 40,000 ^{14}C years before present (B.P.), and display current magnetic alignment. All one can say about their age, at this time, is that they are older than 40,000 ^{14}C years B.P. but younger than 700,000 years, the approximate time of the last magnetic reversal. At this time the only ages that can be assigned to the alluvial sands & gravels in the cores of the hills is Post-Eocene. The loess caps on the hill crests are of Peoria, Roxana, and Loveland ages.

Most of the soils and paleosols that control channel bank stability in the valleys are derivatives of the above mentioned loess materials although some portions are derived from the sands and gravels. The following soil descriptions are from pages 6 & 7 and pages 56 & 57 of the SCS Panola County soil survey, Soil Survey Series 1960, No. 10 (Dent, et al., 1963).

"The Alluvial soils occur in transported material of fairly recent deposition. Horizonation is weak or lacking in these soils because the soil-forming processes have not had enough time to develop a well-developed profile.

Members of the Alluvial great soil group in Panola County are the Collins and Falaya soils.

Collins Series

This series consists of moderately well drained, strongly acid to medium acid soils that formed in silty alluvium on nearly level bottom lands. The dominant slope range is 0 to 3 percent.

In most places the surface layer and upper part of the subsoil are dark-brown silt loam. The lower subsoil is dark-brown silt loam with many gray and yellowish-brown mottles.

The Collins soils occur with the Falaya and the Waverly soils. They are better drained than the Falaya and Waverly soils and are free of mottles to a greater depth.

In this county the Collins soils are mainly on bottom lands in the hilly parts. Small areas are on the delta adjacent to the bluffs. About 65 percent of the acreage is in row crops, 34 percent is in

pasture, and 1 percent is in trees. The principal row crops are cotton and corn.

Collins silt loam (0 to 2 percent slopes)(Cm). -- This is a moderately well drained, friable soil on nearly level bottom lands. The major layers are as follows:

0 to 6 inches, dark-brown, friable silt loam.

6 to 24 inches, brown, friable silt loam with light yellowish-brown mottles.

24 to 48 inches, yellowish-brown, friable silt loam with dark yellowish-brown, light-gray, and very pale brown mottles.

Profile description of Collins silt loam (0 to 2 percent slopes) in a cultivated field 3 miles east of Como (NW $\frac{1}{4}$ NE $\frac{1}{4}$ Sec. 1, T.7S., R.7W.):

A_p - 0 to 6 inches, brown or dark-brown (10YR 4/3) silt loam; weak, fine granular structure; friable; many fine and medium roots; strongly acid or medium acid; clear, wavy boundary.

C₁ - 6 to 24 inches, brown or dark-brown (10YR 4/3) to dark yellowish-brown (10YR 4/4) silt loam with few, fine, faint, light yellowish-brown (10YR 6/4) mottles; structureless; friable; common fine roots; strongly acid or medium acid; clear, wavy boundary.

C₂ - 24 to 48 inches +, yellowish-brown (10YR 5/4) silt loam with many, fine, faint and distinct, dark yellowish-brown (10YR 4/4), light-gray (10YR 7/2), and very pale brown (10YR 7/3) mottles; structureless; friable; few fine, soft, brown concretions; few fine roots; strongly acid.

The A_p horizon ranges from brown or dark brown (10YR 4/3) to brown (10YR 5/3). The depth to the gray mottles is 18 to 30 inches.

Included with this soil are small areas of Vicksburg silt loam and a few small, sandy areas. The Vicksburg soils were not mapped separately in Panola County.

Collins silt loam is well suited to row crops, trees, hay and pasture. It has a high available moisture-holding capacity. The organic-matter content is low, however, and a plowpan forms readily.

Practically all of this soil has been cleared. About 65 percent of the acreage is in row crops, 34 percent is in pasture, and only 1 percent is in trees. Capability unit 3 (A7-IIw-1); woodland suitability group 6.

Collins silt loam, local alluvium (0 to 3 percent slopes) (Co). - This soil is in narrow drainageways of the hilly parts of the county and along the foot of bluffs at the edge of the delta. The soil is in local alluvium that recently washed from hills covered with loess.

In most places this soil has more rapid runoff and better surface drainage than Collins silt loam, as well as slower infiltration. Water generally does not stand for long periods. The layers of this soil vary more in texture than those in Collins silt loam, and they generally contain more sand. A few small areas on slopes of 3 to 5 percent are included.

This soil is well suited to row crops, pasture, and trees. About 65 percent of the acreage is in row crops, 34 percent is in pasture, and 1 percent is in trees. Capability unit 3 (A7-IIw-1); woodland suitability group 6.

Falaya Series

This series consists of somewhat poorly drained, strongly acid to very strongly acid soils that developed in silty alluvium on nearly level bottom lands. The slope ranges from 0 to 3 percent.

Generally, the plow layer is brown silt loam and the subsoil is mottled, gray and brown silt loam.

The Falaya soils occur with the Collins and the Waverly soils. They are better drained and browner than the Waverly soils but are not so well drained as the Collins. The mottles in the Falaya soils are not so close to the surface as those in the Waverly soils but are closer to the surface than those in the Collins soils.

Falaya soils are scattered throughout most of this county. About 63 percent of the acreage is in row crops, 30 percent is in pasture, and 7 percent is in trees. The principal row crops are cotton and corn.

Falaya silt loam (0 to 2 percent slopes) (Fa). -- This is a somewhat poorly drained, nearly level soil on bottom lands. The major layers are:

0 to 7 inches, brown, friable silt loam.

7 to 12 inches, mottled, brown and light brownish-gray, friable silt loam.

12 to 43 inches, light-gray silt loam with strong-brown mottles.

Falaya series. -- The soils of the Falaya series are in recent loess alluvium on nearly level bottom lands. These soils are not so well drained as the Collins soils and are mottled more distinctly and at less depth. The Falaya soils in this county intergrade toward the Low-Humic Gley great soil group.

Representative profile of Falaya silt loam, in a cultivated field 9 miles west of Batesville (NE $\frac{1}{4}$ NW $\frac{1}{4}$ Sec. 23, T.9S., R.9W.):

A_p - 0 to 7 inches, brown (10YR 5/3) silt loam; weak, fine and medium, granular structure; friable; many fine and few medium roots; strongly acid; abrupt, smooth boundary.

C₁ - 7 to 12 inches, mottled, brown (10YR 5/3), and light brownish-gray (10YR 6/2) silt loam; mottles are many, medium, and distinct; structureless, friable; common fine roots; strongly acid; clear, smooth boundary.

C_{2g} - 12 to 26 inches, light-gray (10YR 7/1) silt loam with many, medium, faint, very pale brown (10YR 7/4) mottles and few, fine, distinct, strong-brown (7.5 YR 5/6) mottles; structureless; friable; common fine roots; very strongly acid; clear, wavy boundary.

C_{3g} - 26 to 43 inches +, gray or light-gray (10YR 6/1) and light-gray (10YR 7/2) silt loam with common, fine, distinct, strong-brown (7.5 YR 5/6) mottles; structureless; friable; few fine roots; strongly acid.

The A_p horizon ranges from dark grayish brown (10YR 4/2) to brown (10YR 5/3). Gray mottles begin at a depth of 6 to 18 inches. The C horizon ranges from silt loam to silty clay loam.

Included with this soil are very small areas in which the lower subsoil is silty clay.

This soil has slow internal drainage and a moderate available waterholding capacity. Its content of organic matter is low. A plowpan forms readily in cultivated areas.

Most of this soil has been cleared. About 66 percent of the acreage is in row crops, 30 percent is in pasture, and 4 percent is in trees. The soil is well suited to pasture and hardwood trees and is fairly well suited to row crops. Capability unit 9 (A7-IIIw-1); woodland suitability group 5.

Falaya silt loam, local alluvium (0 to 3 percent slopes) (F1). - This soil occupies narrow drainageways in the hilly parts of the county and is on the delta at the foot of bluffs. The soil developed in local alluvium that recently washed from nearby hills covered with loess.

This soil is not likely to be flooded for long periods. It generally has slightly more rapid runoff and better surface drainage than Falaya silt loam, as well as slower infiltration. The soil layers vary more in texture than those in Falaya silt loam and, in some places, contain a little more sand. A few small areas with slopes of 3 to 5 percent are included.

About 75 percent of the acreage is in row crops, 19 percent is in pasture, and 6 percent is in trees. This soil is well suited to pasture and hardwood trees and is fairly well suited to row crops. Capability unit 9 (A7-IIIw-1); woodland suitability group 5."

The soils described above are developed on valley fill sequences of varying widths and thicknesses. At the Florence property site on lower Johnson Creek the valley fill is approximately 1200' to 1600' wide and is derived from 20.7 square miles of upland watershed area (Fig. 1.3.). On the Woodruff property the valley fill widths vary from approximately 400' to 1000' and are derived from 5.6 square miles of upland watershed area. Likewise the width of alluvium on the Leigh property on lower Goodwin Creek is approximately 900' to 1100' and is the product of 8.2 square miles of upland drainage area. The valley soils at both of the Johnson Creek sites are predominantly Collins silt loam with some Falaya silt loam present. On the Goodwin Creek site the same two soils are present but Falaya predominates (Fig. 1.4.).

The soils and alluvium described above are primarily post settlement (or historically derived) materials. These, however, are not the materials that control bank stability. They only constitute a variable loading factor over the more important underlying paleosol material. Since most

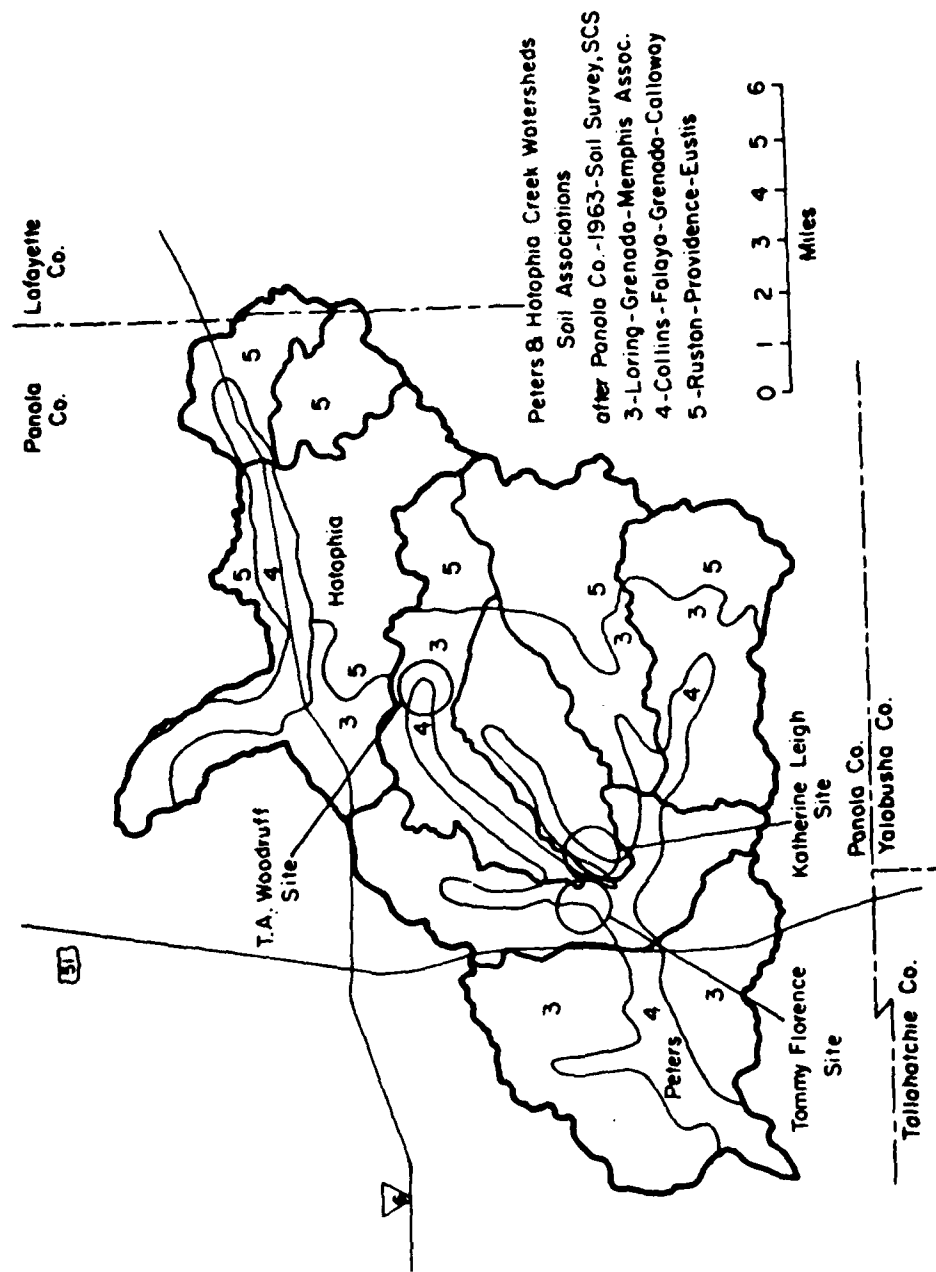
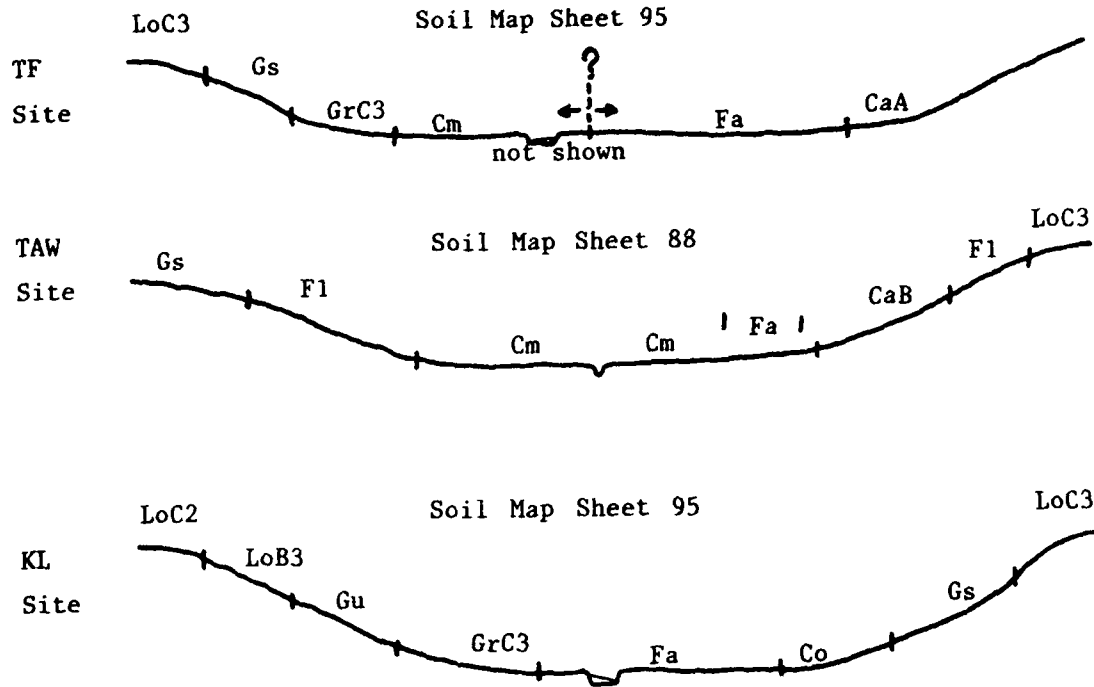


Figure 1.3. Geographic Locations of the Test Sites shown on Soil Map of Area.

Cross sections looking D.S.



Soils data taken from Soil Surv., Panola Co., MS, Series 1960, No. 10,
(Dent, 1963)

CaA	Calloway silt loam, 0-2% slopes
CaB	Calloway silt loam, 2-5% slopes
Cm	Collins silt loam
Co	Collins silt loam, local alluvium
Fa	Falaya silt loam
F1	Falaya silt loam, local alluvium
GrC3	Grenada silt loam, 5-8% slopes, severely eroded
Gs	Gullied land, sandy
Gu	Gullied land, silty
LoB3	Loring silt loam, 2-5% slopes, severely eroded
LoC2	Loring silt loam, 5-8% slopes, eroded
LoC3	Loring silt loam, 5-8% slopes, severely eroded

Figure 1.4. Valley-normal soil transects at each test site (schematic).

present channels in this area were relocated by private or governmental endeavours, the present streams do not often flow in natural channels. As most problems with bank stabilization are concentrated in areas with these "new" banks, this is where sampling and testing efforts were concentrated, ... on the paleosols that are exposed on the middle and lower portions of these banks. Three types of tests were stressed in this study. Borehole Shear Tests (BST) were run in situ and lab tests to determine tension and compression strengths were run on undisturbed samples in the laboratory. Most test sites were adjacent to or within 10 meters of the streambanks.

1.2 TEST SITE LOCATIONS AND DESCRIPTIONS

The geographic location of the three test sites on Johnson and Goodwin Creeks are shown on Figure 1.3, superimposed over a general soil map of the area. Figures 1.5 through 1.25 show the aerial photos, the test site schematic plots, and the channel cross sections of the Florence site (Fig. 1.5 to Fig. 1.11), the Woodruff site (Fig. 1.12 to Fig. 1.18) and the Leigh site (Fig. 1.19 to 1.25). Tables 1.1, 1.2 and 1.3 specify the hole numbers and dates drilled, and the test depth horizons and dates of each strata sampled.

1.3 BOREHOLE PREPARATION & SAMPLING PROCEDURES

The procedures for taking undisturbed samples for unconfined compression and tension tests in the laboratory and for preparation of the boreholes for the BST experiments in the field were as follows. Samples for both the compression and tension tests were, with few exceptions, collected in the same manner, at the same time, and with the same equipment. The field equipment consisted of 1) a trailer-mounted Gidding's Drill Rig Model GSRP-ST* (Fig. 1.26), 2) various 2" and 3" inside diameter thin-wall solid soil tubes similar to Shelby tubes but fitted with double-tapered quick-relief hardened soil tube bits (Fig. 1.27), 3) another set of

*Trade names are used in this publication solely for the purpose of providing specific information. Mention of a trade name does not constitute a guarantee or warranty of the product by the U.S. Department of Agriculture or an endorsement by the Department over other products not mentioned.



Figure 1.5. Aerial Photo of Lower Johnson Creek (Florence) site.

D.133

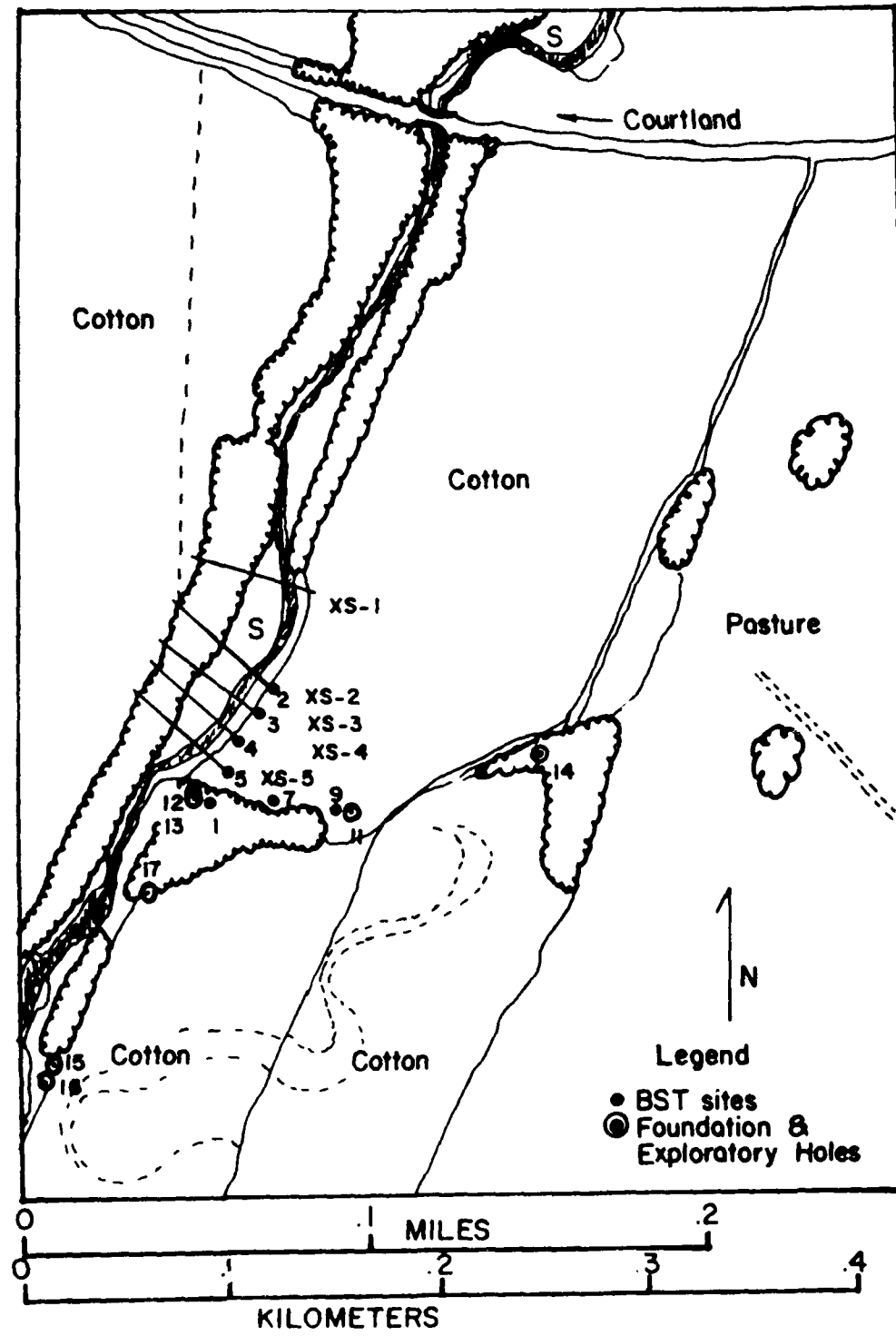


Figure 1.6. Locations of Florence site test holes & cross sections.

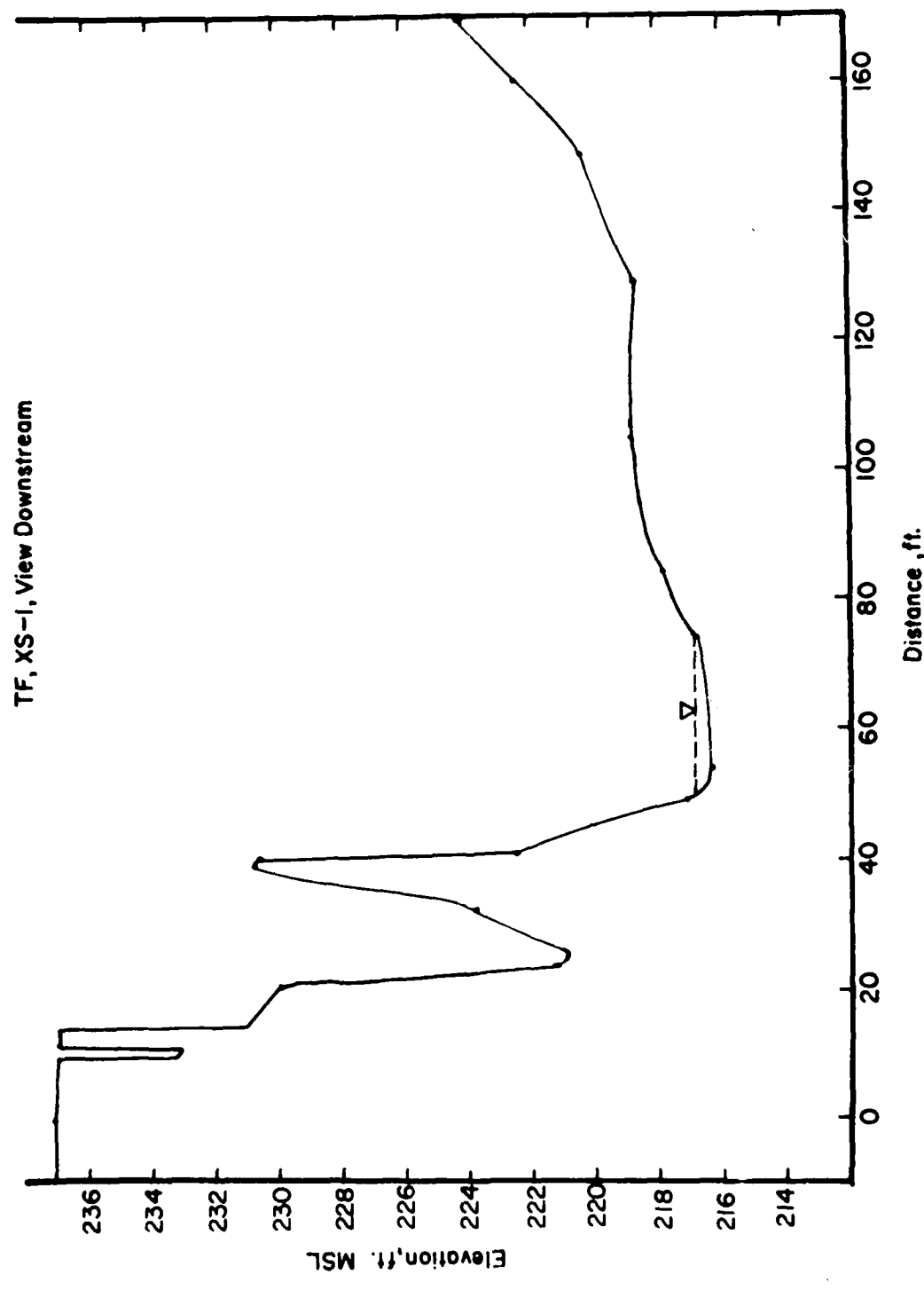


Figure 1.7. Florence site Cross Section XS-1.

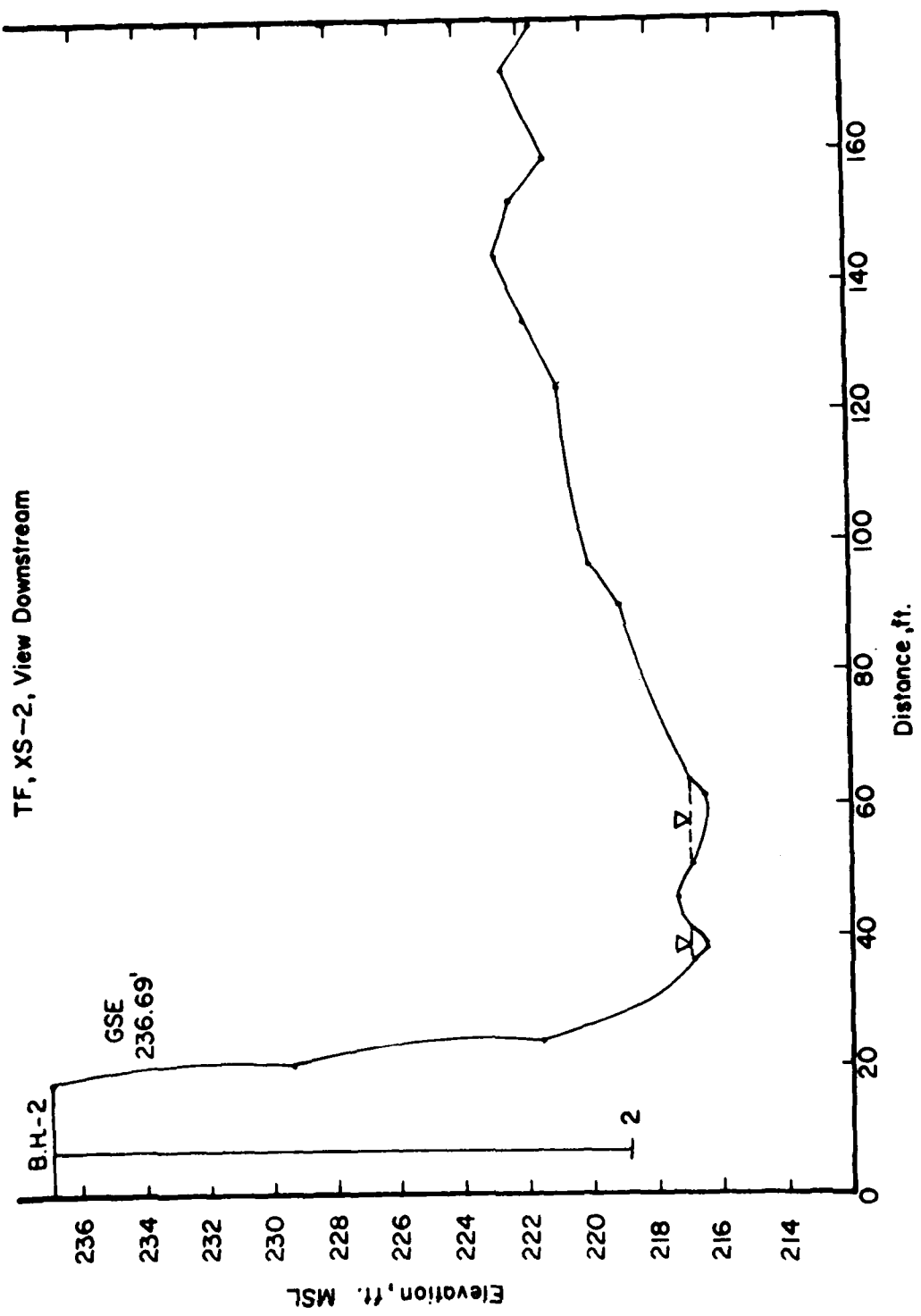


Figure 1.8. Florence site Cross Section XS-2.

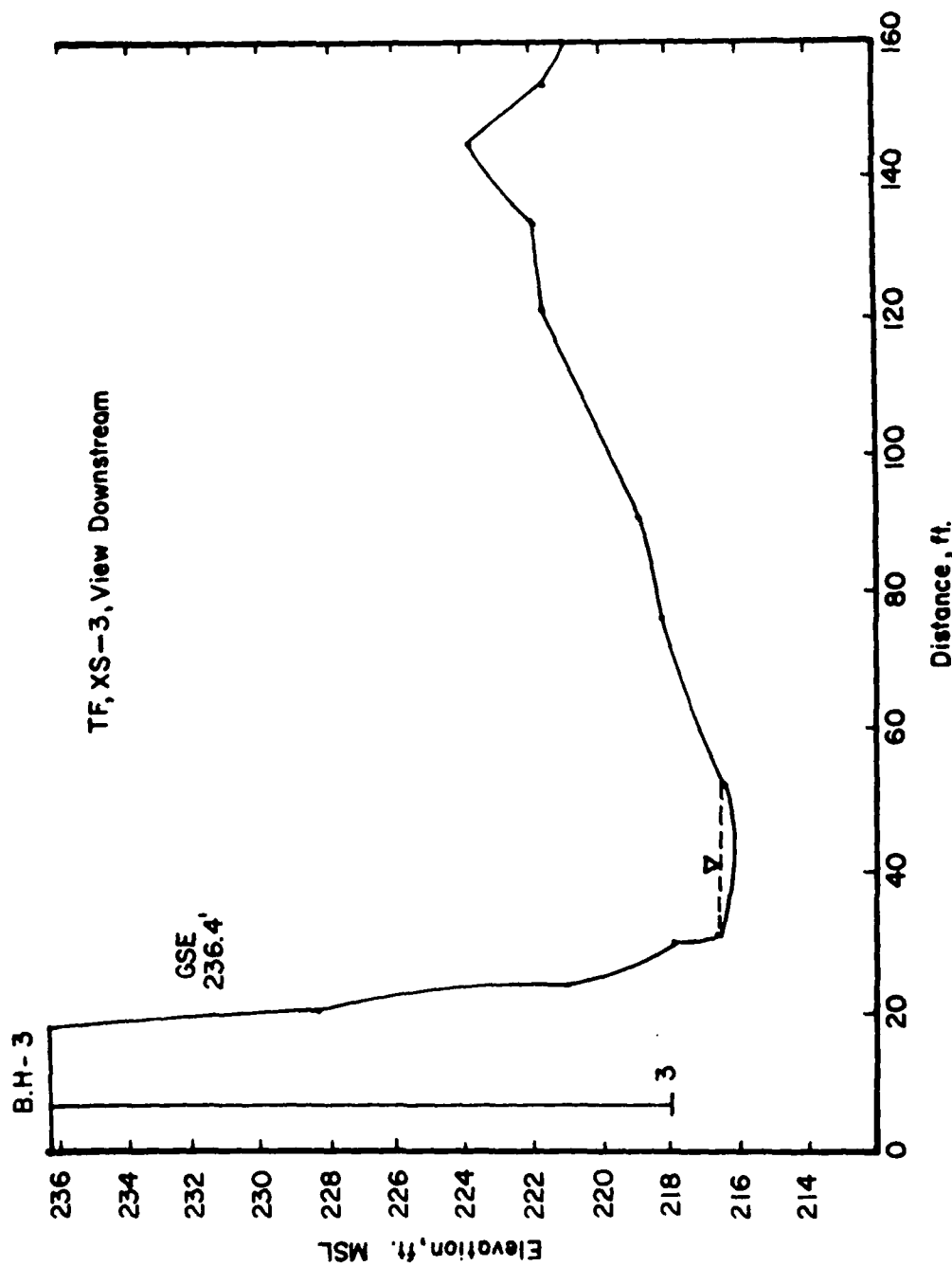


Figure 1.9. Florence site Cross Section XS-3.

D. 137

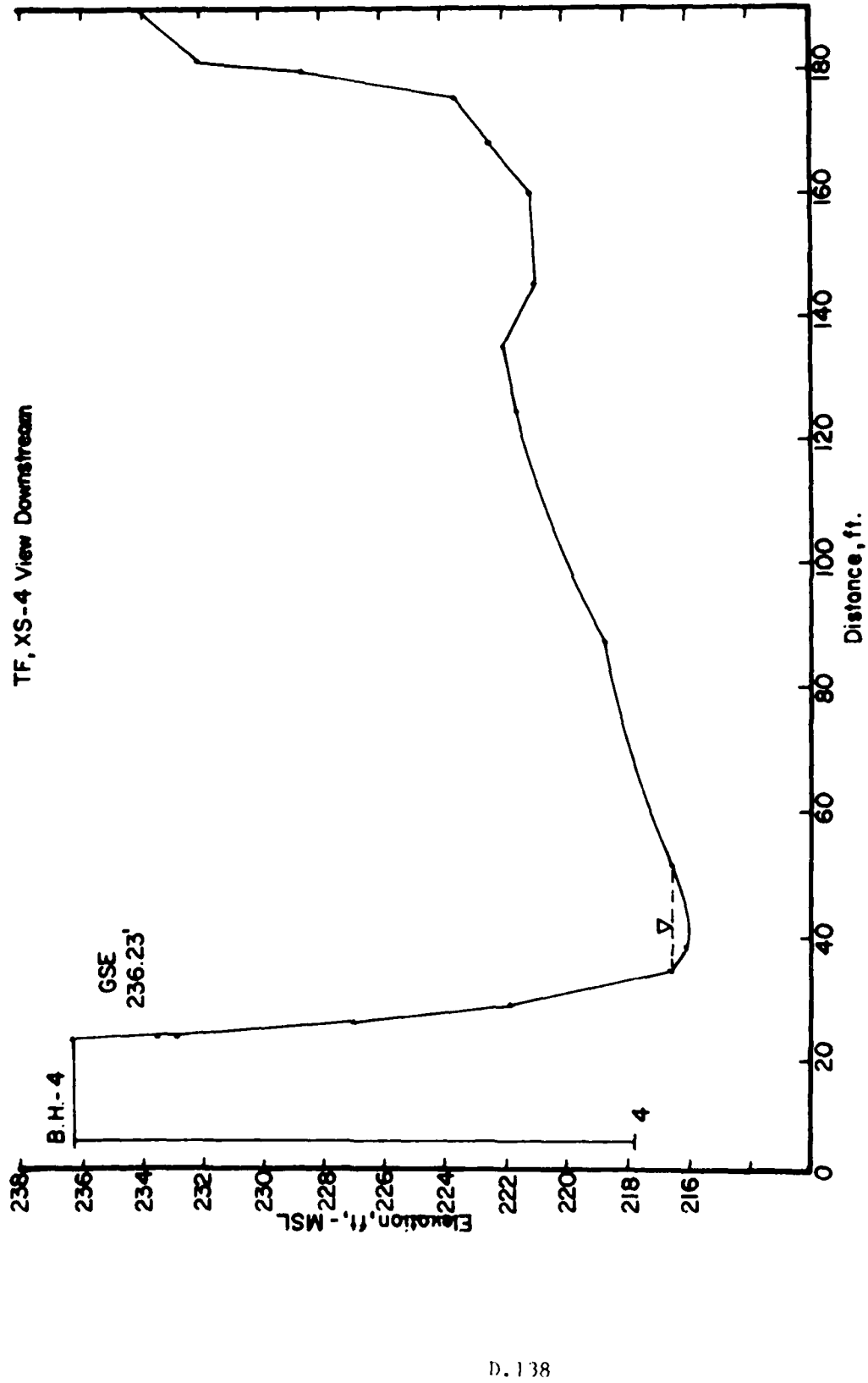


Figure 1.10. Florence site Cross Section XS-4.

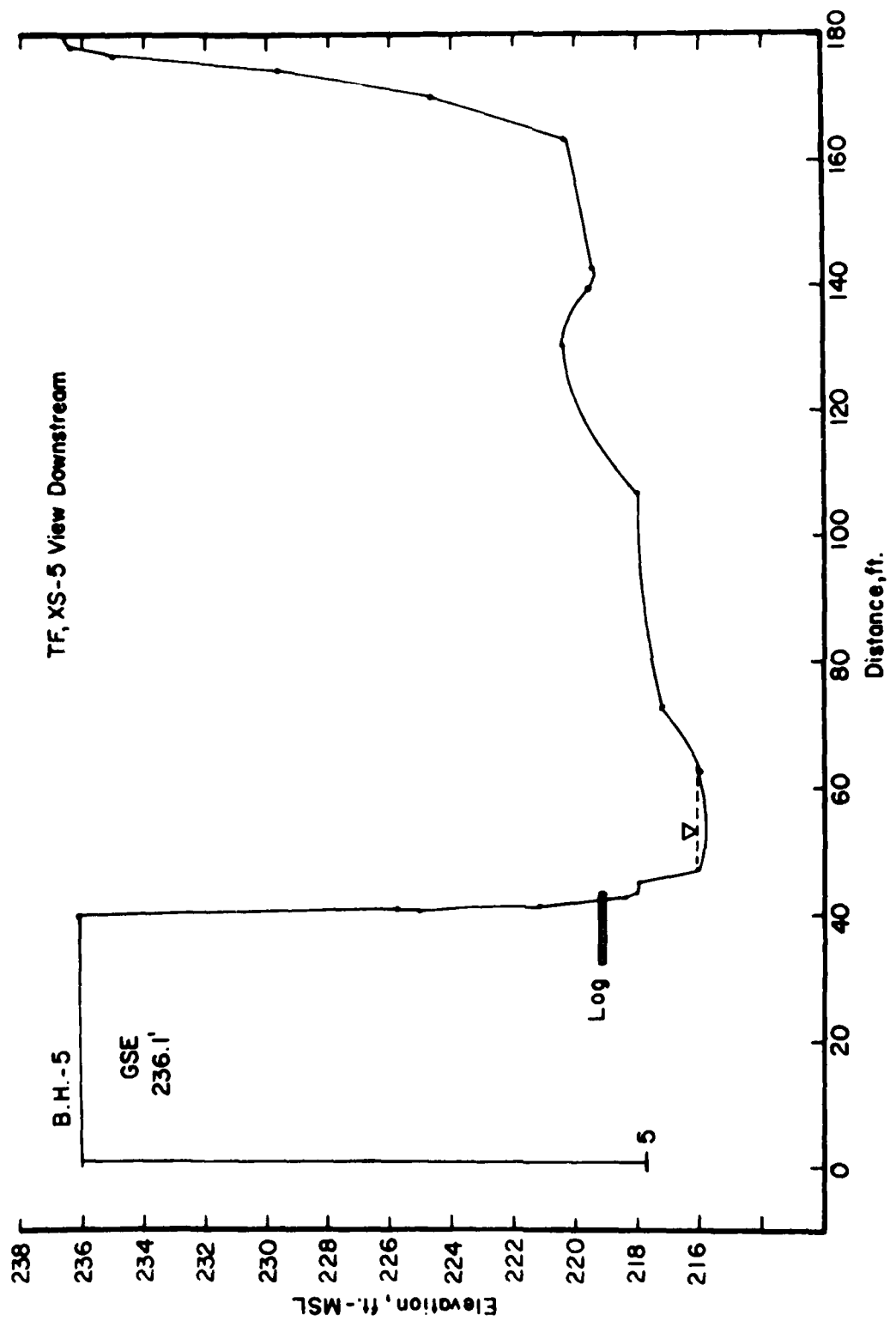


Figure 1.11. Florence site Cross Section XS-5.

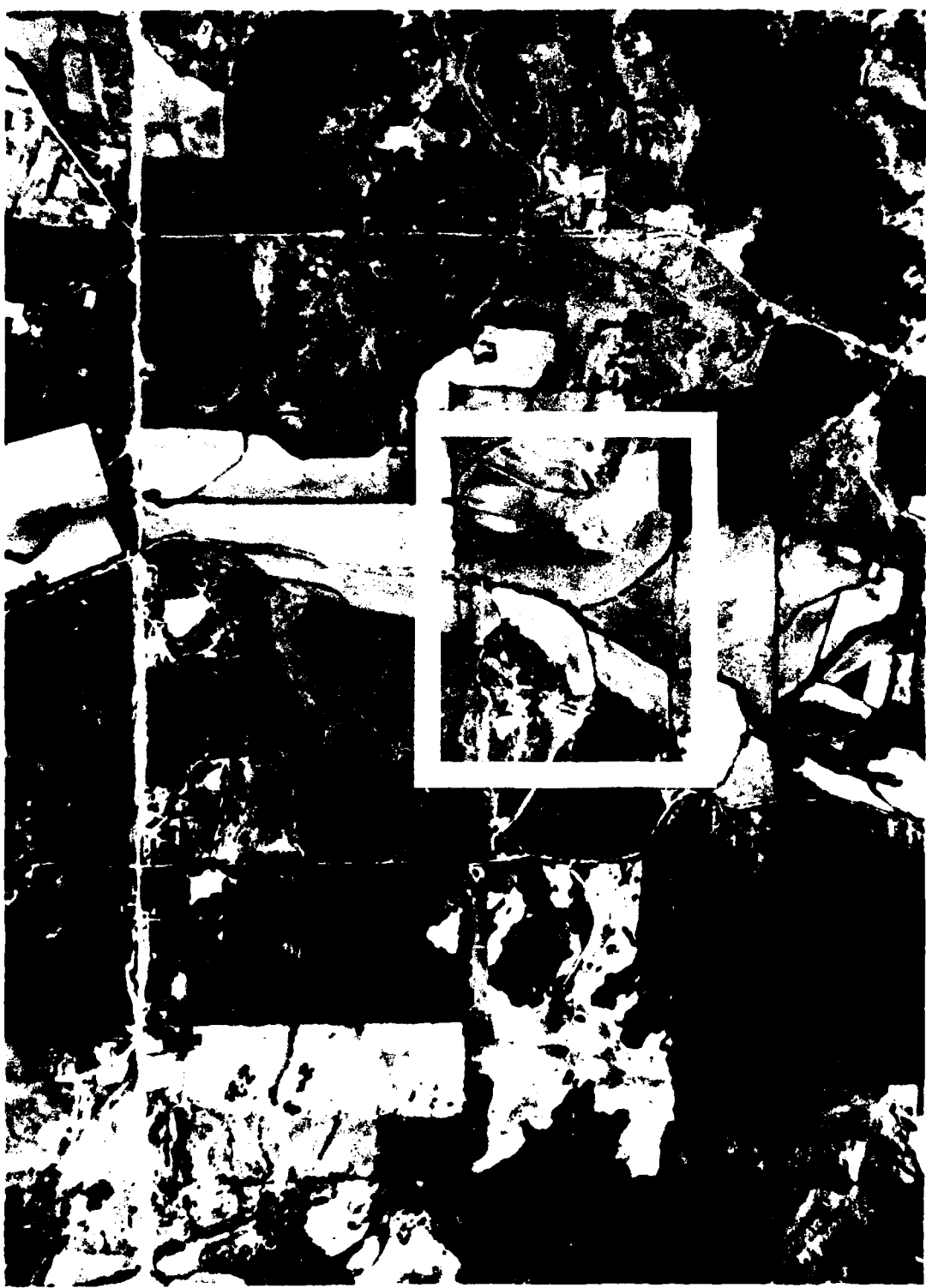


Figure 1.12. Aerial Photo of Upper Johnson Creek (Woodruff) site.

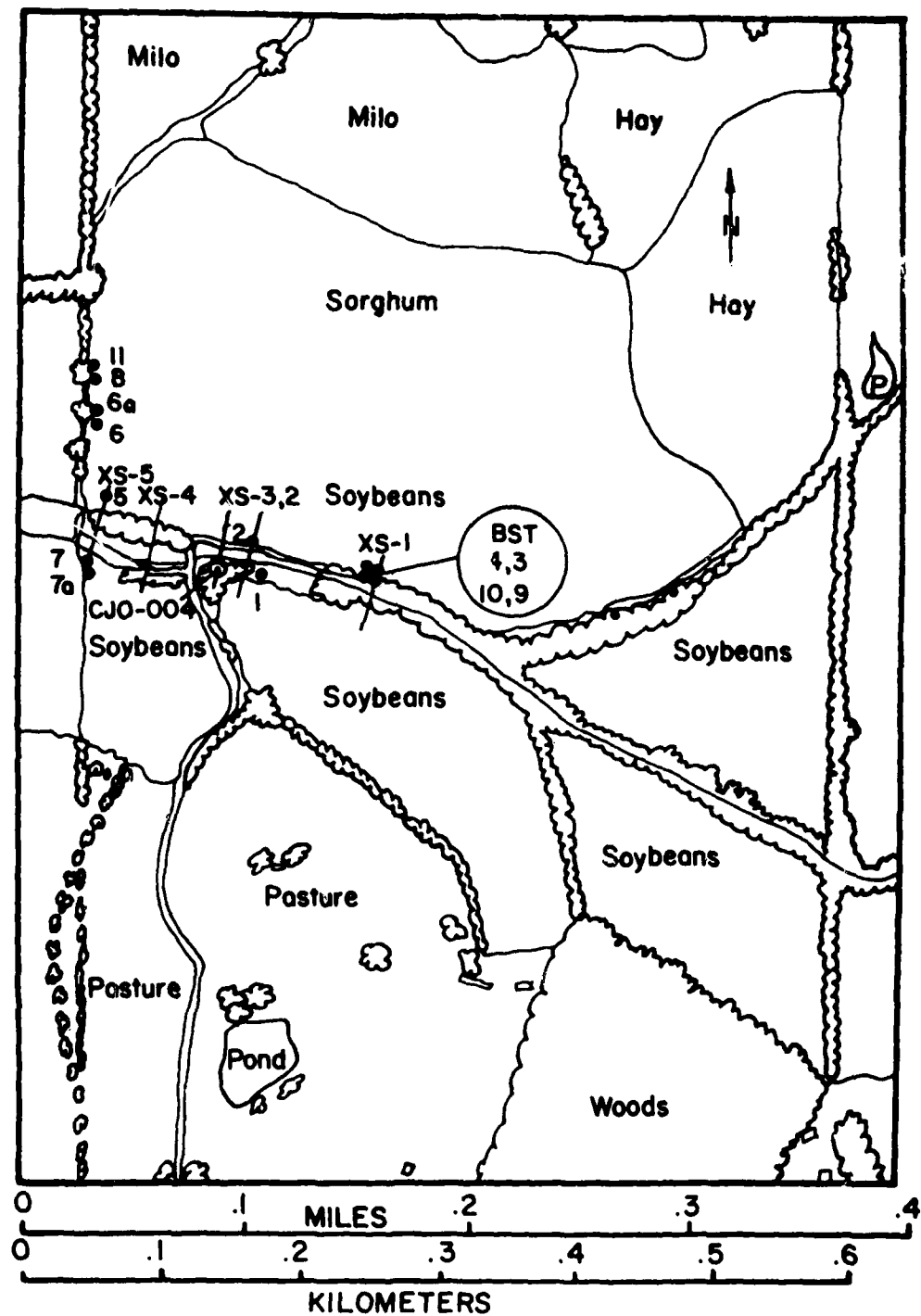


Figure 1.13. Locations of Woodruff site test holes & cross sections.

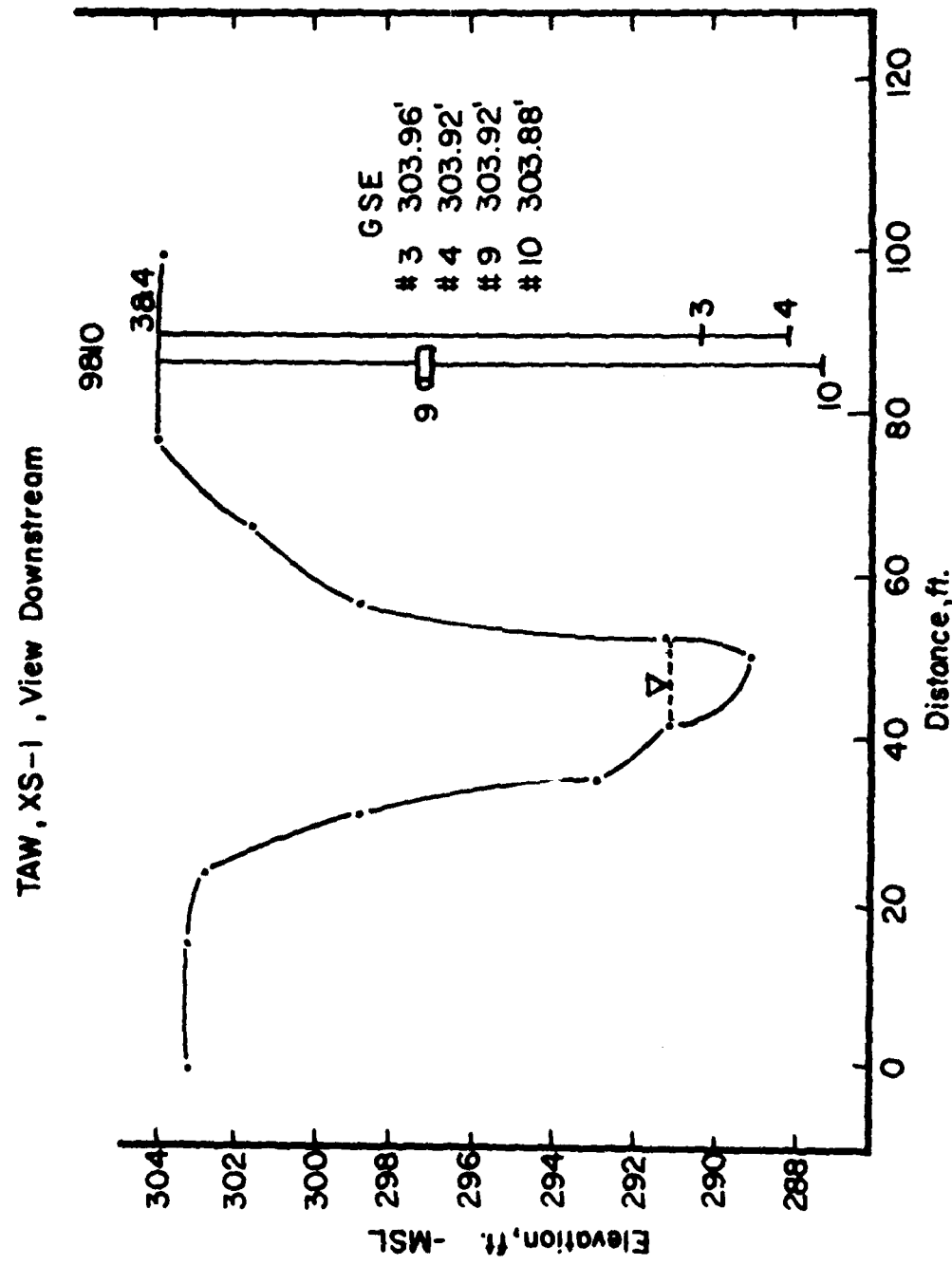


Figure 1.14. Woodruff site Cross Section XS-1.

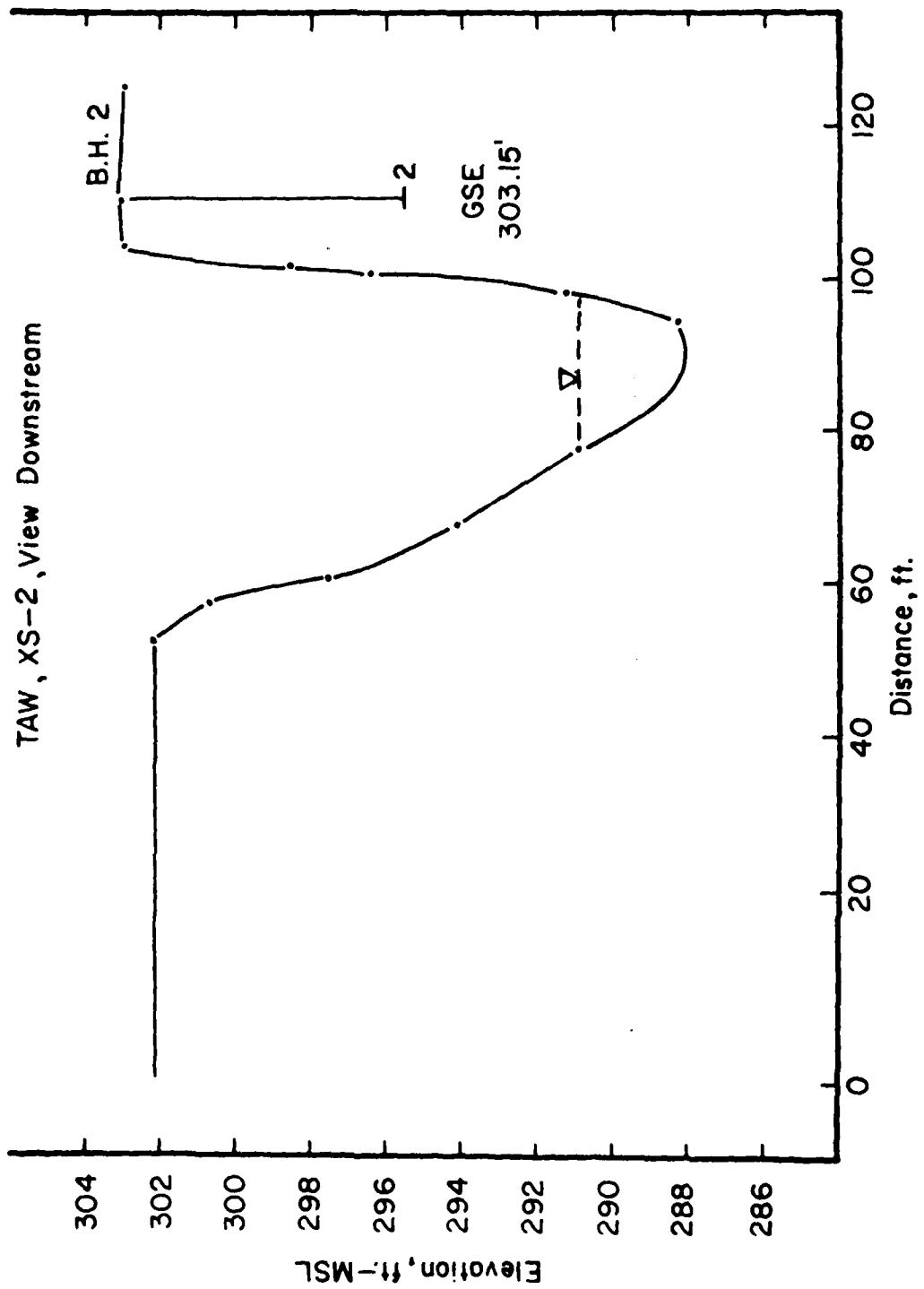


Figure 1.15. Woodruff site Cross Section XS-2.

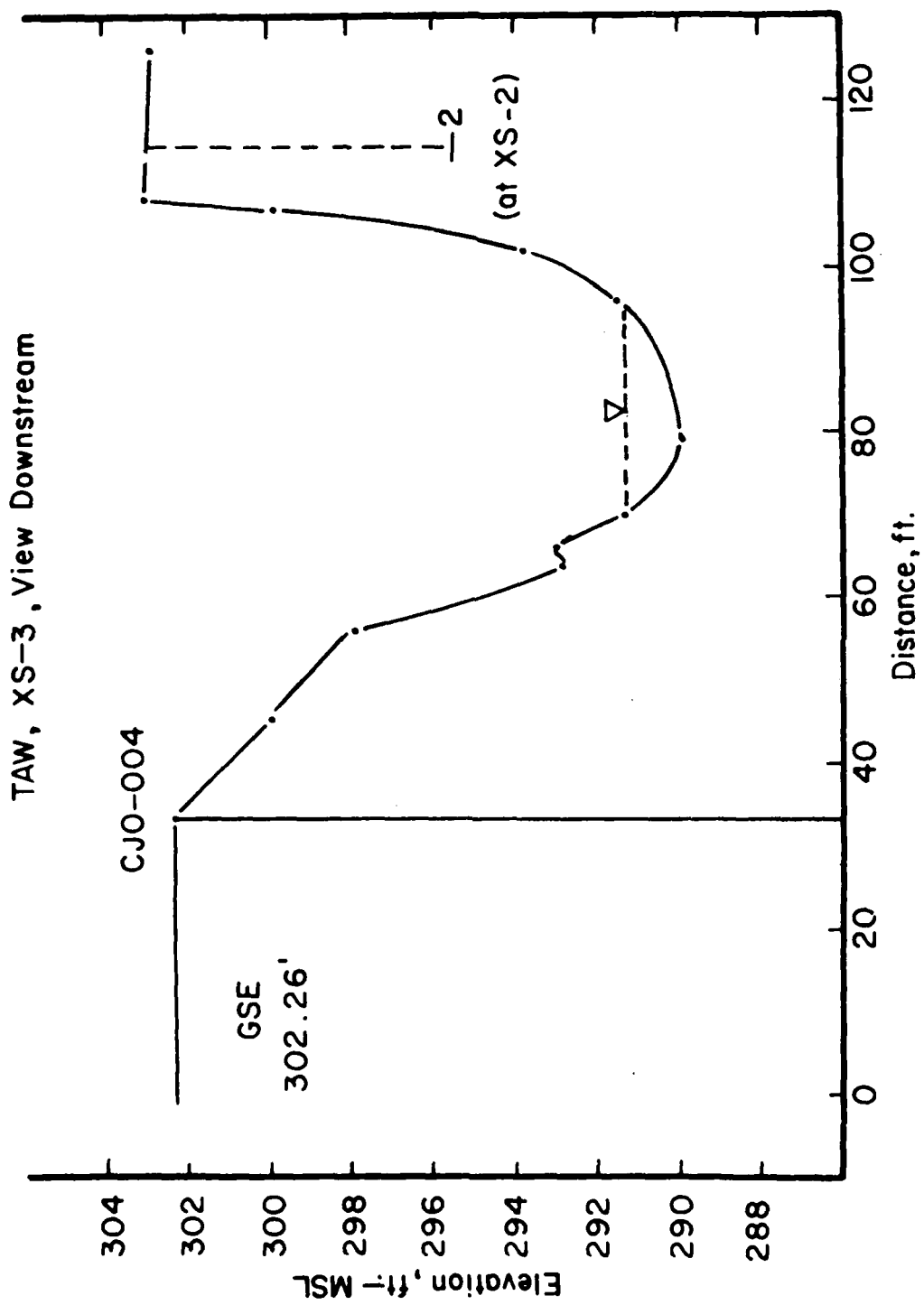


Figure 1.16. Woodruff site Cross Section XS-3.

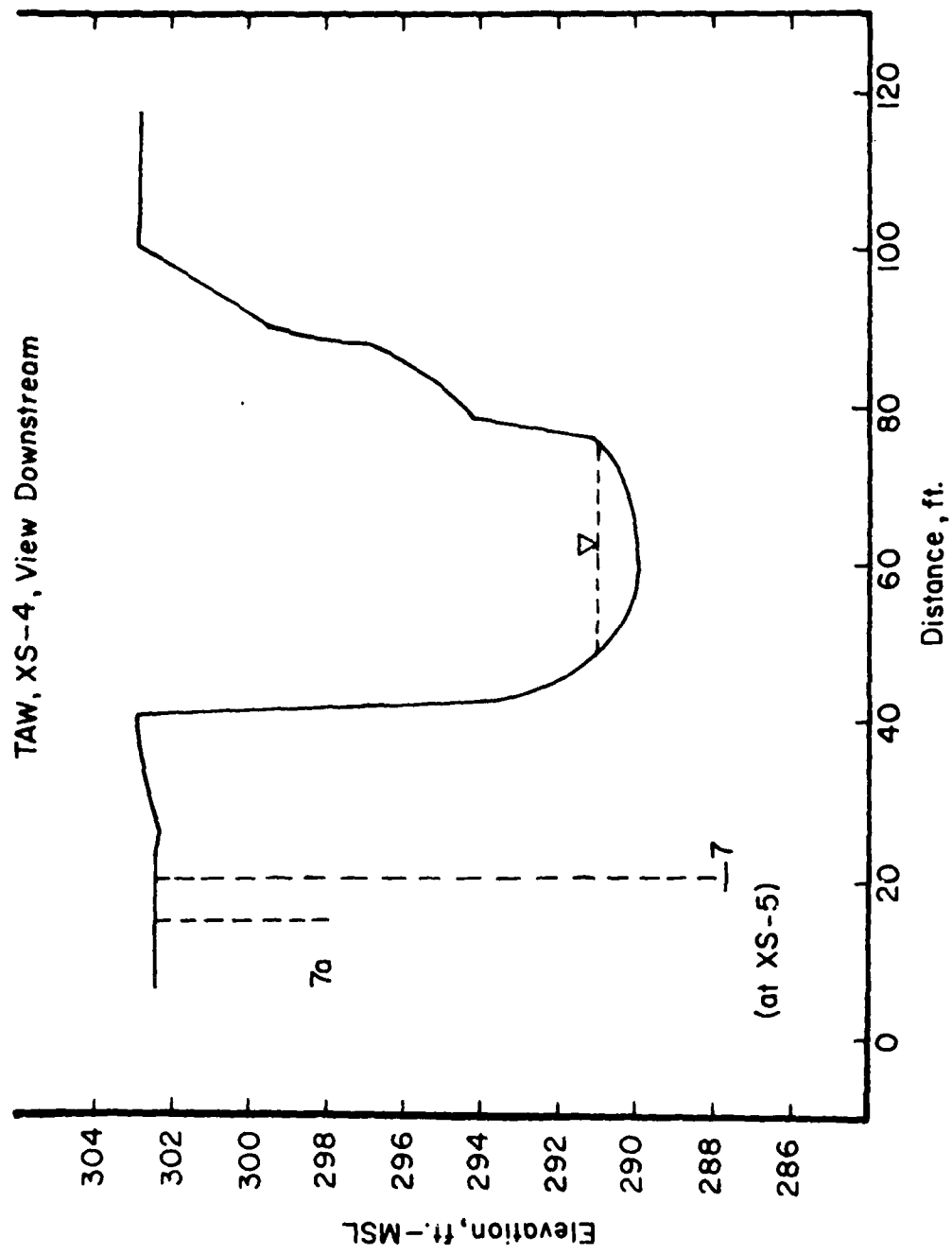


Figure 1.17. Woodruff site Cross Section XS-4.

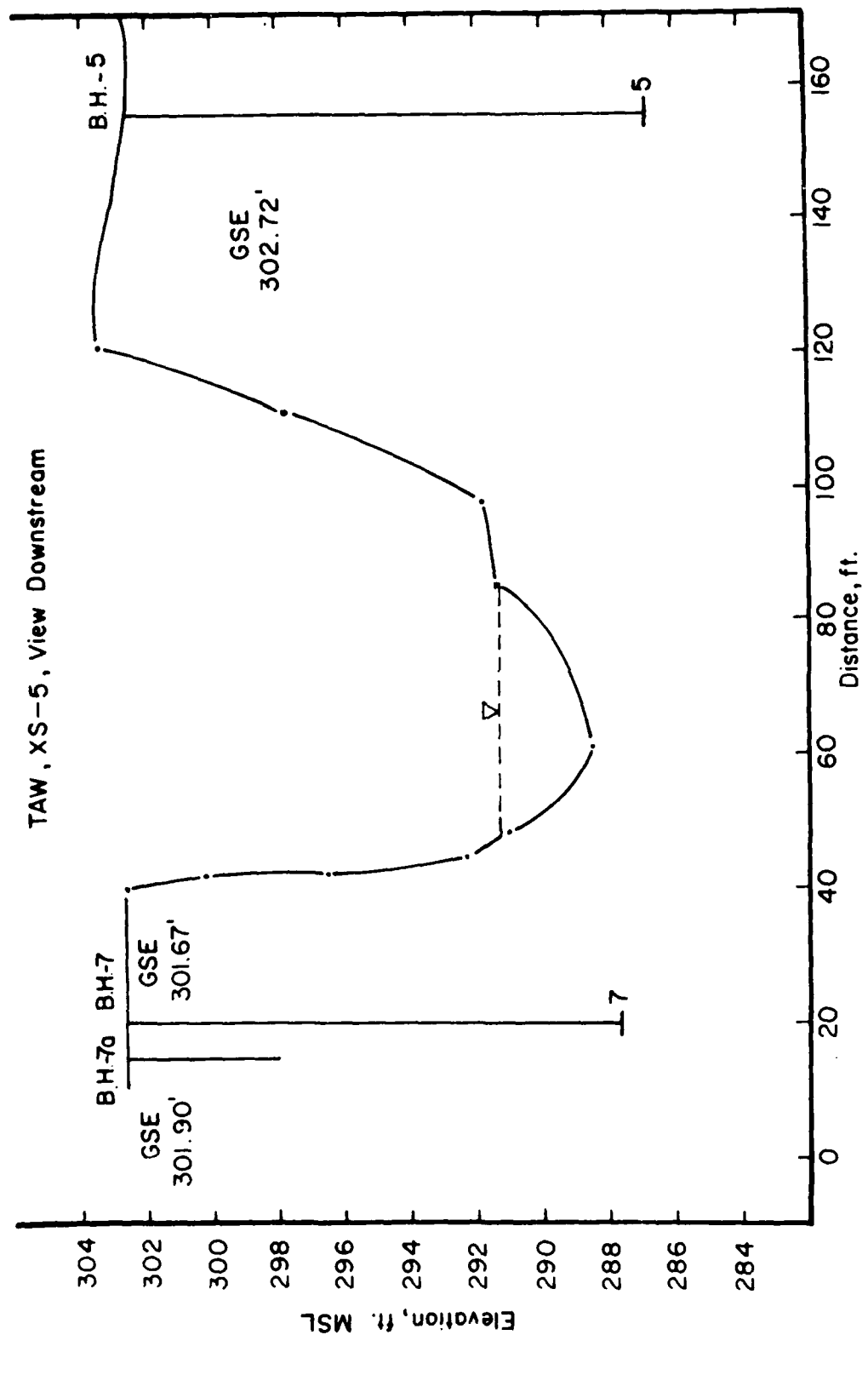


Figure 1.18. Woodruff site Cross Section XS-5.



Figure 1.19. Aerial Photo of Lower Goodwin Creek (Leigh) site.

D.147

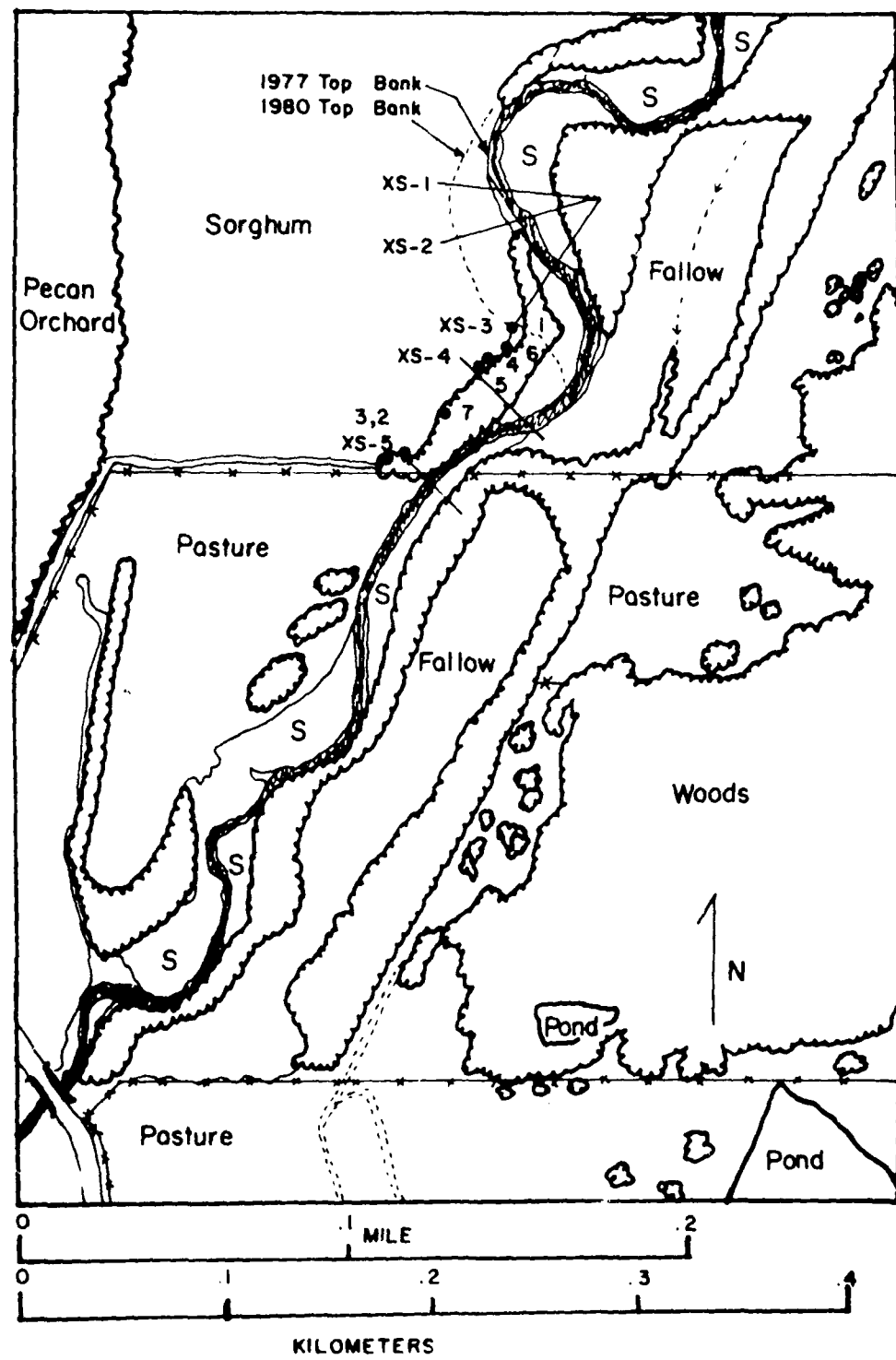
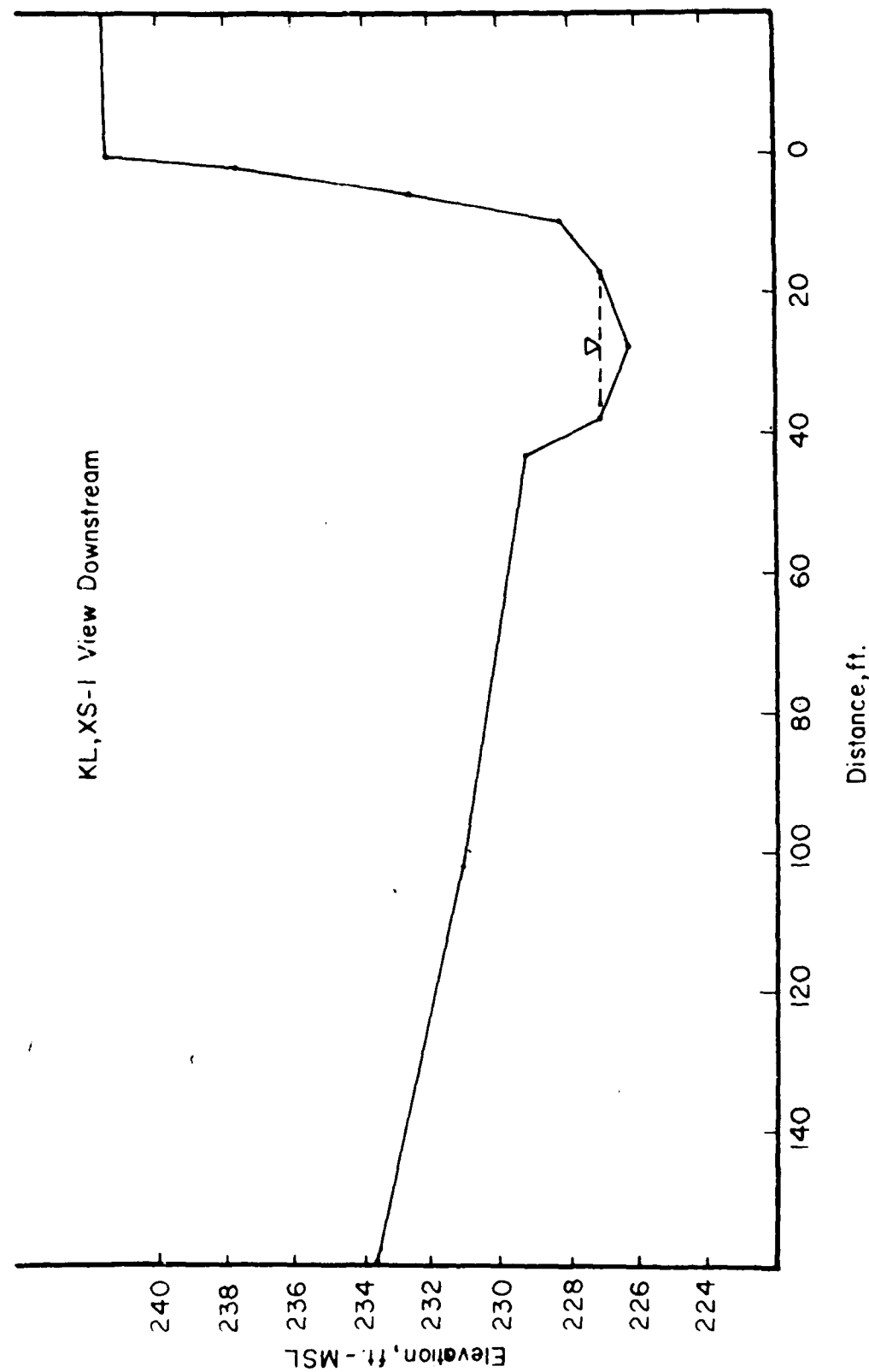


Figure 1.20. Locations of Leigh site test holes & cross sections.



D. 149

Figure 1.21. Leigh site Cross Section XS-1.

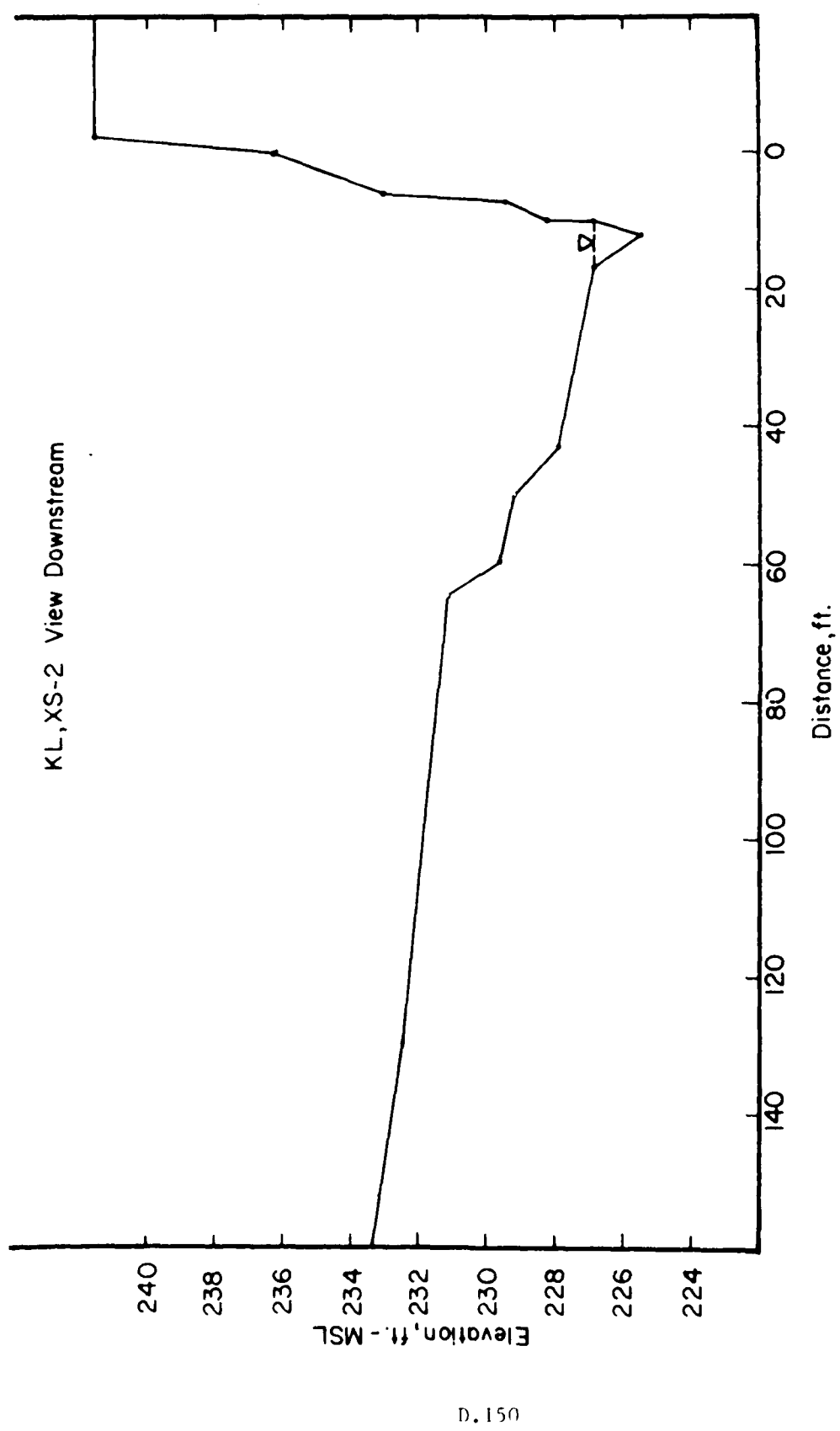


Figure 1.22. Leigh site Cross Section XS-2.

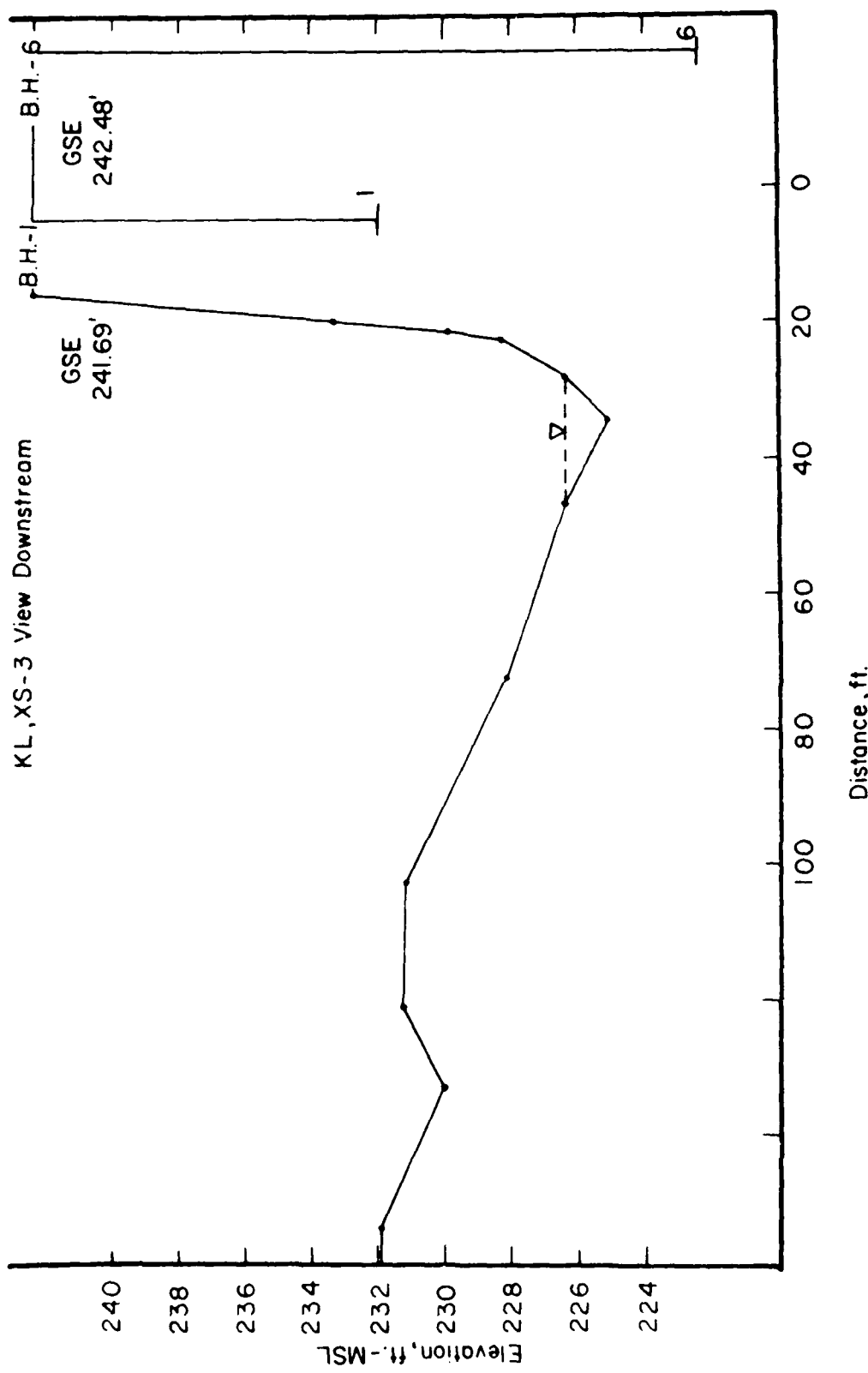


Figure 1.23. Leigh site Cross Section XS-3.

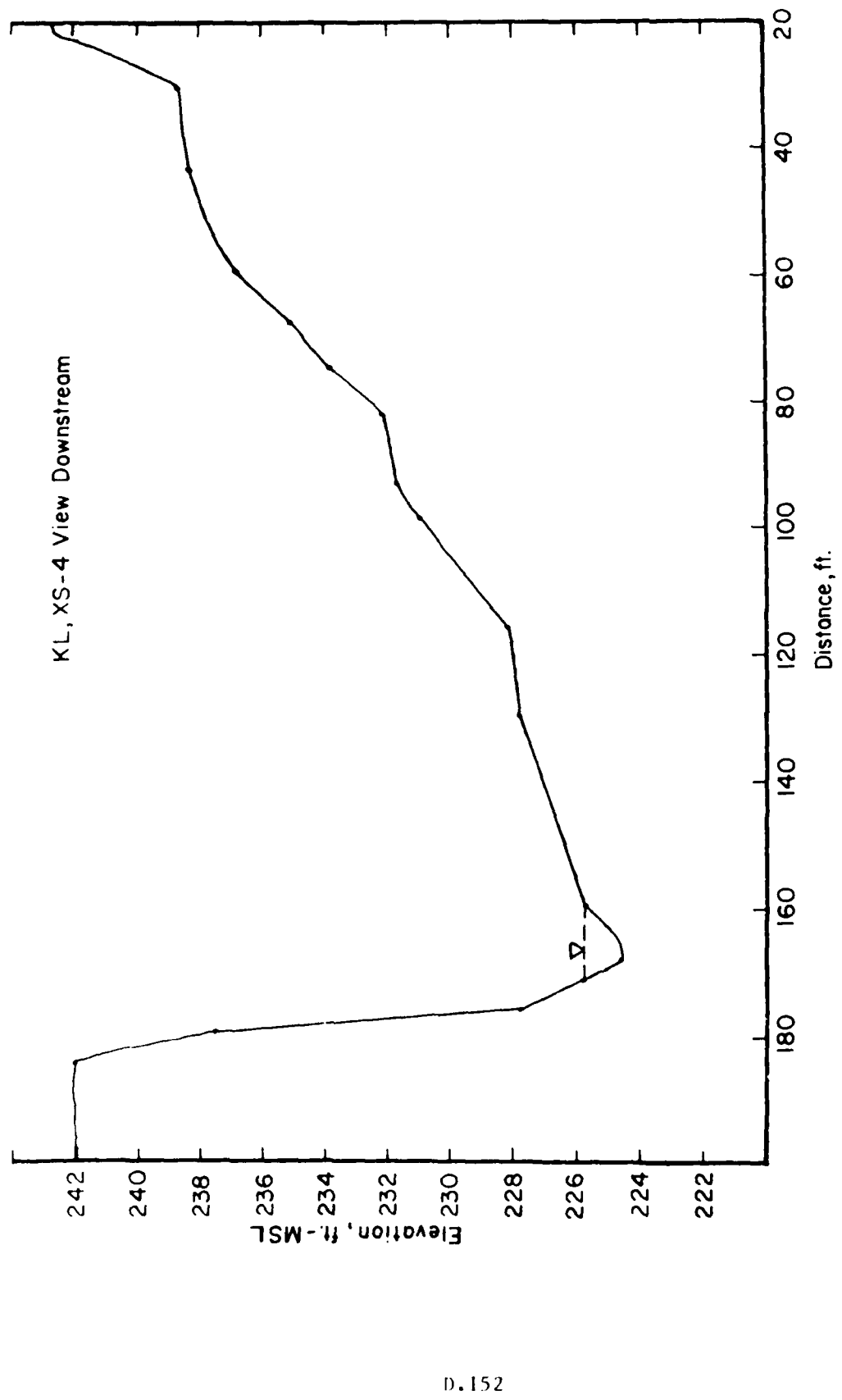


Figure 1.24. Leigh site Cross Section XS-4.

KL,XS-5 View Downstream

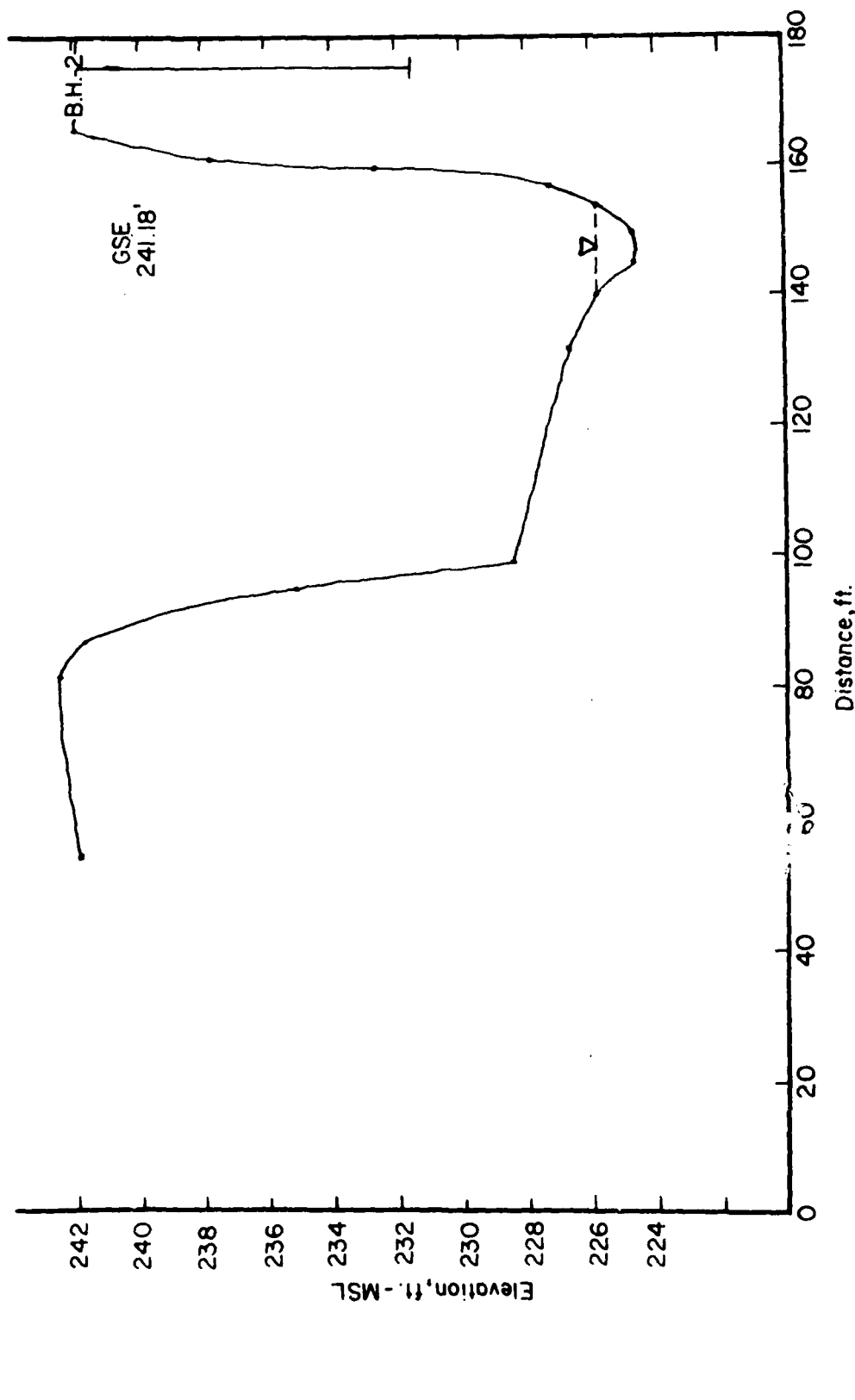


Figure 1.25. Leigh site Cross Section XS-5.

Table 1.1. Boring and Testing Record; Tommy Florence property - Lower Johnson Creek, SE $\frac{1}{4}$, NW $\frac{1}{4}$, SE $\frac{1}{4}$, Sec. 3, T.10S., R.7W.

Hole Number	Field Book Page #	Date(s) Drilled	Strata Tested	Borehole Shear Test Depths	Date(s) or New (N) Tested	Old (O) Test Plate
1		5-06-80	f. sd. bed. PSA	0.66 m	5-06-80	0
2	22-23	7-29-80	PSA	0.59-1.07 m	7-30-80	N
			dense gray sand	1.73-1.98 m	8-07-80	N
			OP	3.05-3.66 m	7-29-80	N
			OP	3.05-3.66 m	8-07-80	N
			fine sand	4.42-4.57 m	8-08-80	N
3	24-25	7-29-80	OP tending to f. dense gray sd.	1.82-2.13 m	8-08-80	N
			OP	1.98-2.29 m	8-06-80	N
			OP	2.44-2.74 m	8-05-80	N
4	26-27	7-30-80	PSA	0.61-0.91 m	8-04-80	N
			PSA	0.91-1.30 m	8-12-80	N
			OP	2.74-3.05 m	8-04-80	N
			OP	3.28-3.50 m	8-12-80	N
5	28-29	8-04-80	soft layer	1.37-1.68 m	8-13-80	N
			soft layer	1.91-2.05 m	8-13-80	N
			OP	3.66-3.81 m	8-14-80	N
6	----	Skipped	--	--	--	--
7	30-31	8-07-80	--	--	--	--
8	----	Skipped	--	--	--	--
9	32-33	8-07-80	--	--	--	--

Table 1.2. Boring and Testing Record; T.A. Woodruff property - Upper Johnson Creek, SW $\frac{1}{4}$, NE $\frac{1}{4}$, Sec. 20, T.9S., R.6W.

Hole Number	Field Book Page #	Date(s) Drilled	Strata Tested	Borehole Shear Test Depths	Date(s) or New (N) Tested	Old (O) Test Plate
1						
2	3	5-28-80	YP OP OP OP	0.84 m 2.13 m 2.21 m 2.29 m	5-28-80 5-28-80 5-30-80 5-30-80	0 0 0 0
3	4-5	5-30-80	YP OP OP	1.52 m 2.74 m 3.20 m	6-02-80 6-02-80 6-02-80	0 0 0
4	6-7	6-02-80	YP OP OP	1.74 m 2.90 m 3.81 m	6-04-80 6-04-80 6-04-80	0 0 0
5	8-9	6-04-80		1.98 m	6-05-80	0
6	10	6-04-80	Ch. Fill	0.76 m	6-13-80	0
6a	11-12	6-16-80	Ch. Fill	2.20 m	6-13-80	0
			Ch. Fill	1.06 m	6-16-80	0
			Yp-Ch. Fill	1.22 m	6-16-80	0
			Ch. Fill	2.13-2.21 m	6-16-80	0
7	13-14	6-09-80				
8	15-16	6-16-80				
9	17	7-09-80	YP	1.5 -1.8 m	7-09-80	N
10	18-19	7-09-80	OP	3.3 -3.5 m	7-11-80	N
11	20-21	7-24-80	PSA	0.69-0.84 m	7-24-80	N

Table 1.3. Boring and Testing Record; Katherine Leigh property - Lower Goodwin Creek, NW $\frac{1}{4}$, SE $\frac{1}{4}$, SW $\frac{1}{4}$, Sec. 2, T.10S., R.7W.

Field Hole Number	Book Page #	Date(s) Drilled	Strata Tested	Borehole		Old (O) or New (N) Test Plate
				Shear Test Depths	Date(s) Tested	
1		5-19-80	PSA	0.52 m	5-19-80	O
			PSA	0.61 m	5-19-80	O
			YP	1.83 m	5-19-80	O
2	2	5-27-80	YP	0.91 m	5-27-80	O
			YP	1.07 m	5-27-80	O
			YP	1.52 m	5-27-80	O
3	2	5-27-80	--	--	--	
4	34-35	8-08-80	--	--	--	
		8-13-80	--	--	--	
5	36-37	8-15-80	PSA	0.76-0.91 m	8-19-80	N
			Grey Clay	3.73-4.27 m	8-19-80	N
6	38-39	8-19-80	PSA	0.91-1.22 m	8-21-80	N
			YP	1.52-1.82 m	8-21-80	N
			YP?	2.44-2.60 m	8-21-80	N
7	40-41	8-19-80	--	--	--	

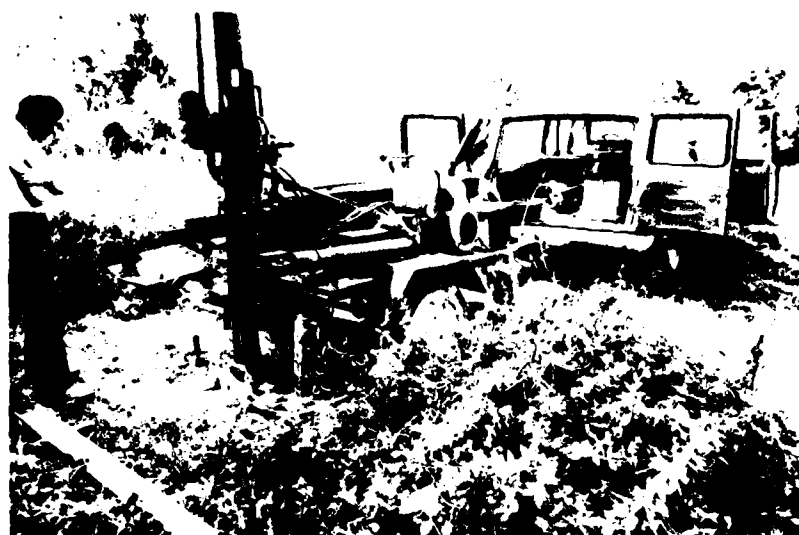


Figure 1.26. Drill rig used in Borehole Shear Test program.

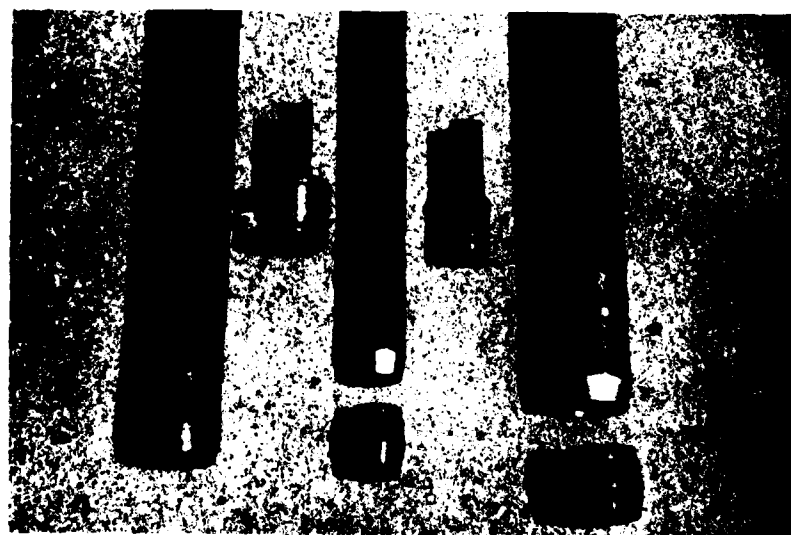


Figure 1.27. 2" & 3" Quick-Relief Soil Tubes, Bits and Vacuum-ball Soil Tube Heads.

the above soil tubes with toolheads modified with neoprene O-rings and vacuum-ball air locks (Fig. 1.27), 4) a third set of soil tubes with slotted sides, 5) both 1.5 inch and 3 inch diameter split-spoon samplers (Fig. 1.28), 6) extrusion tools, 7) 4" diameter PVC extrusion troughs (schedule 40 PVC pipe cut in half) and 8) various other tools and accessories commonly used in well drilling practices. Cover plugs (Fig. 1.29) were made to keep holes sealed to evaporative conditions until BST analyses could be performed.

After selection of a test site, the drill rig was positioned over the desired point and the rig securely anchored to the ground with two 3-foot long x 3-inch diameter anchor-augers flanking the point at about 18 inches to each side. The hydraulic vertical travel piston was then centered and plumbed and the 3" regular soil tube (item 2 above) was fitted to the Kelly-bar. If the soil resistance permitted, the soil tube was then pressed into the soil in up to 5 foot increments and withdrawn. The filled tube was then placed in a horizontal position, the drive head and the soil tube bits were removed from their respective ends, and after the tube was aligned with the half-cylinder extrusion trough, the sample was gently pressed out of the tube and into the trough in one smooth motion with a ramrod-like device slightly underfit to the inside diameter of the particular soil tube. The extruded samples were then carefully shaved to remove the slickensided surface layer, and were described lithologically.

Field data logged included information of the sort listed in the well log legend in Addendum Section 1.4 and features such as Munsell Color Codes and relative moisture status of the sampled horizon. After completing the field descriptions, samples from selected horizons were cut, their elevation (or depth) ranges were noted, and the samples were placed in plastic bags, tied, tagged, and laid in a foam rubber lined box for transportation to the laboratory.

When the surface soil was too hard for the 3" soil tube to be pressed into the ground, the 2" tube was tried. If it failed, then a 3" flight auger was used to start the hole and the undisturbed surface sample was lost. If the 2" soil tube worked where the 3" tube failed, then the hole was overcut with the 3" tube before proceeding. Usually 3 or 4 inches of undisturbed 3" diameter sample was taken at the bottom of the hole to get the overcut waste material to stay in the tube. If the material was soft

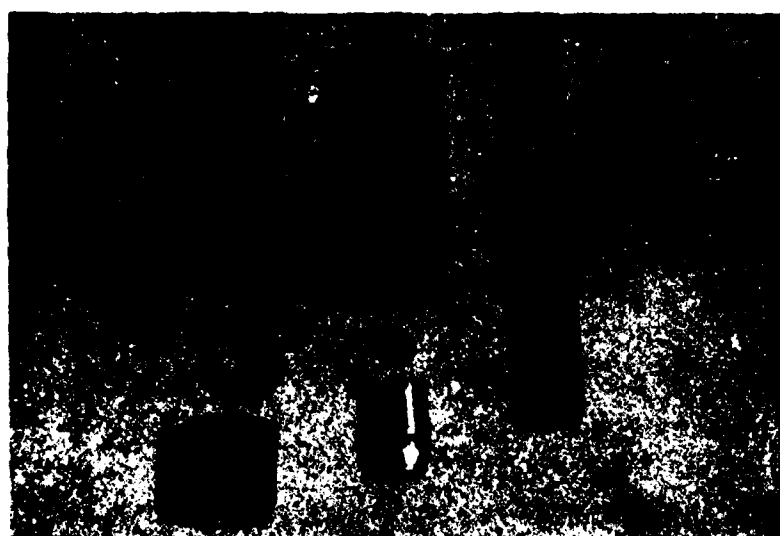


Figure 1.28. Split-spoon Samplers.



Figure 1.29. Borehole Cover Plug.

enough to allow the 3" soil tube to be pressed into the ground but too wet to remain in the tube, then the vacuum tube heads were used. If the sample was both wet and sandy and would not stay in either vacuum soil tube, then a split spoon sampler with a basket-spring retainer (Fig. 1.28) was used. If the material was too hard for the 2" soil tube to be used and a sample was needed, then the split-spoons were driven into the material with a 140 pound drop-hammer instead of being pressed into the material hydraulically. Withdrawal of the tools after the latter process usually requires two tandem hydraulic 10 ton jacks supplementing the drill rig's vertical piston. Samples taken with the hammer-driven split-spoon are acceptable for unconfined compression tests but are seldom, if ever, acceptable for tension tests.

Once the sample has been retrieved, the hole was reamed to a 3 to 3½ inch diameter size, preferably with the 3" soil tube which left a smoother borehole for the BST downhole test head. The area around the reamed hole was then leveled with a flat bladed shovel if BST tests were to begin immediately. If not, a 1 foot long by 3½ inch outside diameter pipe capped with a 1 ft. square steel plate (Fig. 1.29) was pressed into the borehole and the anchor augers carefully unscrewed. The cover plate prevented drying or collapse of the inner walls of the borehole from overhead traffic until BST tests could be made. Most delayed tests were completed within 48 hours of the time the holes were drilled. Where possible, BST tests were run on horizons where undisturbed samples had been successfully taken.

1.4 WELL LOGS OF BOREHOLES

The data recorded in the fieldbook for each borehole was reproduced in Figures 1.31 through 1.56. Figure 1.30 gives the well log legend used in these figures. The reader will note that the stratigraphic symbols for clay, sands, gravels, etc. are seldom used in the drafted column, the primary descriptions used being the genetic rather than the physical ones, i.e., DS, YP, OP, etc. Only those physical characteristics which were recorded in the field are shown on the logs. Where data is not shown in a column of a log, it was not recorded in the field; the primary interest of the drilling was to 1) drill holes suitable for running BST field analyses, 2) gather undisturbed samples for unconfined compression and tension tests and 3) ascertain genetic stratigraphy variations with depth and distributions within the valley fill.

WELL LOG LEGEND

Borehole Shear Test - 1980 Test Program - Peters Creek

TOOLS

- ST - solid soil tube sampler (pushed)
- SST - slotted soil tube sampler (pushed)
- VST - vacuum soil tube sampler (pushed)
- SSp - split spoon (driven) sampler
- AUG - flight auger (rotary)
- 3" - diameter of tool used (OC means overcut)

TESTS

-  - one pt. stage test with old BST plates
-  - zone (multi-point) non-stage test with new BST plates

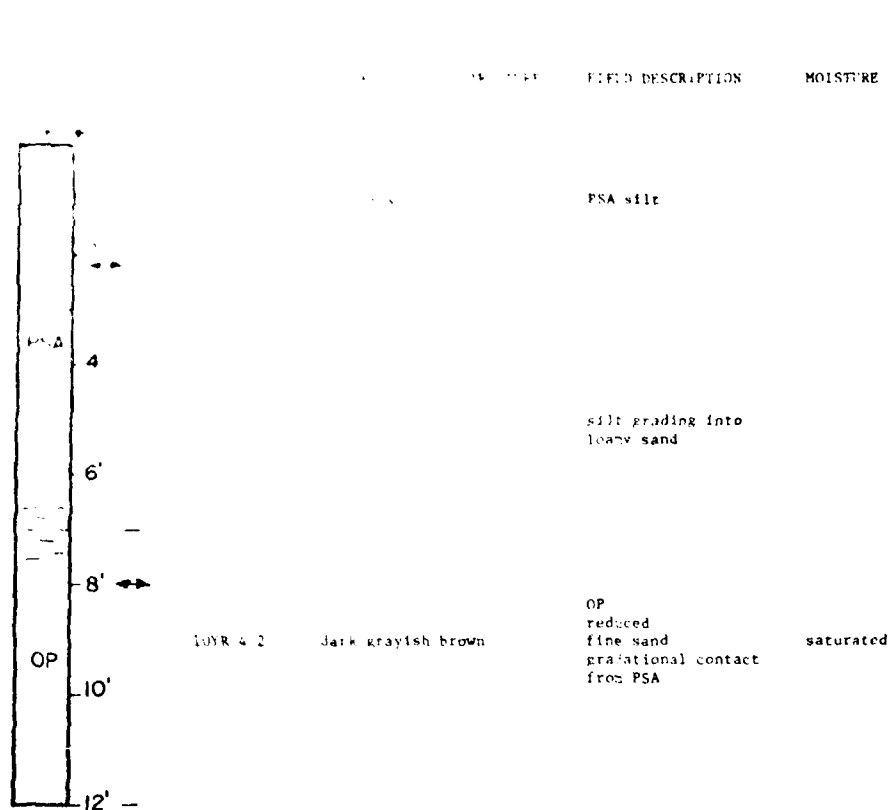
CONTACTS

-  - sharp distinct contact
-  - gradational indistinct contact

STRATIGRAPHY

- PSA - post settlement alluvium
- YP - young paleosol
- OP - old paleosol
- CF - channel fill deposits
- BOG - organic bog deposits
-  - clay balls
-  - iron (Fe) or manganese (Mn) stains
-  - ironstone, wholly or partly indurated
-  - carbon (C14) sample (whether collected or not)
-  - clays or silts
-  - sands
-  - gravels and sands
-  - no sample
-  - water table
-  - logs or limbs of easily identifiable wood

Figure 1.30. Well Log Legend



Hole #1 located within dripline of 14" Cottonwood Tree
on L. R. near (East) of two cased CJO wells.

Figure 1.31. T. Florence site - Borehole #1

Lover Johnson Creek - Tommy Florence prop. - Hole #2 - July 29, 1980
(212' So. Hole #1)

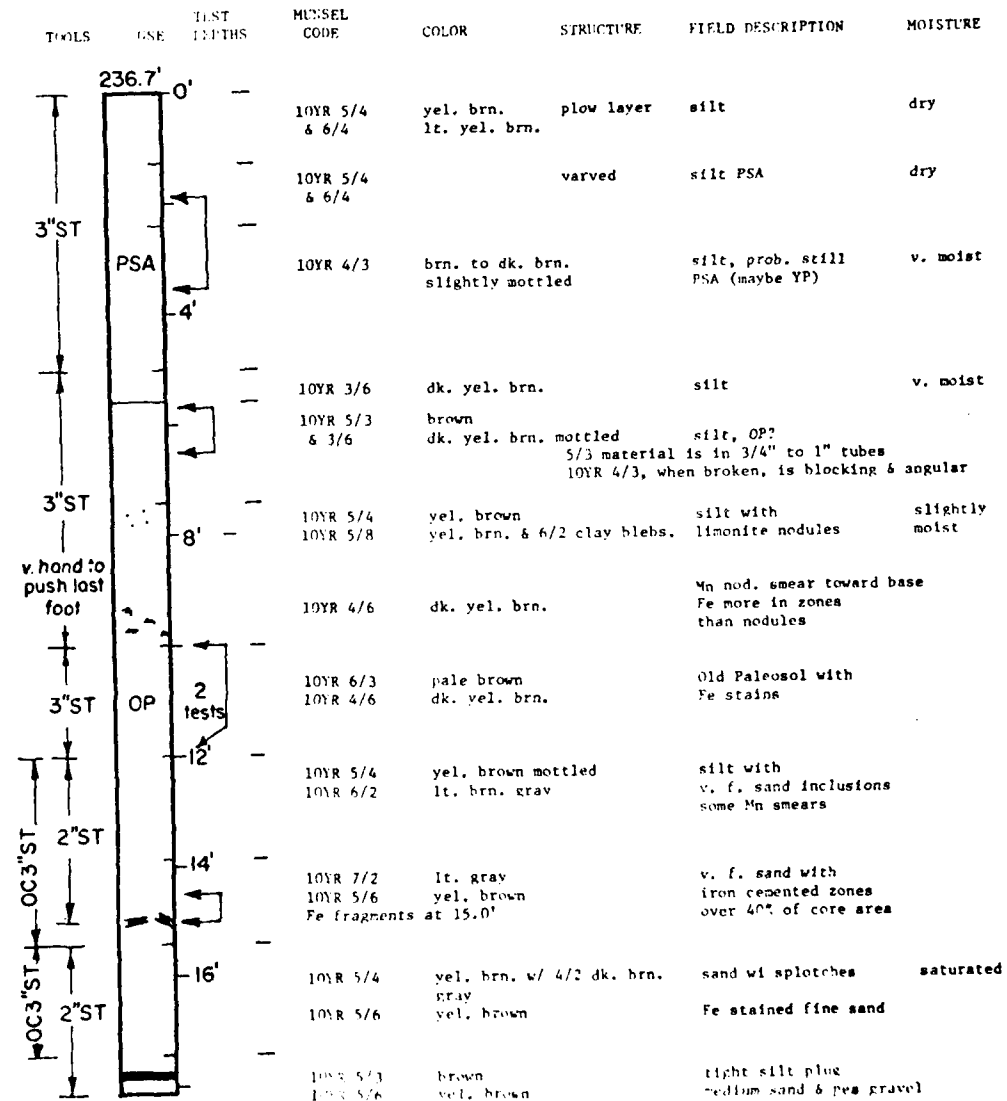


Figure 1.32. T. Florence site - Borehole #2

Lower Johnson Creek - Tomy Florence prep. - Hole #3 - July 29, 1980
(Lat. 44° 56' N., Long. 123° 41' W., #1)

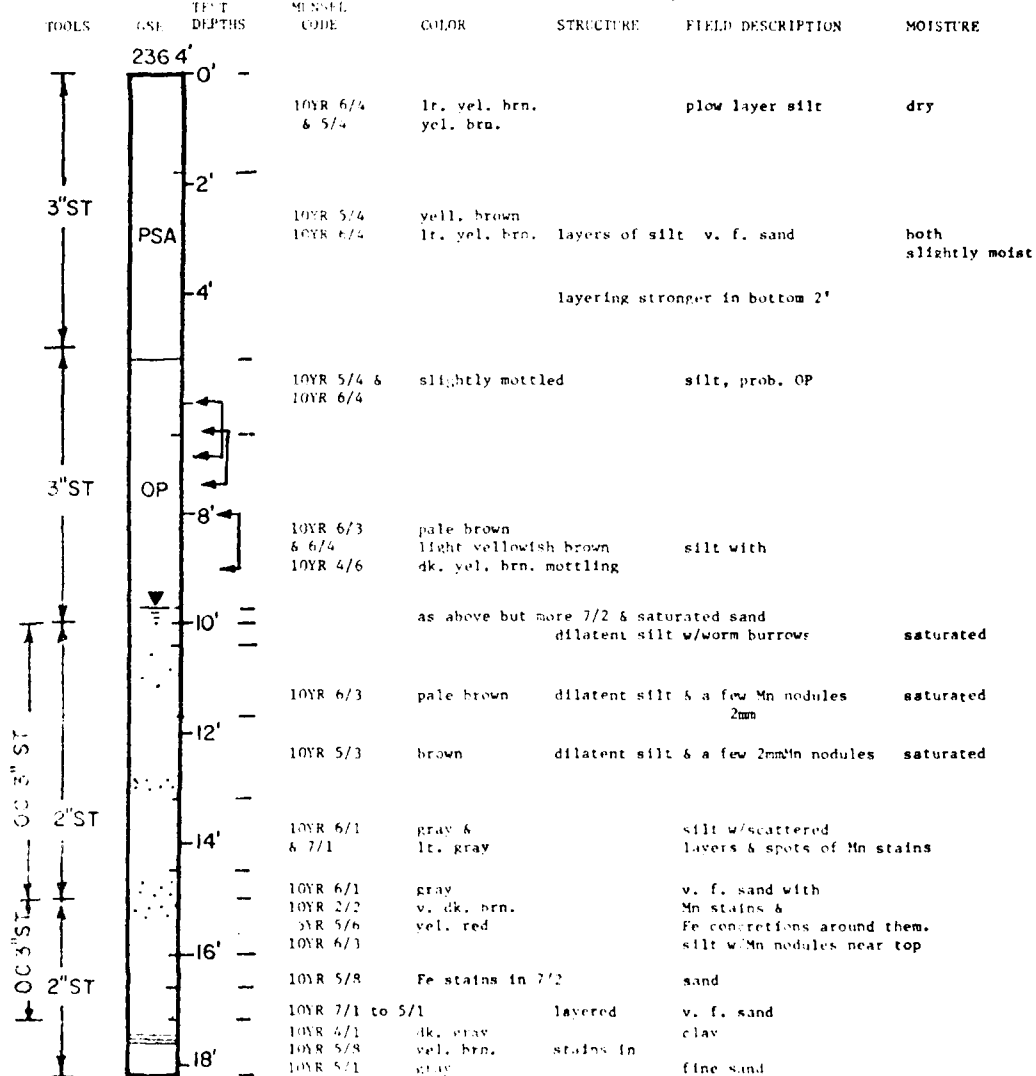


Figure 1.33. T. Florence site - Borehole #3

Lower Johnson Creek - Tommy Florence prop. - Hole #4 - July 16, 1980
(50' South of Hole #3)

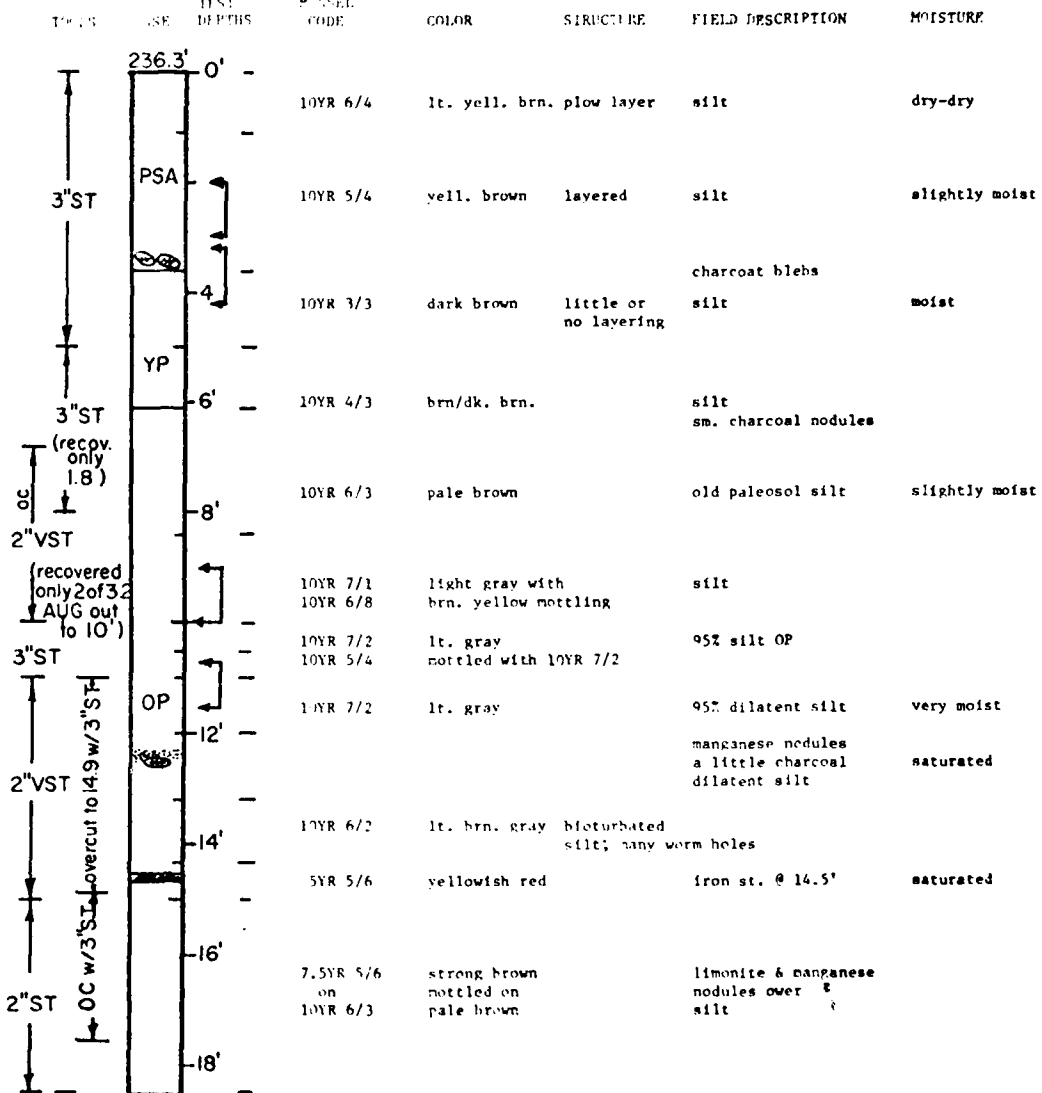


Figure 1.34. T. Florence site - Borehole #4

Lower Johnson Creek - Tomy Florence prop. - Hole #5 - Aug. 4, 1980
 (55° S. #4, 62' N. #1 on left bank)

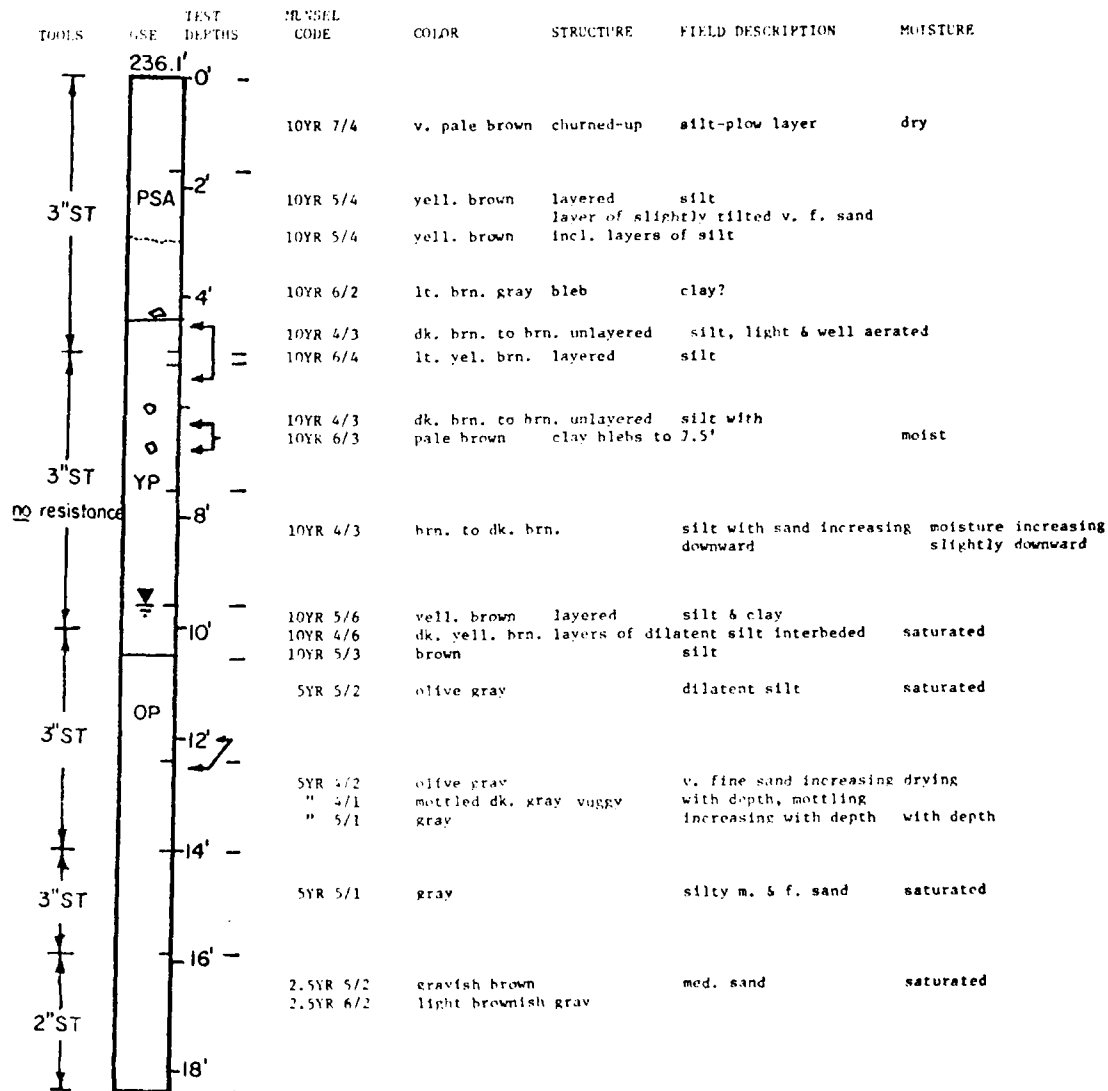


Figure 1.35. T. Florence site - Borehole #5

Lower Johnson Creek - Tommy Florence farm - Hole #7 - Aug. 7, 1980

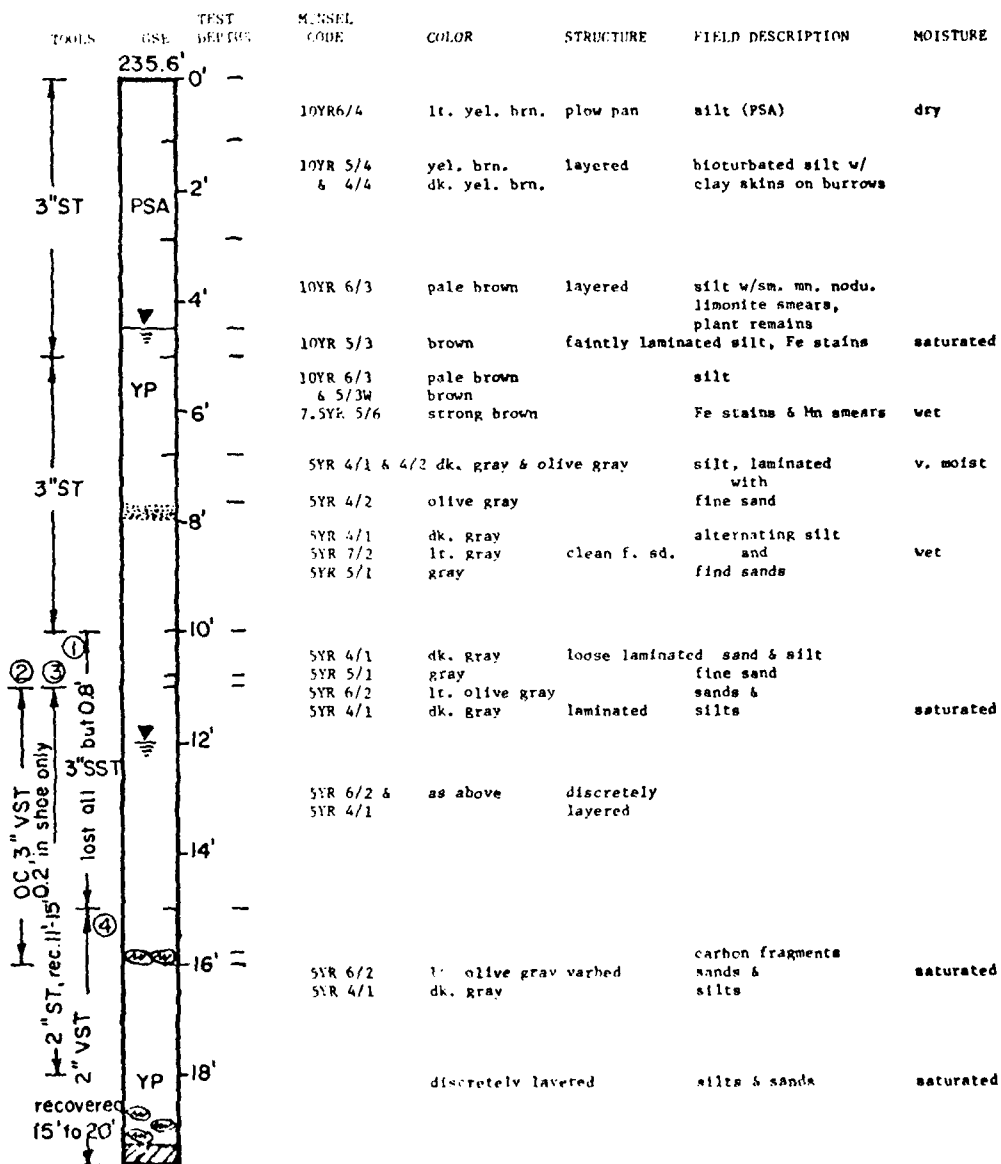


Figure 1.36. T. Florence site - Borehole #7

Lower Johnson Creek - Tommy Florence farm - Hole #9 - August 7, 1980

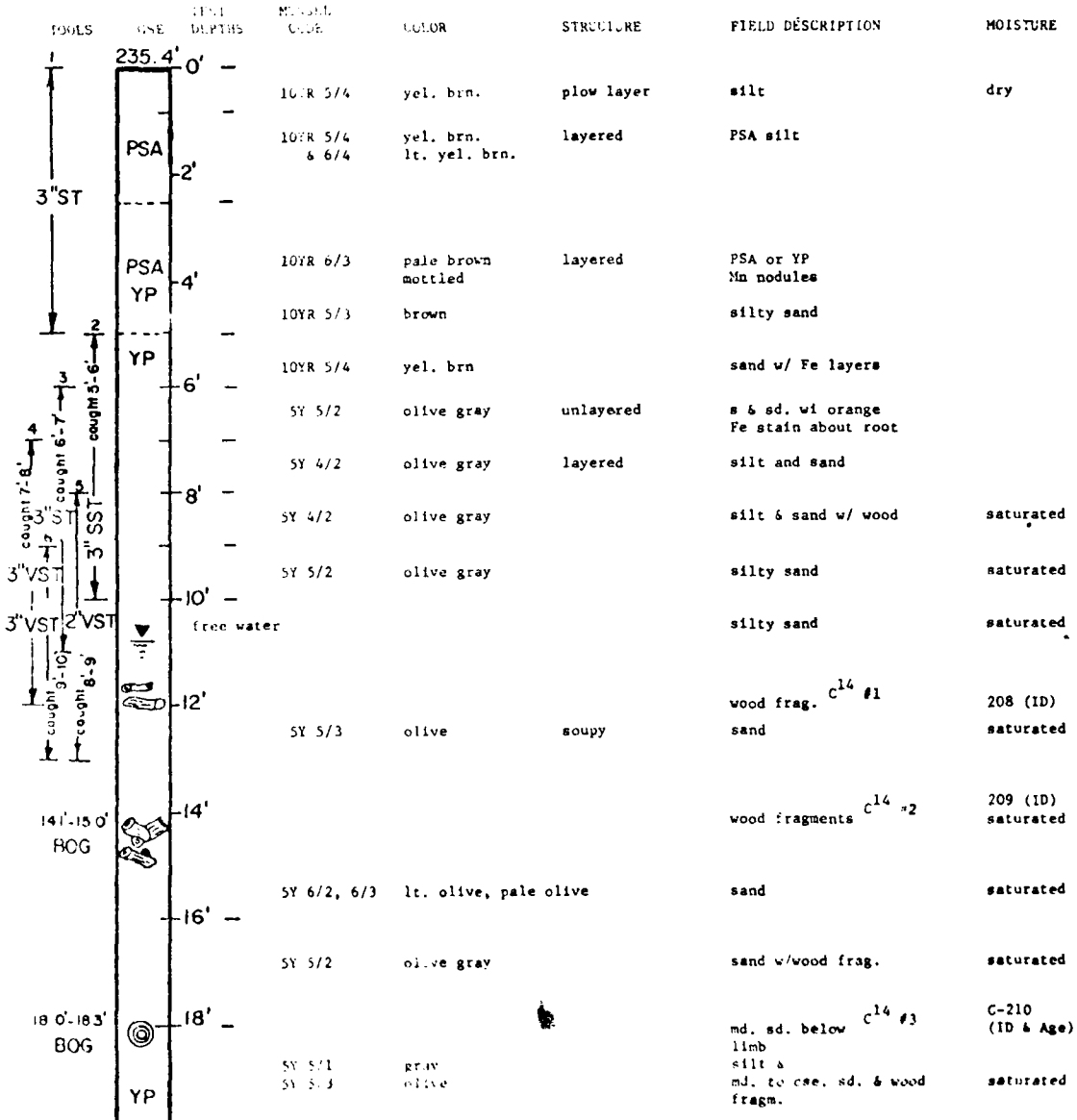


Figure 1.37. T. Florence site - Borehole #9

Upper Johnson Creek - T. A. Woodruff prop. - Hole #1 - May 1980

Hole on L. B. above wooden bridge, above CJ0-004

No Log

Samples taken for tension strength technique development in lab.

Figure 1.38. T. A. Woodruff site - Borehole #1

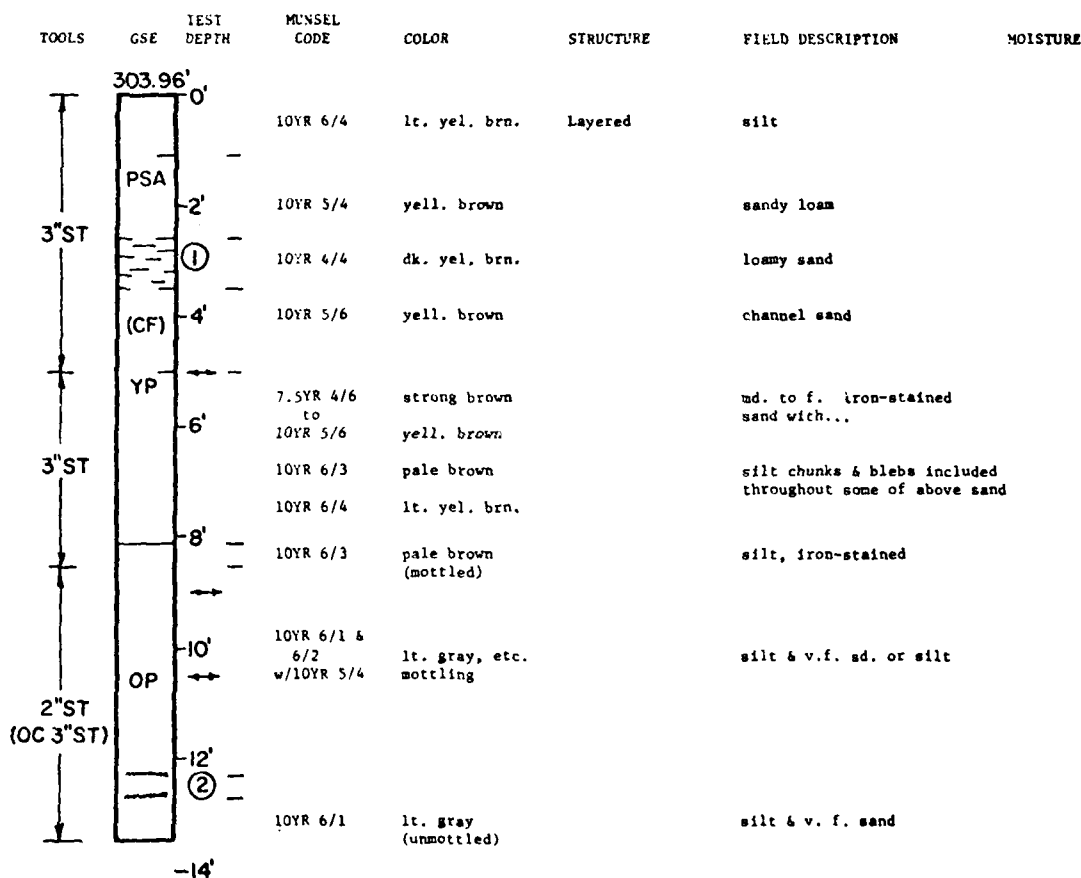
D.169

Upper Johnson Creek - T. A. Woodruff prep. - Hole #2 - May 28, 1980

TOOLS	GSE	TEST DEPTH	MUNSEL CODE	COLOR	STRUCTURE	FIELD DESCRIPTION	MOISTURE
3"ST		303.15' 0'	PL	10YR 6/4 10YR 4/3	lt. yel. brn. mottling		silt (Plow Layer)
3"ST			PSA	10YR 5/4	yell. brown	Layered	silty u.f. sand
				2'			
3"ST			YP	10YR 5/3	mott. brown	Unlayered	silt (w/Mn nodules)
				4'			
3"ST					light gray mottled		hard silty loam
				6'			
3"SSp			OP	lt. gray mottled			very hard silty loam
				8'			

Figure 1.39. T. A. Woodruff site - Borehole #2

Upper Johnson Creek - T. A. Woodruff prop. Hole #3 - May 30, 1980



(1) Occasional sandy layers or silty layers, Mn nodules, sand at base, YP? or PSA?

(2) Strong iron stains, crusting at 12.3' & 12.7'

Figure 1.40. T. A. Woodruff site - Borehole #3

Upper Johnson Creek - T. A. Woodruff prop. - hole #4 - June 2, 1980

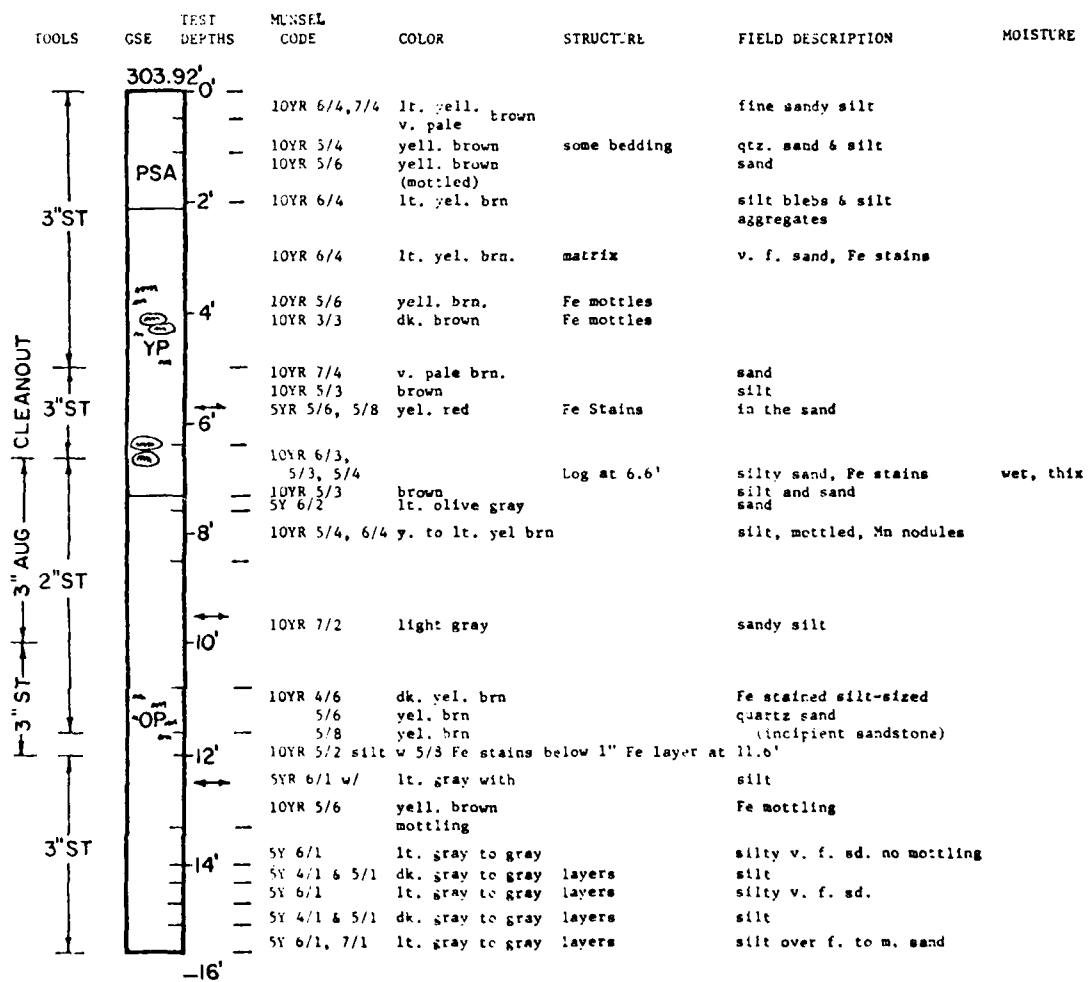


Figure 1.41. T. A. Woodruff site - Borehole #4

Upper Johnson Creek - T. A. Woodruff prop. - Hole #5 - June 4, 1980

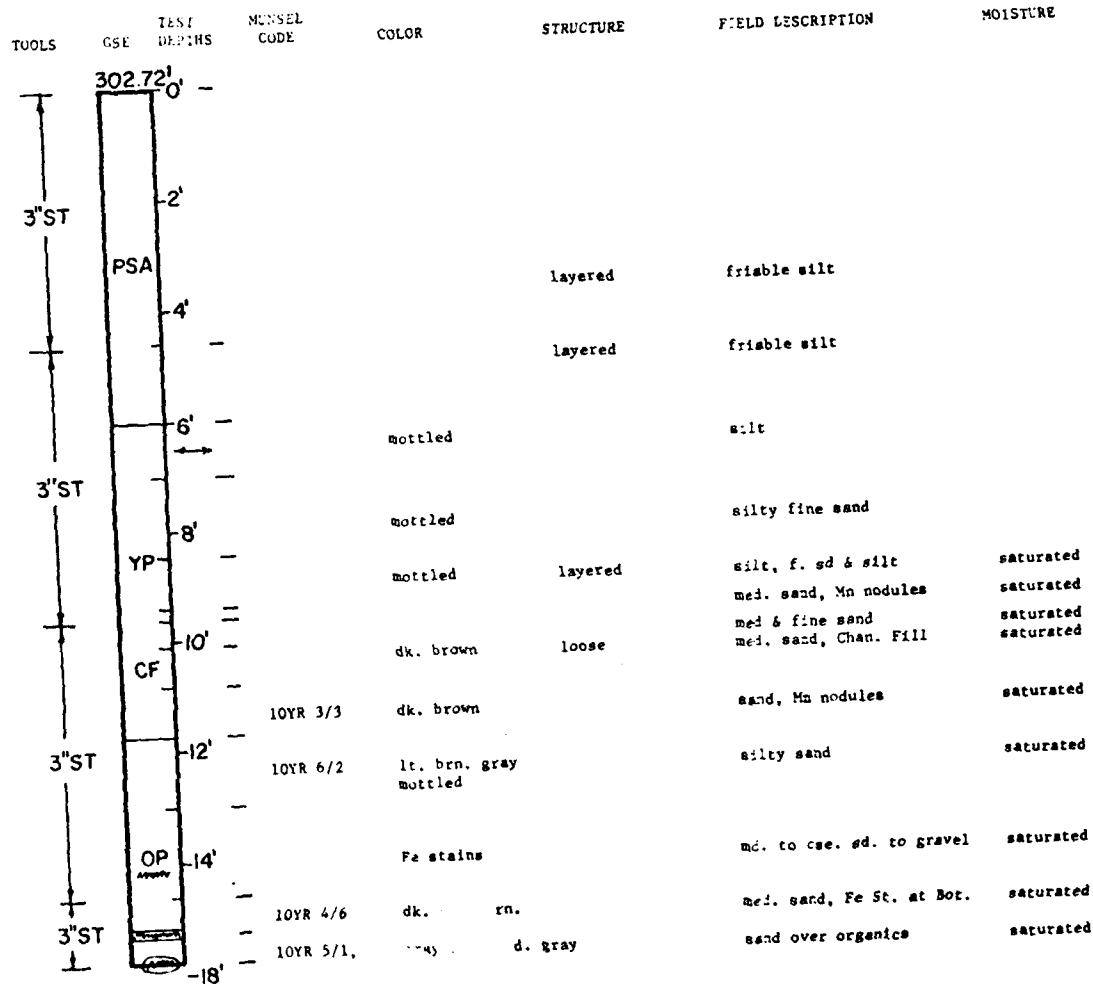


Figure 1.42. T. A. Woodruff site - Borehole #5

Upper Johnson Creek - T. A. Woodruff prop. - Hole #6 - June 4, 1980

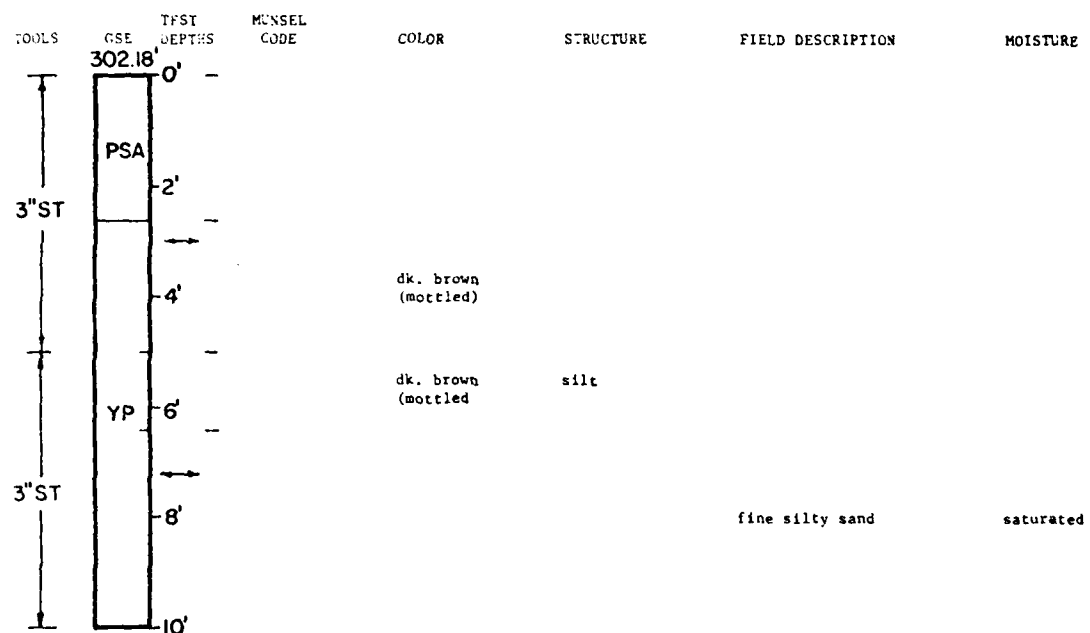


Figure 1.43. T. A. Woodruff site ~ Borehole #6

Upper Johnson Creek - T. A. Woodruff prop. - Hole #6a - June 16, 1980

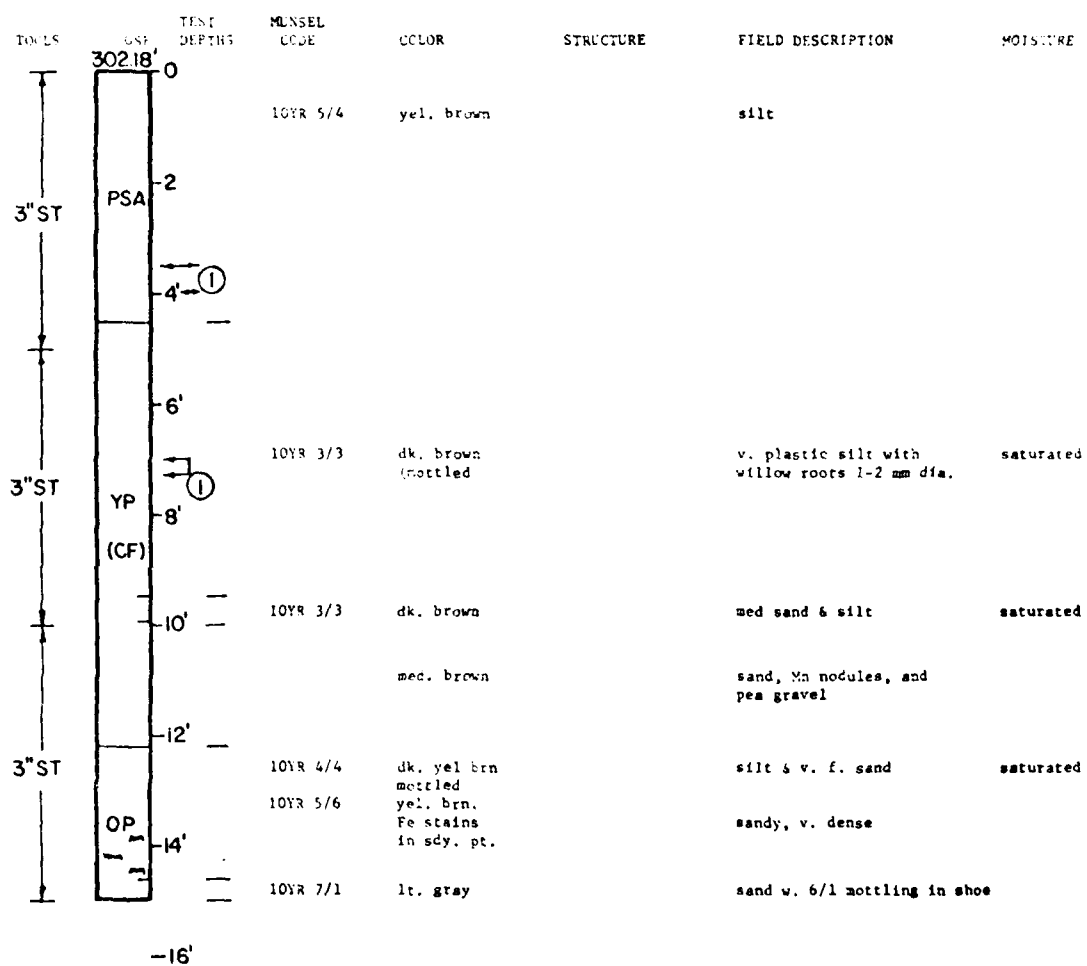
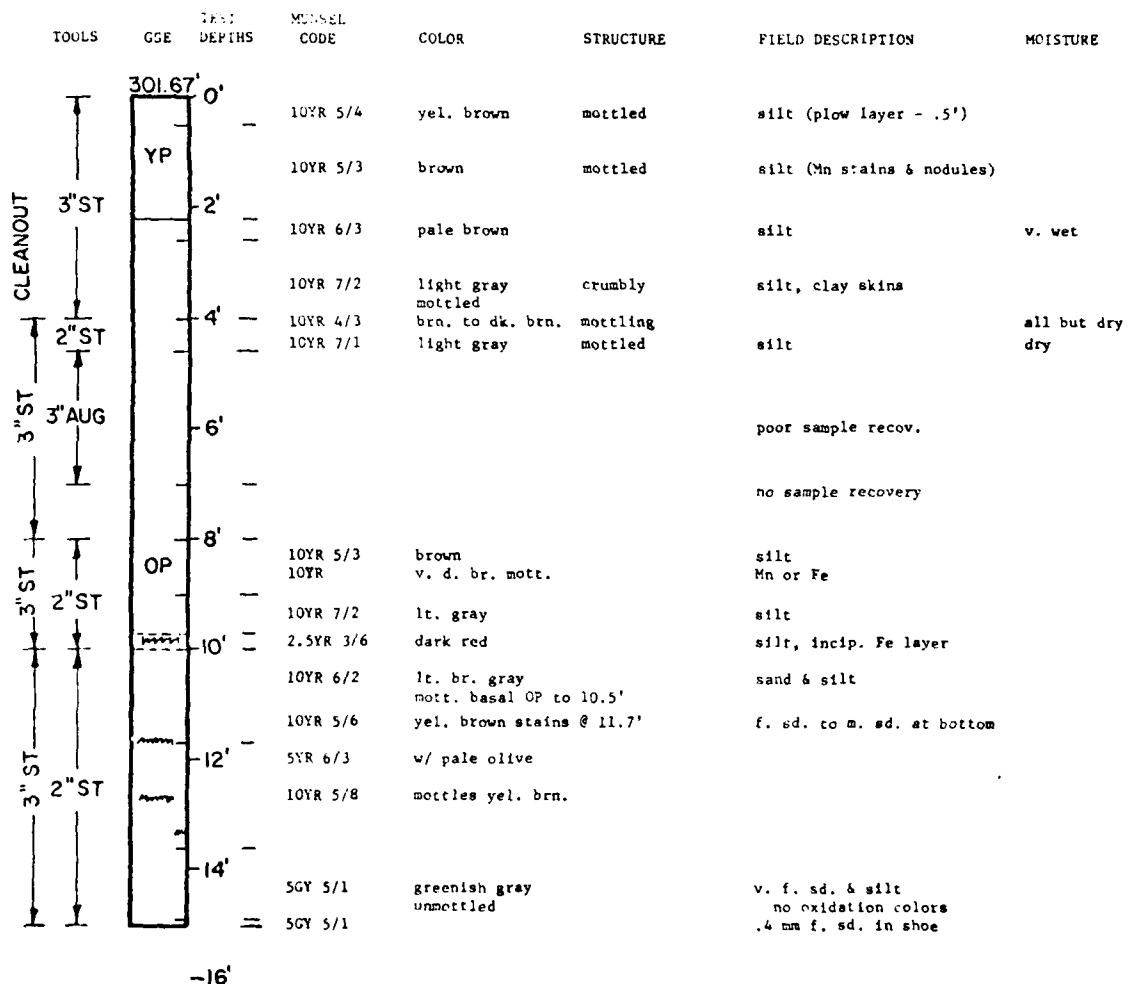


Figure 1.44. T. A. Woodruff site - Borehole #6a

Upper Johnson Creek - T. A. Woodruff prop. - Hole #7 - June 9, 1980



NO BLS tests in this hole

Figure 1.45. T. A. Woodruff site - Borehole #7

Upper Johnson Creek - T. A. Woodruff prop. - Hole #8 - June 16, 1980

TOOLS	USE	TEST DEPTHS	MUNSEL CODE	COLOR	STRUCTURE	FIELD DESCRIPTION	MOISTURE
3"ST		302.64' 0'	-	-		Plow layer	
3"AUG		2'	-			PSA	
3"ST	PSA	4'	10YR 5/4	yel. brown	layered	silt	
		6'	10YR 5/4 & 4/3	yel. brn. & dk. brn.	layered & mottled to 6'	1" cottonwood roots	
		8'			mottled & not layered below 6'	silt	
3"ST		10'	10YR 5/3	brown		Fe stained at 7.5'	saturated
		10'	10YR 5/2 & 5/3	grayish brn brown		v. f. sandy silt	
		12'	10YR 4/2	dk. gray brn.	layered	coarse sand & pea gravel	
3"ST		12'	10YR 5/8 7/1	yel. brn. lt. gray		stained sand	
		14'	10YR 7/1	lt. gray		sand	
3"ST CLEANOOUT	OP	14'	10YR 5/8	ye. brown		sand	saturated
2"ST		16'	7.5YR 5/6	strong brown		Fe stained sand	saturated

NO BHS tests in this hole.

Figure 1.46. T. A. Woodruff site - Borehole #8

Upper Johnson Creek - T. A. Woodruff prop. - Hole #9 - July 9, 1980
(2.5' So. of #3)

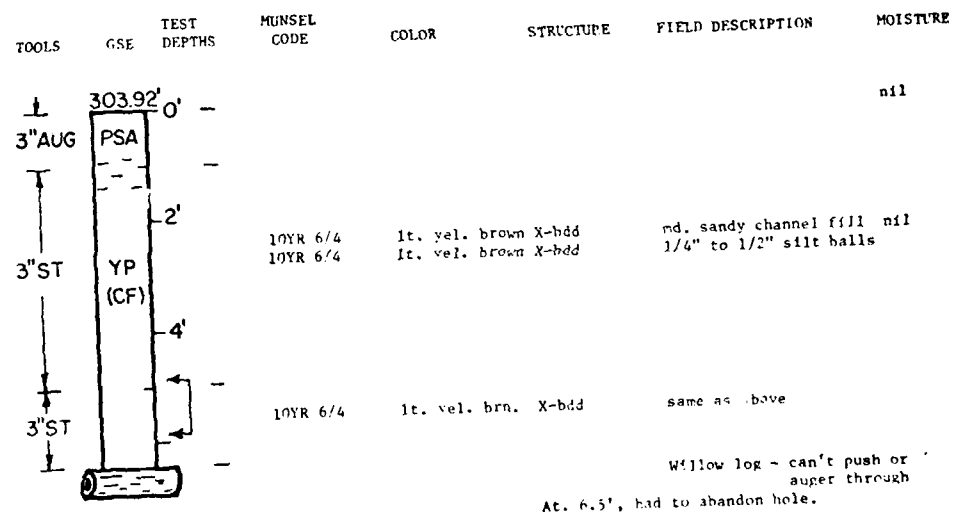


Figure 1.47. T. A. Woodruff site - Borehole #9

Upper Johnson Creek - T. A. Woodruff prop. - Hole #10 - July 9, 1980
(3.0' West of #9)

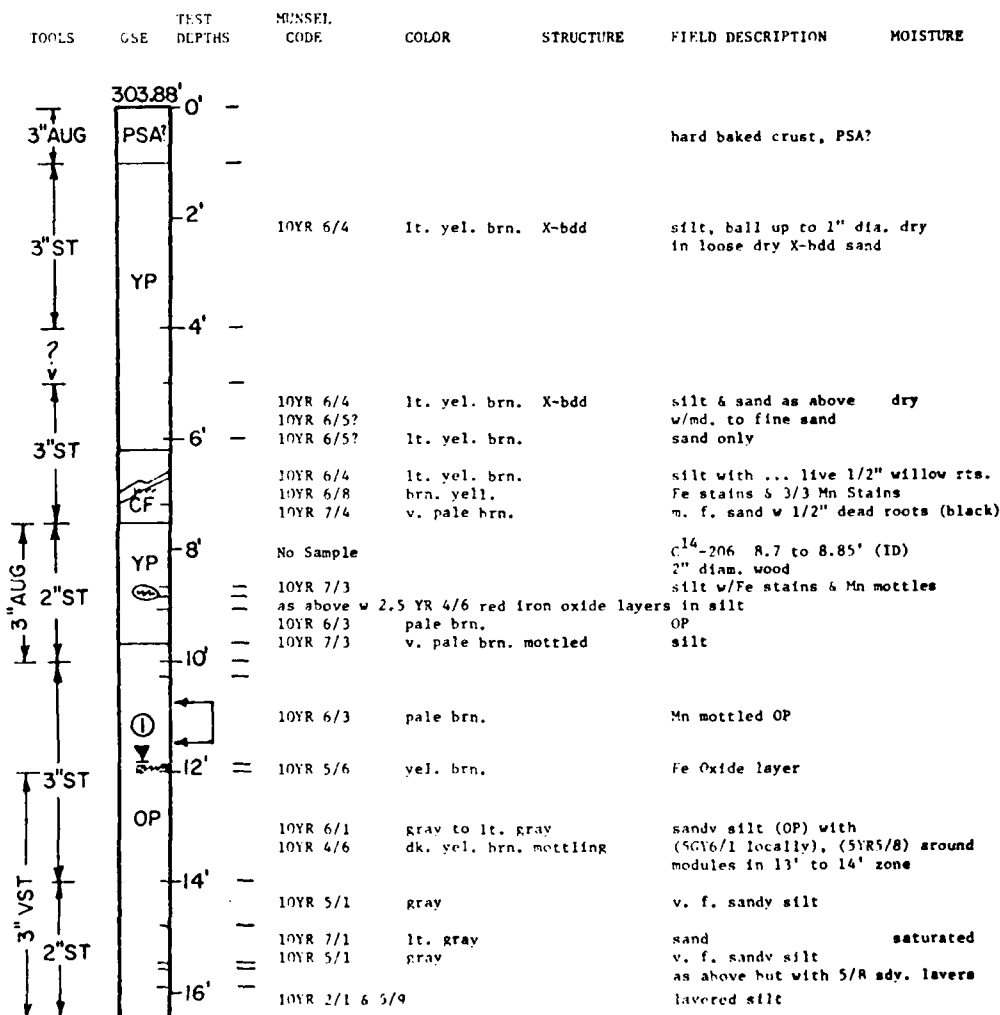


Figure 1.48. T. A. Woodruff site - Borehole #10

Upper Johnson Creek - T. A. Woodruff prop. - Hole #11 - July 24, 1980
 (adjacent to #8 E. of Cottonwood Tree)

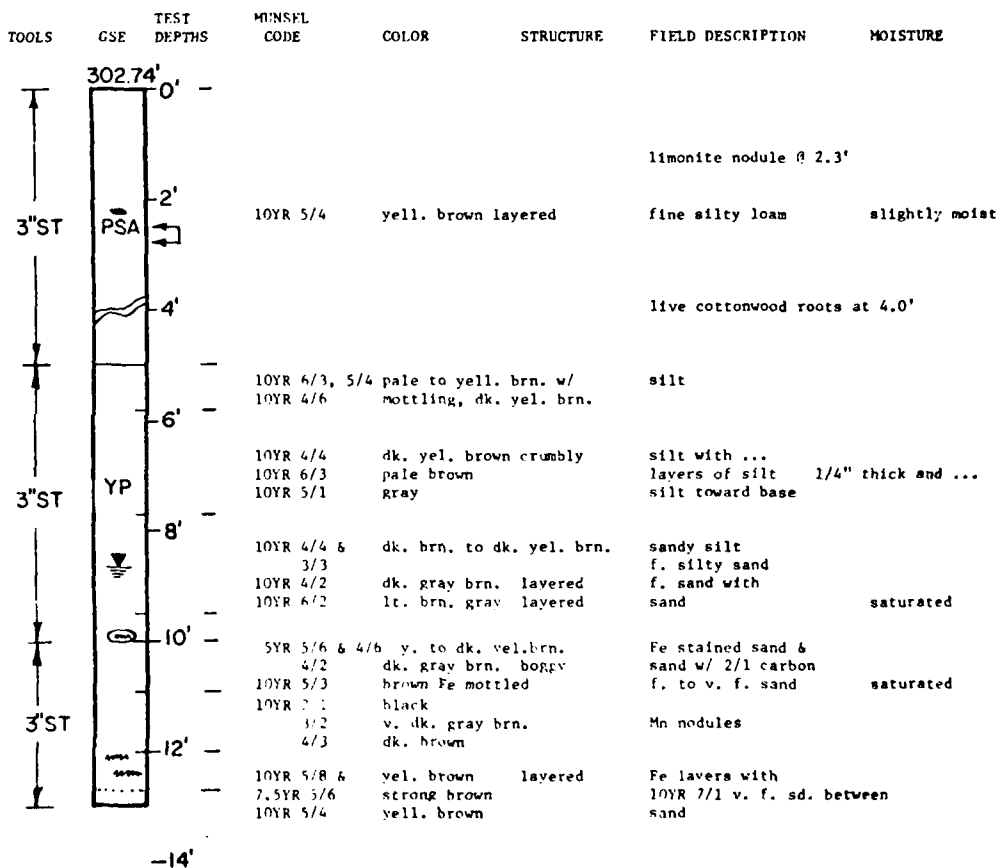


Figure 1.49. T. A. Woodruff site - Borehole #11

Lower Goodwin Creek - Katherine Leigh farm - Hole #1 - May 19, 1980

TOLLS	GSE TEST DEPTHES	MUNSEL CODE	COLOR	STRUCTURE	FIELD DESCRIPTION	MOISTURE
241.21'	0' -			layered	PSA fine silt	
	PSA					
	4'		mottled & rooted		YP	
	YP		richer brown		YP	
	8'	LUR 2/2	mottled & tanned	thin ironstone layer silt	f. sand & clay	saturated
	CF sand	v. dk. brown	layered			
	10'					

Located in corner of field at downstream end of bend on RHB.

Samples of YP taken for UC & UT testing
 1/4 borehole tests run before heavy rains washed out proceedings.

Figure 1.50. K. Leigh site - Borehole #1

Lower Goodwin Creek - Katherine Leigh farm - Hole #2 - May 27, 1980
 (SW Corner of Field beneath Pecan)

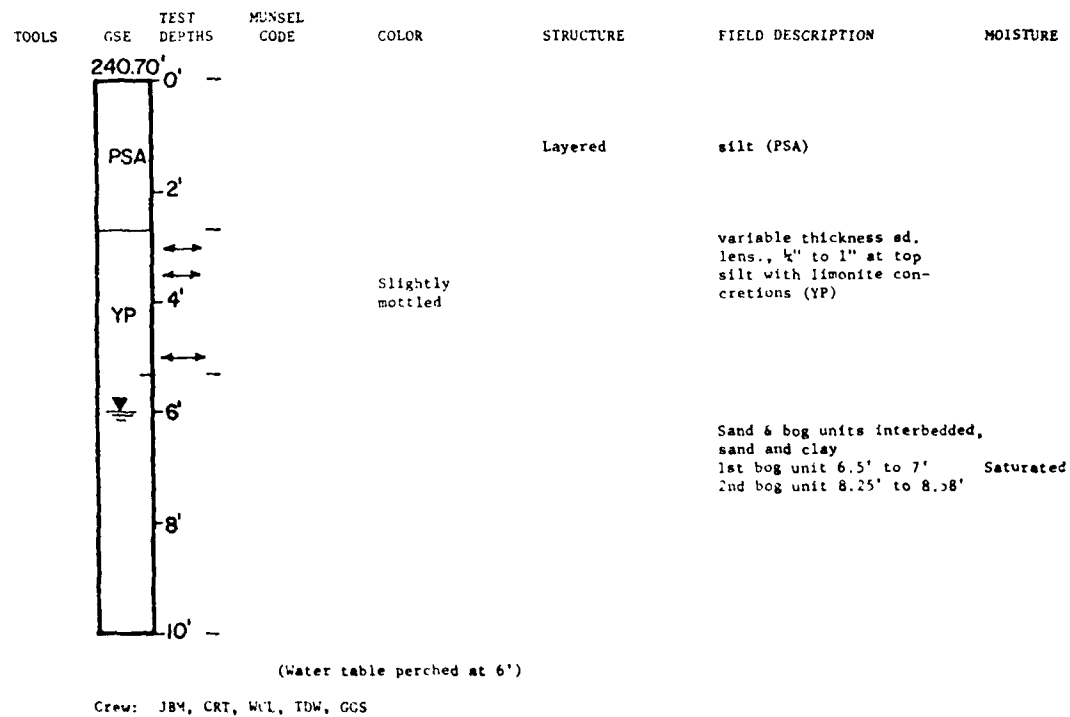


Figure 1.51. K. Leigh site - Borehole #2

Lower Goodwin Creek - Katherine Leigh farm - Hole #3 - May 27, 1980
 (beneath Bodock tree 30' N. of #2)

TOOLS	TEST DEPTHS	MUNSEL CODE	COLOR	STRUCTURE	FIELD DESCRIPTION	MOISTURE
	24.0	0	-		plow layer in silt	
PSA	2'	-	tan	layered	silt (PSA)	
YP	4'	-	light tan mottled		silt w/limonite (YP)	
(CF)	6'	-		X-hdd	md. sand clay skins pt. bars	
	8'	-	gray mottled		sandy YP	
YP	10'	-	gray		fine sand, org. fragm.	saturated
	12'	-	gray		silt w/carbon	saturated
	14'	-	gray		md. sand, pgs organics at 14.0' (YP)	
YP	16'	-	gray		sandy silt (YP)	

Figure 1.52. K. Leigh site - Borehole #3

Lower Goodlin Creek - Katherine Leigh farm - Hole #4 - Aug. 8, 1980

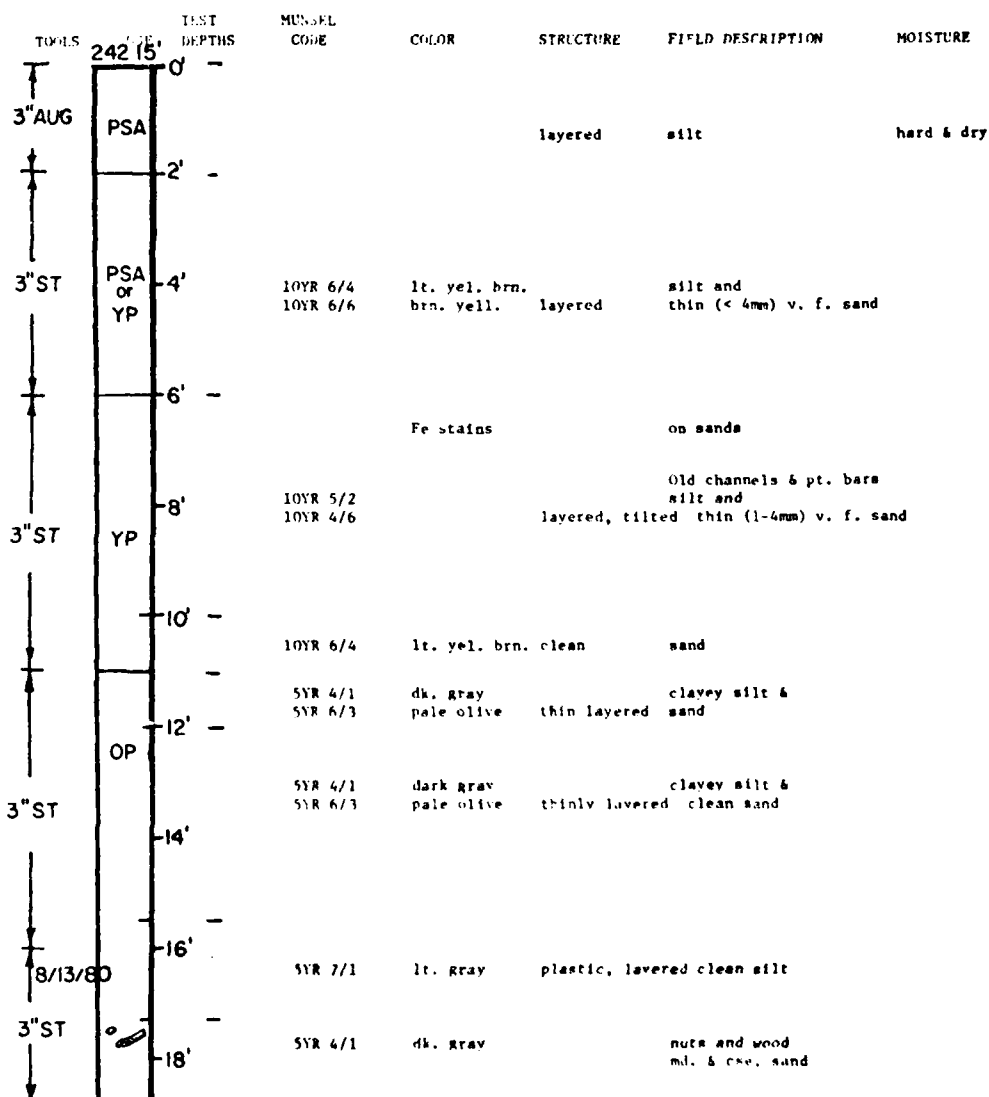


Figure 1.53. K. Leigh site - Borehole #4

Lower Goodwin Creek - Katherine Leigh farm - Hole #5 - Aug. 15, 1980

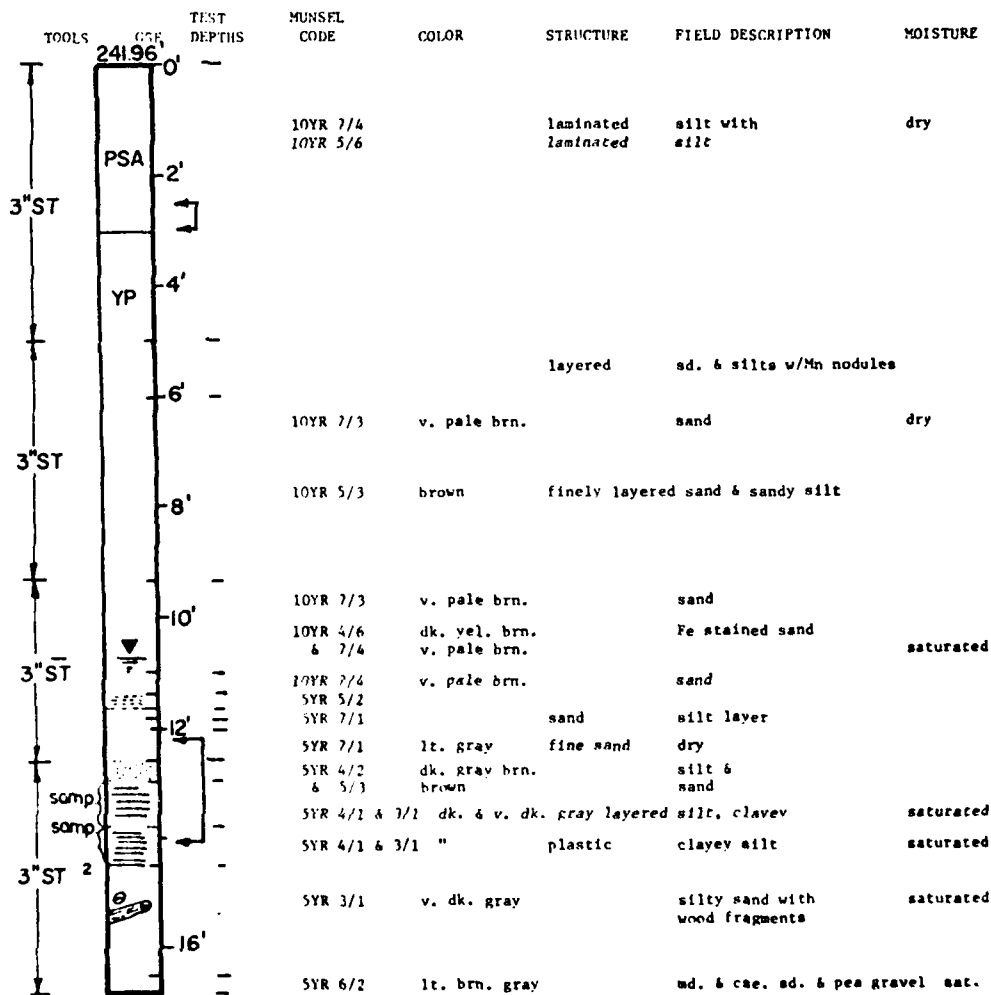


Figure 1.54. K. Leigh site - Borehole #5

Lower Goodwin Creek - Katherine Leigh farm - Hole #6 - Aug. 19, 1980

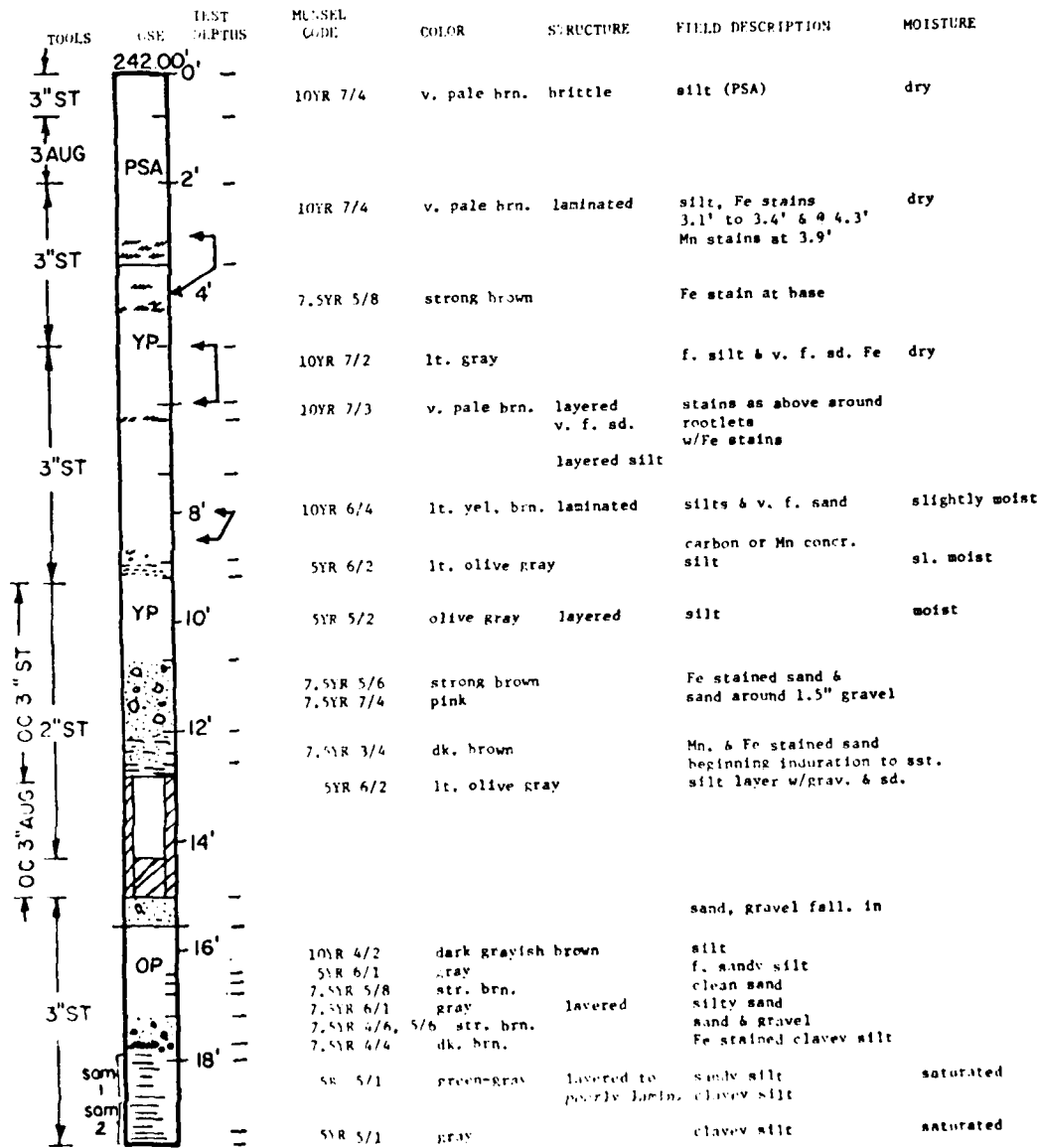


Figure 1.55. K. Leigh site - Borehole #6

Lower Goodwin Creek - Katherine Leigh farm - Hole #7 - August 19, 1980

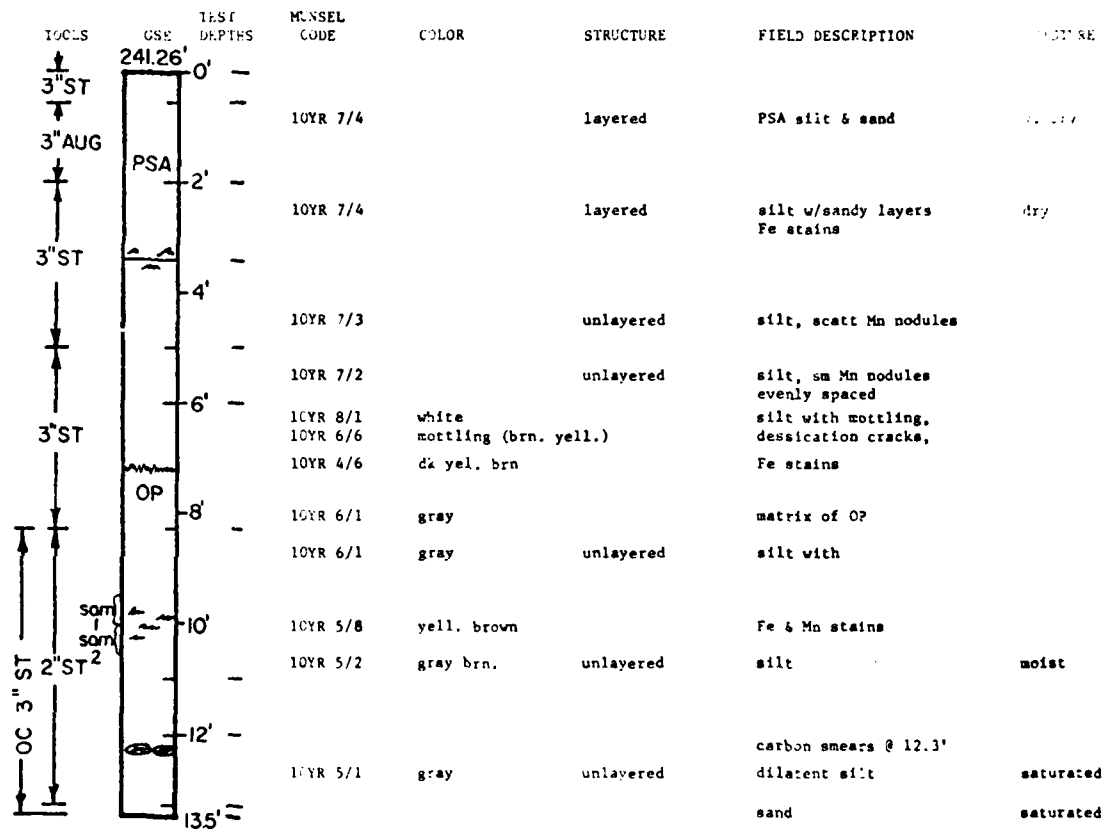


Figure 1.56. K. Leigh site - Borehole #7

ADDENDUM 2
IOWA BOREHOLE SHEAR TESTER

Addendum 2
List of Figures

Figure No.	Title	Page
2.1	Direct Shear Test for Laboratory Testing	191
2.2	Borehole Shear Test, essentially a direct shear test performed on the soil inside the borehole	193
2.3	Borehole Shear Test Apparatus	194
2.4	Shear Head and Connecting Rods ready for insertion into the borehole	195
2.5	Pulling Assembly, Base Plate and Gas Control Console	197
2.6	Pulling force is applied by cranking the handle at a rate of two turns per second	198
2.7	Old and New (High Pressure) Borehole Shear Test Shear Plates . .	201

2.1 INTRODUCTION

The borehole shear tester is a simple device which measures, directly, the shear strength of fine to medium grained soils *in situ*. Its main advantages are: (i) the cohesion and friction angle can be evaluated separately, in about one tenth of the time required for laboratory triaxial or direct shear testing, (ii) test data are plotted on site, during testing, enabling immediate repetition if results are unreasonable, (iii) tests can be carried out at various depths in the bank to locate weak strata, and (iv) test depths may be tailored to provide data on the stratigraphic units identified from the log of the borehole.

2.2 THEORY

The shear strength of a soil can be described by the Coulomb equation. If there is no significant pore water pressure:

$$s = \sigma \tan \phi + c \quad (2.1)$$

s = drained shear strength

ϕ = apparent friction angle

σ = normal stress

c = apparent cohesion.

When values of σ and s are plotted on axes of σ (x-axis) and s (y-axis) they produce a straight line of slope, $\tan \phi$, and intercept c . This line is called the Mohr-Coulomb Rupture line. Actually, the Mohr-Coulomb failure line is concave downward, but for limited ranges of stress, it can be approximated as a straight line.

In a direct shear test a sample of soil is placed in a split box and a normal load is applied (Fig. 2.1). A shearing force is then applied so that the top half of the box tends to slide over the bottom half, producing a shear plane in the soil. The normal load and peak shear force are converted to stresses by dividing by the sample area, and plot as a point on the σ - s graph. Since that combination of σ and s correspond to state of failure in the soil, by definition, the point must lie on the Mohr-Coulomb line. The test is repeated on an identical soil sample, but with a higher normal load. For a frictional material the shear force will also be higher. After several repetitions, sufficient points are generated to define the Mohr-Coulomb line and then calculate c and ϕ .

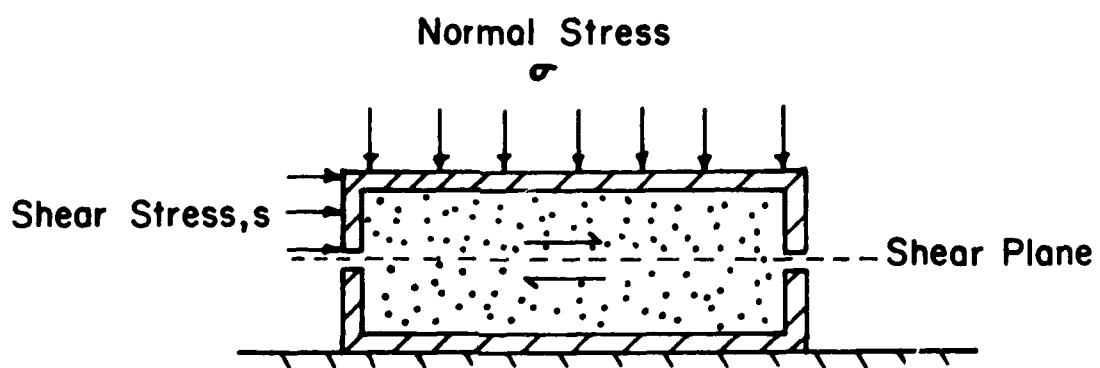


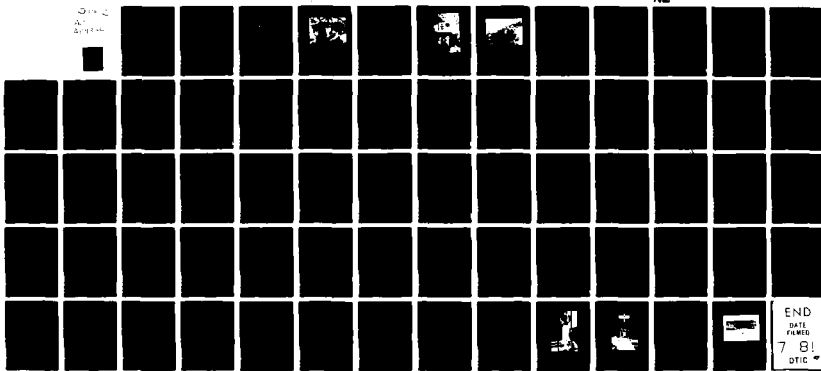
Figure 2.1. Direct Shear Test for Laboratory Testing.

AD-A101 389

SOIL CONSERVATION SERVICE OXFORD MS SEDIMENTATION LAB F/6 8/13
STREAM CHANNEL STABILITY, APPENDIX D, BANK STABILITY AND BANK M--ETC(U)
APR 81 C R THORNE, J B MURPHEY, W C LITTLE

UNCLASSIFIED

NL



END
DATE FILED
7-81
BY

The borehole shear test is essentially a direct shear test performed on the soil inside the borehole. An expanding head provides the normal load (Fig. 2.2.) by expanding out under gas pressure to make two shear plates bite into the soil. The head is then pulled axially up the borehole using connecting rods and a lead screw. Pulling continues until the soil adjacent to the toothed plates shears and the pulling force declines. The maximum pulling force when divided by the area of the plates corresponds to the shear strength, s . The data produce a point on the Mohr-Coulomb line on the σ - s graph. Repetitions at higher σ values produce a series of points which define the Mohr-Coulomb line, c and ϕ . The results obtained seem reasonable for a variety of soil types (Handy and Fox, 1967).

2.3 APPARATUS

The apparatus consists basically of 3 parts: the shear head, pulling device and gas control console (Fig. 2.3.). The head consists of a gas operated piston with a rolling diaphragm to minimize friction, and two curved shear plates. The diameter of the head and plates when contracted is a little less than 76 mm (3 inches). The exact design of the shear plates depends on the type of soil to be tested (Lutenegger, Remmes and Handy, 1978). The console controls gas pressure that is used to expand and contract the head. Liquid CO₂ or compressed Nitrogen may be used to supply gas pressure (Wineland, 1975). The pulling device consists of a flat plate of 0.09 m² (1 ft²) area with a worm gear and lead screw for pulling the rod, which is connected to the head, and a hydraulic pressure measuring system consisting of two hydraulic cylinders, pistons and a hydraulic pressure gauge. The whole device including about 10 m (30 feet) of pulling rod and a reamer for fine finishing of the borehole weighs about 40 kilograms (90 pounds).

2.4 TESTING PROCEDURE

The first step is to drill a borehole to slightly more than the depth required for the deepest test. The inside of the hole is then smoothed using the reamer supplied with the apparatus. The head is attached to the necessary number of connecting rods and lowered into position in the hole (Fig. 2.4.). The head is attached to the pulling device by placing the base plate, thrust bearing and ring gear over the connecting rod so that

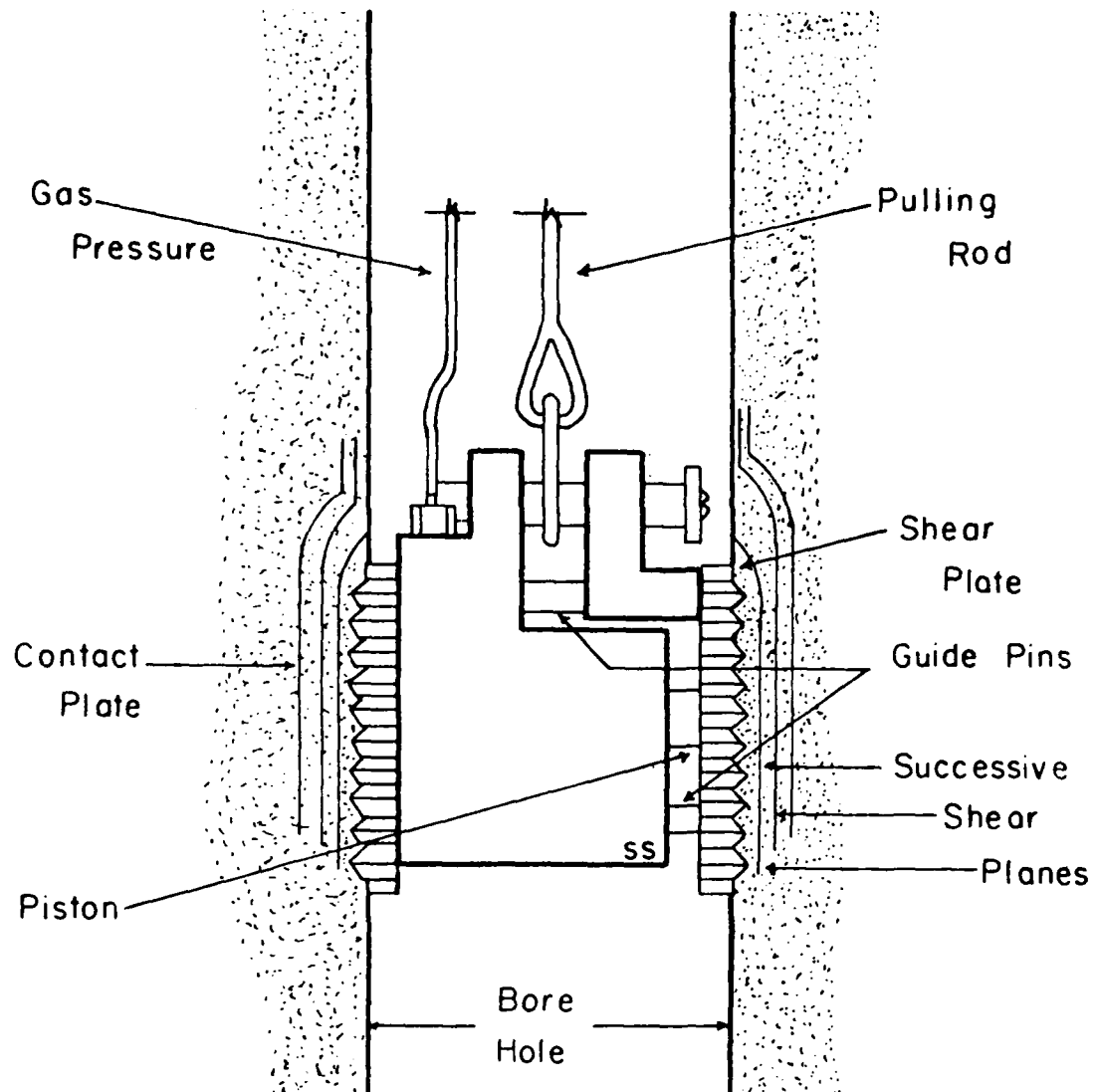


Figure 2.2. Borehole Shear Test, essentially a direct shear test performed on the soil inside the borehole.

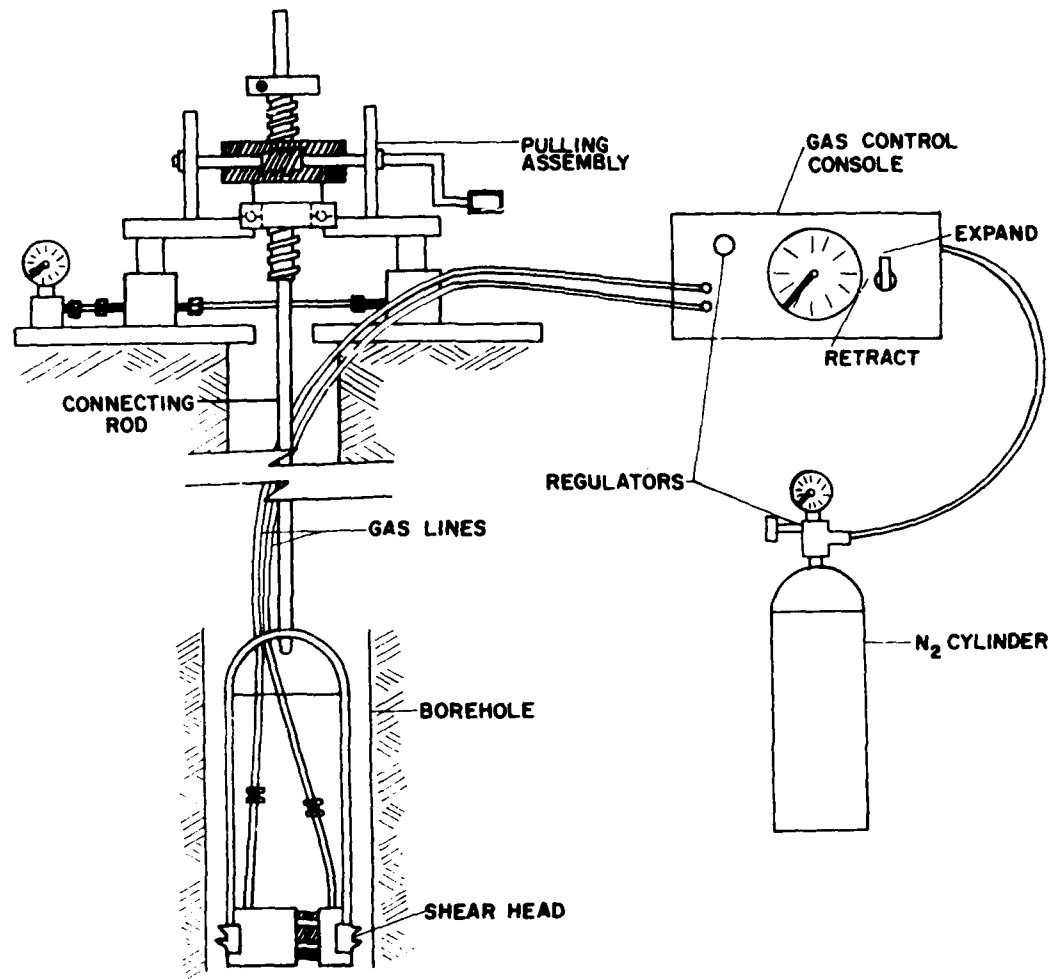


Figure 2.3. Borehole Shear Test Apparatus.

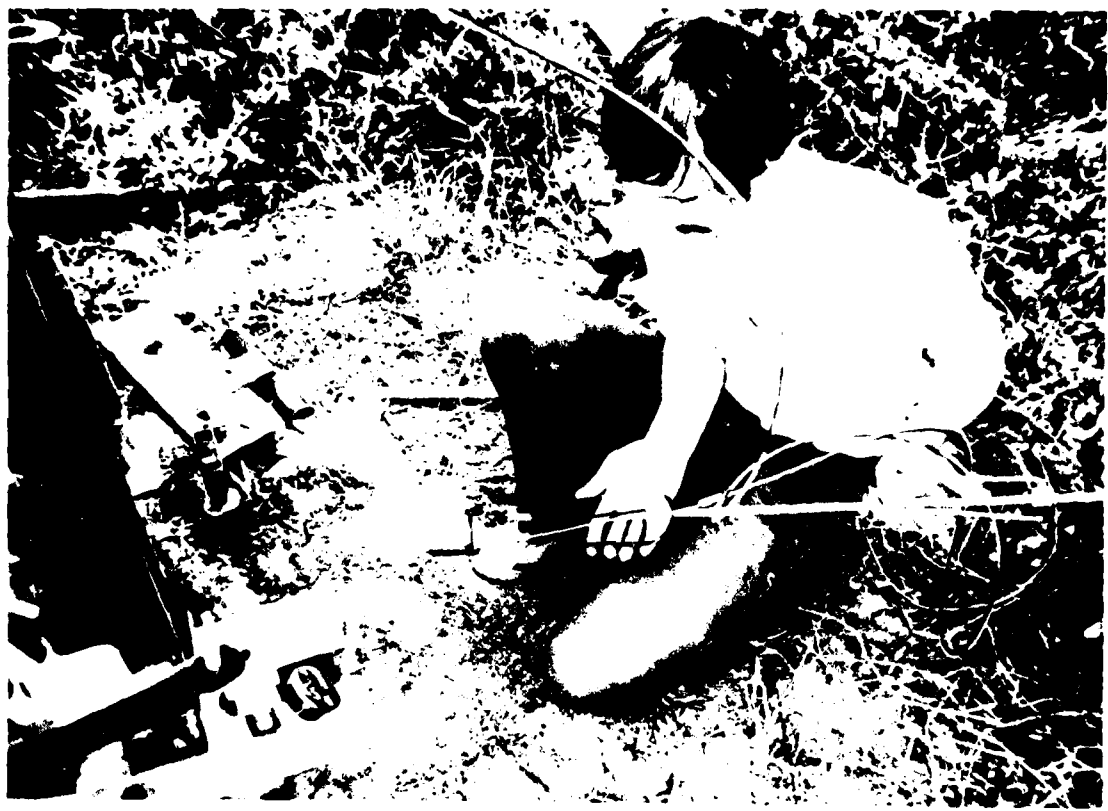


Figure 2.4. Shear Head and Connecting Rods ready for insertion into the borehole.

the ring gear engages a worm drive on the base plate. An acme-threaded screw with locking lugs in the top is screwed down through the ring gear until it is nearly flush at the top. A clamping collett is then dropped over the connecting rod and turned so the cross-wise slots engage the locking lugs. The torque arm fits between the crank bearing blocks and is then tightened in place (Fig. 2.5.). The hydraulic pressure gauge is adjusted to read zero under the combined load of the head, connecting rods and gear assembly. The gas pressure required is set on the console (Fig. 2.5.) and the head expanded. Ten minutes is allowed for the soil to consolidate and any pore pressures to dissipate. The shearing force is applied to the soil by cranking the handle and turning the worm drive (Fig. 2.6.). One turn advances the head 0.0254 mm (0.001 inches). By turning the handle at a rate of 2 turns per second the standard shear rate of 0.0508 mm/sec (0.002 inches/second) is achieved. Typically, with a constant rate of strain, the shear force rises rapidly, then more slowly until it reaches a peak. In some soils the peak value is maintained indefinitely but usually it decreases after a time. The normal pressure and shear force are noted and converted to the normal stress and shear strength using calibration charts supplied with the apparatus. If a stage test is desired, the head is wound back down the hole until the shear force is zero and an increment is added to the normal pressure. Five minutes are allowed for consolidation and then the shearing force is again applied. This procedure is repeated until sufficient points are obtained or there is a sharp decrease in the shear strength, indicating that the head is fully expanded. If it is wished to avoid a stage test, the head is removed after the first test, cleaned and returned to the same depth but rotated through 90°. After the second test the head is again removed, cleaned and returned to the hole but at a slightly greater depth (usually 80 mm deeper (3 inches)) within the same soil layer. This is repeated until the desired number of points are obtained.

The stage test has the advantages of saving time and not requiring duplicate soil conditions along the borehole. However, stage testing involves an assumption that the accumulated stresses and strains of previous tests do not significantly affect the results in the next stage. This is not a tenable assumption for all soils, especially those with sensitive structural features. With the standard shear plates normal stresses usually range from about 28 kPa (4 psi) to 104 kPa (15 psi). The

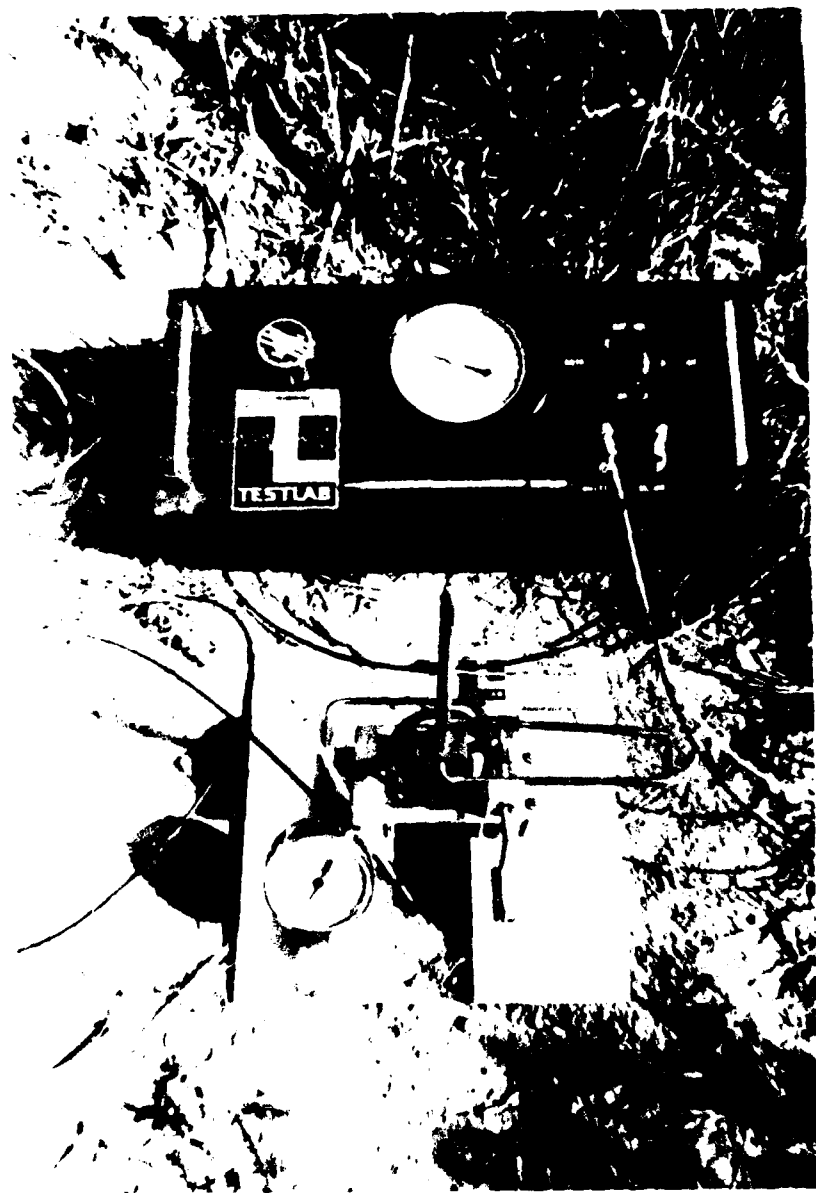


Figure 2.5. Pulling Assembly, Base Plate and Gas Control Console. The required pressure has been set and the shear head piston control switched to 'expand'. The axial stress meter has been set to zero.

D.197

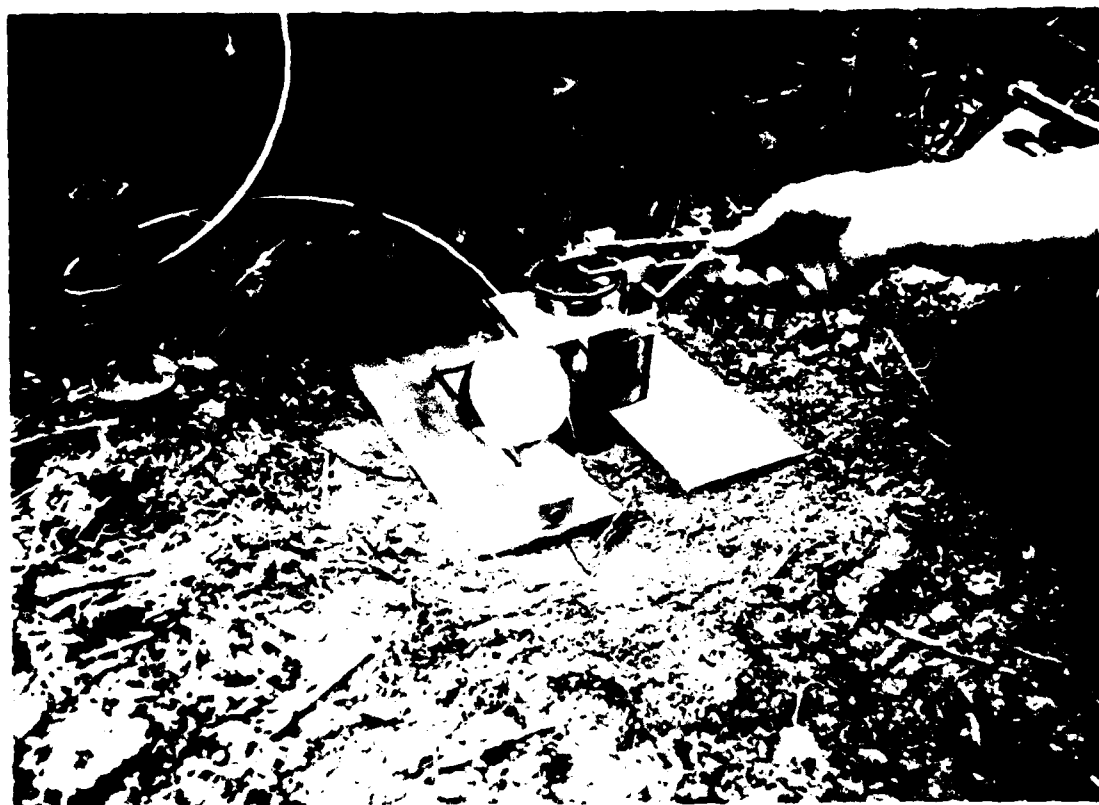


Figure 2.6. Pulling force is applied by cranking the handle at a rate of two turns per second.

high pressure plates for stiff soils generally work in the range 206 kPa (30 psi) to 2,760 kPa (400 psi). A stage test usually takes about one hour to produce 5 points and a non-stage test about two hours.

2.5 DISCUSSION

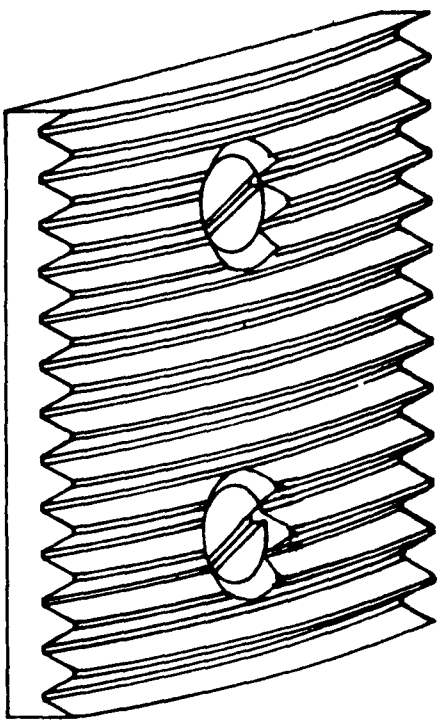
The Borehole Shear Tester is a comparatively new device which has not had years of use and application to develop a sound knowledge of its limitations. Therefore results obtained with the tester are to be treated somewhat cautiously because of doubt which still exists in their interpretation.

The most basic question is whether the BST is a drained or an undrained test. The consolidation and drainage times of 10 minutes (initial) and 5 minutes (stage tests) will certainly be sufficient for full drainage in sands and partially saturated soils but might only allow partial drainage in saturated clay. Hence the BST (Borehole Shear Tester) would be a consolidated-drained test in sands and partially saturated soils, but perhaps a consolidated-undrained test in saturated clays (Schmertmann, 1975). Even more confusing, the test could result in partial but not complete drainage. Handy (1975) considered the problem of drainage and reasoned that BST data will be conservative. His results, in analyzing slope stability, using BST data suggest that c and ϕ estimates may be used without modification in considering the worst case. This would give BST data very wide applications.

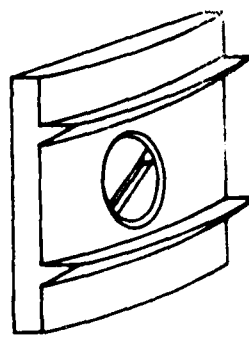
The borehole shear test avoids the serious problem of soil disturbance that is inherent in laboratory tests on field sampled soil cores. However in the BST test there is disturbance to the soil lining the borehole. It would appear at first that this problem would be critical to the BST test, since the test is performed on soil in the highly disturbed "smear zone" at the borehole surface. However, the nature of the test may mitigate the problem of soil disturbance. First, consolidated tests are less sensitive to soil disturbance than unconsolidated tests and second, the consolidation of the soil in the smear zone tends to promote failure in the weaker, deeper, less disturbed soil outside the smear zone. However, this tends to produce an unwanted bearing resistance at the top of the shear plates.

The most widespread problem encountered in the use of the Borehole Shear Tester is that of incomplete seating of the shear plates so that the shear teeth are only partly filled with soil. An associated problem is that the large number and low angle of the teeth introduce serious local soil disturbance, tending to destroy fabric and change the soil from a cohesive to a noncohesive material. These phenomena can result in a serious underestimation of the cohesion. Progressive seating of the plates and filling of the teeth at successively higher normal stresses produce a false linear envelope with a friction angle which is too high (Handy, 1975). These problems were encountered in this study in tests using the original, multi-toothed shear plates. The problem was solved by replacing the old shear plates with high pressure plates of the type described by Luttenegger, Remmes and Handy (1978) (Fig. 2.7.).

The main design changes were developed by Yang (1975) in extension of the BST technique to rock mechanics (Handy *et al.*, 1976). In the new plates the number of teeth is reduced to 2 and are spaced at 5.8 times the tooth height, so that a large percentage of the enclosed soil is undisturbed by tooth incision. The teeth themselves are 30° half-wedges which slide into the soil easily. Plate area is reduced by a factor of 5 to allow higher normal pressures and promote full seating. Working at these high pressures introduces the possibility of the normal load exceeding the bearing capacity of the soil. However this should be obvious by a falling off in the shear strength. Comparative tests show the new plates to give higher, and more reasonable, estimates for cohesion and usually a somewhat lower and likewise more reasonable friction angle (Luttenegger, Remmes and Handy, 1978). The results suggest that the old plates and stage test approach may be used for soft soils but that the new plates and nonstage tests should be used for stiff soils. When this convention is followed the BST seems to be an excellent means of obtaining *in situ* measurements of c and ϕ . The results of this study fully endorse this conclusion.



OLD PLATE



NEW PLATE

Figure 2.7. Old and New (High Pressure) Borehole Shear Test Shear Plates.

ADDENDUM 3
BOREHOLE SHEAR TESTS:
TABLES OF RESULTS

March 4

to

August 21

1980

Addendum 3
List of Tables

Table No.	Title	Page
3.1	Test 1, Davidson Creek, BH1	205
3.2	Test 2, Davidson Creek, BH2	206
3.3	Test 3, Johnson Creek at Tommy Florence site (J/TF), BH1 . . .	207
3.4	Test 4, J/TF, BH1	208
3.5	Test 5, Goodwin Creek at Katherine Leigh site (G/KL), BH1 . . .	209
3.6	Test 6, G/KL, BH1	210
3.7	Test 7, G/KL, BH2	211
3.8	Test 8, G/KL, BH2	212
3.9	Test 9, G/KL, BH2	213
3.10	Test 10, Johnson Creek at T. A. Woodruff site (J/TAW), BH2 . .	214
3.11	Test 11, J/TAW, BH2	215
3.12	Test 12, J/TAW, BH2	216
3.13	Test 13, J/TAW, BH2	217
3.14	Test 14, J/TAW, BH3	218
3.15	Test 15, J/TAW, BH3	219
3.16	Test 16, J/TAW, BH2	220
3.17	Test 17, J/TAW, BH4	221
3.18	Test 18, J/TAW, BH4	222
3.19	Test 19, J/TAW, BH4	223
3.20	Test 20, J/TAW, BH5	224
3.21	Test 21, J/TAW, BH6a	225
3.22	Test 22, J/TAW, BH6	226
3.23	Test 23, J/TAW, BH6a	227
3.24	Test 24, J/TAW, BH9	228
3.25	Test 25, J/TAW, BH10	229
3.26	Test 26, J/TAW, BH11	230
3.27	Test 27, J/TF, BH2	231
3.28	Test 28, J/TF, BH2	232
3.29	Test 29, J/TF, BH4	233
3.30	Test 30, J/TF, BH4	234

3.31 Test 31, J/TF, BH3	235
3.32 Test 32, J/TF, BH3	236
3.33 Test 33, J/TF, BH2	237
3.34 Test 34, J/TF, BH2	238
3.35 Test 35, J/TF, BH3	239
3.36 Test 36, J/TF, BH2	240
3.37 Test 37, J/TF, BH4	241
3.38 Test 38, J/TF, BH4	242
3.39 Test 39, J/TF, BH5	243
3.40 Test 40, J/TF, BH5	244
3.41 Test 41, J/TF, BH5	245
3.42 Test 42, G/KL, BH5	246
3.43 Test 43, G/KL, BH5	247
3.44 Test 44, G/KL, GH6	248
3.45 Test 45, G/KL, GH6	249
3.46 Test 46, G/KL, GH6	250

The following results are summarized in Tables 7 and 8, section 4, main text.

Table No. 3.1
IOWA BORE HOLE SHEAR APPARATUS

Location Davidson Creek at Sedimentation Laboratory Date March 4, 1980
Depth 0.35 m (1.1 ft.) Horizon Silty Sand Tested by Colin Thorne
Description Borehole 1, Next to outdoor flume, top of right bank

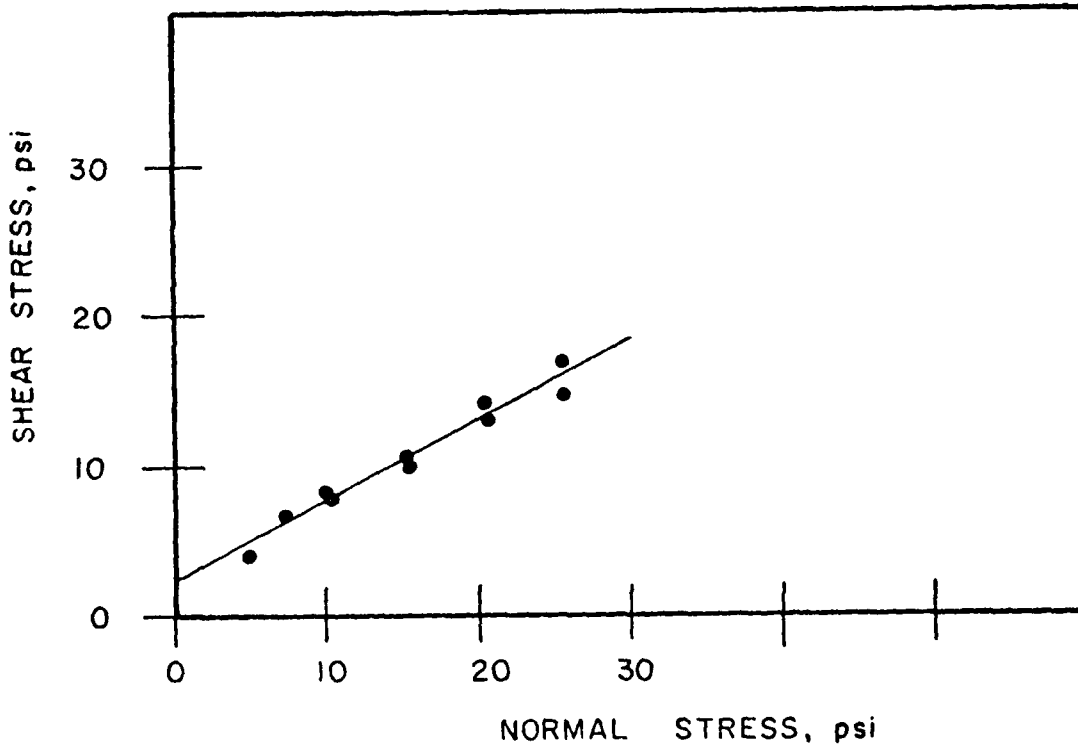


Table No. 3.2

IOWA BORE HOLE SHEAR APPARATUS

Location Davidson Creek at Sedimentation Laboratory Date March 6, 1980

Depth 0.35 m (1.1 ft.) Horizon Medium Sand Tested by Colin Thorne

Description Borehole 2, next to outdoor flume, back from right bank.

Point No.	Normal Stress Gauge	σ_n	Shear Stress Gauge	τ_{max}	Cons. Time	Remarks
1	31	7.9	18.8	5.2	10	$r^2 = 0.968$
2	51	13	31	8.1	5	$m = 0.603$
3	71	17.	44	12	5	$b = 0.288$
4	91	23.5	52	13.7	5	
5	46	11.5	24	6.7	5	
6	62	15.5	35	9.3	5	
7	81	20.7	50	13.3	5	
						$\phi = 35^\circ$
						$c = 0.29 \text{ psi}$
						$= 2 \text{ kPa}$

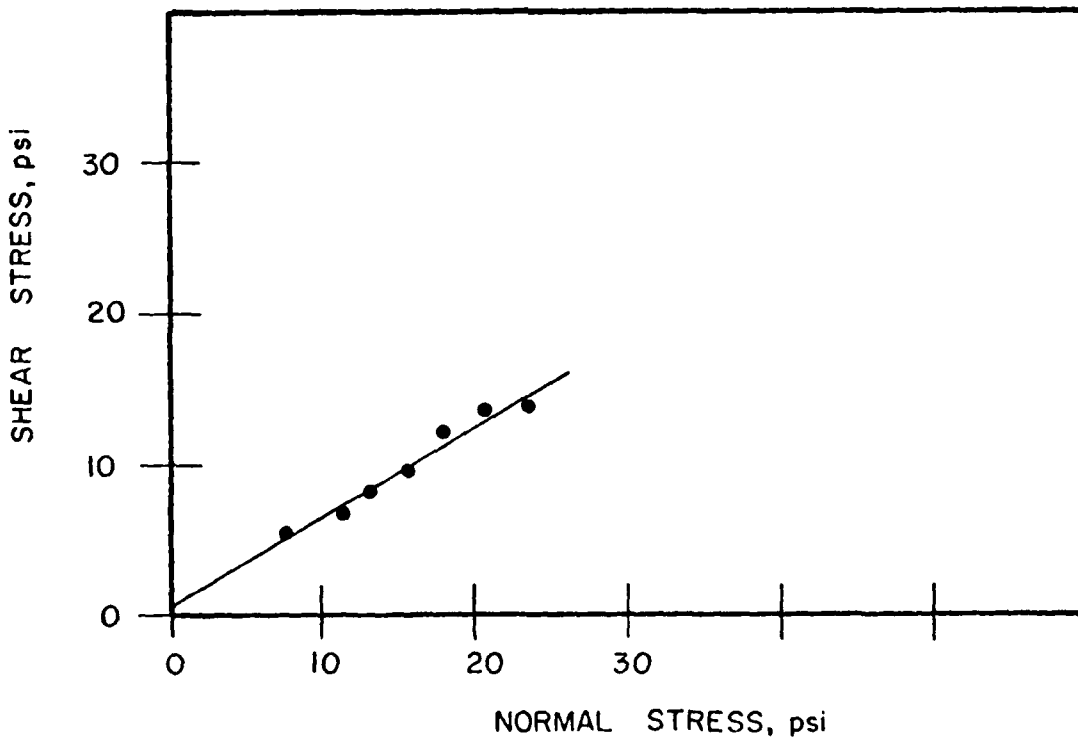


Table No. 3.3

IOWA BORE HOLE SHEAR APPARATUS

Location Tommy Florence's at Johnson Creek **Date** May 6, 1980

Depth 0.66 m (2.2 ft.) Horizon PSA Tested by Thorne/Murphrey

Description In corner of field near wells. LHB of Creek.

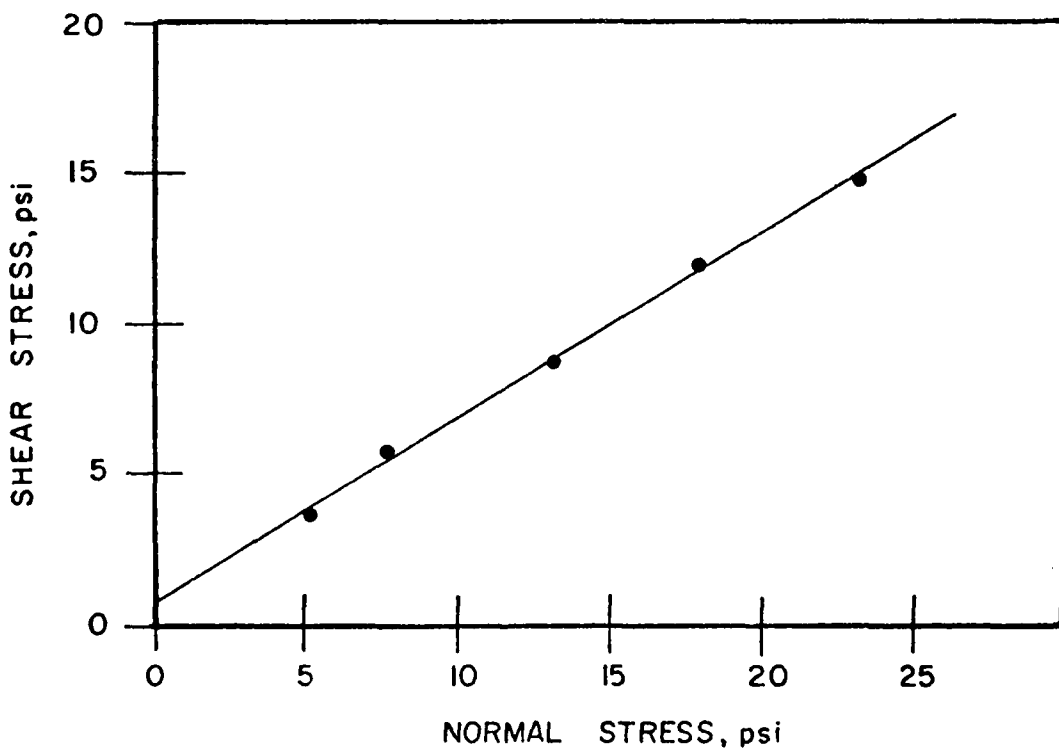


Table No. 3.4

IOWA BORE HOLE SHEAR APPARATUS

Location Johnson Creek, Tommy Florence field Date May 6, 1980

Date May 6, 1980

Depth 2.44 m (8 ft.) Horizon Fine sand Tested by Thorne/Murphree

Description Fine sand below PSA. Borehole near wells at LHB

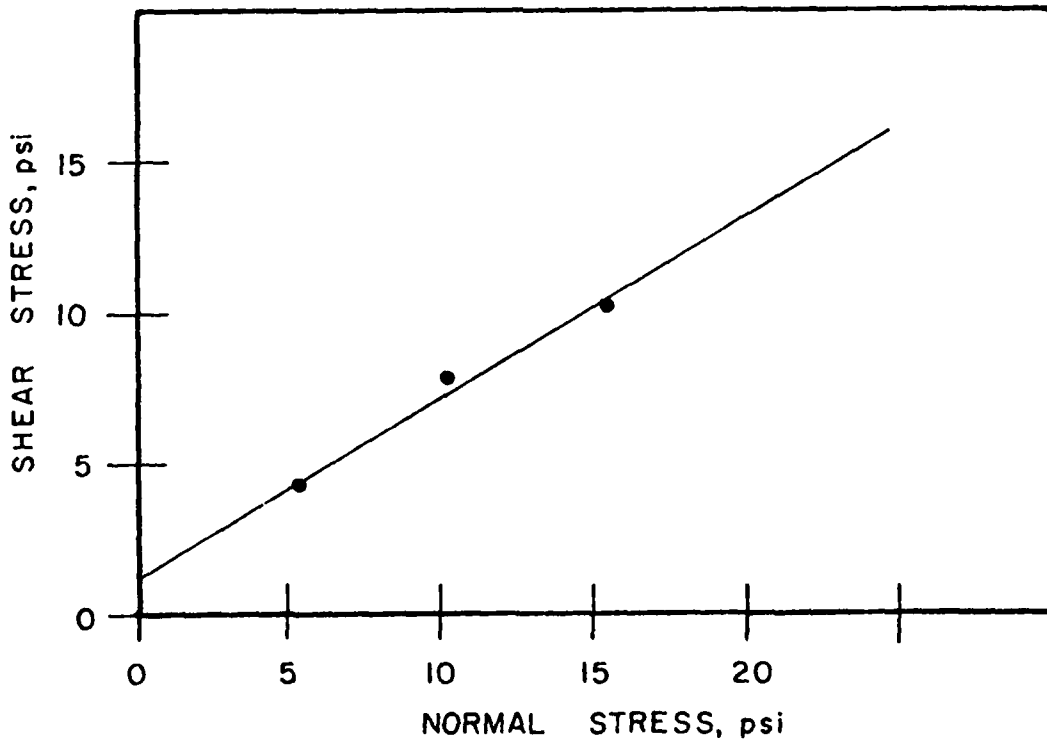


Table No. 3.5

IOWA BORE HOLE SHEAR APPARATUS

Location Katherine Leigh's at Goodwin Creek **Date** May 19, 1980

Date May 19, 1980

Depth 0.61 m (2 ft) Horizon PSA Tested by Thorne/Murphy

Tested by Thorne/Murphy

Description BHi, corner of field near top of right bank

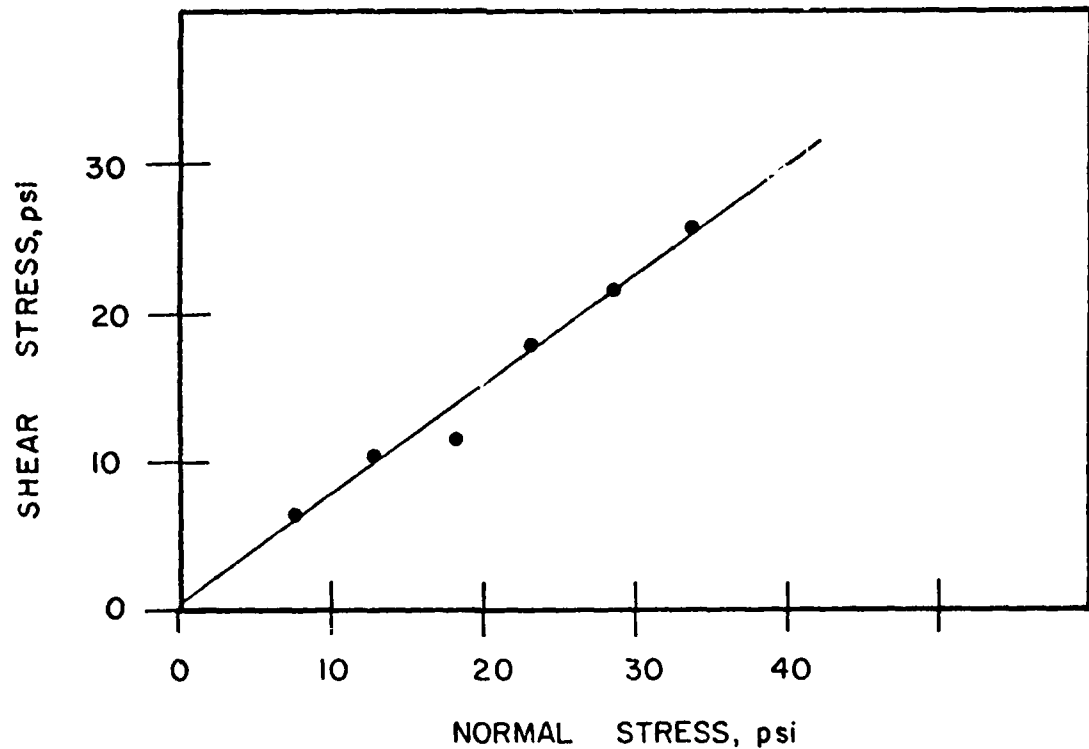


Table No. 3.6

IOWA BORE HOLE SHEAR APPARATUS

Location Katherine Leigh's at Goodwin Creek Date May 19, 1980
Depth 1.83 m (6 ft.) Horizon Y.P. / Tested by Thorne/Murphy
Description Borehole 1, corner of field near top RB of Goodwin Creek

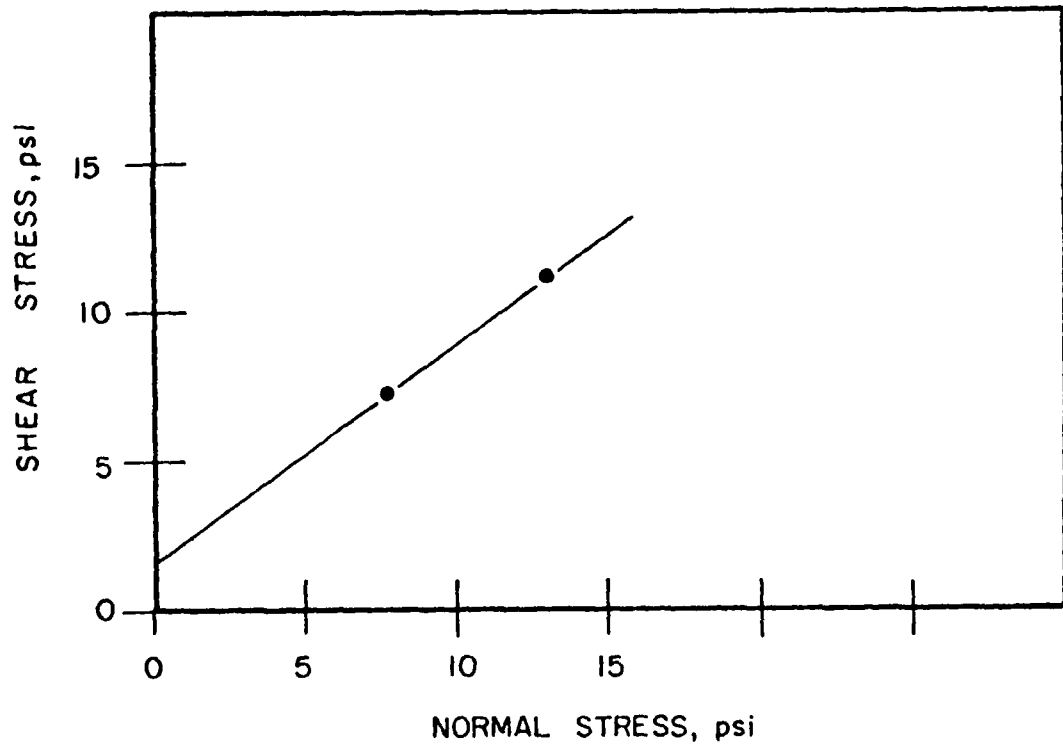


Table No. 3.7

IOWA BORE HOLE SHEAR APPARATUS

Location Katherine Leigh's at Goodwin Creek Date May 27, 1980
 Depth 0.91 m (3 ft.) Horizon Y.P. Tested by Thorne/Murphrey
 Description Borehole 2, Right corner of field 60m back from Goodwin Creek

Point No.	Normal Stress Gauge σ_n	Shear Stress Gauge t_{max}	Cons. Time	Remarks Regression line:
1	18	4.66	8	$r^2 = 0.9991$
2	40	10.29	24	$m = 0.809$
3	60	15.41	39.5	$b = -1.61$
4	80	20.53	57	
5	99	25.39	71	
				$\theta = 39^\circ$
				$c = -1.61 \text{ psi}$
				$= -11.13 \text{ kPa}$
				moisture content 23.5% dry wt.

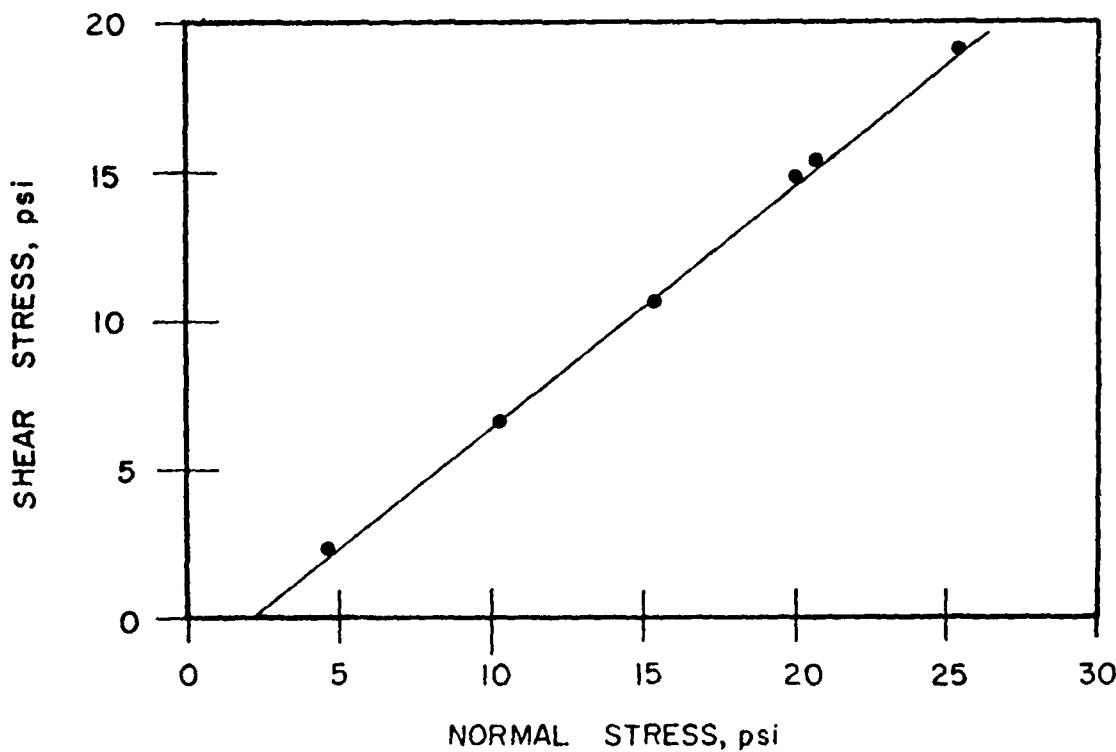


Table No. 3.8

IOWA BORE HOLE SHEAR APPARATUS

Location Katherine Leigh's at Goodwin Creek Date May 27, 1980
 Depth 1.07 m (3.5 Ft.) Horizon Y.P. Tested by Therne/Murphrey/Little
 Description Borehole 2, Right corner of field 60 m back from Goodwin Creek

Point No.	Normal Stress Gauge	σ_n	Shear Stress Gauge	τ_{max}	Cons. Time	Remarks
1	21	5.43	15.5	4.31	10	$r^2 = 0.9994$
2	40	10.29	27	7.33	5	$m = 0.653$
3	60	15.41	39.5	10.62	5	$c = 0.6364$
4	81	20.79	52	13.91	5	
5	100	25.65	66	17.59	5	
6	120	30.77	78.5	20.88	5	
7	141	36.15	91	24.16	5	
						$\theta = 33^\circ$
						$c = 0.636 \text{ psi}$
						$= 4.39 \text{ kPa}$
						moisture content 23.8% dry wt.

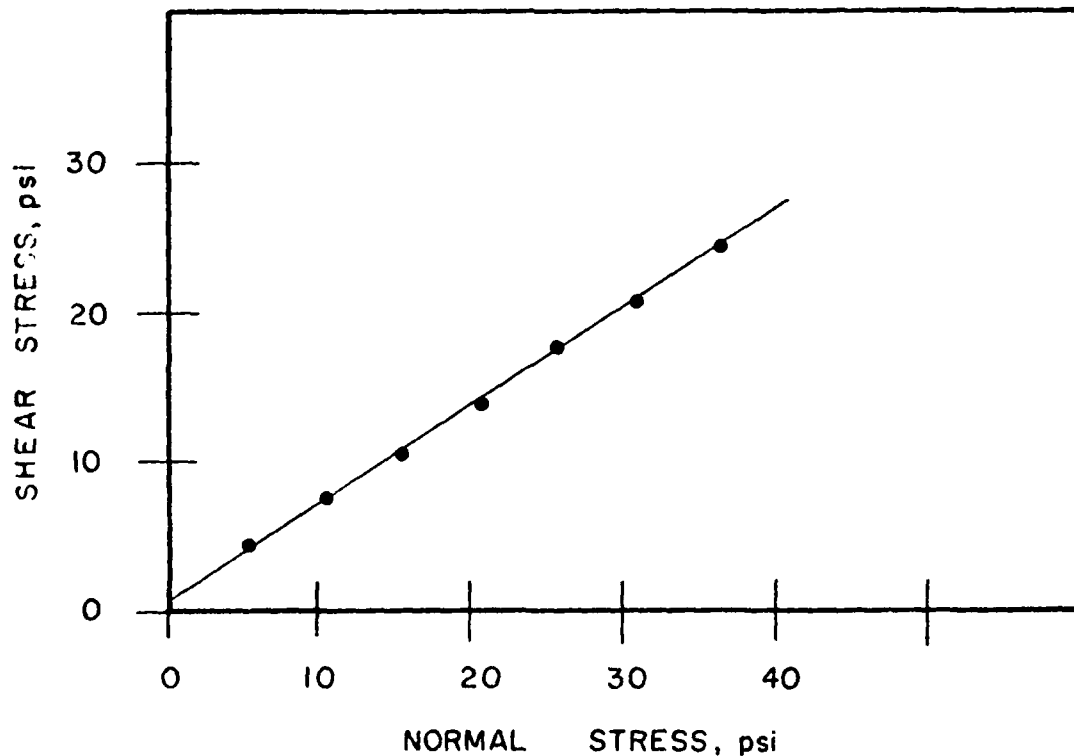


Table No. 3.9

IOWA BORE HOLE SHEAR APPARATUS

Location Katherine Leigh's at Goodwin Creek Date May 27, 1980

Depth 1.52 m (5 ft.) Horizon Y.P. Tested by Thorne/Murphy/Little

Description EH2. RH corner of field 60m back from Goodwin Creek

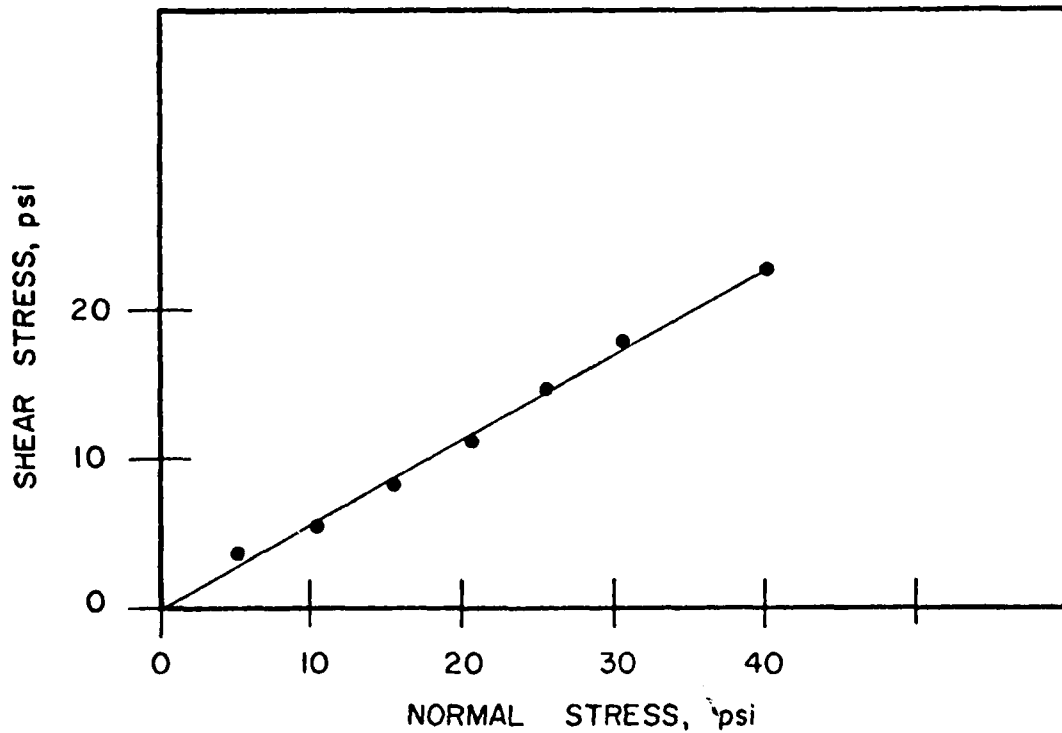


Table No. 3.10

IOWA BORE HOLE SHEAR APPARATUS

Location T.A. Woodruff's at Johnson Creek Date May 28, 1980
 Depth 0.84 m (2.9 ft.) Horizon Y.P. Tested by Thorne/Murphrey/Smith
 Description RH2, RHB over rickety bridge upstream of grade control structure.

Point No.	Normal Stress Gauge σ_n	Shear Stress Gauge τ_{max}	Cons. Time	Remarks
1	21	14	3.91	10 Straight line
2	42	23	6.28	5 $m = 0.4413$
3	60	13	3.65	5 $b = 1.514$
4	80	12	3.39	5 (2 points only)
				$\phi = 24^\circ$
				$c = 1.51 \text{ psi}$
				$= 10.44 \text{ kPa}$
				moisture content 13.6% dry wt.

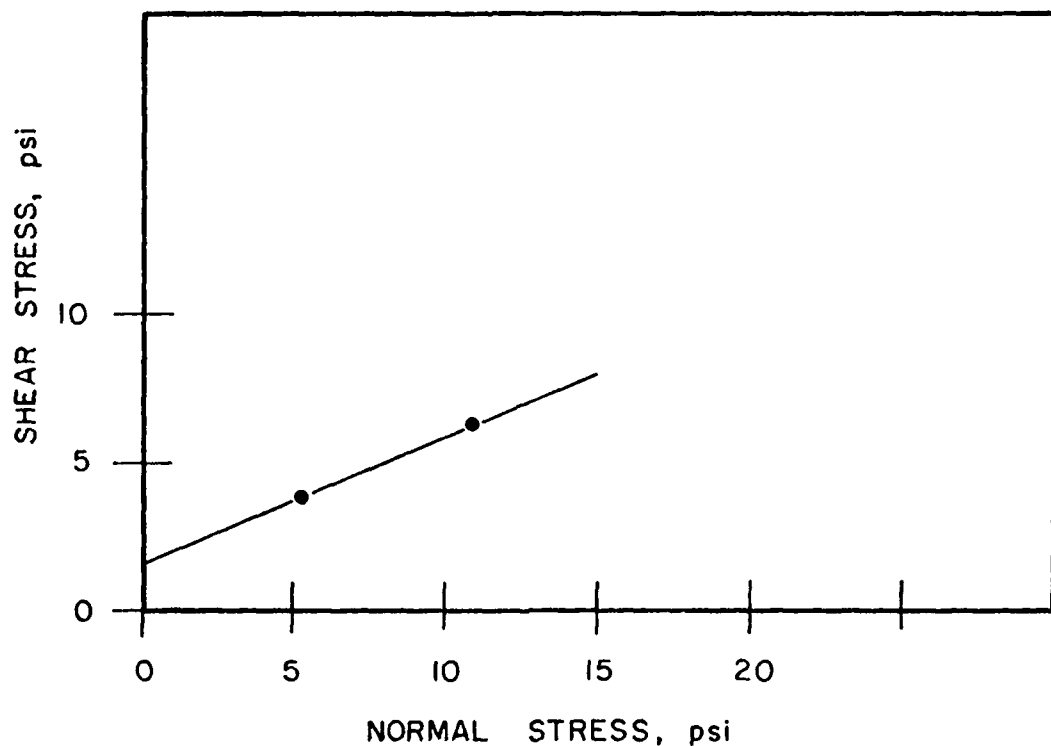


Table No. 3.11

IOWA BORE HOLE SHEAR APPARATUS

Location T. A. Woodruff's at Johnson Creek Date May 28, 1980

Date May 28, 1980

Depth 2.13 m (7 ft.) Horizon O. P. Tested by Thorne/Murphrey/Smith

Tested by Thorne/Murphrey/Smith

Description Borehole 2, Right bank

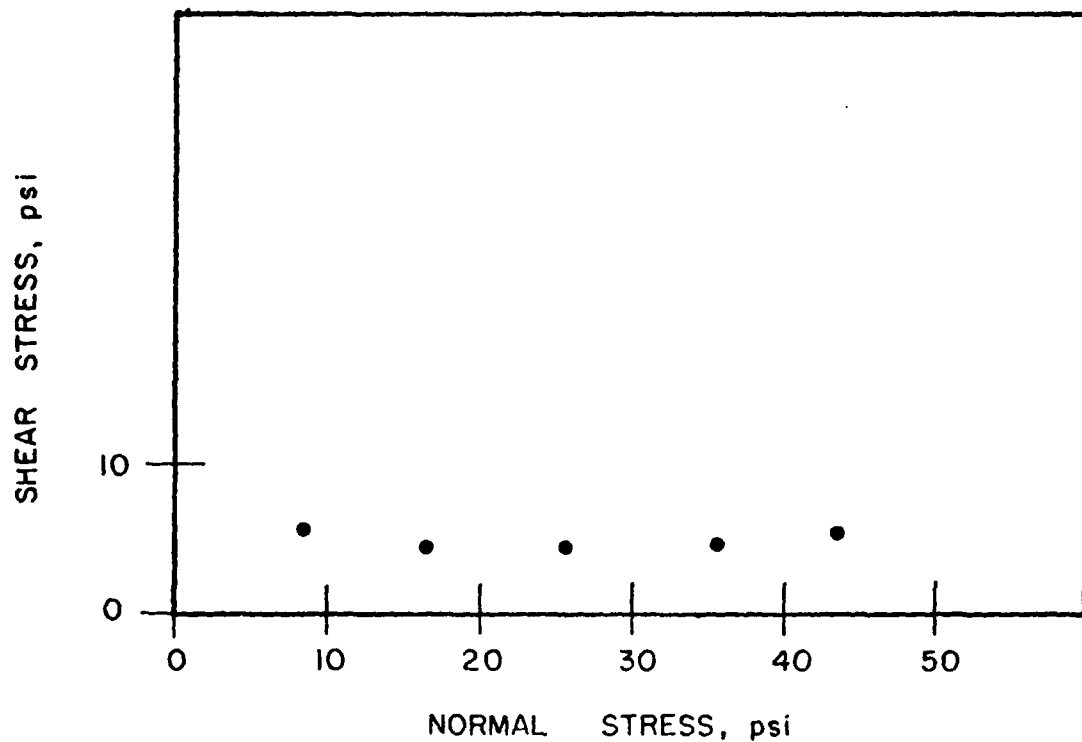


Table No. 3.12

IOWA BORE HOLE SHEAR APPARATUS

Location T. A. Woodruff's at Johnson Creek Date May 30, 1980
Depth 2.21 m (7.25 ft.) Horizon O. P. Tested by Thorne/Murphrey/Smith
Description Borehole 2, Right bank

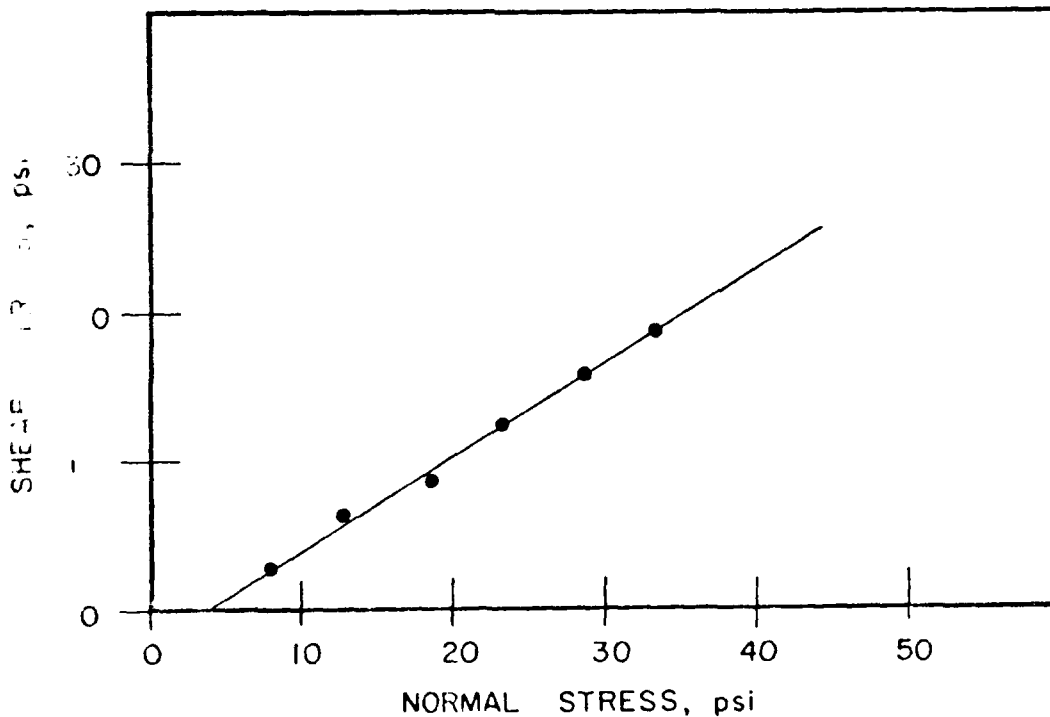


Table No. 3.13

IOWA BORE HOLE SHEAR APPARATUS

Location T. A. Woodruff's at Johnson Creek Date May 30, 1980
 Depth 2.29 m (7.5 ft.) Horizon O. P. Tested by Thorne/Murphrey/Smith
 Description Borehole 2, Right bank

Point No.	Normal Stress Gauge	σ_n	Shear Stress Gauge	t_{max}	Cons. Time	Remarks Regression line:
1	20	5.17	8	2.33	10	$r^2 = 0.991$
2	40	10.29	14	3.91	5	$m = 0.6028$
3	61	15.7	24.5	6.67	5	$b = -1.99$
4	81	20.79	39	10.49	5	
5	104	26.67	52	13.91	5	
6	132	33.84	66	17.59	5	
7	152	38.96	80	21.27	5	
8	170	43.57	96	25.48	5	
						$\phi = 35^\circ$
						$c = -1.99 \text{ psi}$
						$= -13.7 \text{ kPa}$

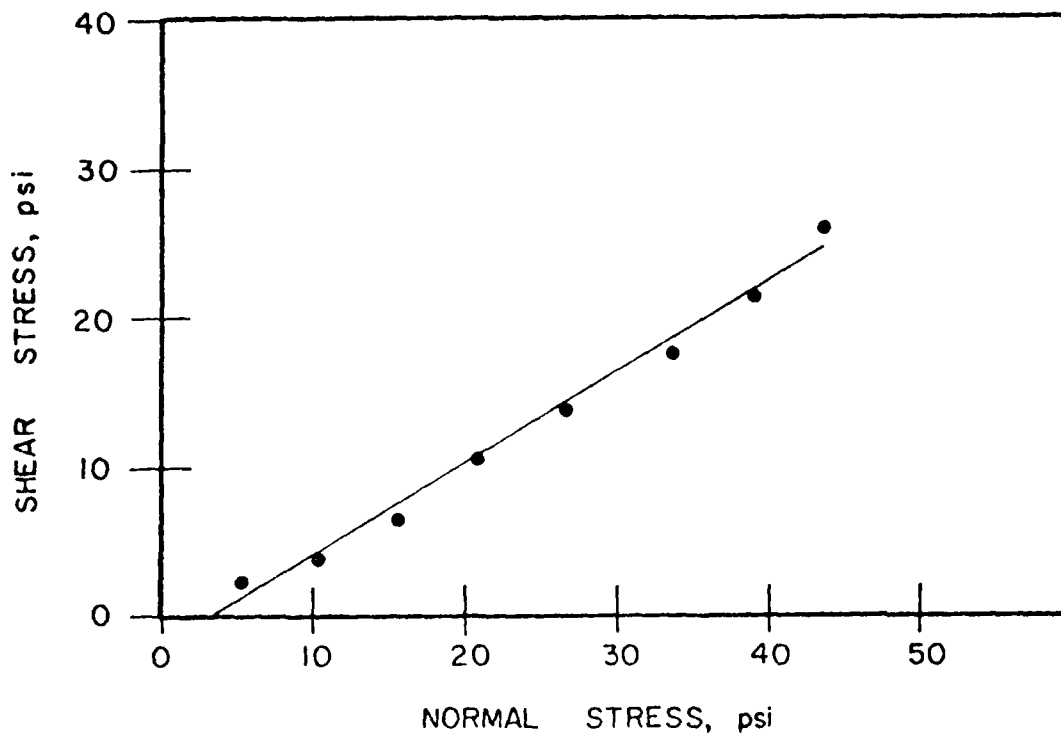


Table No. 3.14
IOWA BORE HOLE SHEAR APPARATUS

Location T. A. Woodruff's at Johnson Creek Date June 2, 1980
 Depth 1.52 m (5 ft.) Horizon Y. P. Tested by Thorne/Murphrey/Smith
 Description Borehole 3, Right bank

Point No.	Normal Stress Gauge	σ_n	Shear Stress Gauge	t_{max}	Cons. Time	Remarks
1	20	5.17	12.8	3.6	10	$r^2 = 0.9983$
2	41	10.55	28	7.59	5	$m = 0.717$
3	60	15.41	42.5	11.41	5	$b = 0.061$
4	80	20.53	56	14.96	5	
5	100	25.56	68	18.11	5	
6	120	30.77	50	13.38	5	Fully expanded?
						$\phi = 36^\circ$
						$c = 0.06 \text{ psi}$
						$= 0.42 \text{ kPa}$
						moisture content 8.45% dw

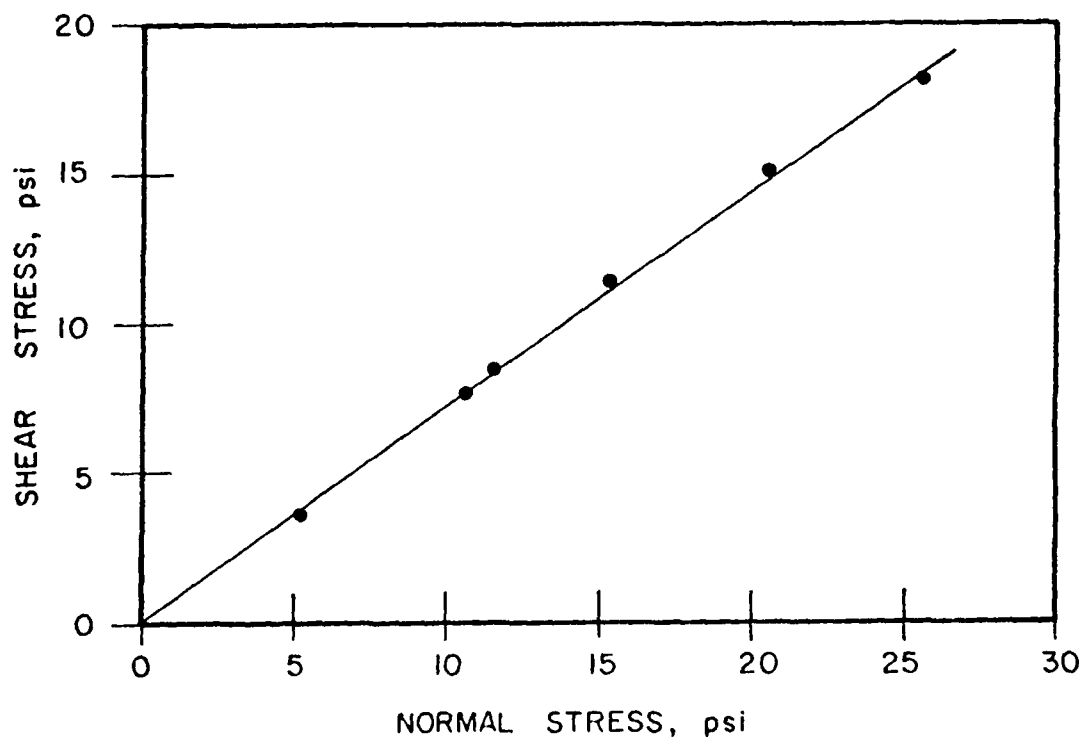


Table No. 3.15

IOWA BORE HOLE SHEAR APPARATUS

Location T. A. Woodruff's at Johnson Creek Date June 2, 1980
3.05 m (1 ft.)
Depth 2.74 m (9 ft.) Horizon O. P. Tested by Thorne/Murphrey/Smith
Description Borehole 3, Right bank

	Point No.	Normal Stress Gauge σ_n	Shear Stress Gauge τ_{max}	Cons. Time	Remarks Straight line:
2.74m	1	16	4.15	13.5	$m = 0.6676$ (only 3 pc)
3.05m	2	32	8.24	24	$b = 1.02$
	3	56	14.39	39.5	10.62
	4	80	20.53	34	9.17
	5	110	28.21	33	8.91
	6	150	38.45	38	10.22
					$\theta = 34^\circ$
					$c = 1.02 \text{ psi}$
					$= 7.04 \text{ kPa}$
					moisture content 17.48% dw

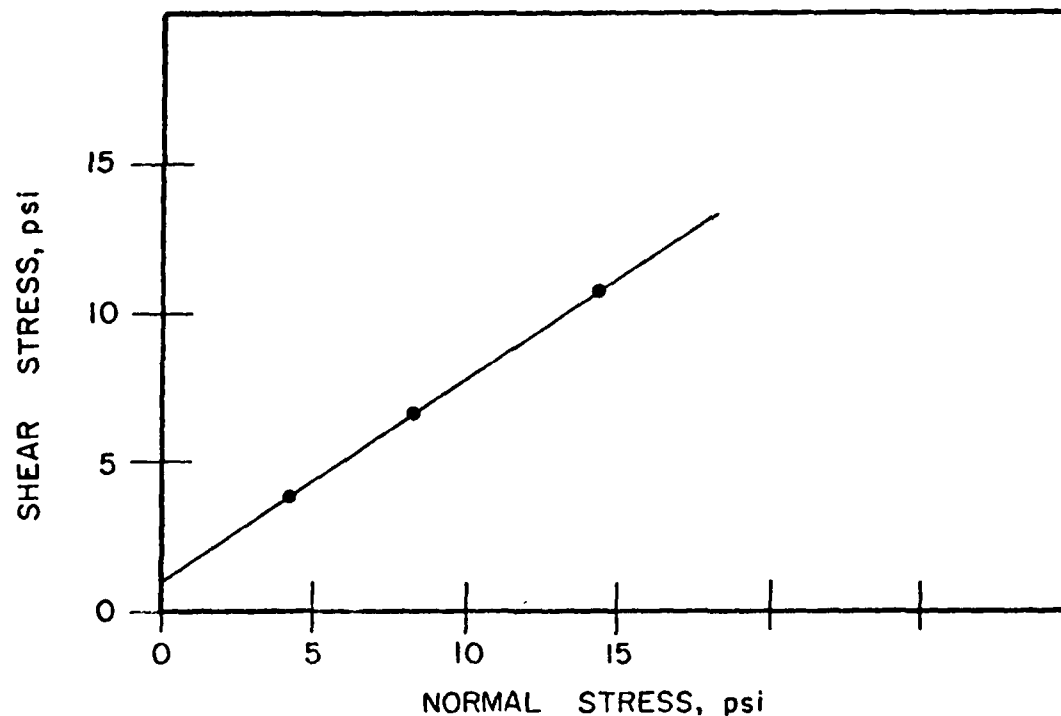


Table No. 3.16

IOWA BORE HOLE SHEAR APPARATUS

<u>Location</u>	T. A. Woodruff's at Johnson Creek	<u>Date</u>	June 2, 1980
<u>Depth</u>	3.20 m (10.5 ft.)	<u>Horizon</u>	O. P.
<u>Description</u>	Tested by Thorne/Murphrey/Smith		
BH 2, 200m upstream of rickety bridge, RHF			

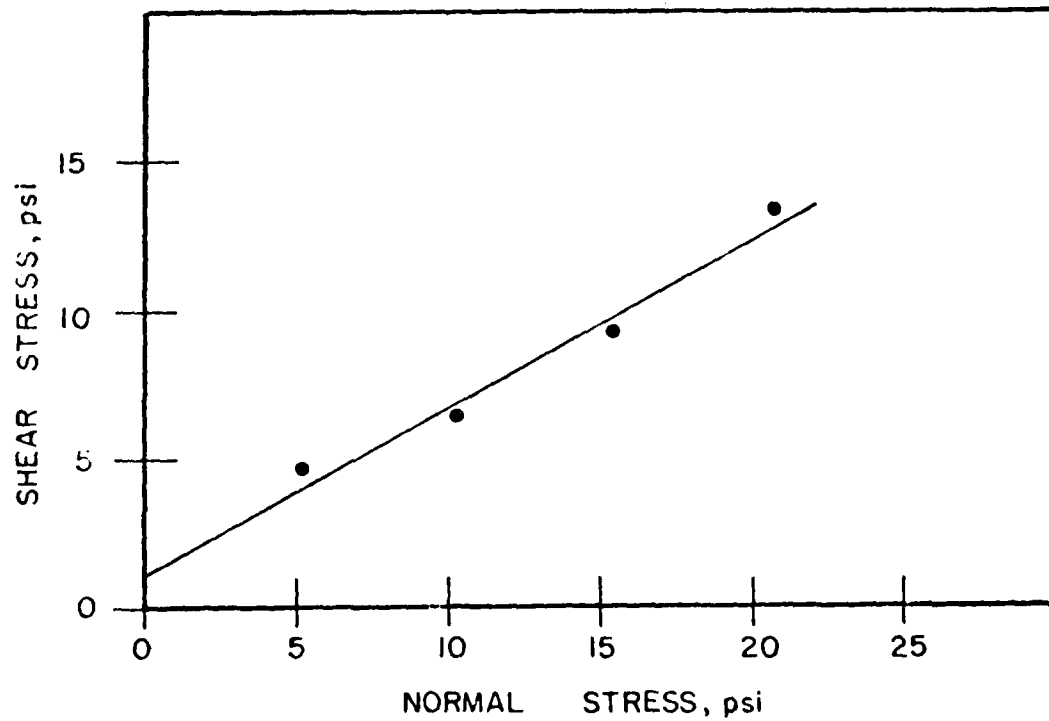


Table No. 3.17

IOWA BORE HOLE SHEAR APPARATUS

Location T. A. Woodruff's at Johnson Creek Date June 14, 1980
 Depth 2.9 m (9.5 ft.) Horizon O. P. Tested by Thorne/Murphrey/Smith
 Description Borehole 4 on right bank

Point No.	Normal Stress Gauge	σ_n	Shear Stress Gauge	t_{max}	Cons. Time	Remarks
1	13	3.38	10.5	2.99	10	$r^2 = 0.9985$
2	23	5.94	17	4.70	5	$m = 0.7709$
3	31	7.99	24	6.54		$b = 0.5329$
4	40	10.29	31	8.38		
5	50	12.85	39.5	10.62		
6	60	15.41	47	12.59		
7	70	17.97	56	14.96		
8	90	23.09	70	18.64		$\phi = 38^\circ$
9	110	28.21	84	22.32		$c = 0.53 \text{ psi}$
10	150	38.45	112	29.69		$= 3.67 \text{ kPa}$
						moisture content 20.38%dw

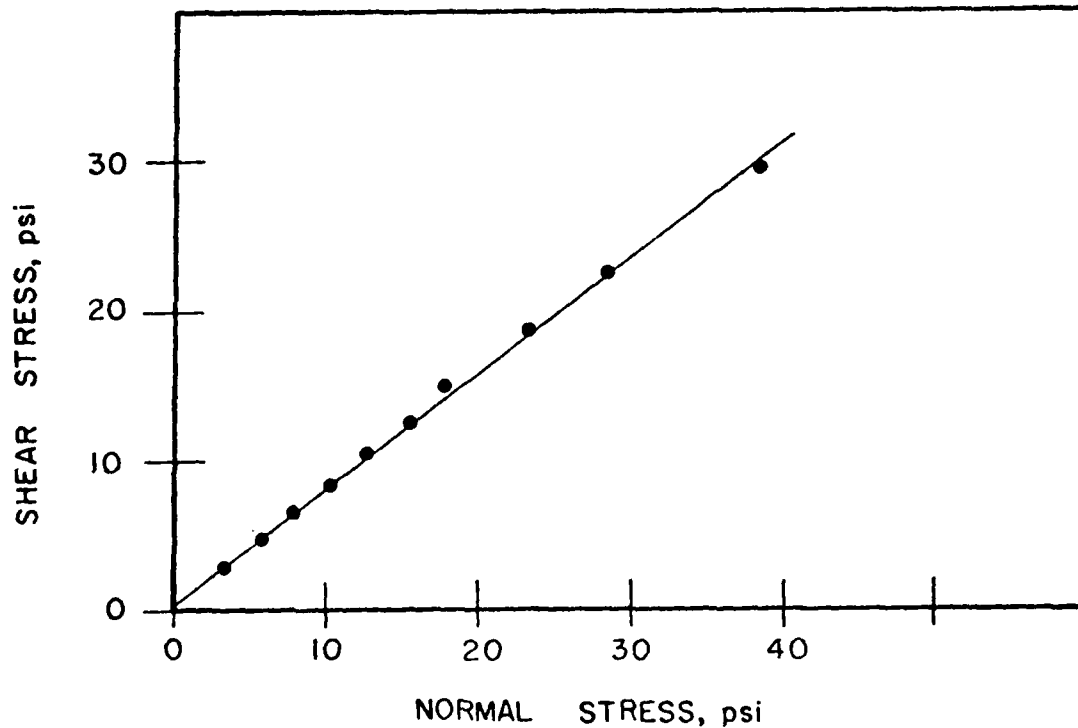


Table No. 3.18
IOWA BORE HOLE SHEAR APPARATUS

Location T. A. Woodruff's at Johnson Creek Date June 4, 1980
 Depth 1.74 m (5.7 ft.) Horizon Y. P. Tested by Thorne/Murphrey/Smith
 Description Borehole 4 on Right Bank

Point No.	Normal Stress Gauge	σ_n	Shear Stress Gauge	t_{max}	Cons. Time	Remarks
1	12	3.12	8	2.33	10	Regression line: $r^2 = 0.9884$
2	21	5.43	16	4.44	5	$m = 0.6418$
3	30	7.73	22	6.02	5	$b = 0.7477$
4	40	10.19	28	7.59	5	
5	50	12.85	32	8.65	5	
6	61	15.67	40	10.75	5	
						Fully expanded?
						$\phi = 33^\circ$
						$c = 0.748 \text{ psi}$
						$= 5.16 \text{ kPa}$
						moisture content 14.70% dry

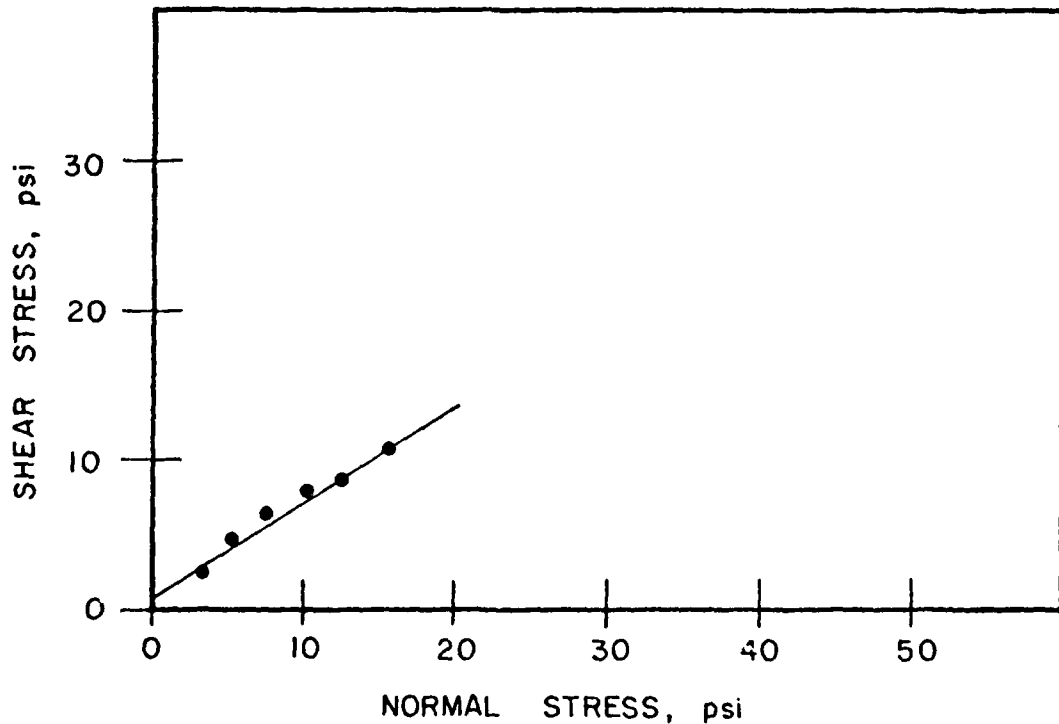


Table No. 3.19

IOWA BORE HOLE SHEAR APPARAT'S

Location T. A. Woodruff's at Johnson Creek Date June 4, 1980
ft.)
Depth 12.5' 3.81 m (12.5 Horizon O. P. Tested by Thorne

Description Borehole 4 on right bank.

Point No.	Normal Stress Gauge	σ_n	Shear Stress Gauge	τ_{max}	Cons. Time	Remarks Regression line:
1	10	2.61	3	1.02	10	$r^2 = 0.9914$
2	20	5.17	7	2.07	5	$m = 0.7022$
3	31	7.99	15	4.18	5	$b = -1.15$
4	41	10.55	23	6.28	5	
5	50	12.85	31	8.38	5	
6	70	17.97	42	11.28	3	
						$\phi = 35^\circ$
						$c = -1.15 \text{ psi}$
						$= 7.93 \text{ kPa}$
						moisture content 35.18%dw

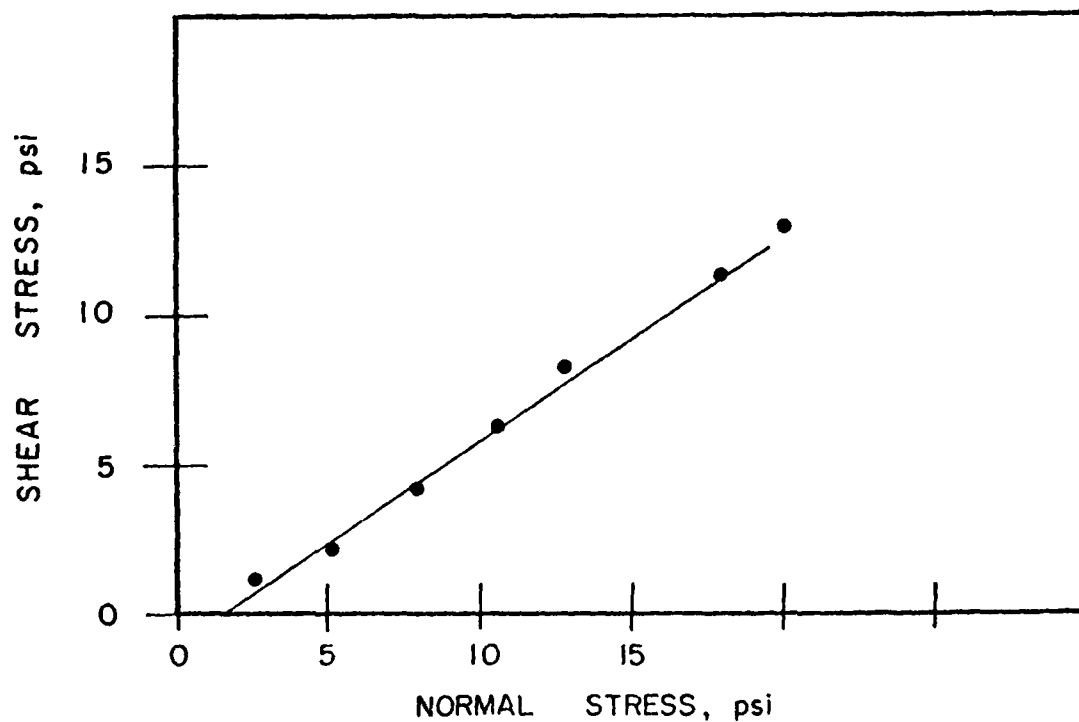


Table No. 3.20
IOWA BORE HOLE SHEAR APPARATUS

Location T. A. Woodruff's at Johnson Creek Date June 5, 1980
 Depth 1.98 m (6.5 ft.) Horizon O. P. Tested by Thorne
 Description Borehole 5 on Right bank

Point No.	Normal Stress Gauge σ_n		Shear Stress Gauge t_{max}		Cons. Time	Remarks
1	50	12.85	32	8.65	10	$m = 0.7441$
2	70	17.97	46.5	12.46	5	$b = -0.8$
						2 points only:
						$\theta = 37^\circ$
						$c = -0.8 \text{ psi}$
						$= -5.52 \text{ kPa}$

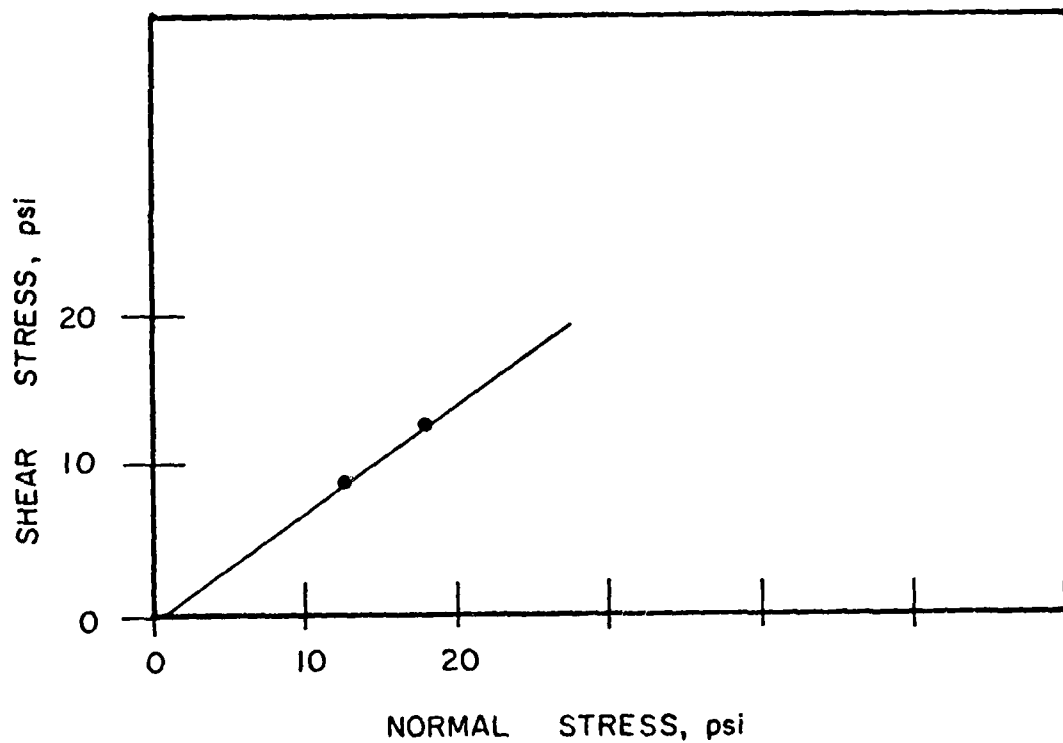


Table No. 3.21

IOWA BORE HOLE SHEAR APPARATUS

Location T. A. Woodruff's at Johnson Creek Date June 13, 1980
0.85, 1.02m and 1.22m
Depth (2.8, 3.5 & 4 ft.) Horizon Channel Fill Tested by Thorne
Description Borehole 6a on Right bank

Point No.	Normal Stress Gauge	σ_n	Shear Stress Gauge	τ_{max}	Cons. Time	Remarks Regression line:
1	160	41.01	103	27.32	10	$0.85m \quad r^2 = 0.7224$
2	170	43.57	117	31.00	.5	$m = 0.6077$
						$b = 1.07$
1	71	18.23	45.5	12.2	10	1.22m
2	87	22.32	62.5	16.67	5	
3	100	26.65	74	19.69	5	
1	130	33.33	54	14.43	10	1.02m
2	140	35.89	77	20.48		$\phi = 31^\circ$
						$c = 1.07 \text{ psi}$
						$= 7.37 \text{ kPa}$

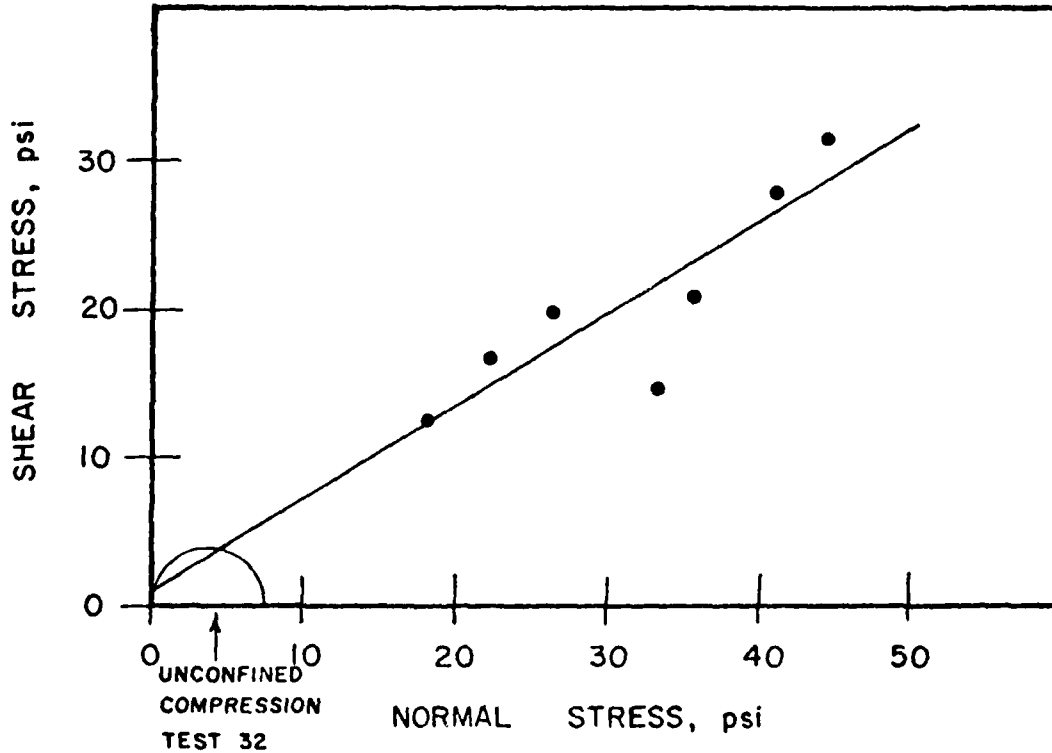


Table No. 3.22
IOWA BORE HOLE SHEAR APPARATUS

Location T. A. Woodruff's at Johnson Creek Date June 13, 1980
Depth 0.76 m (2.5 ft.) Horizon Channel Fill /YP Tested by Thorne/George
Description Borehole 6 on Right Bank

Point No.	Normal Stress Gauge	Shear Stress Gauge	Cons. Time	Remarks
1	21	5.43	13	3.65
2	32	8.24	24	6.54
3	43	11.06	32	8.65
4	55	14.13	40.5	10.88
5	70	17.97	50.5	13.51
6	100	25.65	72.5	19.30
				Not Seated?
				$r^2 = 0.9997$
				$m = 0.7295$
				$b = 0.5348$
				$\emptyset = 36^\circ$
				$c = 0.53 \text{ psi}$
				$= 3.69 \text{ kPa}$
				moisture content 17.13%dw

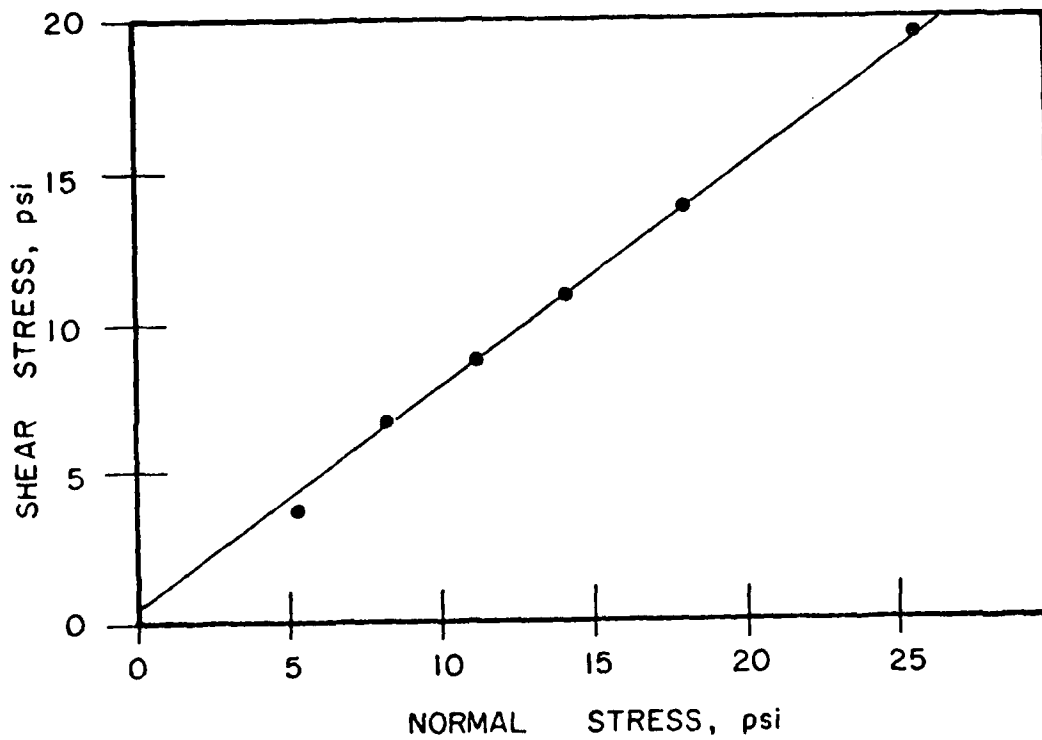


Table No. 3.23

IOWA BORE HOLE SHEAR APPARATUS

Location T. A. Woodruff's at Johnson Creek Date June 16, 1980
2.13 m (7 ft.)
Depth 2.2 m (7 ft. 3in.) Horizon Channel Fill/YP Tested by Thorpe
Description Borehole 6a on Right bank

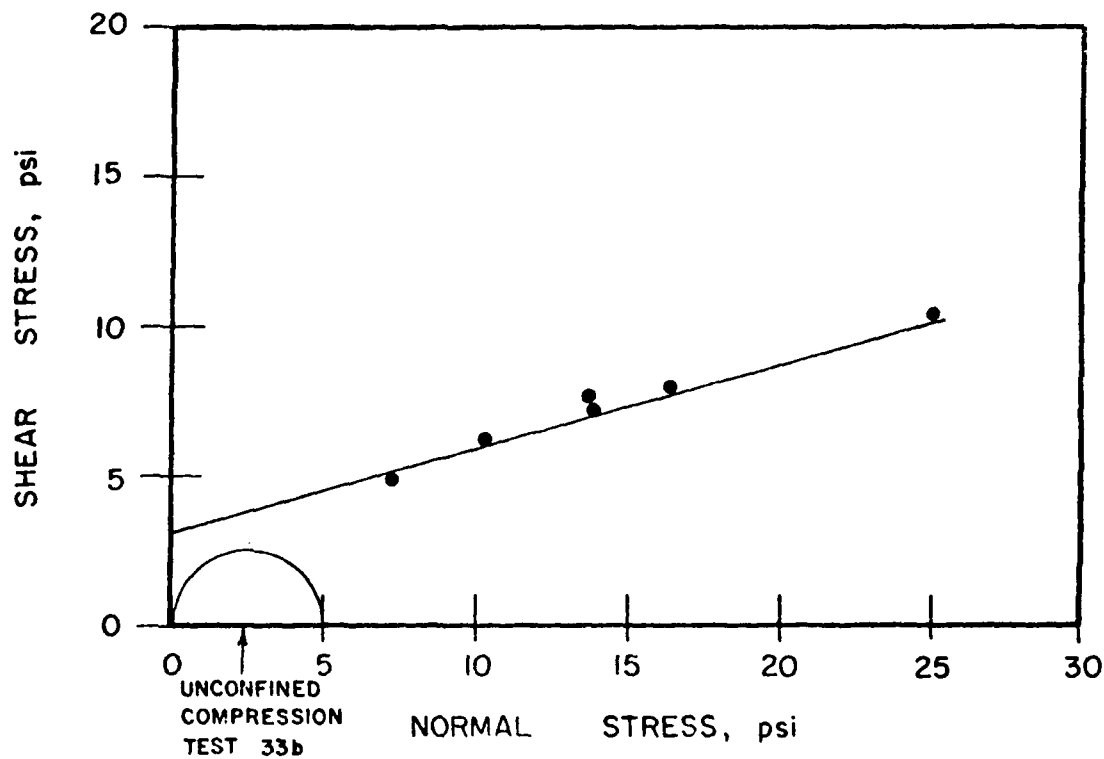


Table No. 3.24

IOWA BORE HOLE SHEAR APPARATUS

Location T. A. Woodruff's at Johnson Creek Date July 9, 1980

Depth 1.5 - 1.8 m Horizon Young Palaeosol Tested by Thorne

Description Borehole 9 (next to BH 3). Right bank upstream of grade control structure.

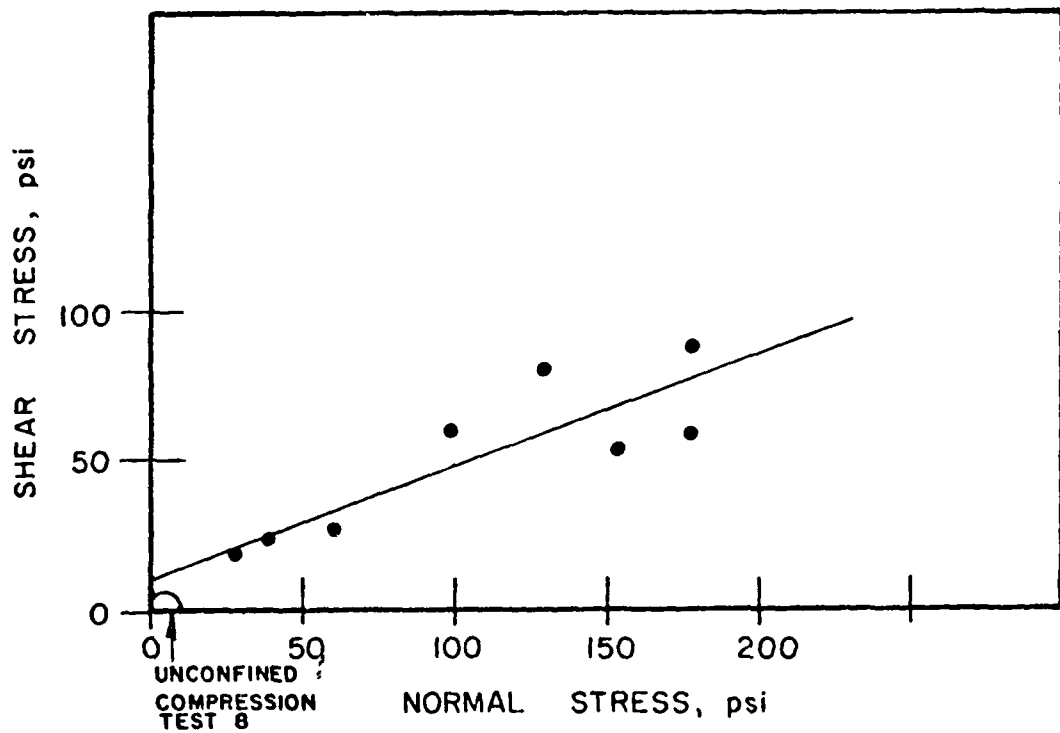


Table No. 3.25

IOWA BORE HOLE SHEAR APPARAT'S

Location T. A. Woodruff's at Johnson Creek Date July 11, 1980
 Depth 3.3 - 3.5 m Horizon Old Paleosol Tested by Thorne
 Description Borehole 10 (Right Bank)

Point No.	Normal Stress Gauge	σ_n	Shear Stress Gauge	t_{max}	Cons. Time	Remarks
1	30	38.5	7.5	10.1	10	$m = 0.186$
2	121	154.9	24	31.8	10	$b = 2.92$
3	150	192.1	8	10.8	10	
4	60	76.9	3	4.2	10	
5	101	129.3	3.5	4.8	10	
						(only 2 points)
						$\phi = 11^\circ$
						$c = 2.92 \text{ psi}$
						$= 20.1 \text{ kPa}$

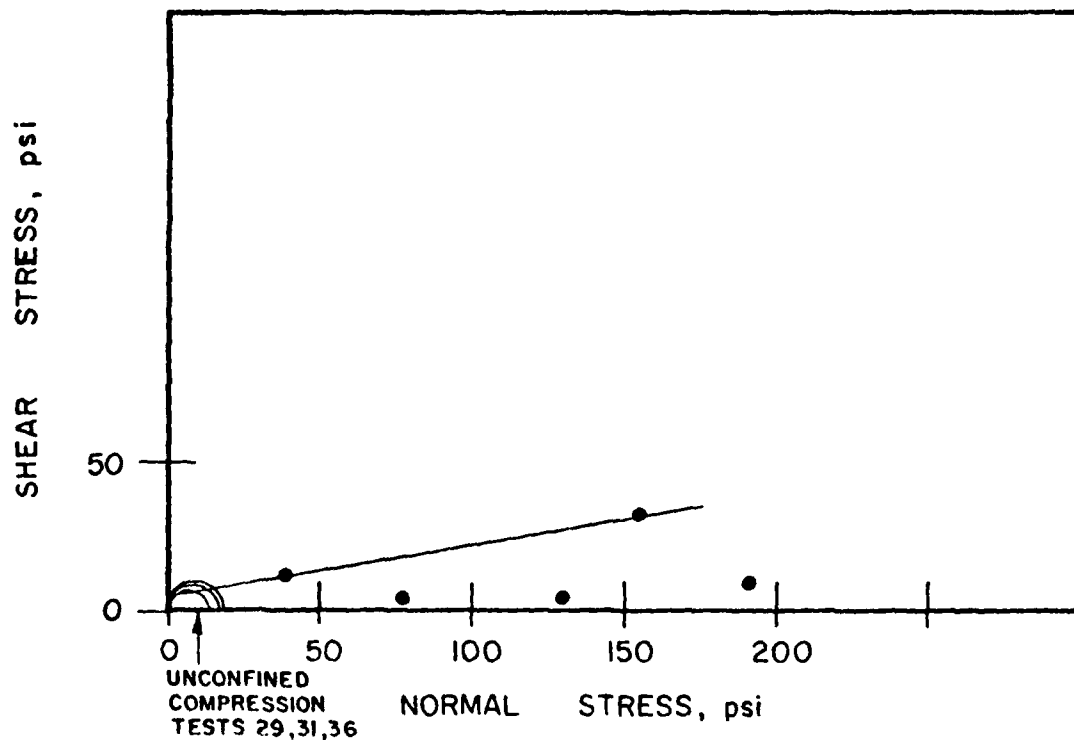


Table No. 3.26

IOWA BORE HOLE SHEAR APPARATUS

Location T. A. Woodruff's at Johnson Creek Date July 24, 1980
0.69 - 0.84 m
Depth (2.25 - 2.75 ft.) Horizon PSA Tested by Thorne/Smith
Description Borehole 11 (Under Cottonwood, 70m back from right bank at Grade Control Structure).

Point No.	Normal Stress Gauge	Shear Stress Gauge	Cons. Time	Remarks
	σ_n	t_{max}		
1	30	38.5	10	$2'3"$ } $r=0.9$ } $r=0.95$
2	61	78.1	10	$2'3"$ } $r^2=0.8$ } $r^2=0.9$
3	72	92.2	10	$2'6"$ } $m=0.39$ } $m=0.47$
4	90	115.3	10	$2'6"$ } $b=12.8$ } $b=7.897$
5	106	135.7	10	$2'9"$
6	106	135.7	10	$2'9"$
				Best Fit line-points
				2, 3 and 4.
				$\phi = 28.6^\circ$
				$c = 31 \text{ kPa}$
				(Reject 1-too low, poor reading reject 5,6-too high, caving)

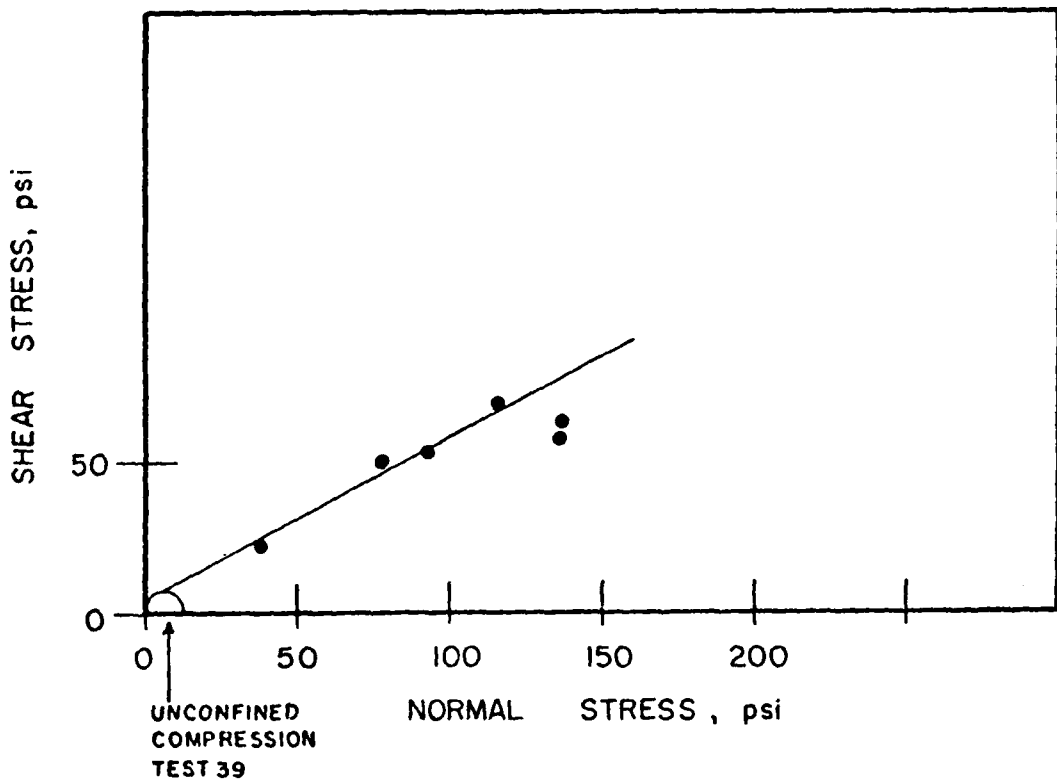


Table No. 3.27
IOWA BORE HOLE SHEAR APPARATUS

Location Tommy Florence's at Johnson Creek Date July 29, 1980
3.05 - 3.66
Depth (10 - 12 ft.) Horizon O. P. Tested by Thorne
Description Borehole 2, left bank

Point No.	Normal Stress Gauge σ_n	Shear Stress Gauge τ_{max}	Cons. Time	Remarks Regression line:
1	50	64.1	31	41
2	123	157.5	44.5	58.7
3	61	78.1	34	45
4	61	78.1	36	$r^2 = 0.99$
5	84	108.8	44	$m = 0.506$
6	108	138.3	60	$b = 6.34$
7	132	169.0	69	10
8	34.5	44.2	20.5	27.2
				$\emptyset = 27^\circ$
				$c = 6.34 \text{ psi}$
				$= 44 \text{ kPa}$

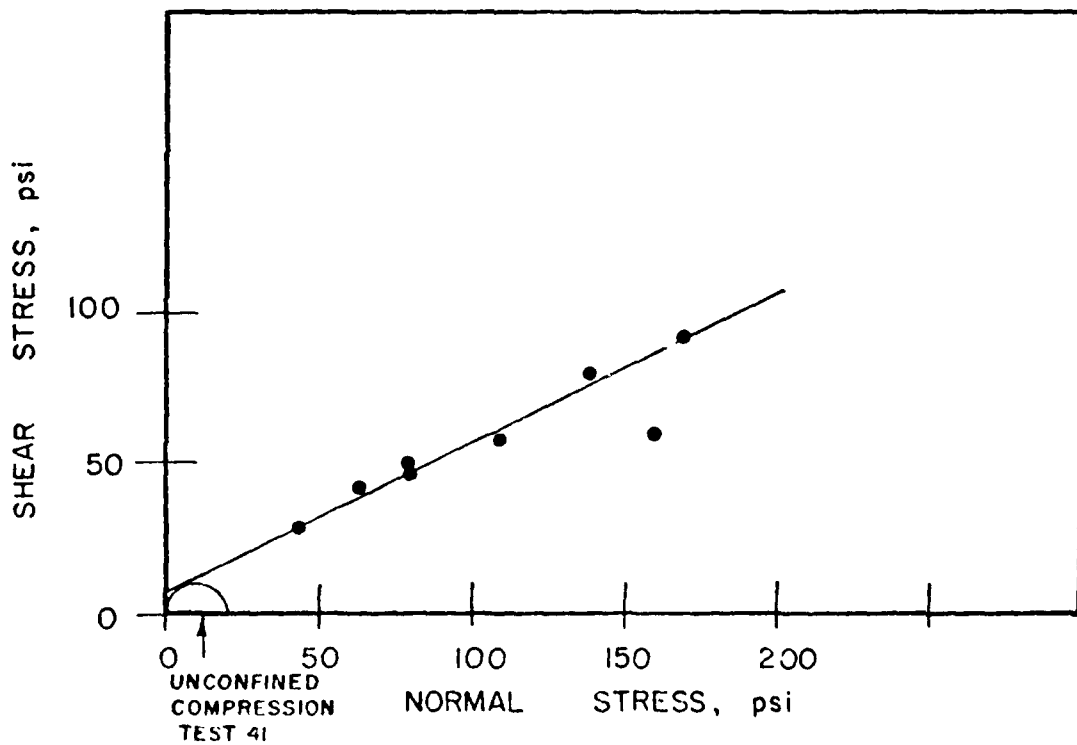


Table No. 3.28
IOWA BORE HOLE SHEAR APPARATUS

Location Tommy Florence's at Johnson Creek Date July 30, 1980
0.76 - 1.07 m
Depth (2.5 - 3.5 ft.) Horizon PSA Tested by Thorne
Description Borehole 2 on left bank.

Point No.	Normal Stress Gauge	σ_n	Shear Stress Gauge	t_{max}	Cons. Time	Remarks
1	80	102.5	18	23.9	10	$2'6'' \quad r^2 = 0.8549$
2	30	38.5	7.5	10.1	10	$2'6'' \quad m = 0.2108$
3	120	153.7	23.5	31.1	10	$2'9'' \quad b = 3.472 \text{ psi}$
4	120	153.7	29.5	39.0	10	$2'9''$
5	52	66.6	15.5	20.6	10	$3'3''$
6	144	184.4	38	50.2	10	$2'3''$
7	144	184.4	27	35.7	10	$3'6''$
						$\phi = 12^\circ$
						$c = 3.47 \text{ psi}$
						$= 23.9 \text{ kPa}$
						moisture content 11.6%dw

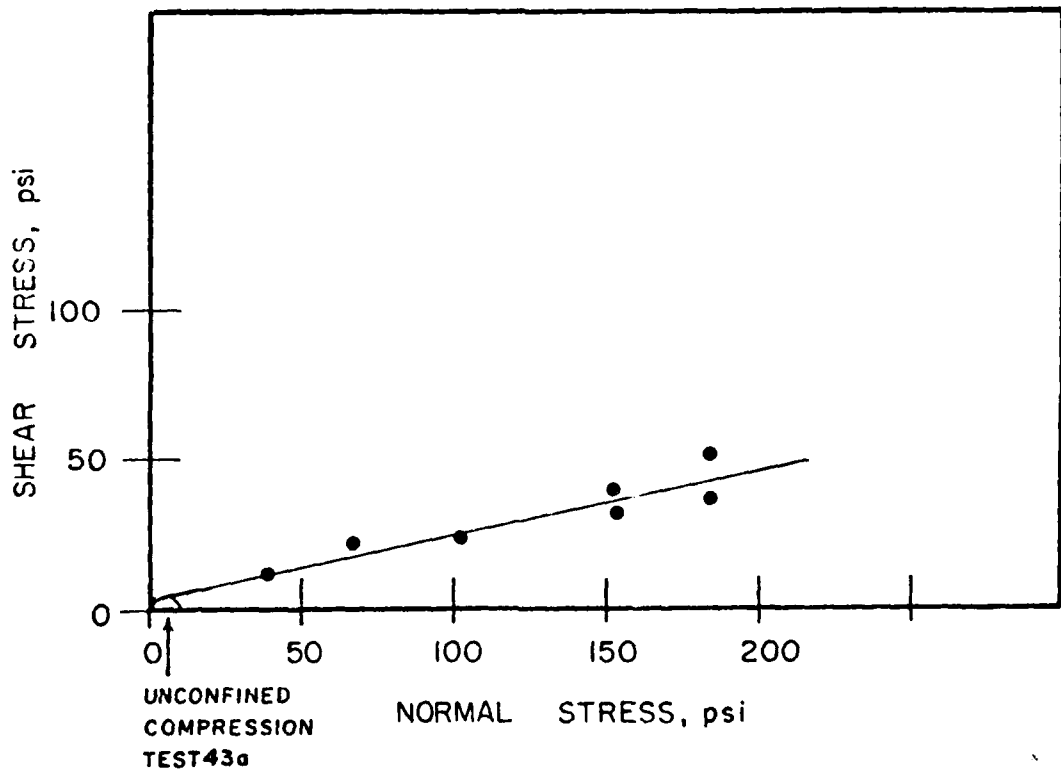


Table No. 3.29

IOWA BORE HOLE SHEAR APPARATUS

Location Tommy Florence's at Johnson Creek Date August 4, 1980
 Depth 0.61-0.91m(2-3 ft.) Horizon PSA Tested by Thorne
 Description Borehole 4 on left bank.

Point No.	Normal Stress Gauge	σ_n	Shear Stress Gauge	\uparrow_{max}	Cons. Time	Remarks
1	20	25.7	8.5	11.4	10	$2'$ $r^2 = 0.97$
2	94	120.4	51	67.3	10	$2'$ $m = 0.4197$
3	64	82	37	47.6	10	$2'3''$ $b = 9.316$
4	42	53.8	23	30.5	10	$2'3''$
5	150	192.1	70	92.3	10	$2'6''$
6	130	164.5	53	70	10	$2'6''$
7	120	153.7	55	72.6	10	$2'9''$
						$\phi = 23^\circ$
						$c = 9.32 \text{ psi}$
						$= 64.2 \text{ kPa}$
						moisture content 14.3%dw

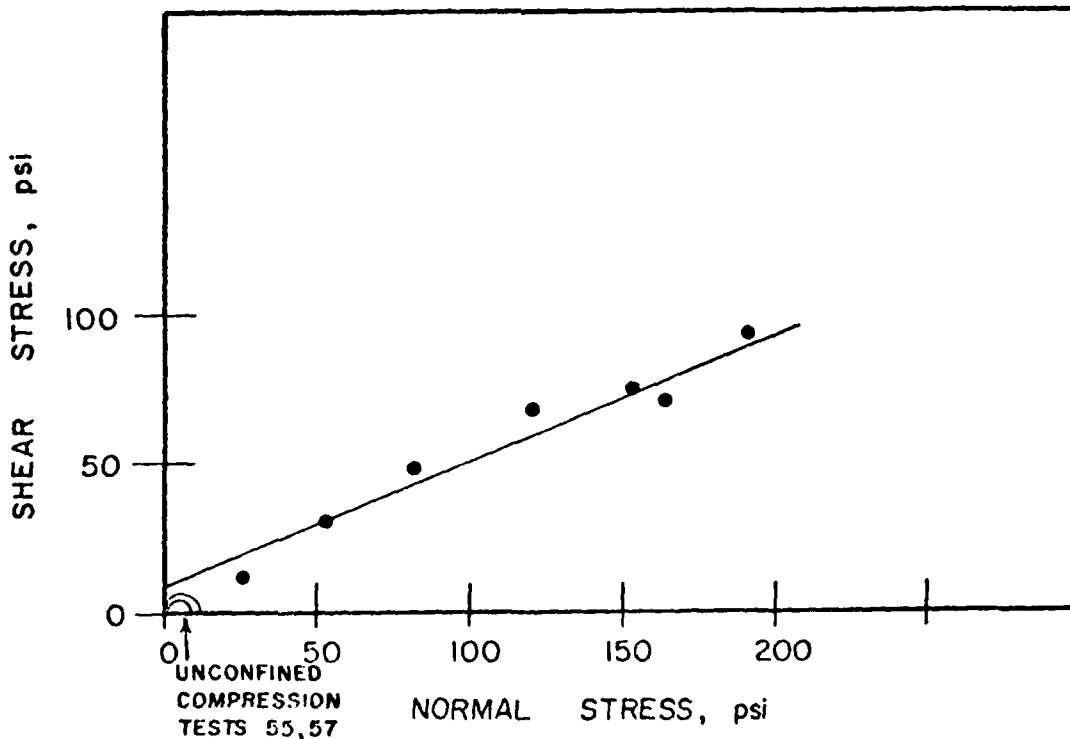


Table No. 3.30
IOWA BORE HOLE SHEAR APPARATUS

Location Tommy Florence's at Johnson Creek Date August 4, 1980
2.74 - 3.05 m
Depth (9 - 10 ft.) Horizon Old Paleosol Tested by Thorne
Description Borehole 4, on left bank top

Point No.	Normal Stress Gauge	σ_n	Shear Stress Gauge	τ_{max}	Cons. Time	Remarks
1	27	34.6	13	17.3	10	10' not bedded (reject)
2	51	65.3	33	43.6	10	10' $r^2 = 0.88$
4	76	97.3	39	51.5	10	10' 3" $m = 0.4946$
5	112	143.4	59	77	10	10' 6" $b = 7,899 \text{ psi}$
9	109	139.6	54	71.3	10	9' 9"
11	93	119.1	60	79.1	10	9' 6"
12	41.5	53.2	23	30.5	10	9' 6"
						$\theta = 26^\circ$
						$c = 54.5 \text{ kPa}$
						moisture content 21.2%dw

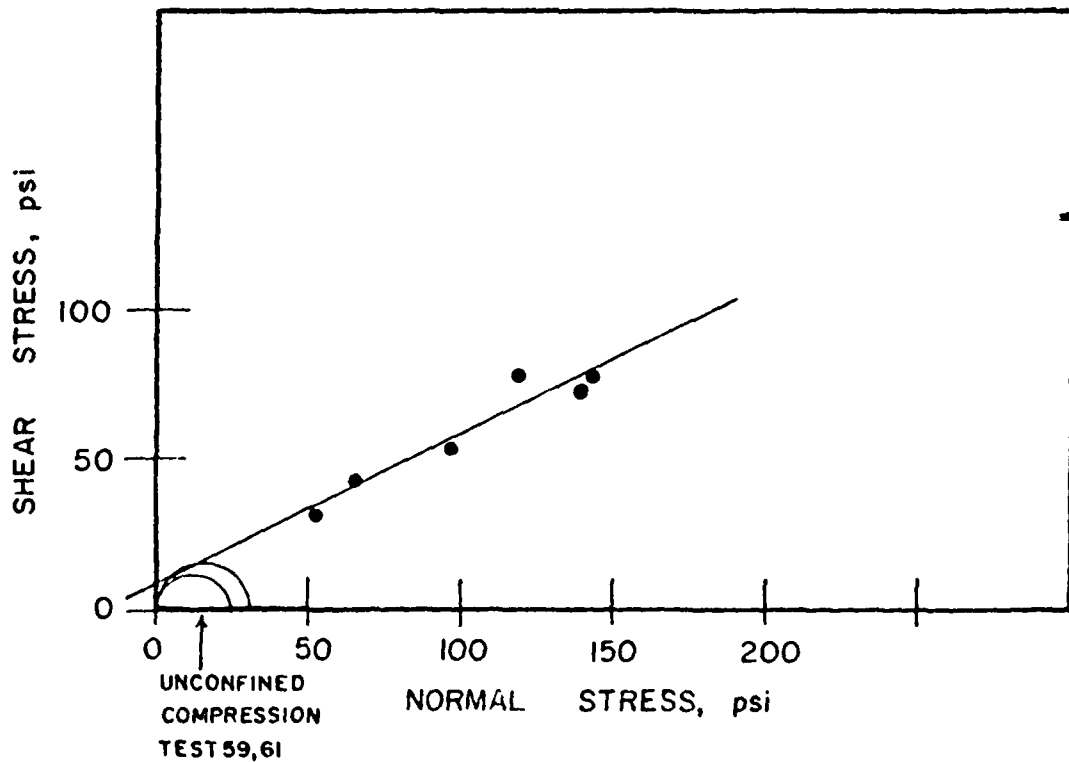


Table No. 3.31
IOWA BORE HOLE SHEAR APPARATUS

Location Tommy Florence's at Johnson Creek Date August 5, 1980
2.36 - 2.74 m
Depth (7.75 - 9 ft.) Horizon Old Paleosol Tested by Thorne/Smith
Description Borehole 3 on left bank

Point No.	Normal Stress Gauge	σ_n	Shear Stress Gauge	τ_{max}	Cons. Time	Remarks
1	31	39.7	22	29.2	10	$9'$ $r^2 = 0.92$
2	61	78.1	29	38.4	10	$9'$ $m = 0.3777$
3	91	116.1	45	59.4	10	$8'$ $b = 14.3 \text{ psi}$
4	121.5	155.6	53	70	10	$8'$
5	81	103.7	46	60.7	10	$7'9''$
						$\phi = 21^\circ$
						$c = 14.3 \text{ psi}$
						$= 98.5 \text{ kPa}$
						moisture content 23.4%dw

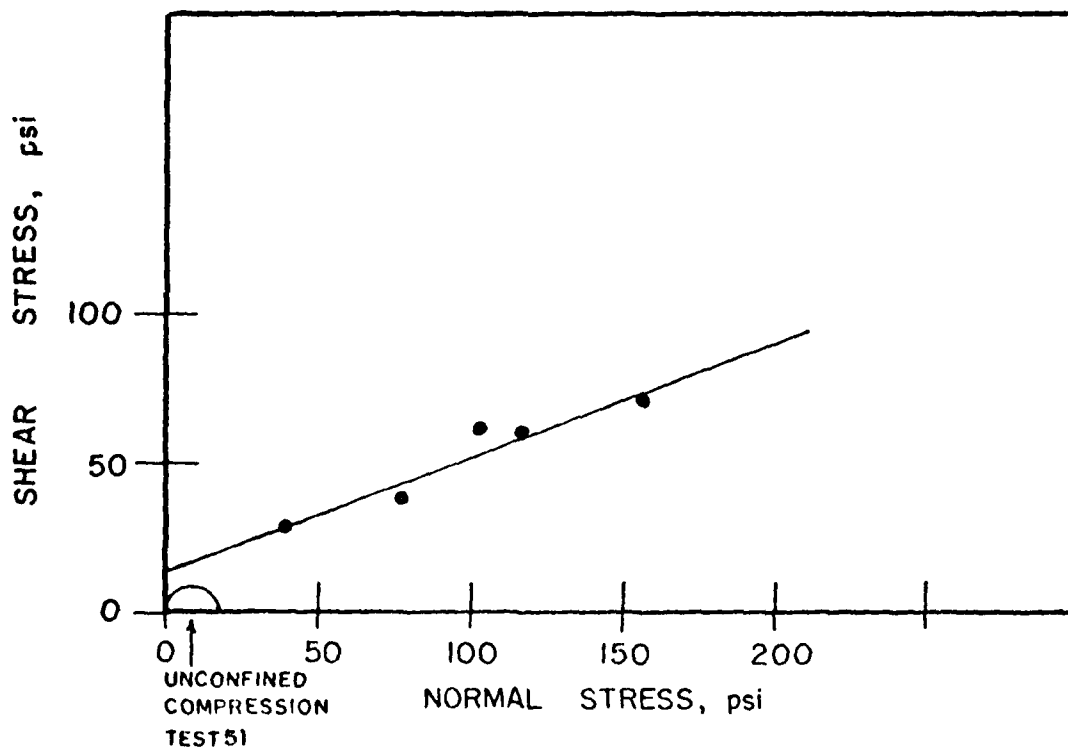


Table No. 3.32								
IOWA BORE HOLE SHEAR APPARATUS								
Location	Tommy Florence's at Johnson Creek			Date	August 6, 1980			
1.98 - 2.29 m								
Depth (6.5 - 7.5 ft.)			Horizon	Old Paleosol				
Description Borehole 3 on left bank			Tested by Thorne/Smith					

Point No.	Normal Stress Gauge	Shear Stress Gauge	σ_n	t_{max}	Cons. Time	Remarks
1	31	19	39.7	25.2	10	$r^2 = 0.99$
2	60	33	76.9	43.6	10	$m = 0.4630$
3	90	44	115.3	58.1	10	$b = 7.542 \text{ psi}$
5	48	28	61.5	37.1	10	$6'9''$
6	75	40	96.1	52.8	10	$6'9''$
7	112	57	143.4	75.2	10	$6'6''$
						$\phi = 25^\circ$
						$c = 7.54 \text{ psi}$
						$= 52.0 \text{ kPa}$
						moisture content 23.9%dw

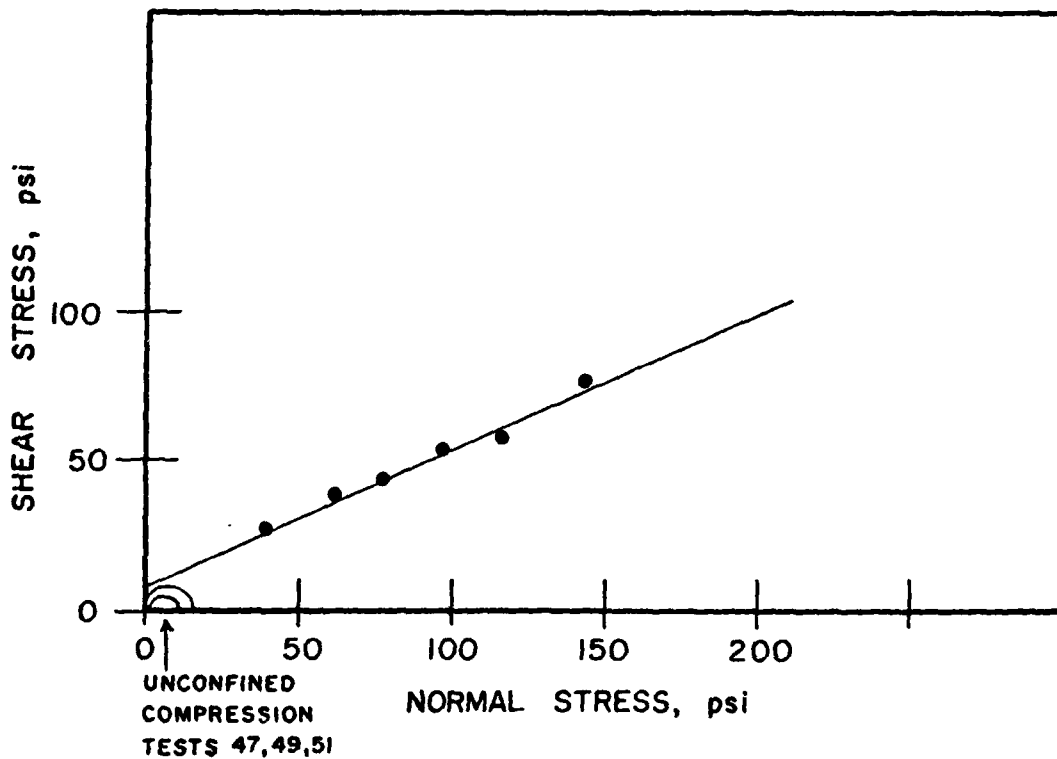
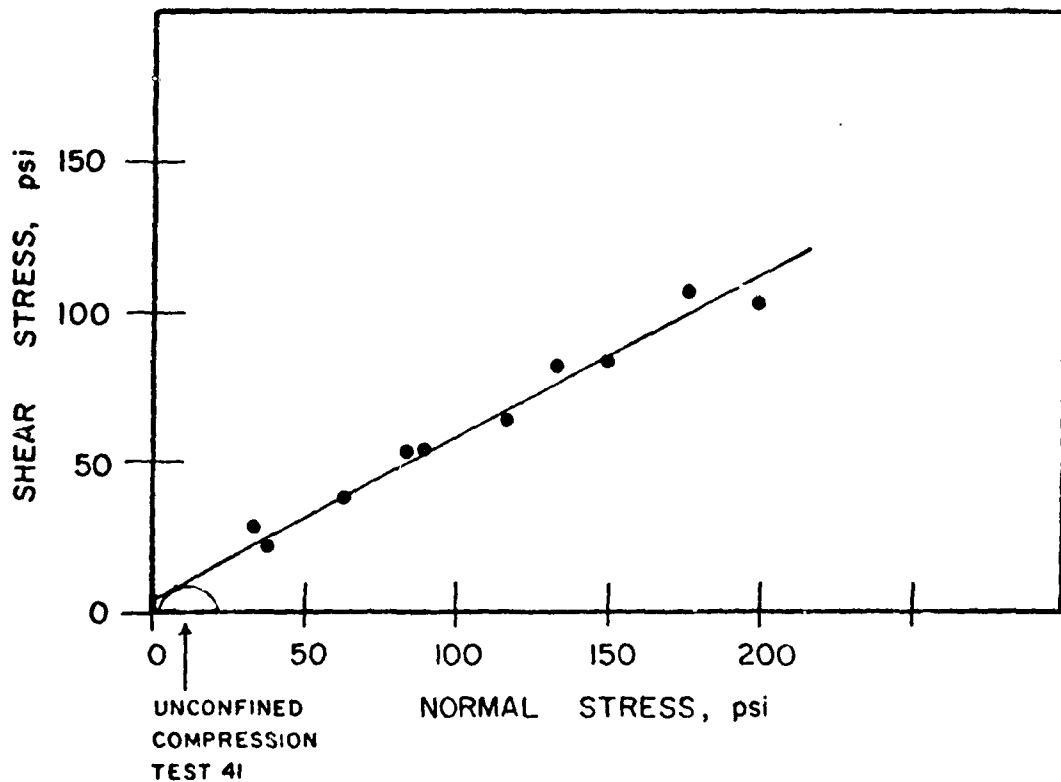


Table No. 3.33
IOWA BORE HOLE SHEAR APPARATUS

Location Tommy Florence's at Johnson Creek Date August 7, 1980
2.97 - 3.51 m
Depth (9.75-11.5 ft.) Horizon Old Paleosol Tested by Thorne
Description Borehole 2 on left bank

Point No.	Normal Stress Gauge σ_n	Shear Stress Gauge τ_{max}	Cons. Time	Remarks
1	103	61	80.4	10 9'9" $r^2 = 0.97$
2	65	40	52.8	10 9'9" $m = 0.53$
3	30	16	21.3	10' b = 5 psi
4	90	49	64.7	10'
5	70	40	52.8	10 10'3" $\phi = 28^\circ$
6	50	29	38.4	10 10'3" c = 34.5 kPa
7	117	64	84.4	10 10'6" = 5 psi
8	137	80	105.4	10 10'6"
9	156	77	101.5	11'3"
10	134	54	71.3	11'3" not bedded?
11	34.5	21	27.8	11'6"
				moisture content 22.6%dw



IOWA BORE HOLE SHEAR APPARATUS					
Location	Tommy Florence's at Johnson Creek		Date	August 7, 1980	
	1.60 - 1.83 m				
Depth (5.25 - 6 ft.)	Horizon	Dense Sand	Tested by	Thorne	
Description Borehole 2 on left bank					

Point No.	Normal Stress Gauge	Shear Stress Gauge	Cons. Time	Remarks
1	34	43.6	29	38.4
2	62	79.4	50	66
3	88	112.7	72	95
4	48	61.5	27	35.7
5	79	101.2	62	81.8
6	103	131.9	85	112
7	52	66.6	42	55.5
				10
				5'3"
				m = 0.8317
				5'6"
				b = 0.5709 psi
				5'9"
				not bedded
				6'
				6'
				$\phi = 40^\circ$
				c = 0.57 psi
				= 3.9 kPa
				moisture content 20.2%dw

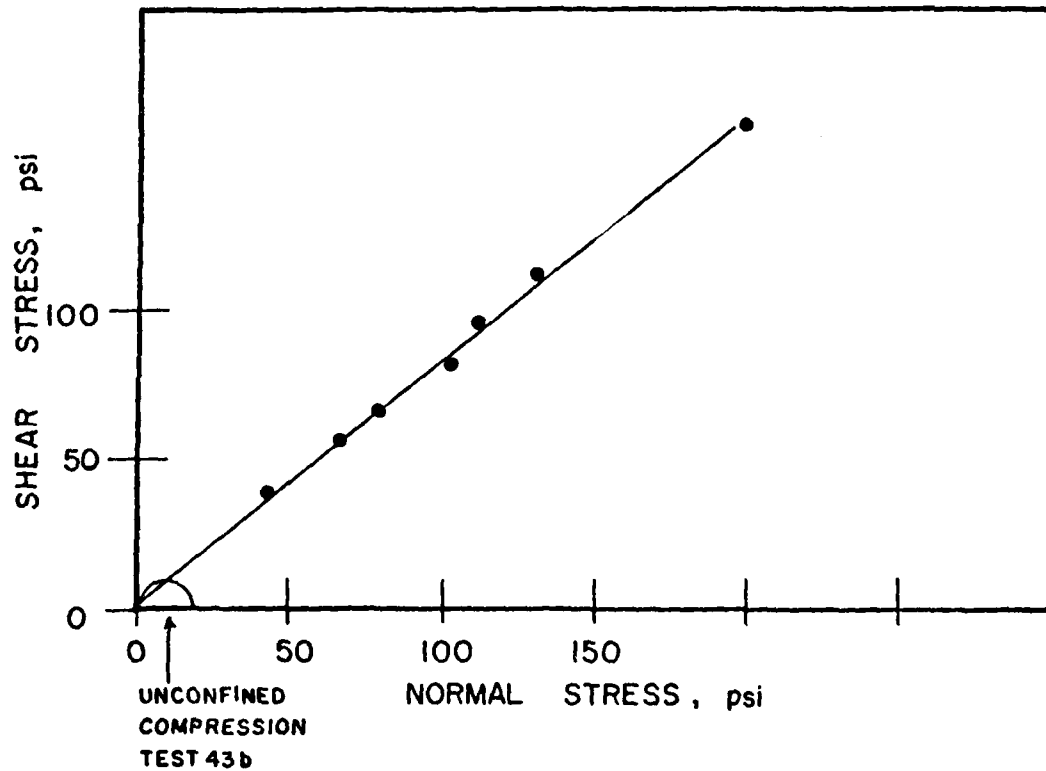


Table No. 3.35

IOWA BORE HOLE SHEAR APPARATUS

Location Tommy Florence's at Johnson Creek Date August 8, 1980
 Depth 1.83-1.98m(6-6.5ft) Horizon Old Paleosol Tested by Thorne
 Description Borehole 3 on left bank

Point No.	Normal Stress Gauge	σ_n	Shear Stress Gauge	t_{max}	Cons. Time	Remarks
1	58	74.3	29.5	39.0	10	6'
2	19	24.4	6.5	8.8	10	6' not bedded?
3	42	53.8	19.5	29.5	10	6'3"
4	80	102.5	39.5	52.2	10	6'6"
5	101	129.3	51	67.3	10	6'6"
						$r^2 = 0.998$ (4 pts. only)
						$m = 0.4979$
						$b = 2.20$ psi
						$\phi = 27^\circ$
						$c = 2.20$ psi
			moisture content	21.4%dw		= 15.2 kPa

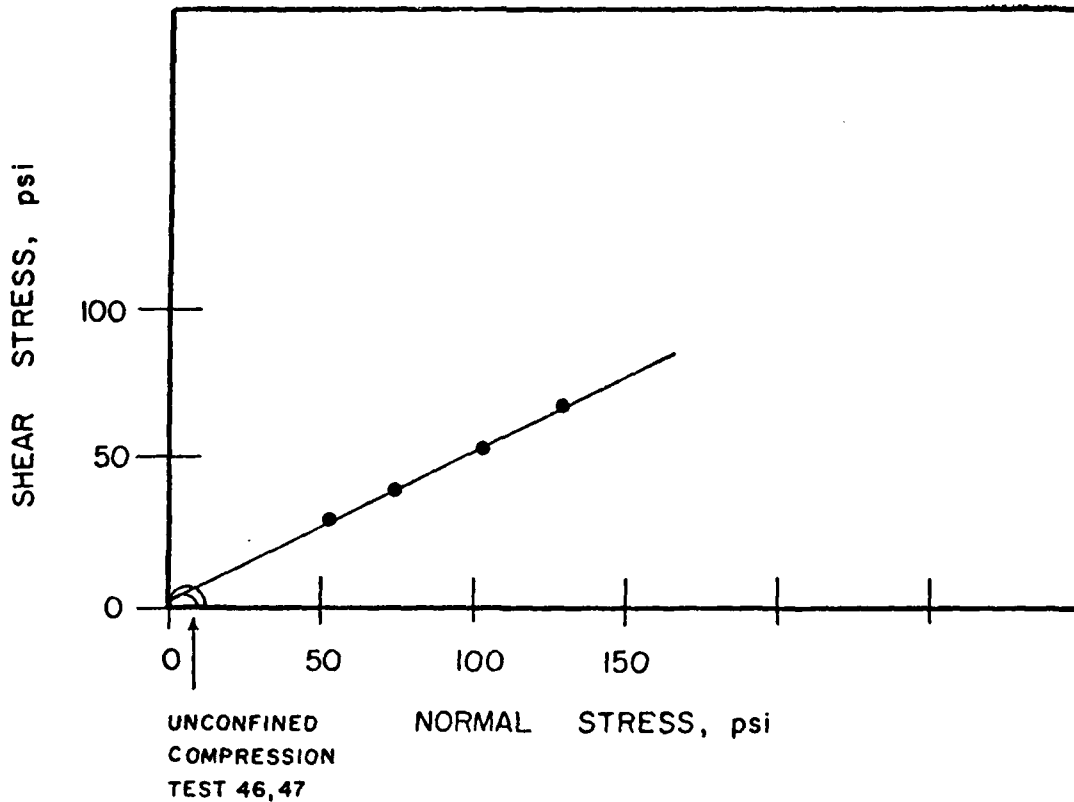


Table No. 3.36
IOWA BORE HOLE SHEAR APPARATUS

Location Tommy Florence's at Johnson Creek Date August 8, 1980
4.42 - 4.50 m
Depth (14.5 - 14.75 ft) Horizon Fine Sand/ Silt Tested by Thorne
Description Borehole 2 on left bank

Point No.	Normal Stress Gauge	σ_n	Shear Stress Gauge	τ_{max}	Cons. Time	Remarks
1	35	44.9	24.5	32.4	10	14'9"
2	61	78.1	30	39.7	10	14'9" not bedded?
5	94	120.4	54	71.3	10	14'6"
6	58	74.3	38	50.2	10	14'6"
						$r^2 = 0.99$ (only 3 points)
						$m = 0.5101$
						$b = 10.6$ psi
						moisture content 17.7%dw
						$\phi = 27^\circ$
						$c = 10.6$ psi
						= 72.8 kPa

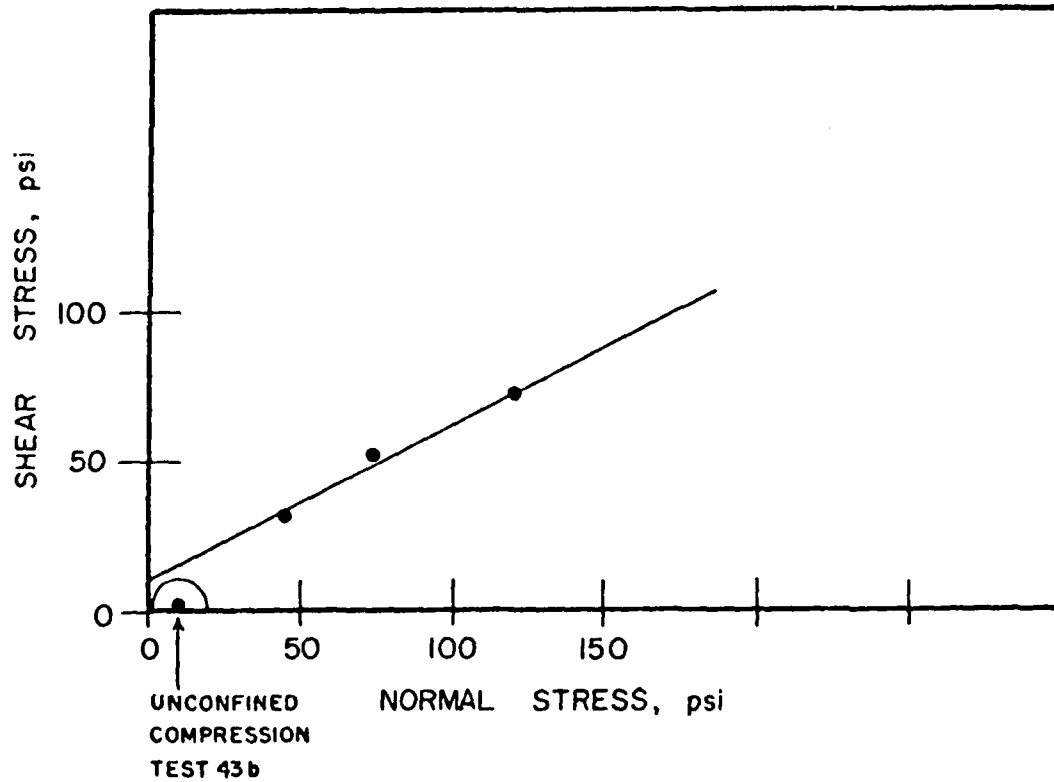


Table No. 3.37
IOWA BORE HOLE SHEAR APPARATUS

Location Tommy Florence's at Johnson Creek Date August 12, 1980
3.28 - 3.50 m
Depth (10.75-11.5 ft.) Horizon Old Paleosol Tested by Thorne
Description Borehole 4 on left bank

Point No.	Normal Stress Gauge	σ_n	Shear Stress Gauge	t_{max}	Cons. Time	Remarks
1	110	140.9	43	56.8	10	11'6" $r^2 = 0.73$
2	92	117.8	44	58.1	10	11'6" $m = 0.34$
3	70	89.7	44	58.1	10	11'8" $b = 15.4$
4	48	61.5	29.5	39.0	10	11'3"
5	33	42.3	17	22.6	10	11'
6	71	90.9	32	42.3	10	11'
7	110	140.9	73	96.2	10	10'9" Flyer?
						$\phi = 19^\circ$
						$c = 15.4 \text{ psi}$
						$= 106 \text{ kPa}$
						moisture content 23.1%dw

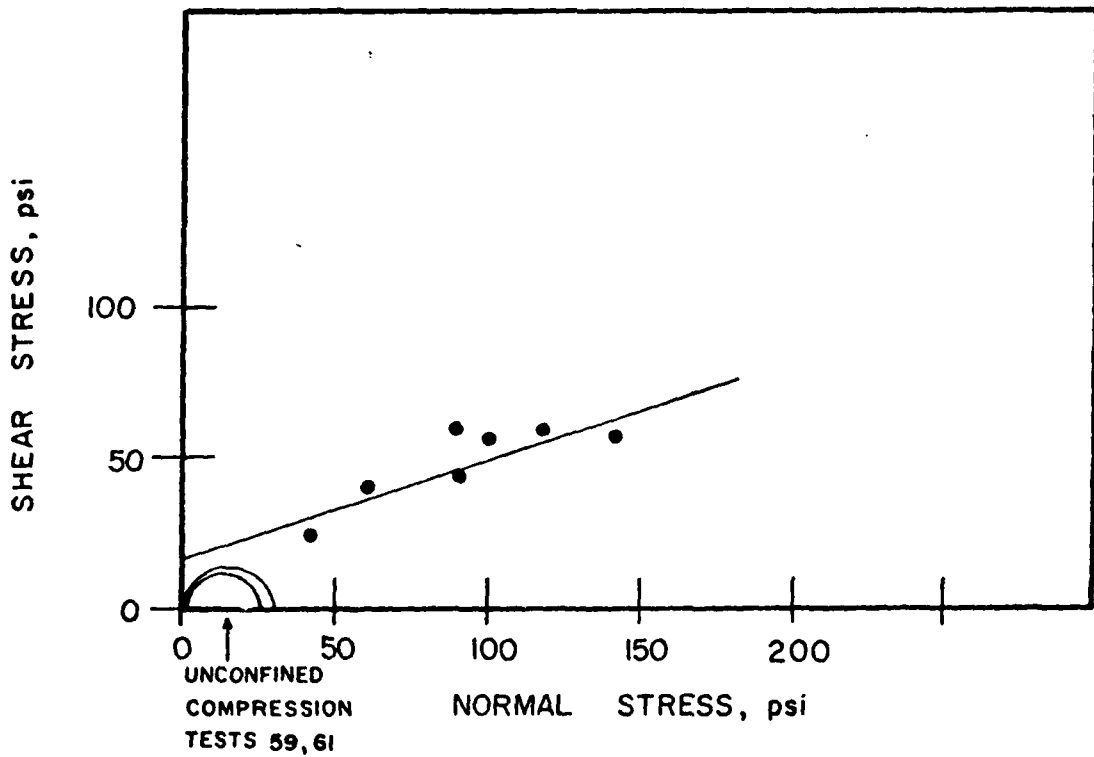
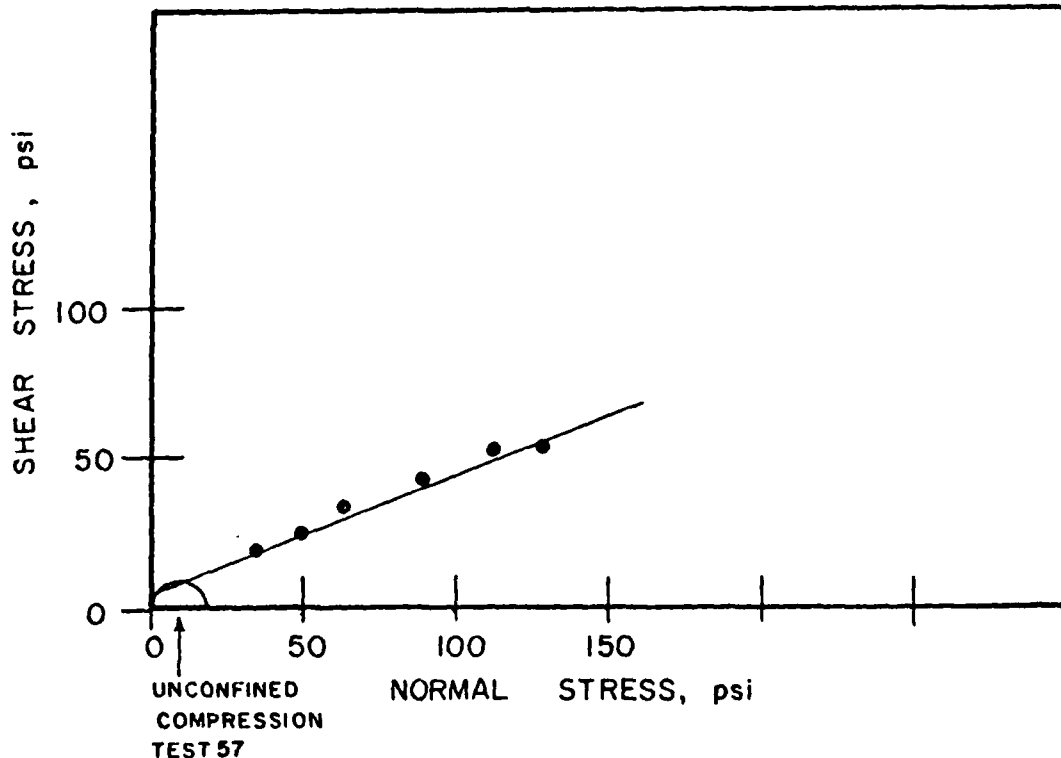


Table No. 3.38

IOWA BORE HOLE SHEAR APPARATUS

Location Tommy Florence's at Johnson Creek Date August 12, 1980
1.07 - 1.22 m
Depth (3.5 - 4 ft.) Horizon PSA Tested by Thorne
Description Borehole 4 on Left bank

Point No.	Normal Stress Gauge	σ_n	Shear Stress Gauge	τ_{max}	Cons. Time	Remarks
2	31	39.7	13.5	18	10	3'9"
3	50	64.1	25	33.1	10	3'9"
4	70	89.7	30.5	40.3	10	3'6"
5	88	112.7	39.5	52.2	10	4'
6	100	128.1	26	34.4	10	4' Fully expanded
7	100	128.1	40	52.8	10	4'3"
						$r^2 = 0.96$ (5 points)
						$m = 0.3983$
						$b = 4.69$
						$\theta = 22^\circ$
						$c = 4.69$ psi
			moisture content	18.5%dw		= 32.3 kPa



Results Table 39

Table No. 3.39

IOWA BORE HOLE SHEAR APPARATUS

Location Tommy Florence's at Johnson CreekDate August 13, 19801.91 - 2.06 mDepth (6.25 - 6.75 ft.) HorizonYPTested by ThorneDescription Borehole 5 (Soft Layer) on Left Bank

Point No.	Normal Stress Gauge	σ_n	Shear Stress Gauge	τ_{max}	Cons. Time	Remarks
1	90	115.3	45	59.4	10	$6'3"$ $r^2 = 0.950$
2	107	137.0	41	54.1	10	$6'3"$ $m = 0.49$
3	64	82	33	43.6	10	$6'6"$ $b = 8.0 \text{ psi}$
4	35	44.9	20	26.5	10	$6'6"$
5	60.5	77.5	30.5	40.3	10	$6'9"$
6	50	64.0	27.5	36.4	10	$6'9"$ Fully Expanded?
						$\phi = 24.1^\circ$
						$c = 8.0 \text{ psi}$
						$= 55.2 \text{ kPa}$
						moisture content 18.5%dw

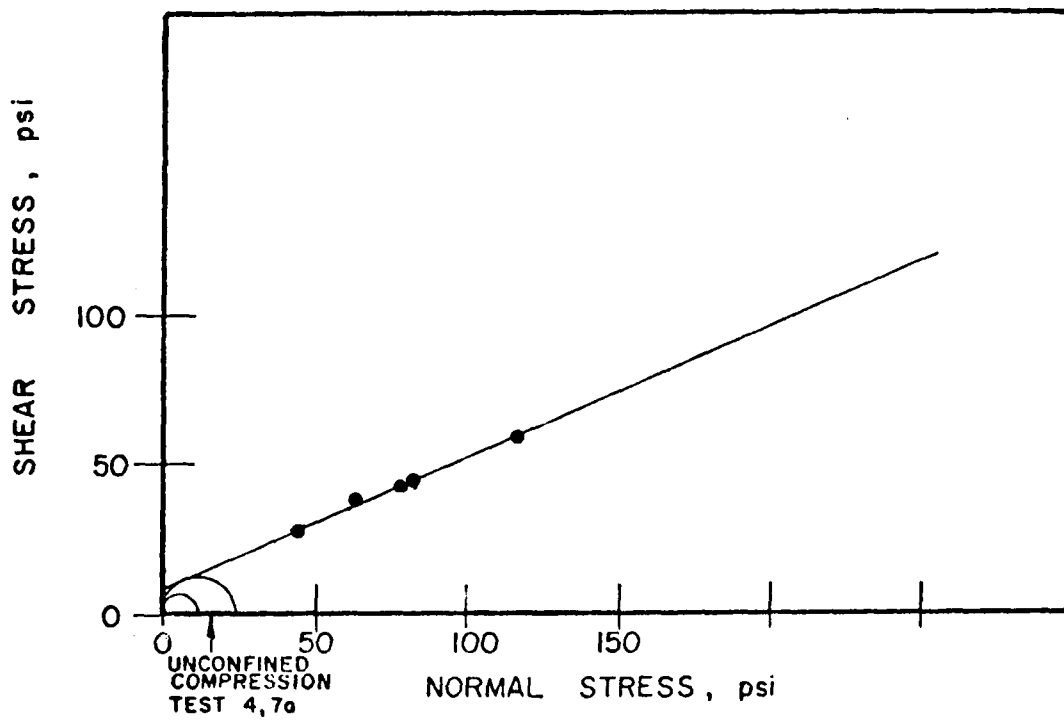


Table No. 3.40
IOWA BORE HOLE SHEAR APPARATUS

Location Tommy Florence's at Johnson Creek Date August 13, 1980
1.37 - 1.68 m
Depth (4.5 - 5.5 ft.) Horizon Soft Layer / YP Tested by Thorne
Description Borehole 5

Point No.	Normal Stress Gauge	σ_n	Shear Stress Gauge	t_{max}	Cons. Time	Remarks
1	41	52.5	24	31.8	10	4'6"
2	56	71.7	35	46.3	10	4'6"
3	70	89.7	41	54.1	10	4'9"
4	90	115.3	40	52.8	10	5' Caving?
6	65	83.3	35	46.3	10	5'3"
7	46	58.9	31.5	41.6	10	5'6"
8	90	115.3	36	47.6	10	5'6" Caving?
						$r^2 = 0.85$
						$m = 0.48$
						$b = 9.95$
						$\phi = 26^\circ$
		moisture content	19.0%dw			$c = 9.95 \text{ psi}$
						$= 68.6 \text{ kPa}$

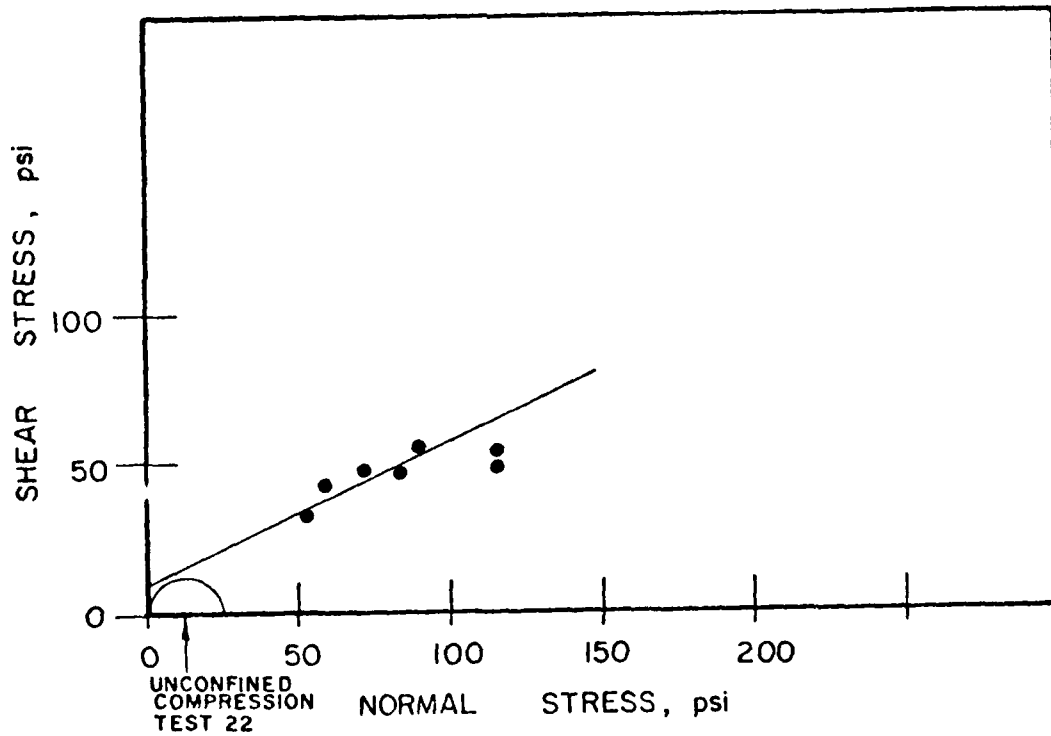


Table No. 3.41
IOWA BORE HOLE SHEAR APPARATUS

Location Tommy Florence's at Johnson Creek Date August 14, 1980
 Depth 3.66 - 3.81 m Horizon Old Paleosol Tested by Therne
 Description Borehole 5 on Left Bank

Point No.	Normal Stress Gauge	σ_n	Shear Stress Gauge	\uparrow_{max}	Cons. Time	Remarks
1	36	46.1	21	27.8	10	$12'$ $r^2 = 0.99$
2	90	115.3	35	46.3	10	$12'$ $m = 0.25$
4	53	67.9	26	34.4	10	$12'3''$ $b = 17.2$ psi
5	73	93.6	31.5	41.7	10	$12'6''$
6	110	140.9	39	51.5	10	$12'6''$
						$\phi = 14^\circ$
						$c = 17.2$ psi
						$= 118.3$ kPa

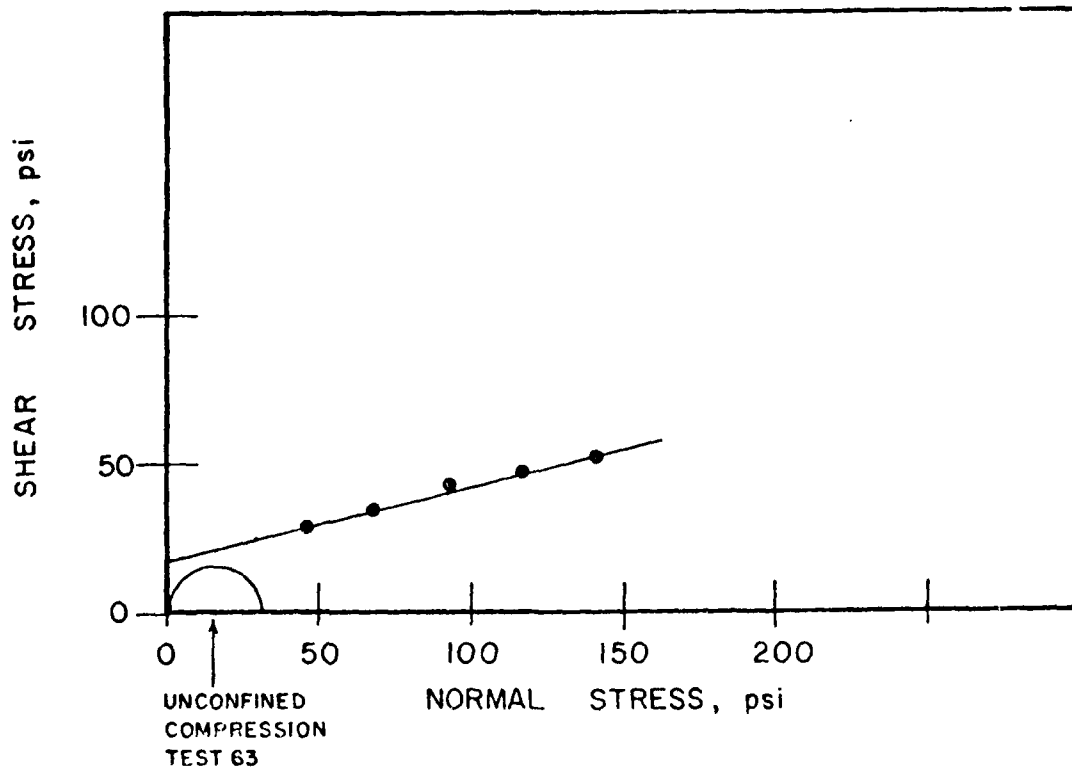


Table No. 3.42

IOWA BORE HOLE SHEAR APPARATUS

Location Katherine Leigh's at Goodwin Creek Date August 19, 1980
 Depth 0.76-0.91m(2.5-3ft.) Horizon PSA Tested by Thorne
 Description Borehole 5 on Right Bank

Point No.	Normal Stress Gauge σ_n	Shear Stress Gauge t_{max}	Cons. Time	Remarks
1	61	25	33.1	10 2'6" $r^2 = 0.99$
2	28	35.9	12.5	10 2'9" $m = 0.374$
3	41	52.5	17	10 2'9" $b = 3.02 \text{ psi}$
4	54	69.2	21	10 3'
				$\phi = 20.5^\circ$
				$c = 3.02 \text{ psi}$
				$= 20.8 \text{ kPa}$
				moisture content 23.0%dw

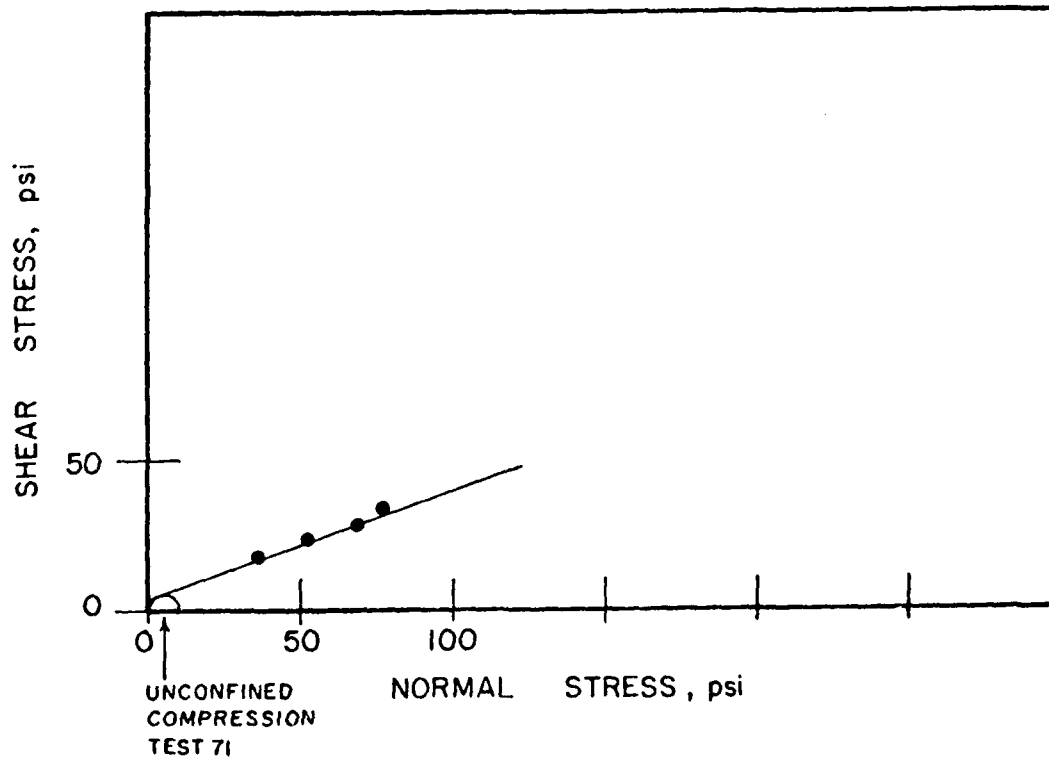


Table No. 3.43

IOWA BORE HOLE SHEAR APPARATUS

Location Katherine Leigh's at Goodwin Creek Date August 19, 1980
3.73 ~ 4.27 m
Depth (12.75 - 14 ft.) Horizon Old Paleosol-Grey Clay Tested by Thorne
Description Borehole 5 on Right Bank

Point No.	Normal Stress Gauge	σ_n	Shear Stress Gauge	τ_{max}	Cons. Time	Remarks
1	91	116.5	21.5	28.5	10	$13'$ $r^2 = 0.674$
2	114	146	29.5	39	10	$13'$ $m = 0.14$
3	71	90.9	25.5	33.8	10	$13'3''$ $b = 15.2 \text{ psi}$
4	51	65.3	21.5	28.5	10	$13'3''$
5	38	48.7	13.5	18	10	$13'6''$
6	41	52.5	17	22.6	10	$13'9''$
7	65	83.3	18.5	24.6	10	$13'9''$
8	83	106.3	12	16	10	$14'$
9	81	103.7	20.5	27.2	10	$12'9''$
10	119	152.4	25.5	33.8	10	$12'9''$
						$\phi = 7.90$
						$c = 15.2 \text{ psi}$
						$= 104.5 \text{ kPa}$
						moisture content 19.7% dw

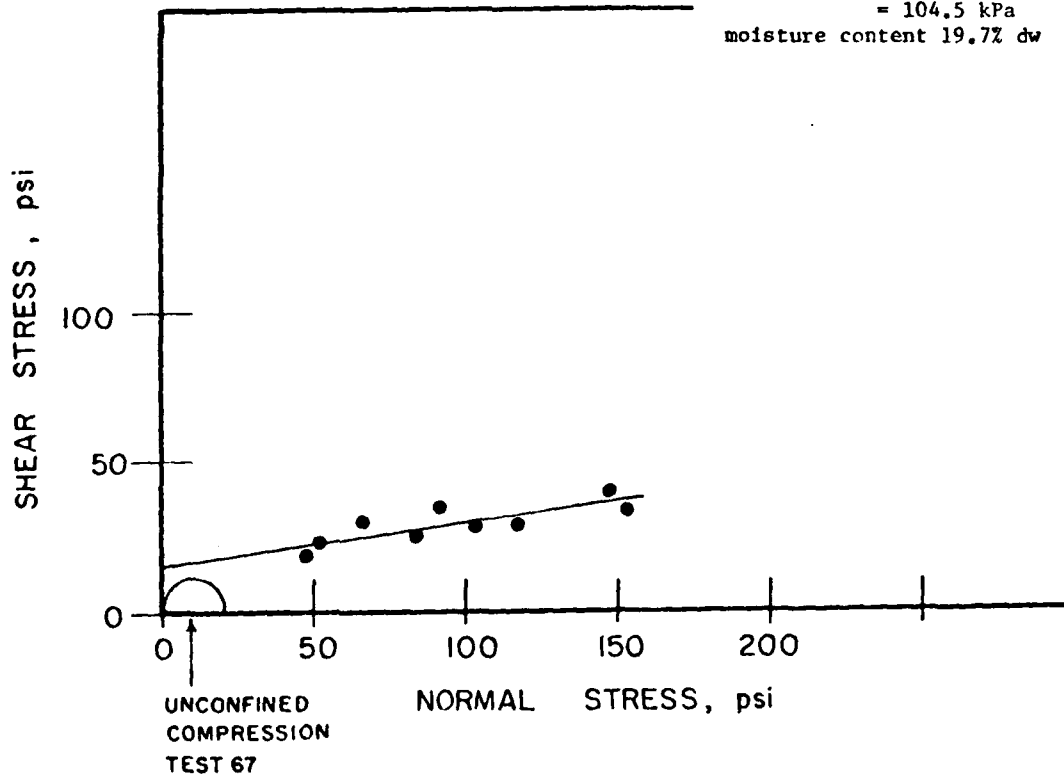


Table No. 3.44
IOWA BORE HOLE SHEAR APPARATUS

Location Katherine Leigh's at Goodwin Creek Date August 21, 1980
Depth 0.91-1.22 m (3-4ft) Horizon PSA Tested by Thorne
Description Borehole 6 on Right Bank

Point No.	Normal Stress Gauge	σ_n	Shear Stress Gauge	τ_{max}	Cons. Time	Remarks
1	68	87.1	30	39.7	10	$3'$ $r^2 \approx 0.79$
2	28	35.9	13.5	18	10	$3'3''$ $m = 0.38$
3	56	71.7	24	31.8	10	$3'9''$ $b = 6.0$
4	36	46.1	20	26.5	10	$3'9''$
5	44	56.4	17	22.6	10	$4'$
6	45	57.7	25	33.1	10	$4'$
						$\emptyset = 20.9^\circ$
						$c = 6.0 \text{ psi}$
						$= 41.4 \text{ kPa}$

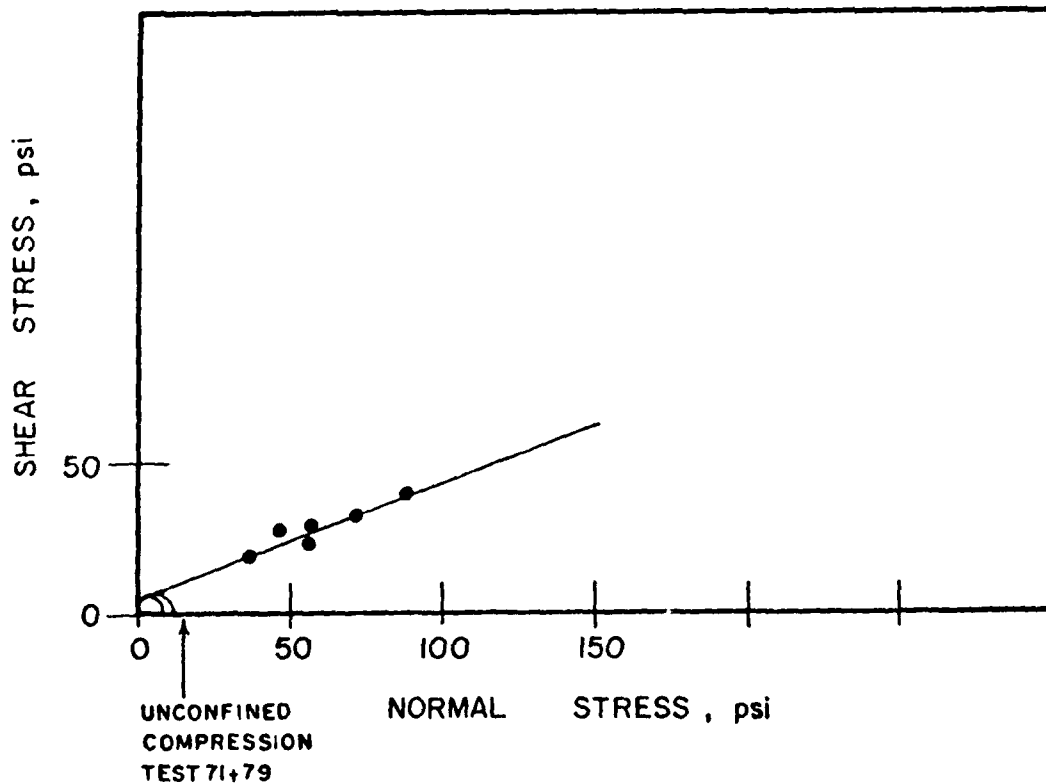


Table No. 3.45
IOWA BORE HOLE SHEAR APPARATUS

Location Katherine Leigh's at Goodwin Creek Date August 21, 1980
 Depth 1.52-1.82 m (5-6 ft) Horizon Y. P. Tested by Thorne
 Description Borehole 6 on Right Bank

Point No.	Normal Stress Gauge	Shear Stress Gauge	τ_{max}	Cons. Time	Remarks
1	80	102.5	23	30.5	5' $r^2 = 0.99$
2	101	129.3	33.5	44.3	5' $m = 0.275$
3	64	82	33	43.6	10' 3" $b = 9.2$
4	62	79.4	23	30.5	10' 3"
5	41	52.5	17	22.6	10' 6"
6	56	71.7	23	30.5	5' 6"
7	74	94.8	27	35.7	10' 9"
8	94	120.4	32	42.3	6'
					$\theta = 15^\circ$
					$c = 9.2 \text{ psi}$
					$= 63.5 \text{ kPa}$

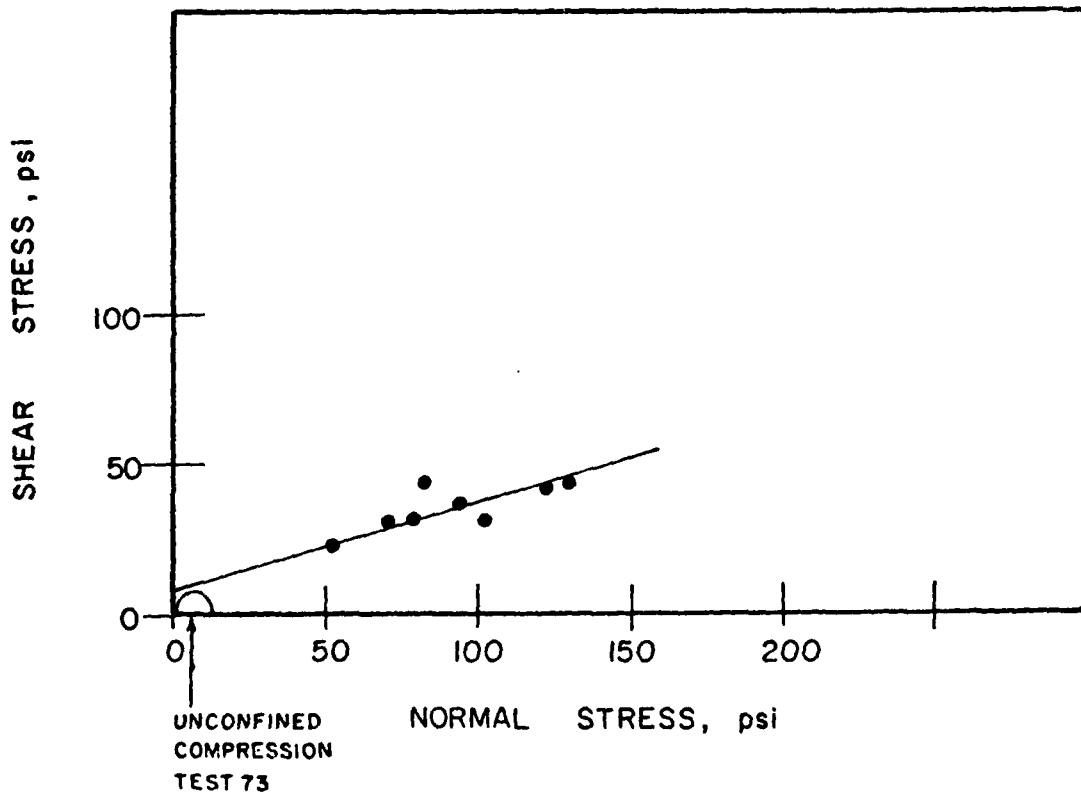
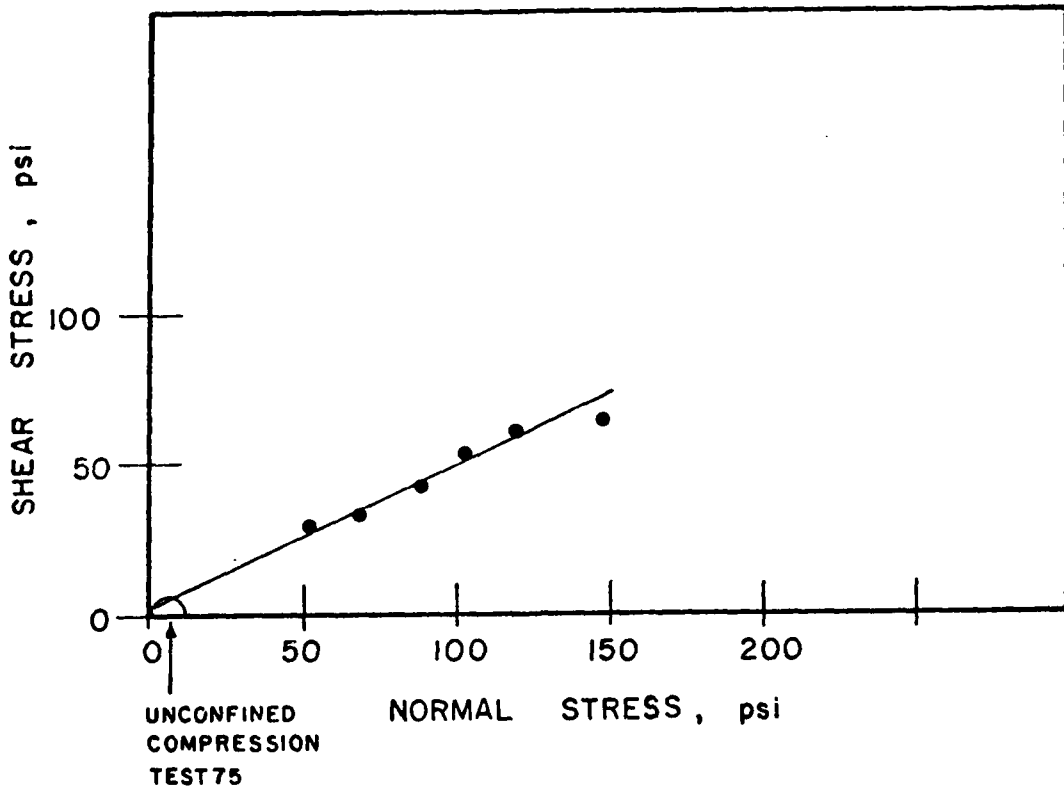


Table No. 3.46

IOWA BORE HOLE SHEAR APPARATUS

Location Katherine Leigh's at Goodwin Creek Date August 21, 1980
Depth 2.44 - 2.6 m
(8 - 8.5 ft.) Horizon Young Paleosol Tested by Thorne
Description Borehole 6 on Right Bank



ADDENDUM 4
UNCONFINED COMPRESSION AND TENSION TESTER

D.251

Addendum 4
List of Figures

Figure No.	Title	Page
4.1	Unconfined compression test on a sample of young paleosol	255
4.2	Unconfined compression apparatus modified for unconfined tension testing	256
4.3	Soil lathe for turning down samples strong in tension	258

4.1 INTRODUCTION

An unconfined compression test is a uniaxial compression test in which the soil core is provided no lateral support while undergoing vertical compression. The test measures the unconfined compression strength of a cylindrical sample of cohesive soil and, indirectly, the shear strength. The unconfined tension test is identical except that uniaxial tension replaces uniaxial compression and the unconfined tension strength is measured.

These tests were carried out on undisturbed soil cores taken from holes bored for the shear test. Compression tests were performed to supply additional shear strength data with which to check the BST measurements. Unconfined tension tests were performed to provide data on the behaviour of undisturbed alluvial soils in tension, for use in stability equations (section 3.2). Carrying out unconfined compression and tension tests on identical samples from within stratigraphic units also allowed evaluation of the ratio between the tensile and compression strength. This has important ramifications for the linearity of the Mohr-Coulomb line close to the ordinate and the permissibility of extrapolating it left of the ordinate into the tension quadrant.

4.2 UNCONFINED COMPRESSION TESTS

The unconfined compression tester used in this study is a Soil Test Incorporated, Model U-560* hand operated apparatus. Axial Load is measured using a proving ring. Two proving rings were available. The heavier ring had a range of 110 N (25 pounds) and the lighter one 22 N (5 pounds). Tests were performed on 76 mm (3 inches) and 51 mm (2 inches) nominal diameter soil cores cut to lengths of approximately 190 mm (7.5 inches) and 95 mm (3.75 inches) respectively to give a length to diameter ratio of about 2.5. Core dimensions were measured using a vernier caliper. Soil

*Trade names are used in this publication solely for the purpose of providing specific information. Mention of a trade name does not constitute a guarantee or warranty of the product by the U.S. Department of Agriculture or an endorsement by the Department over other products not mentioned.

cores were weighed prior to testing to obtain data on the field unit weight. Tests were strain controlled by turning the hand crank at a constant rate to advance the lower platten at about 0.05 mm per second (0.002 inches per second). Dial gauges were used to monitor axial deformation (1 dial unit \equiv 0.001 inches) and proving ring deformation (1 dial unit \equiv 0.0001 inches). Measurements of deformation were taken every 0.01 inches until failure occurred (Fig. 4.1.). After failure the soil moisture content was determined by oven drying at 105° C. Some soil samples were retained for mechanical and chemical analyses.

4.3 UNCONFINED TENSION TESTS

The unconfined compression tester was also used to perform tension tests. Only slight modifications were necessary. These modifications consisted of calibration of the lighter proving ring in tension as well as compression (by the manufacturers) and the manufacture of end caps to connect the soil column to the end plattens. End caps were made in the machine shop at the Sedimentation Laboratory (Fig. 4.2.). This tension tester is an improvement over previous versions, in that the measurement of axial load and deformation are of much greater accuracy and precision (Thorne, 1978; Thorne, Tovey and Bryant, 1980).

The soil cores were held in the end caps using paraffin wax. The technique for wax bonding is described in detail in a recent technical note (Thorne, Tovey and Bryant, 1980). This technique was also developed, independently, by Lutton (1974), however until very recently the authors were unaware of this. In previous studies 38 mm (1.5 inch) samples of alluvial bank material had been tested and strength of the wax had been sufficient to bond even the strongest cores successfully. However, when 76 mm (3 inch) soil cores from the banks of the bluff line streams were tested in a preliminary study some of them proved to be remarkably strong in tension, so much so that the bonding strength of the wax (about 35 kPa (5 psi)) was insufficient. Lutton (1974) encountered this problem and, to overcome it, he necked down the soil cores to an hour glass shape. A similar solution was used in this study (again without knowlege of Lutton's work), but with one significant difference. Instead of turning down the cylindrical core to an hour glass shape, the central section of the core was necked down at a constant radius. The ends of the sample core were not

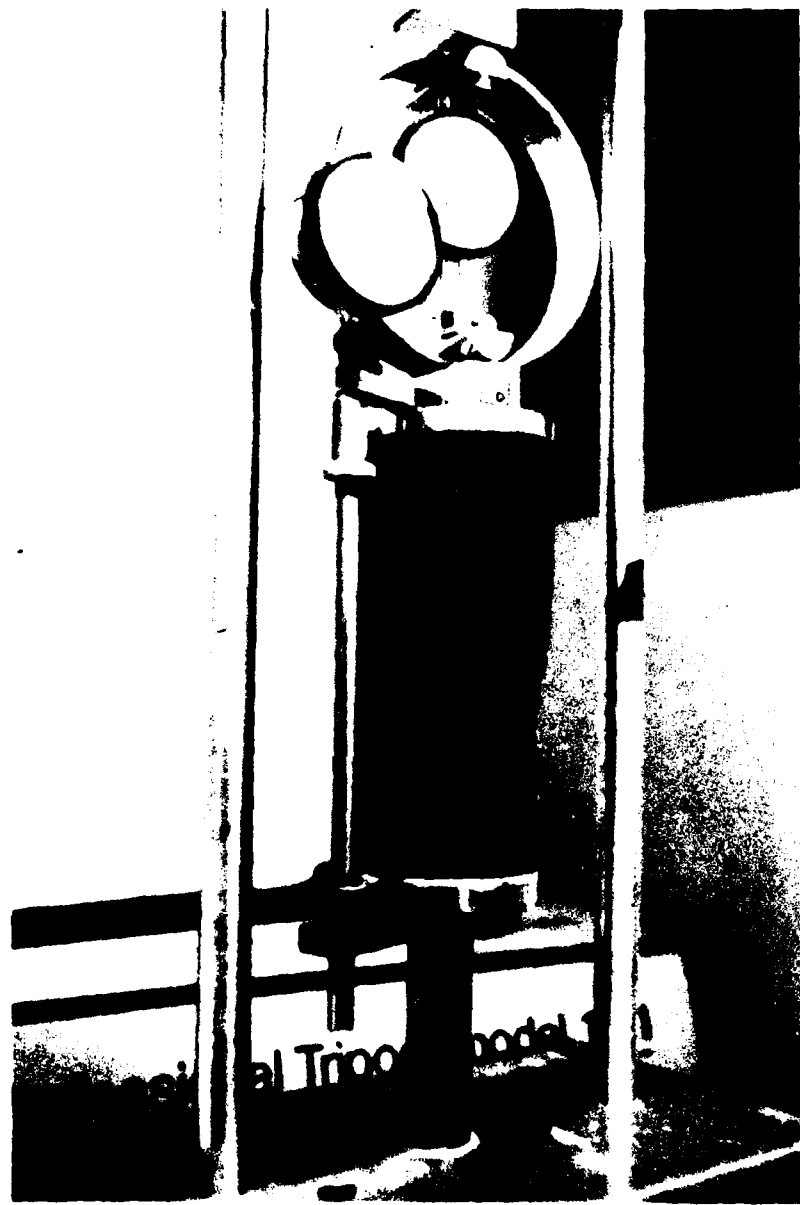


Figure 4.1. Unconfined compression test on a sample of young paleosol.

D.255

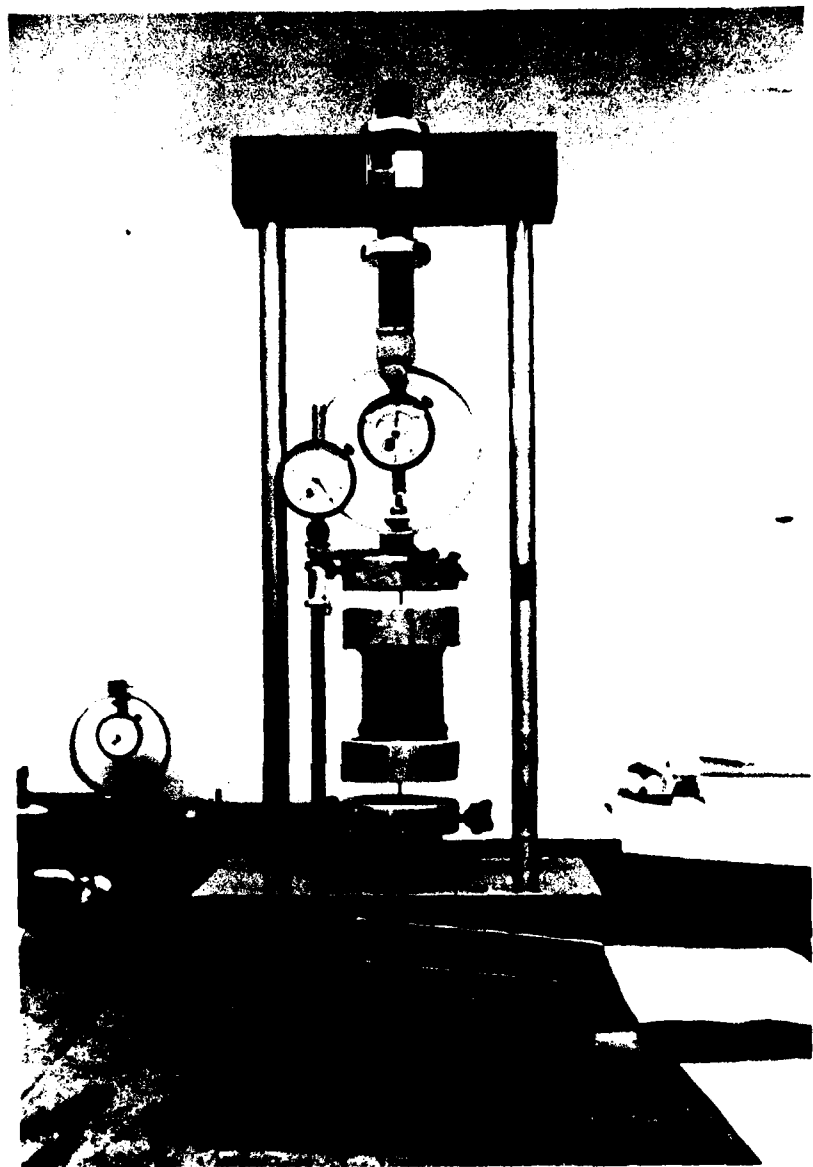


Figure 4.2. Unconfined compression apparatus modified for unconfined tension testing.

necked down but were grooved to provide a key for the wax-to-soil bond (Fig. 4.2.). By using a uniform diameter in the test section of the soil core the location of the failure surface was not specified as it was in Lutton's tests, but was free to develop along any bedding planes or lines of weakness in the soil. This proved to be significant in layered soils (see discussion of results in section 4.3.3).

Samples were turned down and grooved on a special soil lathe designed and built at the Sedimentation Laboratory (Fig. 4.3.). The soil core rested on two plastic rollers. Cutting was carried out using modeling knives. A profiled tool-rest was used to produce sample shape of uniform diameter over the test length and to ensure reproducibility between samples. The diameter of the necked-down portions of the 76 mm (3 inch) and the 51 mm (2 inch) samples were about 58 mm (2.3 inches) and 37 mm (1.5 inches) respectively. The lathe worked very well for the fine to medium grained soils encountered in this study. Problems arose with samples which contained gravel and with very wet samples. The latter samples tended to be thixotropic when rotated on the lathe and could not be shaped in this way. These problems were not too important however because the gravelly and wet samples were usually weak enough to be tension tested without necking down.

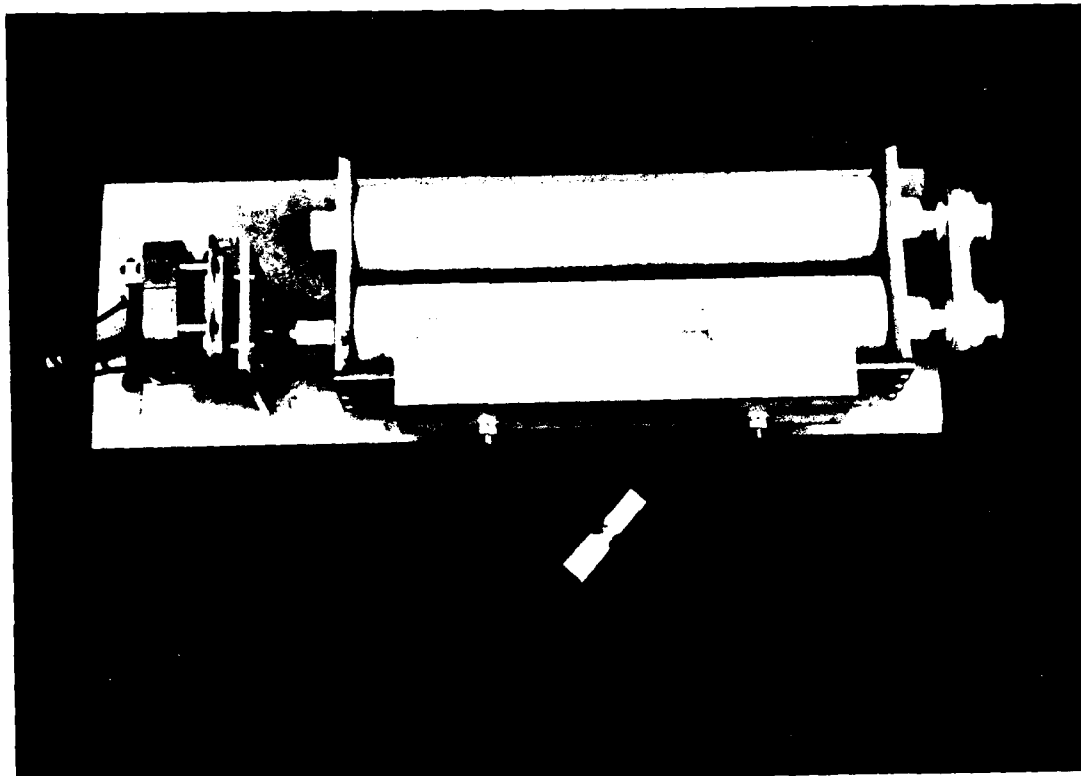


Figure 4.3. Soil lathe for turning down samples strong in tension.

